19th World Congress of Soil Science

Symposium 2.4.1
Soil minerals and sustainability

Soil Solutions for a Changing World,

Brisbane, Australia

1 – 6 August 2010

Table of Contents

Table of Contents (Cont.)

A comparison of extraction methods to assess potassium availability for Thai upland soils

Timtong Darunsontaya[A], Anchalee Suddhiprakarn[A*], Irb Kheoruenromne[A], and Robert J. Gilkes[B]

[A]Department of Soil Science, Faculty of Agriculture, Kasetsart University, Bangkok 10900, Thailand. *Corresponding author. Email agrals@ku.ac.th
[B]School of Earth and Environment, Faculty of Natural and Agricultural Sciences, University of Western Australia, Crawley, WA 6009, Australia.

Abstract
The effectiveness of several extraction procedures for K in predicting K uptake by Guinea grass in the glasshouse was determined for 18 upland soils from Thailand. NH_4OAc solution extracted exchangeable K that is closely related (R^2=0.97) to plant K uptake at 168 days, by which time most plants had died from K deficiency. This linear relationship has near unit slope so that plant uptake of K is quantitatively determined as exchangeable K. HNO_3-K and NaTPB-K determine different forms of non-exchangeable K in these soils that were relatively weakly related to the plant K uptake (R^2=0.62 for HNO_3-K and R^2=0.45 for NaTPB–K). These relationships indicate that exchangeable K is the K available to plants and non-exchangeable K was not readily available for plant growth over the time scale of the experiment. The XRD patterns of clay from the soils after cropping mostly show no change from that of the initial soil confirming that plant growth did not affect mineral forms of K. XRD patterns for samples extracted with NaTPB show a decrease in illite (001) peak-intensity with a concomitant increase in vermiculite (001) peak-intensity due to K removal from interlayer site in illite by NaTPB.

Key Words
Non-exchangeable K, HNO_3-K, NaTPB-K, NH_4OAc-K, highly weathered soils

Introduction
In Thailand, potassium deficiency is widespread under a tropical monsoonal climate in crops on highly weathered upland soils which are deficient in K bearing minerals. Critical assessment of the ability of soils to release K for plant uptake is important for the proper management of K in crop production. Exhaustive cropping techniques in a glasshouse study combined with chemical analyses of soils are useful for relating plant uptake of K to the various forms of soil K (Martin and Sparks 1985). For particular soil–plant systems, the suitability of a soil test extractant for predicting K supply depends on how closely the extracted K indicates the actual uptake of K by plants. Most extractants determine readily available K, which is generally assumed to be solution K plus exchangeable K. Replenishment of plant available K will depend on the release of mineral forms of K. For effective K management of Thai upland soils it is necessary to identify forms of K including mineral species containing K in these soils and establish which forms of K are released to plants.

Methods
Site sampling and physico-chemical analyses
Surface and subsurface samples of 18 upland agricultural soils from the Southeast Coast and Peninsular Thailand were used for this study. The physico-chemical properties were analyzed using standard methods (National Soil Survey Center 1996). Bulk soil samples were air–dried and crushed to pass through a 2 mm sieve before laboratory analysis. Soil pH was determined in water and in 1M KCl using 1:1 soil:liquid. Organic carbon (OC) was determined by the Walkley and Black wet oxidation procedure (Nelson and Sommers 1996) and calculation of organic matter content (OM) used the relationship OM = OC × 1.724. Cation exchange capacity (CEC) was determined by saturating the exchange sites with an index cation (NH_4^+) using 1M NH_4OAc at pH 7.0. Extractable acidity was measured by barium chloride-triethanolamine ($BaCl_2$-TEA) buffered at pH 8.2. Available phosphorus was determined by the Bray II method. Particle size distribution was determined by the pipette method.

X–ray diffraction (XRD) analysis of the clay fraction used CuKα radiation with a Philips PW–3020 diffractometer equipped with a graphite diffracted beam monochromator. Oriented clay was prepared on ceramic plates and XRD patterns were obtained from 4–35° 2θ with a step size of 0.02° 2θ and a scan speed

of 0.04°/second after various pretreatments to aid the identification of clay minerals (Brindley and Brown 1980).

Potassium study
Exchangeable K was determined by extraction in 1M NH_4OAc at pH 7.0. Non-exchangeable K was determined using two chemical extractants. One molar HNO_3-extractable K (HNO_3-K) was determined by boiling 2 g of soil in 20 mL 1M HNO_3 at 113°C for 25 minutes (Pratt 1965). NaTPB-K was extracted by shaking 1g of clay in 10 mL of 0.3M NaTPB for 168 hours. One milliliter of 1M NH_4OAc was immediately added to the suspension to prevent continuing K exchange from the suspended clay and to block subsequent fixation of dissolved K. The KTPB precipitate was then dissolved in 50 mL of 70% acetone. The acetone was then collected from the sample by filtration and acidified with 5 mL 6M H_2SO_4. The resulting solution was heated on a hot plate for 2 hours at 60°C to concentrate the H_2SO_4 which was then made up to a final volume of 100 mL with deionized water. Potassium in this solution was determined with a flame photometer (Schulte and Corey 1963 1965). The values of K released from the clays to NaTPB solution were converted to a whole soil basis by multiplying by the clay proportion. HNO_3-K and NaTPB-K also included NH_4OAc-K. Total K in soils was determined using X-ray fluorescence spectrometry.

An exhaustive K depletion glasshouse experiment was conducted on these soils using Guinea grass (*Panicum maximum*) to assess their K supply capacities. One kilogram of air-dry soil per pot was used for cropping and basal nutrients were applied initially and after each harvest to ensure that general nutrient supply did not limit plant growth. Thirty grass seeds were sown in each pot and thinned to 4 uniform plants after emergence. Soils were watered daily to field capacity with deionised water. The grass was harvested every 30 days and the K content of plants was determined after acid digestion.

Results
Classification and general properties
These Thai upland soils are highly weathered and highly developed. They are classified as Oxisols and Ultisols and all soils experience a udic soil moisture regime. They exhibit a wide range of general properties (Table 1). The pH in water and in 1M KCl ranges from 3.7 to 6.5 and from 3.4 to 5.6 respectively. The CEC of these soils ranges from 1.4 to 28 cmol/kg, OM ranges from 0.3 to 30 g/kg, EA ranges from 1.1 to 27 cmol/kg and available P ranges from 0.3 to 176 mg/kg. Soil texture ranges from sand to clay. Most of soil samples have low values of pH, CEC and organic matter because of their advanced weathering due to the high rainfall and elevated temperatures in this region.

Table 1. Range and mean value of some properties of Thai upland soils.

Property	min	max	mean
pH (1:1 H_2O)	3.7	6.5	5.0
pH (1:1 KCl)	3.4	5.6	4.1
CEC (cmol/kg)	1.4	28	6.9
EA (cmol/kg)	1.1	27	7.6
OM (g/kg)	0.3	30	5.6
Available P (mg/kg)	0.3	176	25
Sand (g/kg)	43	811	471
Silt (g/kg)	35	453	160
Clay (g/kg)	76	872	369
NH_4OAc-K (mg/kg)	8.0	212	37
HNO_3-K (mg/kg)	25	248	79
NaTPB-K (mg/kg)	7.5	189	57
Total K (mg/kg)	67	29931	3366

Soil potassium determined by various extraction methods
NH_4OAc extractable K in these soils ranges from 8.0 to 212 mg/kg (mean 37 mg/kg) and includes water soluble and exchangeable K. The Oxisols have higher values of this K form than the Ultisols due presumably to the higher clay content of Oxisols. HNO_3-K ranges from 25 to 248 mg/kg (mean 79 mg/kg) and NaTPB-K ranges from 7.5 to 189 mg/kg (mean 57 mg/kg). The mean value of NaTPB extractable K is less than HNO_3-K because nitric acid extractable K includes non-exchangeable K from the destructive

dissolution of silicate minerals, whereas NaTPB extraction is less severe and only extracts structural K from interlayer sites in micaceous minerals. However, K removed by all three extractants represents only a small proportion of total soil K, as has commonly been reported for other highly weathered soils (Markewitz and Richter 2000)

Relationships between K removed by the extraction procedures and plant K uptake
The values of K removed by the three extractants have been compared with the K taken up by plants during 180 days of growth in a glasshouse experiment, by which time most plants had died from K deficiency (Figure 1). The results show that cumulative K uptake by plants has weak exponential relationships with NaTPB-K (R^2=0.45) and HNO_3-K (R^2=0.62). There is a much closer linear relationship between plant K content and NH_4OAc-K (R^2=0.97) with the plant K content being numerically equal to the exchangeable K content of the soil (*i.e.* slope of regression line is nearly unity) (Figure 1c). This relationship indicates that exchangeable K is practically the only form of K available to plants and that non-exchangeable K is not readily available for plant growth over a period of 180 days.

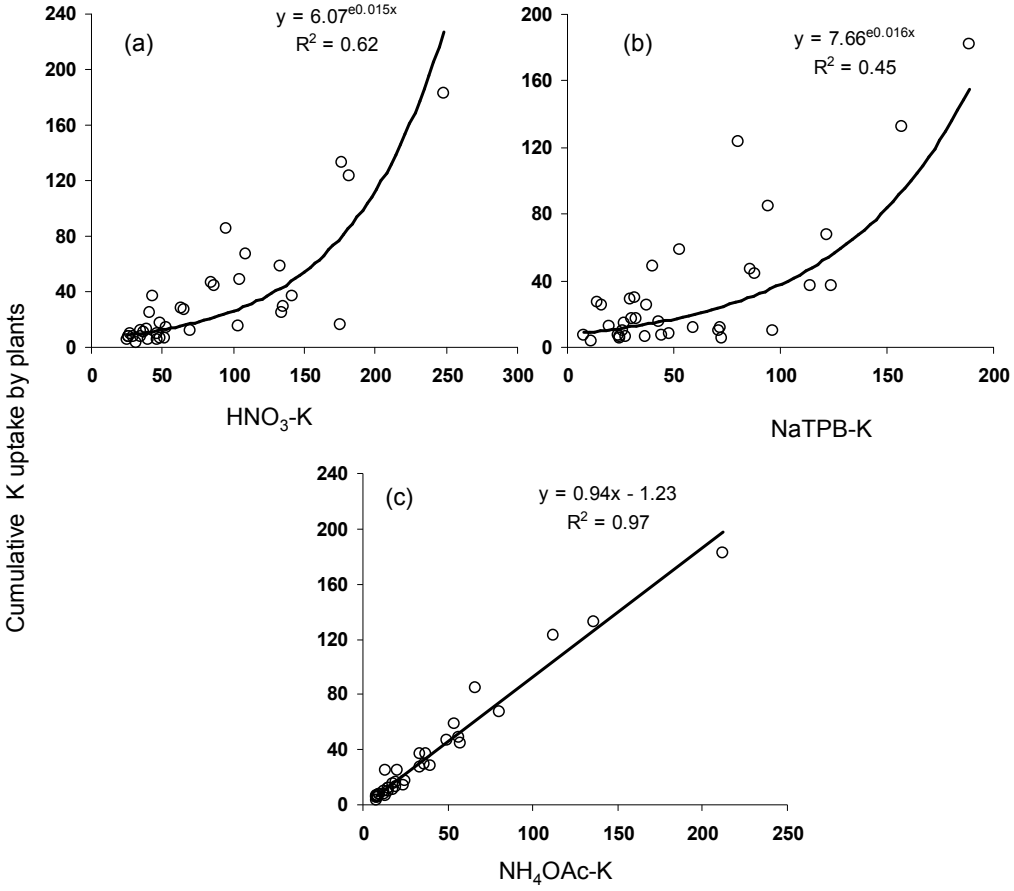

Figure 1. Relationships between soil K removed by extractants and cumulative K uptake by Guinea grass in 180 days.

Availability of K to plants in relation to clay mineralogy
The clay fractions of these soils contain much kaolin and various amounts of minor accessory minerals including illite, gibbsite, anatase, quartz, maghemite, hematite, goethite and hydroxyl Al interlayered vermiculite. XRD patterns of clays shows that there was no change in clay mineralogy due to plant growth indicating that the structure of the clay minerals was not affected by K depletion due to plant growth. This is consistent with K being provided to plants from the exchange sites and not from the structural sites in layer silicates. However, the XRD pattern from a sample extracted with NaTPB for 168 hours and that contains illite shows a decrease in illite (001) peak-intensity with a concomitant increase in vermiculite (001) peak-intensity due to K removal from illite by NaTPB (Figure 2).

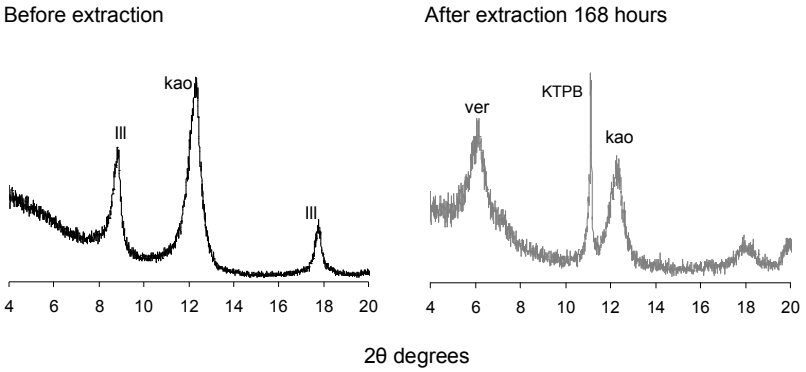

Figure 2. Diffraction patterns of basally oriented, Mg-saturated clay from Chumphon (Cp) surface soil showing changes in the relative peak intensities of vermiculite and illite resulting from 168 hours of shaking with NaTPB. (Ver=vermiculite, Ill= illite, Kao= kaolinite). The reflection at 11˚ 2Ɵ is due to KTPB.

Conclusions

This study has identified NH_4OAc-K as being a highly predictive indicator of the availability of K to plants grown in the glasshouse for these highly weathered upland soils whereas NaTPB-K and HNO_3-K are not readily available to plants. The K-exhaustion glasshouse experiment involved small volumes of soil that were intensively exploited by roots and the removal of plant tops ensured that there was limited recycling of K. Under field conditions plant roots can exploit a much larger volume of soil and recycling of K from foliage can occur. Furthermore, under a humid tropical climate the weathering process can promote the release of K from K-minerals. Consequently, K exhaustion of soils will occur at a slower rate in the field. However these soils clearly contain little exchangeable K and the non-exchangeable K is not readily available to plants so that soil K will eventually become too low to support annual field crops if K fertilizers are not provided.

Acknowledgments

The authors are grateful to The Royal Golden Jubilee Ph.D. Program under the Thailand Research Fund for financial support and to the laboratory staff at the School of Earth and Environment, UWA.

References

Brown G, Brindley GW (1980) X–ray diffraction procedures for clay mineral identification. In 'Crystal structures of clay minerals and their X–ray identification'. (Eds GW Brindley, G Brown) pp. 305–359. (Spottiswoode Blallantyne Ltd.: London).

Markewitz D, Richter DD (2000) Long-term soil potassium availability from a Kanhapludult to an agrading loblolly pine ecosystem. *Forest Ecology and Management* **130**, 109-129.

Martin HW, Sparks DL (1985) On the behavior of non-exchangeable potassium in soils. *Communication in Soil Science and Plant Analysis* **16**, 133-162.

National Soil Survey Center (1996) Soil survey laboratory methods manual, Soil survey investigations report No. 42. Natural Resources Conservation Service. pp. 400. (United States Department of Agriculture: Washington D.C.)

Pratt PF (1965) Potassium. In 'Methods of soil analysis, Part 2: chemical and microbiological properties'. (Ed. Black CA), pp. 1023-1031. (American Society of Agronomy: Madison, Wisconsin)

Schulte EE, Corey RB (1963) Flame photometric determination of potassium precipitated in soils as potassium tetraphenylboron. *Soil Science Society Proceedings* **27,** 358-360.

Schulte EE, Corey RB (1965) Extraction of potassium from soils with sodium tetraphenylboron. *Soil Science Society Proceedings* **29,** 33-35.

A study on mineralogy of soils under two parent rocks in higher rainfall areas of Iran

Masoomeh Poormasoomi[A] and Hasan Ramezanpour[B]

[A] Department of Soil Science, University of Guilan, Iran, Email masoomeh_poormasoomi@yahoo.com
[B] Department of Soil Science, University of Guilan, Iran, Email hasramezanpour @ guilan.ac.ir

Abstract
Morphology, mineralogy and geochemistry of soils derived from granite and andesitic basalt was investigated in western part of Lahijan. Two representative soil pedons were selected in mountain landform. Mineral weathering was characterized by petrographic microscope and comparison was made with total elemental analysis (XRF) and X-ray analysis (XRD).All evidences showed that there is a close structured relationship between the host mineral and the weathering products however, the weathered rock has also been hydrothermally altered. Mineral composition (confirmed by thin section and XRD) in granite were quartz, orthoclase (including perthitizing zone) albitic plagioclase and minor amount of biotite however in andesitic basalt were pyroxene, olivine, amphibole, plagioclase (labradorite) and quartz. Furthermore, sericite, chlorite, smectite (in soils from andesitic basalt) and vermiculite were the most alteration products. Total elemental content of Ca, Mg and Fe as well as solum thickness in field observation and clay mineral content were higher in soils from andesitic basalt which can be attributed to the presence of more susceptible ferromagnesian minerals to weathering.

Key Words
Diffractogram, Crystalline rock, Primary mineral

Introduction
Chemical weathering of rocks is one of the major processes that modify the earth's surface and is one of the vital processes in the geochemical cycling of elements. The rate and nature of chemical weathering vary widely and are controlled by many variables such as parent rock type, topography, climate and biological activity (Islam *et al.* 2002). Petrographic and mineralogical analyses are useful tools for the interpretation of the factors controlling the weathering of crystalline rocks and their influence on the typical development of weathered lanforms. Thus, relations between the parent rock materials and secondary clay minerals can help assist in determining different degrees of weathering (Jimenez-Espinosa *et al.*2007).The present work undertaken in order to characterize the alteration of primary minerals, formation of secondary minerals and their relation with results of geochemical and mineralogical analyses.

Methods
Study area located in Lahijan in north of Iran with annual precipitation of 1200mm, udic soil moisture and thermic soil temperature regime. Two sites of granite (P1) and andesitic basalt (P2) parent material on mountains were selected. Each site consist of one pedon (forest) on shoulder. The studied soil pedons have been characterized by field description bulk and undisturbed sampling, routine physical and chemical analyses, total elemental analyses (Page 1982), X-ray diffraction analyses by XRD and thin sections study by petrographic microscope (Bullock *et al.* 1985).

Results
Mineralogical composition of selected horizons by XRD in two soil profiles are summarized in table 1. The results in soils of P1 showed a dominance of quartz (peak of 3.34 Å), muscovite (10 Å), feldspar (3.18-3.24 Å) and clay minerals (illite) in slightly weathered bedrock (Figure1) and vermiculite, kaolinite and mica in surface and deeper horizons (Ramezanpour *et al.* 2006). Thin sections of this pedon (Table 2) contain mainly quartz, K-feldspar (mostly orthoclase as shown in Figure3b), little amount of plagioclase feldspar (albite) and higher content of muscovite (sericite) together with minor amounts of biotite and chlorite (in Crt1 and Crt2). Geochemical analyses (Table 3) showed the presence of some amounts of Na, K and Fe. Furthermore feldspars to sericite (Figure 3a) and biotite alteration to chlorite was an important process which decreased with depth.

Table 1: Mineralogical composition of selected horizons based on X-ray diffraction

Profile horizons	Minerals				
	Qu	Mu/Il	Ka	Ve	Se
Profile 1(granite)					
A	X	X	X	X	.
Crt2	X	X		X	.
Profile 2(andesitic basalt)					
A	X	.	.	.	X
Bt2	X	X	X	X	.
2Crt2	X	X	.	X	X

Qu= Quartz, Mu/Il= Muscovite/Illite, Ka= Kaolinite, Ve= Vermiculite, Se= Smectite

Table 2. Mineralogical composition of soil pedons based on microscopic observation

Profile horizons	Minerals								
	Qu	FK	Pl	Bi	Mu	Ch	Ol	Px	Am
Profile 1									
A	X	X	X	.	.	.	.	.	.
Crt1	X	X	X	X	X	X	.	.	.
Crt2	X	X	X	X	X	X	.	.	.
Profile 2									
A	X	.	X	.	.	.	X	X	.
Bt1	X	.	X	.	.	.	X	X	X
Bt2	X	.	X	.	.	.	X	X	X
Bt3	X	.	X	.	.	.	X	X	X
Crt1	X	.	.	.	.	X	.	X	.
2Crt2	X	.	X	.	.	.	.	X	.

Qu= Quartz, FK= K-feldspar, Pl= Plagioclase, Bi= Biotite, Mu= Muscovite, Ch= Chlorite, Ol= Olivine, Px= Pyroxene, Am= Amphibole

The XRD patterns of the horizons in P2 showed a composition with a dominance of quartz, muscovite, feldspar, pyroxene (peak of 2.99 Å) and clay minerals in weathered bedrock (Figure2) and smectite, vermiculite, kaolinite and mica in A,Bt2 and Crt2 horizons (Ramezanpour and Zanjanchi 2007).

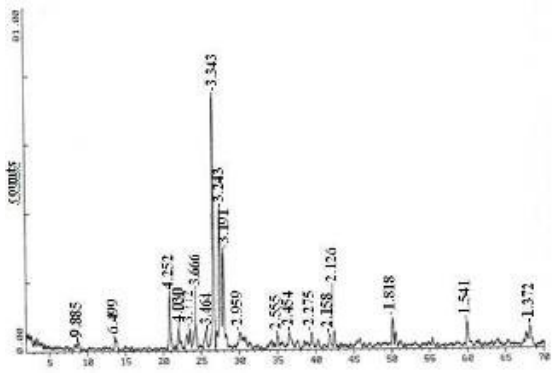

Figure 1. The X-ray diffractograms of the slightly weathered bedrock of P1

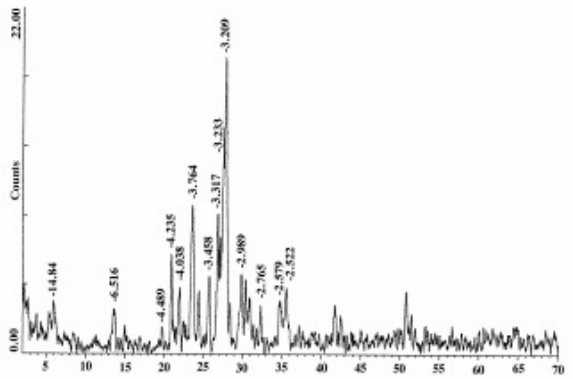

Figure 2. The X-ray diffractograms of the weathered bedrock of P2

Thin section studies revealed that this pedon contain abundant quartz, plagioclase phenocrysts (labradorite), pyroxene, olivine and opaqe minerals. Geochemical analyses showed high amounts of Ca (related to feldspar (labradorite) and mafic minerals) and Mg (is related to mafic minerals) than K and Na in this pedon (Table 3). Alteration of plagioclase to chlorite (Figure 3c,d) and clay minerals as well as pyroxene to amphiboles (Figure 3e, f) was distinc.

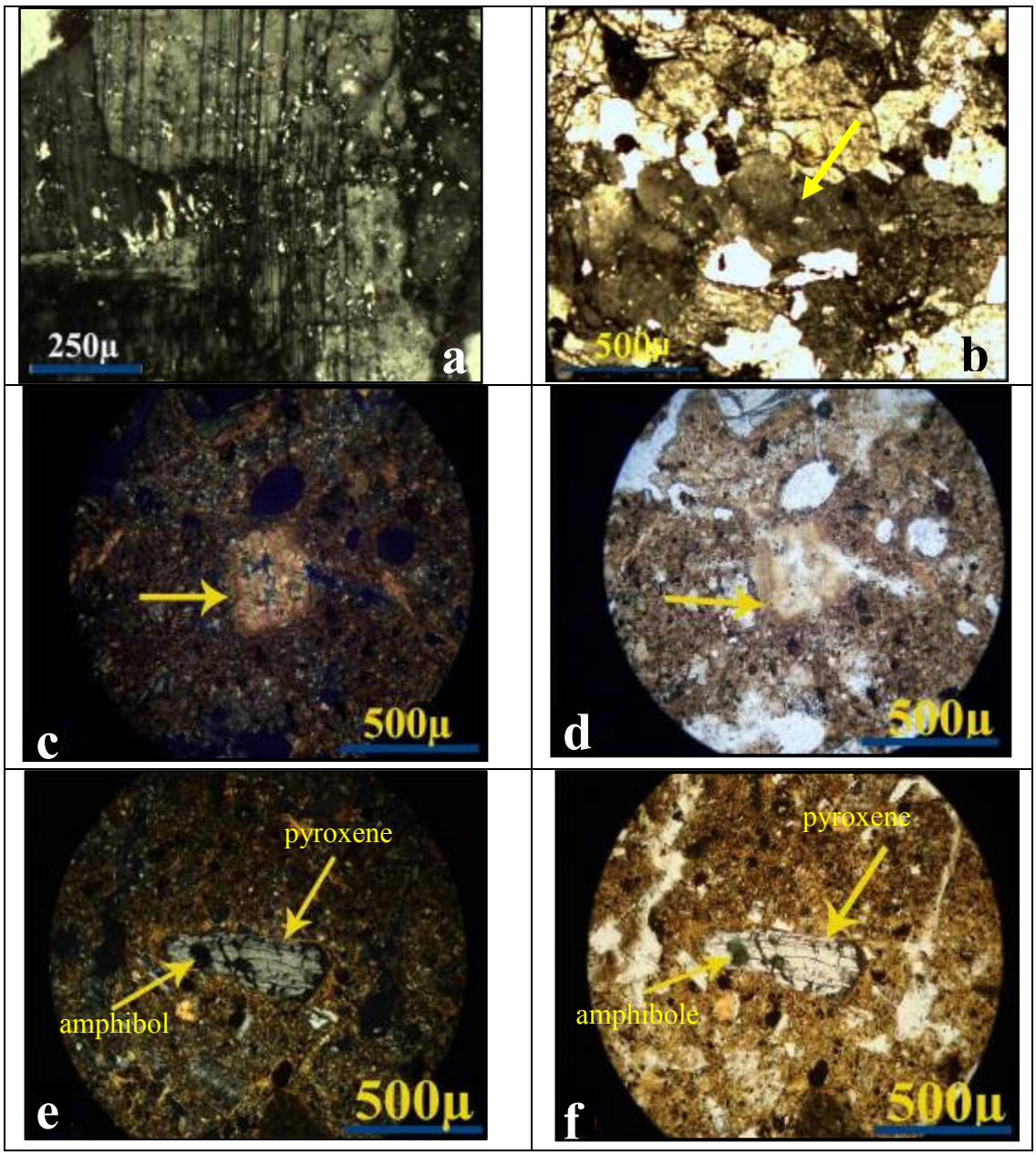

Figure 3: a) Sericitization of plagioclase in Crt horizon from P1- XPL; b) Micrograph of relatively fresh orthoclase in P1-XPL; c) Chlorite pseudomorph after plagioclase in Bt2 horizon from P2- XPL; d) same view in PPL; e) Pyroxene with amphibole as a alteration product in Bt2 horizon from P2- XPL; f) same view in PPL.

Table 3. Total elemental analysis of soil pedons

XRF analyses % / Samples	Na_2O	MgO	K_2O	Cao	Fe_2O_3
Profile 1					
A	2.20	0.75	2.51	0.42	2.11
Crt1	1.35	1.81	2.58	0.7	3.84
Crt2	1.61	0.73	2.13	0.37	2.86
Profile 2					
A	0.93	6.05	1.11	3.03	11.24
Bt1	0.71	5.15	1.03	2.78	12.33
Bt2	0.67	5.95	1.29	3.65	11.63
Bt3	1.03	5.22	1.30	2.44	12.94
Crt1	1.16	8.76	0.65	3.57	8.85
2Crt2	0.67	6.11	1.53	3.37	10.06

It can be concluded that most of the clay minerals in soils from two pedons were originated from the presence of weatherable primary minerals. In the study area, however, morphological properties indicated higher solum thickness for andesitic basalt pedon than granite pedon which is further supported by microscopical study and X-ray data.

References

Bullock P, Fedoroff N, Jongerius A, Stoops G, Turina T (1985) Handbook for soil thin section description. Waine Research Publishing Albrighton, U.K.

Islam MR, Stuart R, Risto A, Vesa P (2002) Mineralogical changes during intense chemical weathering of sedimentary rocks in Bangladesh. *Journal of Asian Earth Sciences* **20,** 889-901.

Jiménez-Espinosa R, Vázquez M, Jiménez-Millán J (2007) Differential weathering of granitic stocks and landscape effects in a Mediterranean climate, Southern Iberian Massif (Spain). *Catena* **70,** 243–252.

Page AL (1982) Methods of Soil Analysis . Part 2: Chemical and Microbiological Methods.ASA, Soil Sci of Am. Madison, Wisconsin. USA.

Ramezanpour H, Hesami R, Farhangi N (2006) Identification of silicate clay in soils derived from granite and limestone in Lahijan area. Proceedings of the 14th Iranian Crystalography and Mineralogy Congress, Birjand univercity, (Iranian society of crystallography and mineralogy).

Ramezanpour H, Zanjanchi MA (2007) Clay mineralogy and geochemistry of the Soils derived from three mafic igneous and metamorphic bedrocks in Lahijan area. *Iranian Journal of Crystalography and Mineralogy* **2,** 383-400.

Abiotic catalysis of the Maillard reaction and polyphenol-Maillard humification pathways by Al, Fe and Mn oxides

Ailsa G. Hardie[A,B], James J. Dynes[B], Leonard M. Kozak[B] and Pan Ming Huang[B†]

[A]Department of Soil Science, Stellenbosch University, Stellenbosch, South Africa, Email aghardie@sun.ac.za
[B]Department of Soil Science, University of Saskatchewan, Saskatoon, SK, Canada
[†]In memoriam

Abstract
The Maillard reaction and integrated polyphenol-Maillard reaction are regarded as important pathways in natural humification. Little is known on the abiotic catalysis of these pathways by poorly crystalline Al and Fe(III) oxides. Therefore, the objective of this study was to compare catalysis of these humification pathways by poorly crystalline Al and Fe oxides and Mn oxide, which has been widely studied. Treatments containing an equimolar amount of glucose and glycine (Maillard reaction) or catechol, glucose and glycine (polyphenol-Maillard reaction) in the presence or absence of metal oxides, were conducted under environmentally relevant conditions, for 15 days under sterile conditions. The humification products were examined using C and Al K-edge, and Al, Fe and Mn L-edge NEXAFS spectroscopy. The redox-reactive Mn and Fe oxides enhanced humification in the Maillard and integrated catechol-Maillard systems to a greater extent than Al oxide. The Mn oxide sequestered substantially more C during humification than the other oxides, and the humic substances formed were more carboxylic in nature. Humification altered the surface chemistry of the oxides, especially the Mn oxide. The findings of this study are of fundamental importance in understanding the role of metal oxides in abiotic humification pathways and C stabilization in soils and sediments.

Key Words
Oxidative polymerization, sesquioxides, birnessite, soft x-ray absorption spectroscopy, organo-mineral complexes

Introduction
In the environment, humification is pivotal in transforming biomolecules originated from organized structures typical of organisms to randomly polymerized, heterogeneous humic substances characteristic of biogeochemical systems. Abundant research evidence at the molecular level shows that mineral colloids, acting as electron acceptors, can enhance the oxidative polymerization and/or polycondensation of biomolecules such as amino acids, sugars, and polyphenols, derived from the breakdown of biological residues and from biological metabolites (Huang and Hardie 2009). The polyphenol pathway and Maillard reaction are regarded as important pathways in natural humification (Huang and Hardie 2009). Furthermore the significance of linking these two pathways into an integrated polyphenol-Maillard pathway has been shown using birnessite (δ-MnO_2) as catalyst (Jokic *et al.* 2004; Hardie *et al.* 2007). Little is known on the abiotic catalysis of the Maillard reaction and especially the integrated polyphenol-Maillard reaction by poorly crystalline Al and Fe(III) oxides, which are common in nature. Sesquioxides, especially poorly crystalline Fe and Al oxides, also play a critical role in long-term carbon stabilization in soils (Kögel-Knabner *et al.* 2008). Therefore, the objective of this study was to investigate the catalysis of the Maillard reaction and integrated polyphenol-Maillard reaction by poorly crystalline Al and Fe(III) oxides, and to investigate the effect of humification reactions on C sequestration and surface chemistry of the oxides. A further aim of the study was to compare the reaction processes and products of the Al- and Fe-oxide-catalyzed Maillard and catechol-Maillard reaction systems with that of previously- investigated, Mn oxide-catalyzed systems.

Methods and Materials
Poorly crystalline Al and Fe(III) oxides were synthesized according to the method described by Huang *et al* (1977). Manganese(IV) oxide (birnessite) was synthesized according to the method described by McKenzie (1971). The BET specific surface areas of the Al, Fe and Mn oxide was 221.1 m^2/g, 164.7 m^2/g and 63 m^2/g, respectively. Treatments containing an equimolar amount (0.05 mol) of glucose and glycine (Maillard reaction) or catechol, glucose and glycine (polyphenol-Maillard reaction) in the presence of 2.5 g metal oxides, and absence (control), were conducted under environmentally relevant conditions, i.e., pH 7.0 and 45° C, for a period of 15 days under sterile conditions. At the end of the reaction period the pH and Eh of the

systems was determined, and then the solution and solid phase were separated using ultracentrifugation. The extent of humification in the supernatant was measured using visible absorbance. The humic acid (HA) fraction from the supernatant and organo-mineral solid residue (SR) were isolated and characterized using C and Al K-edge and Al, Fe and Mn L-edge NEXAFS spectroscopy, on the SGM and PGM beamlines at the Canadian Light Source (CLS), Saskatoon, SK, Canada. The organic C content of the SR was determined using a dry combustion method.

Results

The presence of the redox-reactive Mn and Fe oxides significantly enhanced browning (humification) in all of the reaction systems, most notably in the catechol-Maillard system (Table 1). The presence of Al oxide in the Maillard system actually appeared to decrease visible absorbance compared to the control system (Table 1). This is most likely due to the sorption of humic polymers on the surface of the Al oxide, as indicated by its darkening in colour and the gain in organic C after humification reactions (Table 1). The Mn oxide-catalyzed catechol-Maillard system showed the greatest accumulation of humified organic C in the solid residue (2.41 g) compared to the Al oxide (0.34 g) and Fe oxide (0.45 g) systems (Table 1). The data indicate that much of the humic substances in the Fe oxide remained suspended in the supernatant, whereas, in the Mn oxide system, the supernatant and solid phase contained considerable amounts of humic substances (Table 1). In the Al oxide system most of the humic substances were found sorbed in the solid phase as the visible absorbance of the supernatant was even lower than that of the control system (Table 1). This could be attributed to the availability of dissolved metals for coprecipitation, as well as, the relative affinity of the dissolved metals for organic functional groups of the humic polymers. The Mn oxide-catalyzed systems had the lowest redox status (Table 1) which indicates that more oxidative polymerization took place than in the other systems. The Fe oxide systems had the second lowest redox status, while the control and Al oxide systems were the highest. Even though the visible absorbance was higher at 600 nm in the Fe oxide-catalyzed catechol-Maillard system (Table 1), the redox status and C content of the solid phase indicated that the Mn oxide system was the strongest promoter of humification in the catechol-Maillard system. Thus, the order of reactivity of the oxides in both the Maillard and catechol-Maillard systems was Mn oxide > Fe oxide >> Al oxide. The stronger catalytic ability of the Mn and Fe oxides compared to the Al oxide can be attributed to the higher redox potential of the Mn and Fe oxide reaction systems compared to the Al oxide system which is not subject to redox reactions. The standard electrode potential values of the overall redox reaction of catechol oxidation by Mn(IV) oxide and Fe(III) oxide are +0.509 V and +0.071 V, resp. (Liu and Huang 2001), which also explains the order of catalytic reactivity observed in the metal oxide systems. Furthermore, the lower electronegativity of Mn (1.55) versus Fe (1.83) or Al (1.61) accelerates the formation of semiquinone free radicals from catechol (Liu and Huang 2001).

Table 1. Visible absorbances of the supernatants (400 and 600 nm), redox status (pH + pE) and net organic C (g) gain in the solid residues in Maillard and integrated catechol-Maillard reaction systems with 2.5 g metal oxides.

Treatment	Absorbance			Gain in
	400 nm	600 nm	pH + pE	org. C (g)
Al oxide Maillard	0.15	0.00	11.65	0.12
Al oxide Integrated[a]	6.01	2.10	8.07	0.34
Fe oxide Maillard	8.28	0.85	7.19	0.13
Fe oxide Integrated	86.96	128.43	7.65	0.45
Mn oxide Maillard	32.61	3.00	7.07	0.17
Mn oxide Integrated	100.59	44.21	6.62	2.41
Control Maillard	0.74	0.12	11.44	-
Control Integrated	2.84	0.42	9.05	-

[a]Integrated catechol-Maillard system

The metal oxides substantially influenced the chemical nature of the resultant humic products in the supernatant and solid residues in the Maillard reaction and integrated catechol-Maillard reaction humification pathways. The humic products (supernatant and solid phase) from the catechol-Maillard systems catalyzed by Mn oxide (Figure 1f and h) had a much higher content of aliphatic carboxylic groups (288.6 eV) than those from the control (Figure 1c) and Al and Fe oxide-catalyzed systems (Figure d and e), which were more aromatic in nature. This is largely attributed to the higher redox potential of the Mn oxide system, which implies more aggressive oxidation. The HA from the Fe oxide- and Mn oxide-catalyzed Maillard reaction systems appeared quite similar, as both were strongly aliphatic carboxylic in nature (Figure 1f and h). The solid residues from all the metal oxide-catalyzed Maillard systems were strongly aliphatic

carboxylic in nature (data not shown) in comparison the HA fractions isolated from the supernatants (Figure 1). This is attributable to the chemical partitioning of the humic substances between the solution and solid phases by the preferential coprecipitation of multivalent metals with humic substances possessing aliphatic carboxylic groups (Hardie *et al.* 2007) or to the preferential adsorption of these functional groups on the positively charged surfaces of Al or Fe oxides (Kögel-Knabner *et al.* 2008). The HA in the control system appeared to be relatively strongly aliphatic carboxylic in nature (Figure 1c). However, in contrast to the other systems, there were no metal oxides or dissolved multivalent metals in the control system, and therefore, the chemical partitioning of the humic polymers between the solution and solid phases based on their functional groups would not occur.

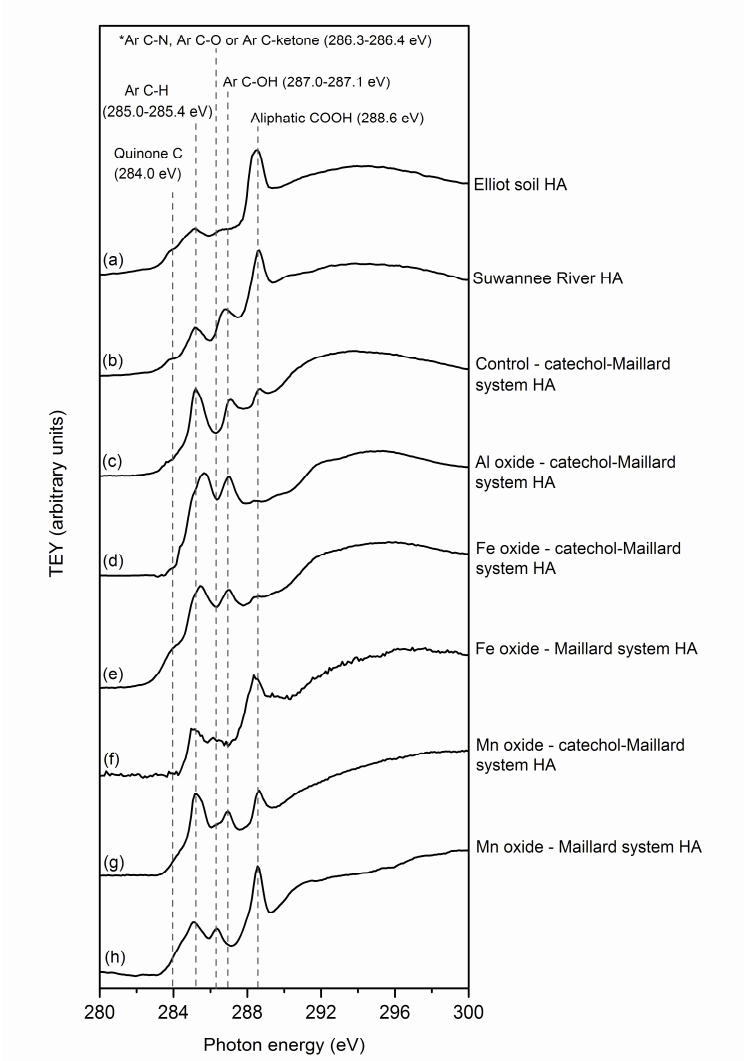

Figure 1. Comparison of the effect of the presence of Al-, Fe- and Mn-oxide on the visible absorbance (400-600 nm) of the supernatant from (a) Maillard reaction and (b) the integrated catechol-Maillard system. The absorbances are scaled by the dilution factor.

The Al K-edge (TEY) (Figure 2) and L-edge (FLY) (not shown) NEXAFS spectra of the Al oxide reacted in the catechol-Maillard system indicated that the residue had a greater content of tetrahedral-Al than the unreacted Al oxide. This indicates the effect of organic humic polymers bound to the Al (either through surface complexation or by co-precipitation with Al from solution) on Al speciation of the solid residues. There was very little change in the nature of the Al oxide reacted in the Maillard system (not shown). The Fe L-edge NEXAFS (TEY and FLY) spectra of the Fe oxides reacted in the Maillard and catechol-Maillard systems (not shown) indicate that the residues from these systems contained more Fe(II) than the unreacted Fe oxide. The Mn oxide-catalyzed Maillard system contained predominantly $MnCO_3$ (rhodochrosite), which was confirmed by XRD (data not shown). This was attributed to the higher pH of the Mn oxide Maillard system (pH 8.0) as a result of the reductive dissolution of birnessite which is favourable for the formation of $MnCO_3$. The Mn oxide-catalyzed catechol-Maillard system contained only Mn(II), mainly as organically-complexed Mn(II) (not shown).

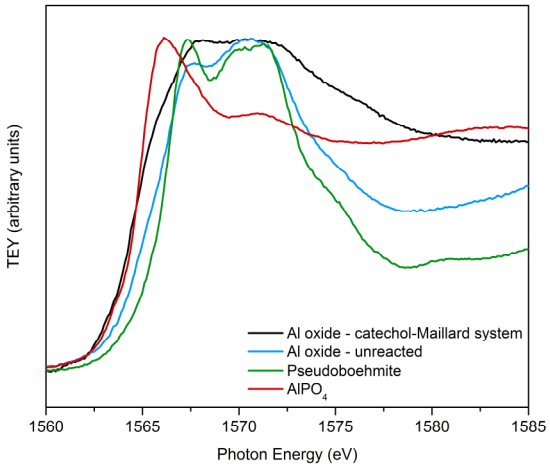

Figure 2. Aluminum K-edge NEXAFS TEY spectra of (blue) the unreacted Al oxide catalyst, (black) the Al oxide after reaction in the integrated catechol-Maillard reaction system, and the reference compounds, (red) $AlPO_4$ (4-coordinated), and (green) pseudoboehmite (6-coordinated).

Conclusions

The results show that the Al, Fe(III) and Mn(IV) oxides catalyzed humification to different extents in the Maillard and catechol-Maillard reaction systems. The Mn oxide was the strongest promoter of browning in the supernatants from the Maillard and catechol-Maillard systems. The greatest enrichment of organic C in the solid phase was found in the Mn oxide-catalyzed catechol-Maillard system (2.41 g), which was about 5 times greater than that of the Fe oxide system (0.45 g) and about 7 times greater than the Al oxide system (0.34 g). The humic products produced in the Mn oxide-catechol-Maillard system were the most aliphatic carboxylic in nature compared to the other metal oxide-catalyzed catechol-Maillard reaction systems, which is largely attributed to the higher redox potential of the Mn oxide system. The humification processes also affected the surfaces of the oxides to different extents. The Al oxide reacted in the catechol-Maillard system had a greater content of tetrahedral-Al after reaction with the biomolecules, indicating the effect of organic humic polymers bound to the Al on the Al coordination. The Fe oxide reacted in the Maillard and catechol-Maillard systems contained more Fe(II) than the unreacted Fe oxide. In contrast, the Mn(IV) oxide was found to be completely reduced to Mn(II) after reaction with the biomolecules. The order of catalytic reactivity of the oxides was as follows: Mn oxide > Fe oxide >> Al oxide. The findings of this study are of fundamental importance in understanding the role of metal oxides in abiotic humification pathways and C stabilization in soils and sediments.

References

Hardie AG, Dynes JJ, Kozak LM, Huang PM (2007) Influence of polyphenols on the integrated polyphenol-Maillard reaction humification pathway as catalyzed by birnessite. *Ann. Environ. Sci.* **1**, 91-110.

Huang PM (2000) Abiotic catalysis. In *'Handbook of soil science'* (Ed. ME Sumner), pp. B302-B332. (CRC Press, Boca Raton).

Huang PM and Hardie AG (2009) Formation mechanisms of humic substances in the environment In: *'Biophysico-chemical processes involving nonliving natural organic matter in the environment. Vol. 2'* (Eds. N Senesi, B Xing and PM Huang). pp. 84-98 (John Wiley & Sons: Hoboken).

Huang PM, Wang TSC, Wang MK, Wu MH, Hsu NW (1977) Retention of phenolic acids on noncrystalline hydroxy-aluminum and -iron compounds and clay minerals of soils. *Soil Sci.* **123**, 213-219.

Jokic A, Wang MC, Liu C, Frenkel AI, Huang PM (2004) Integration of the polyphenol and Maillard reactions into a unified abiotic pathway for humification in nature: The role of δ-MnO_2. *Org. Geochem.* **35**, 747-762.

Kögel-Knabner I, Guggenberger G, Kleber M, Kandeler E, Kalbitz K, Scheu S, Esterhues K, Leinweber P (2008) Organo-mineral associations in temperate soils: Integrating biology, mineralogy, and organic matter chemistry. *J. Plant Nutr. Soil Sci.* **171**, 61-82.

Liu C, Huang PM (2001) The influence of catechol humification on surface properties of metal oxides. In *'Humic substances: Structure, models and functions'* (Eds. EA Ghabbour, G Davies), pp 253-270 (Royal Chemical Society, Cambridge).

McKenzie RM (1971) The synthesis of birnessite, cryptomelane, and some other oxides and hydroxides of manganese. *Mineral Magazine* **38**, 493-502.

Ameliorating acid soil infertility by application of basalt, ground magnesium limestone and gypsum

Shamshuddin Jusop[A] and Che Fauziah Ishak[B]

Department of Land Management, Faculty of Agriculture, Universiti Putra Malaysia, 43400 Serdang, Selangor, Malaysia, [A]Email samsudin@agri.upm.edu.my; [B]Email fauziah@agri.upm.edu.my

Abstract
Ultisols and Oxisols are often acid, having high Al, but are deficient in Ca, Mg, K and P. Studies were conducted to determine the effects of basalt, ground magnesium limestone (GML) and gypsum applications on the soils and crop growth. Results showed that basalt application increased soil pH with concomitant decrease in pHo, which in turn increased cation exchange capacity (CEC). Dissolution of basalt had released Ca, Mg, K and P into the soil making them available for crop consumption. In the soils treated with GML, Ca remained in the zone of incorporation. When GML was applied together with gypsum, Ca moved deeper into the soil profile. SO_4 adsorption onto the surfaces of oxides resulted in an increase in pH and negative charge. The increase in pH was due to the replacement of OH by SO_4.

Key Words
Basalt, ground magnesium limestone, gypsum, maize, Ultisol, Oxisol.

Introduction
Malaysia grows oil palm, rubber and cocoa on Ultisols and Oxisols, which are dominated by kaolinite, gibbsite, goethite and hematite (Shamshuddin and Ismail 1995; Anda *et al.* 2008). The charges on the mineral surfaces change with changing pH. The soils are sometimes used for field crops, but their yields are limited by low pH, high Al and Ca and/or Mg deficiencies (Shamshuddin *et al.* 1991). This paper describes the effects of basalt, GML and gypsum applications on the soils and maize growth.

Material and Methods
Two Ultisols and one Oxisol were used for this study. The ameliorants tested in this study were basalt, GML and gypsum. The soils were treated with these amendments in pot and field experiments for specified periods.

Results and Discussion
Effects of basalt application
Basalt application had increased pH slightly. The increase in pH resulted in reduction of exchangeable Al. The increase in pH resulted in the increase of CEC (by NH_4Cl). The CEC increase may also be due to the lowering of pHo. The dissolution of basalt had released Ca, Mg, K and P into the soil. Hence, exchangeable Ca, Mg and K and available P had increased.

Movement of Ca
Calcium remained in the zone where the lime was originally incorporated. Highly weathered soils of Malaysia are dominated by kaolinite and sesquioxides (Anda *et al.* 2008) and the charge on the exchange complex of these minerals increases with increasing pH. When the GML was applied, pH increased, followed by an increase in CEC. Hence, Ca was held by the negatively-charged surfaces. When GML was applied together with gypsum, some Ca moved deeper into the soil profile, ameliorating the subsoil.

Adsorption of SO_4
SO_4 from the gypsum was adsorbed specifically on the surface of oxides. As a consequence, the pH and negative charge on the oxides increased. However, the resultant increase in pH was only observed in the Oxisol. In the Ultisol, the pH tended to decrease. Obviously, there was another opposing reaction that took place simultaneously as SO_4 adsorption when gypsum was applied. This second reaction was the replacement of Al on the exchange complex by Ca. Al went into the solution and pH was lowered accordingly. Both SO_4 adsorption and Al replacement by Ca occurred in the Oxisol and Ultisol, but the former was more dominant in the Oxisol as the soil contained higher amount of oxides. On the other hand, exchangeable Al was high in the Ultisol and, therefore, Al replacement was more dominant.

Amelioration of acid soil infertility
Our study indicated that Al toxicity can be overcome by GML application at the rate of 2 t/ha or to a limited extent by gypsum application (Shamshuddin *et al.* 1991). It seems that a good agronomic option is to apply GML together with gypsum in the topsoil.

Ca itself is able to detoxify Al. When GML and/or gypsum were applied onto the soils, Ca was made available in large quantities, and consequently reduced Al toxicity. A 10% drop in relative top maize weight corresponds to a Ca/Al concentration ratio of 79. It shows that Ca needs to be considerably high in the soil solution of Ultisols and Oxisols in order to alleviate Al toxicity.

Long-term effect of GML application
The field experiment was started in 1986. It was monitored till 1993. At high rate of GML application, the exchangeable Ca in July 1991 remained reasonably high. After 1991 the exchangeable Ca began to decrease. In the case where 2 t GML/ha were applied, the exchangeable Ca was reduced to the level of the untreated soil. In 1993, at the GML rate of 4 and 8 t/ha, the exchangeable Ca was considered to be within the range suitable for maize growth. This means that the ameliorative effect of GML at the rate 4 t/ha or higher can last up to 8 years. Data on exchangeable Al show consistent results with those of the exchangeable Ca.

Conclusion
Basalt and GML are good soil ameliorants. GML application is only able to alleviate topsoil acidity. In order to alleviate subsoil Ca deficiency of Ultisols and Oxisols GML has to be applied together with gypsum. Gypsum can be used to ameliorate Oxisols having high oxides content, but not to be applied single handedly onto Ultisols having high exchangeable Al. SO_4 adsorption by oxides increased pH and negative charge via replacement of OH by SO_4. Liming at the rate of 4 t/ha or higher is effective for about 8 years.

References
Anda M**,** Shamshuddin J, Fauziah I, Syed Omar, SR (2008) Mineralogy and factors controlling charge development of three Oxisols developed from different parent materials. *Geoderma* **143,** 153-167.

Shamshuddin J, Che Fauziah I, Sharifuddin, HAH (1991) Effects of limestone and gypsum applications to a Malaysian Ultisol on soil solution composition and yield of maize and groundnut. *Plant and Soil* **134,** 45-52.

Shamshuddin J, Ismail, H (1995) Reactions of ground magnesium limestone and gypsum in soils with variable-charge minerals. *Soil Science Society of America Journal* **59,** 106-112.

BET surface area of phosphoric acid treated tropical soils

Amin Eisazadeh[a], Khairul Anuar Kassim [a], Hadi Nur[b]

[a] Geotechnic & Transportation Department, Faculty of Civil Engineering, Universiti Teknologi Malaysia
[b] Ibnu Sina Institute for Fundamental Science Studies, Universiti Teknologi Malaysia, 81310 UTM Skudai, Malaysia
[*] Corresponding author. Tel.: +60177080315; fax: +6075566157. E-mail address: A.Eisazadeh@yahoo.com.

Abstract
The specific surface area is an important property in assessing the physical interaction of clay particles with additives. In this paper, the time-dependent changes induced in surface area of phosphoric acid treated tropical soils comprised mainly of kaolinite mineral were investigated. Comparison between the BET results indicated that the effects of acidic stabilizer on the surface area of soil particles were significant. Furthermore, it was found that the presence of free iron oxides in the form of micro-aggregates on the surface of soil particles contributed to achieving higher surface area values while limiting the attack of phosphoric acid on the clay particles.

Key words
Laterite clay, Kaolin soil, Acid stabilization.

Introduction

The specific surface area is an important characteristic in determining the chemical and physical interaction of the soil with its surroundings. This is due to the fact that most of the chemical reactions in soils take place at the surface of particles (Mitchell and Soga 2005). Furthermore, the surface area developed by soil minerals is related to many other soil properties such as ion exchange capacity, reactivity, and etc. Therefore, the measurement of this property has received much attention during the past decades (Aylmore 1974).

The tendency of all solid surfaces to attract surrounding gas molecules gives rise to a process called gas sorption. Physisorption is the most common type of adsorption. Physisorbed molecules are fairly free to move around the surface of the sample. As more gas molecules are introduced into the system, the adsorbate molecules tend to form a thin layer that covers the entire adsorbent surface. One can estimate the number of molecules (N_m) required to cover the adsorbent surface with a monolayer of adsorbed molecules. Multiplying N_m by the cross sectional area of an adsorbate molecule yields the sample's surface area. One of the most common methods for determining the surface area of finely divided materials is that of Brunauer, Emmett and Teller (Brunauer *et al.* 1938), known as the BET method. The method is based on collecting isotherm data for the physical adsorption of an inert gas and modeling the adsorption data using the BET isotherm equation.

Throughout these years considerable research has been carried out in studying the effect of traditional stabilizers such as lime on various properties of soil (Locat *et al.* 1990; Bell 1996; Narasimha Rao and Rajasekaran 1996). However, the use of phosphoric acid as a stabilizer has been limited.

Materials and experimental programme

Materials

Two soil types formed under extreme weathering conditions were chosen for this study. The first type was the slightly acidic White Kaolin (WK) sample. The soil was dominated by kaolinite and illite minerals along with minor constituents of quartz. Also, a reddish Laterite Clay (LC) rich in iron oxide excavated from a hillside located in Southern part of Malaysian Peninsular was used for this investigation. The physical properties and chemical composition of the untreated samples are presented in Table 1. It should be noted that the phosphoric acid used in this research was a Merck analysed, 85% H_3PO_4, of specific gravity 1.71.

Table 1 The physical properties and chemical composition of the natural soil

Physical properties	values		Chemical composition (oxides)	values (%)	
	Laterite clay	White kaolin		Laterite clay	White kaolin
pH (L/S = 2.5)	4.86	4.34	**SiO_2**	21.55	48.18
External surface area (m^2/g)	57.89	19.87	**Al_2O_3**	24.31	31.10
Liquid Limit, LL (%)	75.8	42.20	**Fe_2O_3**	29.40	1.03
Plastic Limit, PL (%)	39.60	21.30	**MgO**	-	0.86
Plasticity Index, PI (%)	36.20	20.90	**Na_2O**	0.07	-
IS Classification	MH	CL	**CO_2**	3.65	1.34
ICL (%)	5	2	**P_2O_5**	16.71	9.37
Maximum dry density (Mg/m^3)	1.33	1.64	**K_2O**	0.11	4.01
Optimum moisture content (%)	34.00	18.40	**SO_3**	3.98	2.07

Preparation of specimens

According to the previous studies conducted on phosphoric acid stabilization of clayey soils, different amounts of phosphoric acid were selected for each individual soil (Demirel *et al.* 1962; Medina and Guida 1995). Samples were then compacted into a thin wall PVC tubes (50 mm diameter × 100 mm length) under constant compactive effort as specified in clause 4.1.5 of BS 1924: Part2. They were sealed to the atmosphere with rubber tight lids and stored in a room with constant temperature (27±2°C) until being tested at 1 month, 4 months, and 8 months curing period.

Testing programme

The surface area value was obtained by physical adsorption of nitrogen gas using Quantachrome Autosorb-1 surface area analyzer. Hence, approximately 0.15g of the cured sample was deposited into the sample holder. After degassing for 20hr at 300°C, nitrogen gas was injected and the surface area value was calculated using the multipoint BET method.

Results and discussion

As shown in Figure 1, the acid treated White Kaolin samples revealed a sharp reduction in the surface area at the early stages of curing. This was caused by the ion exchange reactions between H^+ ions introduced by the stabilizer and the kaolinite mineral exchange sites which rendered a material with larger particles. Furthermore, the acid treated samples retained their low surface area values for all curing periods. The latter was consistent with the transformation of the natural soil to a completely new material. On the other hand, in Laterite Clay samples, based on the BET results, it was apparent that the presence of iron oxides as part of soil's secondary constituents, contributed to obtaining higher surface area values (Feller *et al.* 1992). Furthermore, the coating action of free iron oxides impeded the attack of acid on clay particles. As can be seen in Figure 2, the free oxides present in the soil environment have bonded the soil particles together, whereas, the neatly arranged book-like kaolinite particles were the predominant feature of the natural White Kaolin soil.

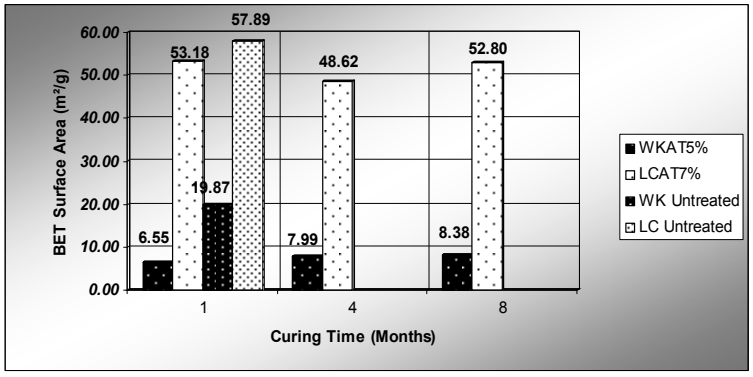

Figure 1 BET results for phosphoric acid treated White Kaolin (WK) and Laterite Clay (LC)

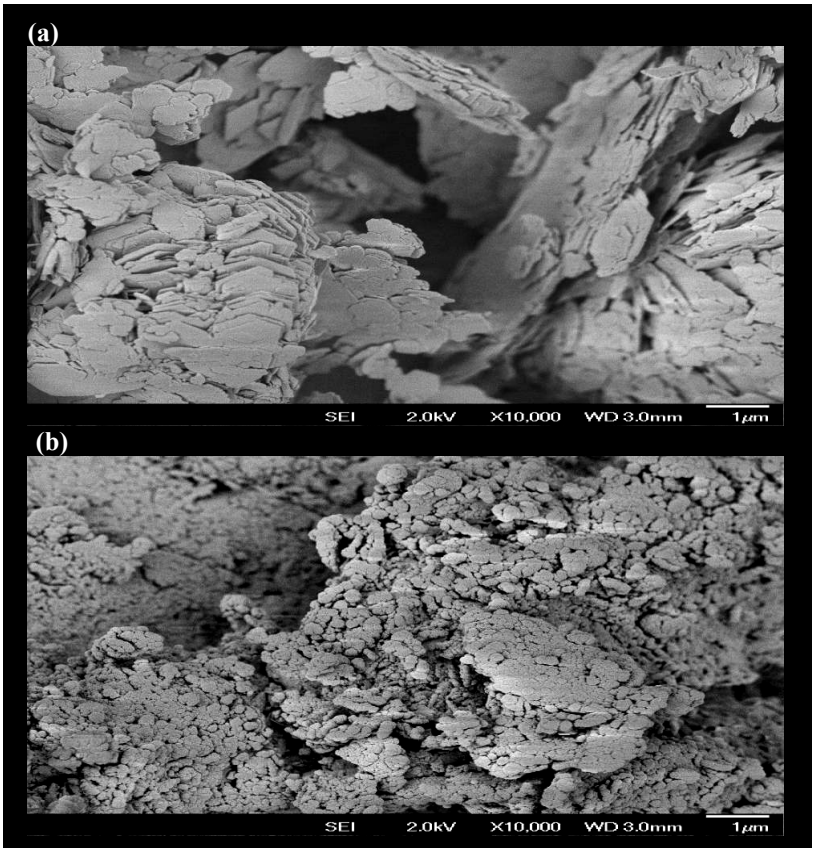

Figure 2 FESEM of untreated (a) White Kaolin and (b) Laterite Clay soil

Conclusions

This research was carried out in an attempt to further elucidate the effects of acidic stabilizers on soil's physical properties. In general, at the early stages of the curing, the substitution of exchangeable ions with H^+ introduced by the stabilizer lowered the surface area values for kaolinitic soils. However, in Laterite Clay samples due to the fact that clay particles were heavily coated and protected by iron oxides, these changes were rather limited. Also, it was found that the presence of free iron oxides in the form of micro-aggregates contributed to achieving higher surface area values.

References

Aylmore LAG (1974) Gas sorption in clay mineral systems. *Clays and Clay Minerals* **22**, 175-183.

Bell FG (1996) Lime stabilization of clay minerals and soils. *Engineering Geology* **42**, 223-237.

British Standards Institution (1990) Stabilized materials for civil engineering purposes: Part 2, Methods of test for cement-stabilized and lime-stabilized materials. London.

Brunauer S, Emmett PH, Teller E (1938) Adsorption of gases in multimolecular layers. *Journal of American Chemical Society* **60**, 309-319.

Demirel T, Benn CH, Davidson DT (1962) Use of Phosphoric Acid in Soil Stabilization. Highway Research Board Bulletin No. 282, 38-58.

Feller C, Schouller E, Thomas F, Rouiller J, Herbillon AJ (1992) N_2-BET Specific Surface Areas of Some Low Activity Clay Soils and their Relationships with Secondary Constituents and Organic Matter Contents. *Soil Science Journal* **153**, 293-299.

Locat J, Berube MA, Choquette M (1990) Laboratory investigations on the lime stabilization of sensitive clays: shear strength development. *Canadian Geotechnical Journal* **27**, 294-304.

Medina J, Guida HN (1995) Stabilization of Lateritic soils with phosphoric acid. *Journal of Geotechnical and Geological Engineering* **13**, 199-216.

Mitchell JK, Soga K (2005) 'Fundamentals of Soil Behavior.' (John Wiley and Sons: New York)

Narasimha Rao S, Rajasekaran G (1996) Reaction products formed in lime-stabilized marine clays. *Journal of Geotechnial Engineering* **122**, 329-336.

Characteristics of soil kaolin on various parent materials in Thailand

W. Wiriyakitnateekul[A], A. Suddhiprakarn[B], I. Kheoruenromne [B], M. Saunders[C] and R.J. Gilkes[C]

[A]Office of Science for Land Development, Land Development Department, Phaholyothin rd., Chatuchak, Bangkok 10900, Thailand
Corresponding author: wwanphen@gmail.com
[B]Department of Soil Science, Faculty of Agriculture, Kasetsart University, Phaholyothin rd., Chatuchak, Bangkok 10900, Thailand
[C]School of Earth and Environment, University of Western Australia, Crawley, Australia 6009

Abstract
The nature of kaolin in Thai soils developed on sandstone, shale/limestone, granite and basalt has been investigated. Mineralogical, chemical and morphological properties of kaolins were determined using X-ray diffraction, transmission electron microscopy, and chemical analysis. Clay concentrates from Thai soils consist of >70% kaolin group minerals with minor amounts of inhibited vermiculite, illite, interstratified clay mineral, gibbsite, quartz and anatase. Soil kaolins exhibit a wide range of crystal sizes, (0.02-0.83 μm, median 0.02 μm) with a variety of morphologies including euhedral platy crystals, laths and tubes. Euhedral hexagonal platy crystals predominate in soils derived from sandstone, lath-shaped crystals in soils derived from basalt and anhedral crystals in soils on shale/limestone.
There are considerable variations in other soil kaolin properties; d(001) ranged from 0.7121-0.7275 nm, coherently scattering domain size (CSD001) 10.3-43.7 nm, Hughes and Brown crystallinity index (HB) 4.1-11.7, specific surface area 34-76 m^2/g and cation exchange capacity 4.2-13.9 cmol/kg. Kaolin in soils on sandstone has the highest value of HB index and largest crystal size, in contrast to kaolin in soils on basalt which has the lowest values of crystallinity index and crystal size. The CEC of soil kaolin (median 9.4 cmol/kg) did not differ systematically between parent materials but was much higher than values for reference mineral kaolin (3.2 cmol/kg). The median value of structural Fe_2O_3 in soil kaolin is 1.84% being highest for soils developed on basalt (median 2.67%) and lowest for soils on shale/limestone (1.39).

Key Words
XRD, TEM, clay mineral, tropical soil

Introduction
Highly weathered soils of the tropics often consist mostly of kaolin group minerals, oxides of Fe, Al and Ti and resistant minerals such as quartz and zircon inherited from the parent material. Chemical properties of these soils reflect this mineralogy as they have low CEC, high zero point of charge, high P sorption and low nutrient reserves (Schwertmann & Herbillon 1992). Kaolin is the most common clay mineral in soils that cover about 47% of the total area in Thailand. Throughout tropical regions plant yield on these soils is highly dependent on fertilization and liming (Yoothong *et al.* 1997). With the growing demand for food, optimum utilization of these common tropical soils will be an important factor in the development of most tropical countries. Consequently the influences of soil mineralogy on agricultural production and land management need to be identified.
Sixty three representative soil samples which developed on sandstone, shale/limestone, granite or basalt, were chosen after screening by XRD for the dominance of kaolin group minerals henceforth the deferrated clay is referred to as '*kaolin*'. These soils are representative of the soils that are extensively used for agriculture in Thailand and elsewhere in the tropics. The sites are nearly flat to undulating with slopes of 2-8%. The soils are classified as belonging to the kaolinitic mineralogical classes of Ultisols, Oxisols and Alfisols.

Methods
Prior to analysis the soil samples were air-dried, crushed using a ceramic mortar and pestle and then passed through a 2 mm stainless steel sieve. The purified soil kaolins were analysed as followings:
1. Mineral composition of the kaolins was determined for random powders and basally oriented clay on ceramic plates using X-ray diffraction with CuKα radiation and a Philips PW3020 diffractometer equipped with a diffracted beam graphite monochromator.
2. Accurate XRD measurement of basal spacings was made using both quartz and octacosane as internal standards (Brindly & Wan 1974).
3. Coherently scattering domain size (CSD) was calculated from the width at half height of the XRD patterns of kaolins via the Scherrer equation (Klug & Alexander 1974).

4. A random powder XRD pattern was used to determine the HB index (Hughes & Brown 1979).
5. The size and shape of kaolin crystals were obtained from electron micrographs using a JEOL 3000F Field Emission Gun TEM.
6. Cation exchange capacity was measured using 0.01M silver thiourea solution at pH 4.7 to displace the exchangeable cations (Rayment & Higginson 1992).
7. Specific surface area was measured using the N_2-BET method (Aylmore *et al.* 1970) with a Micrometrics Gemini III 2375 surface area analyser.

Results and discussion

General soil characteristics

Field soil texture of the soils ranged from sandy loam to clay, some soils contained minor amounts of particles larger than 2 mm. Particle size analysis confirmed the field observations, the soils developed on sandstone and granite generally contained much sand whereas those on shale/limestone and basalt mostly have more than 50% clay. Values of soil pH in water ranged from 3.8 to 7.7 (mean 5.0). Some of the surface soils were near neutral with a pH in water of 6.0-7.7, this may be due to applications of lime that is used in agriculture in these areas.

Mineralogy of the deferrated clay fraction

Kaolin is the major clay mineral (70-90%) present in the deferrated clay fraction of 63 soil samples. Small or trace amounts of inhibited vermiculite, illite, interstratified clay minerals, quartz, gibbsite and anatase occur in most kaolin samples with quartz, gibbsite and/or illite being moderate constituents of 11 samples. Clays from soils developed on basalt contain less inhibited vermiculite and illite compared to soils developed from other parent materials. A relatively high amount of quartz is present for the soils developed on sandstone. Gibbsite is present only in some soils derived from granite, sandstone and shale/limestone which possibly indicating that they are more highly weathered. Anatase is relatively abundant in most of the soils derived from basalt which may be due to the relative abundance of Ti in mafic rocks and it is concentrated considerably during weathering (Anand & Gilkes 1987).

XRD Measurements of soil kaolin

Basal spacing

The 001 spacing (d001) of Thai soil kaolins ranges from 0.7121 to 0.7293 nm (mean 0.7209 nm) which is slightly higher than for standard Georgia kaolin (0.7180 nm). Values of d001 for the soil kaolins developed on basalt (mean 0.7233 nm) were higher than those on granite (0.7208 nm), shale/limestone (0.7204 nm) and sandstone (0.7197 nm), respectively. Linear correlation coefficients (*r*) for relationships between properties of purified soil kaolins are shown in Table 1. There is a highly significant positive linear relationship between 001 spacing of kaolin and structural Fe concentration ($r = 0.50^{***}$) so the higher basal spacing of kaolin may be partly due to isomorphous substitution of Fe affecting unit cell dimensions (Brindley & Brown 1980). However the 001 spacing of these kaolins increases with decreasing crystal size ($r = -0.62^{***}$ for CSD001 and $r = -0.49^{**}$ for CSD060).

Table 1. Linear correlation coefficients (*r*) for relationships between properties of Thai soil kaolins.

Properties		1	2	3	4	5	6
1	d 001	1.00					
2	CSD 001	**-0.62*****					
3	CSD 060	**-0.49*****	**0.47*****				
4	HB	-0.22	**0.43*****	0.22			
5	Structural Fe	**0.50*****	**-0.59*****	**-0.51*****	**-0.27***		
6	CEC	**0.30***	**-0.31***	**-0.38****	**-0.52*****	**0.33***	
7	SSA	**0.40****	**-0.53*****	**-0.52*****	**-0.50*****	**0.46*****	**0.79*****

Number of samples for properties 1-5 (n=63), 6 (n=35), 7 (n=49) which does not include data that would be affected by the presence of moderate amounts of impurities). *** Significant at P = .001, ** P = 0.01 and * P = 0.05
d = d spacing, CSD = crystal size dimension, HB = Hughes & Brown index, CEC = cation exchange capacity, and SSA = specific surface area

Coherently Scattering Domain size (CSD)

Values of the CSD of these kaolins, calculated from 001 and 060 reflections, range from 9.3 to 43.7 nm (mean 17.2 nm) and 10.7 to 25.2 nm (19.1 nm), respectively. The kaolin in soils developed on shale/limestone had the largest CSD001 (mean 20.5 nm) followed by sandstone (18.5 nm), granite (15.6 nm) and basalt (12.6 nm), respectively. CSD for both 001 and 060 reflections decreased with increasing structural Fe (r = -0.59*** for CSD001, and r = -0.51*** for CSD060) (Table 1).

Crystallinity Index

Values of the Hughes and Brown index (HB) for Thai soil kaolins range from 4.1 to 11.7 (mean 6.4). The Thai soil kaolins developed on basalt that has the lowest value of HB index (range 4.7-7.6, mean 5.6) whereas the highest values were for soils on shale/limestone (4.7-11.4, 7.0) followed by sandstone (4.1-11.7, 6.6) and granite (5.4-7.5, 6.3). There is a very weak inverse linear relationship between HB index and Fe content for the kaolins (r = -0.27*) (Table 1).

Transmission electron microscopy investigation of single crystals of soil kaolin

Sizes of platy kaolin crystals expressed as the longest dimension (width), ranged from 0.02-0.84 μm. Some Thai kaolins contain large crystals (>0.4 μm) similar to those in the standard Georgia kaolin (0.4-0.8 μm) but for those soil kaolins, the median size is smaller than 0.2 μm. The largest crystal sizes are for the soil kaolins derived from sandstone (0.023-0.829 μm (median 0.108 μm) followed by those for shale/limestone 0.017-0.835 μm (0.098 μm), granite 0.040-0.364 μm (0.099 μm) and basalt 0.015-0.657 μm (0.106 μm), respectively. Thai kaolins consist mostly of platy crystals (ranging from euhedral and anhedral), some are lath-shaped and there are rare tubular crystals as shown in Figure 1.

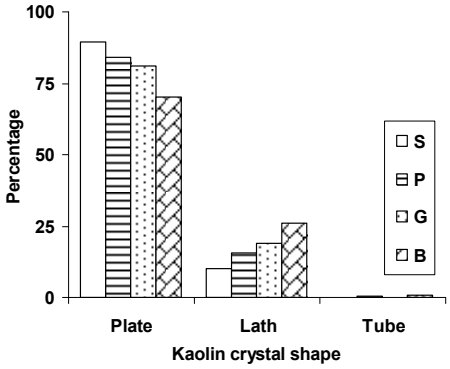

Figure 1. Median values of crystal shape measured from electron micrographs for kaolin in soils on various parent materials. (S = sandstone, P = shale/limestone, G = granite, B = basalt).

Specific Surface Area (SSA)

Values of SSA for the soil kaolins range from 34 to 76 m^2/g (median 50 m^2/g) which are similar to values for kaolins from Western Australian soils (44-56 m^2/g) (Singh & Gilkes 1992) and Indonesian red soils (59-88 m^2/g) (Siradz 2000). The Thai soil kaolins developed on basalt had a high SSA (47-76 m^2/g, mean 62 m^2/g) compared to those for the soils developed on shale/limestone (34-66 m^2/g, 48 m^2/g), granite (39-55 m^2/g, 47 m^2/g), and sandstone (4-60 m^2/g, 45 m^2/g), respectively.

Cation Exchange Capacity (CEC)

CEC of these kaolins ranges from 4.2 to 17.4 cmol/kg (mean 9.2 cmol/kg) whereas the Thai soil kaolins developed on basalt had the highest values of CEC (5.9-17.4 cmol/kg, mean 10.5 cmol/kg) followed by those on sandstone (4.2-12.4 cmol/kg, 9.3 cmol/kg), shale/limestone (4.4-14.3 cmol/kg, 8.9 cmol/kg) and granite (4.9-11.0 cmol/kg, 8.2 cmol/kg), respectively. The CEC of the Thai kaolins had a wider range of values compared to those for Western Australian soils (2.9-8.2 cmol/kg) (Singh & Gilkes 1992) and Indonesian red soils (5.2-12.9 cmol/kg) (Siradz 2000). There is a strong positive linear relationship between CEC and surface area for these Thai soil kaolins (R^2 = +0.62) as shown in Figure 2.

Conclusion

Kaolin group of clay mineral dominated in the deferrated clay fractions with minor amounts of inhibited vermiculite, illite, interstratified clay mineral, quartz, gibbsite and anatase, only those developed on basalt contained less inhibited vermiculite and illite whereas quartz is present highly in the soils on sandstone.

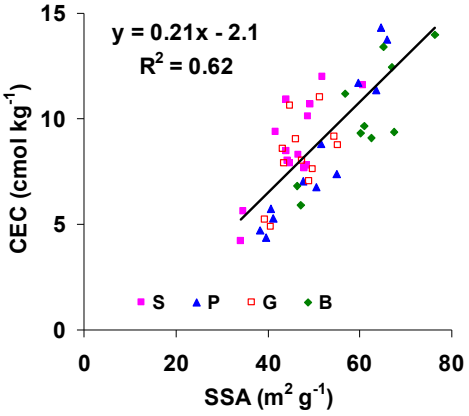

Figure 2. Relationships between CEC and SSA for Thai soil kaolins of soils developed on various parent materials (n=49). (S = Sandstone, P = Shale/limestone, G = Granite, B = Basalt).

Anatase is relatively abundant in most of the samples particularly in those derived from basalt. The larger crystal sizes for soil kaolins, the larger of crystal order exists especially for the soil kaolin of soils developed on sandstone. In contrast to the soil kaolins derived from basalt which have small crystal size, low crystallinity, high SSA, CEC and structural Fe concentration, this may be because of Fe substitution for Al in kaolin crystal. Higher Fe content, higher variation for kaolin properties can be observed for Thai soil kaolins. Electron micrographs show that these Thai soil kaolins consist of a wide variation of crystal sizes and shapes. High content of platy kaolin crystals are mostly found in kaolins of soils developed on sandstone, inversely to lath-shape crystals in those on basalt. Lath-shaped crystal mostly found for the soil kaolins derived from basalt.

Acknowledgment
We gratefully acknowledge support by the Royal Golden Jubilee PhD programme under the Thailand Research Fund for financial support. The TEM analysis was carried out at the Centre for Microscopy and Microanalysis at the University of Western Australia, Crawley, Australia.

References

Anand RR, Gilkes RJ (1987) Variations in the properties of iron oxides within individual specimens of lateritic duricrust. *Australian Journal of Soil Research* **25**, 287-302.

Aylmore LAG, Sills ID, Quirk JP (1970) Surface area of homoionic illite and montmorillonite clay minerals as measured by the sorption of nitrogen and carbon dioxide. *Clays & Clay Minerals* **18**, 91-96.

Brindley GW, Wan HM (1974) Use of long spacing alcohols and alkanes for calibration of long spacings from layer silicates, particularly clay minerals. *Clays & Clay Minerals* **22**, 313-317.

Hart RD, Wiriyakitnateekul W, Gilkes RJ (2003) Properties of soil kaolins from Thailand. *Clay Minerals* **38**, 71-94.

Hughes JC, Brown G (1979) A crystallinity index for soil kaolins and its relation to parent rock, climate and maturity. *Journal of Soil Science* **30**, 557-563.

Klug HP, Alaxander LE (1974) X-ray diffraction Procedures for Polycrystalline and Amorphous Materials, 2nd ed. John Wiley & Sons Inc. New York.

Rayment GE, Higginson ER (1992) Australian Laboratory Handbook of Soil and Water Chemical Methods. Australian Soil and Land Survey Handbook. Inkata, Melbourne.

Schwertmann U, Herbillon AJ (1992) Some aspects of fertility associated with the mineralogy of highly weathered tropical soils. In 'Myths and Science of Soils of the Tropics' (Eds. R Lal, PA Sanchez), pp. 47-60. (Soil Science Society American Special Publication No. 29).

Singh B, Gilkes RJ (1992) Properties of soil kaolins from south-western Australia. *Journal of Soil Science* **43**, 645-667.

Siradz, SA (2000) Mineralogy and chemistry of red soils of Indonesia. Ph.D. Thesis, University of Western Australia, Soil Science and Plant Nutrition, Faculty of Agriculture, WA.

Yoothong K, Moncharoen L, Vijarnsorn P, Eswaran H (1997) Clay mineralogy of Thai soils. *Applied Clay Science* **11**, 357-371.

Charcoal (biochar) as a carbon sequestration approach and its effect on soil's functions

Siva (Sivalingam) Sivakumaran[a], Samuel Dunlop[a, d], Stephanie Caille[b], Markus Deurer[a], Robert Simpson[c], Ian McIvor[a], Paramsothy Jeyakumar[d], Steve Green[a], Tessa Mills[a], Iris Vogeler and Brent Clothier[a].

[a] Sustainable Production: Soil, Water & Environment and Systems Modelling & Biometrics, The New Zealand Institute for Plant & Food Research Limited (Plant & Food Research), Palmerston North, 4442, New Zealand. siva.sivakumaran@plantandfood.co.nz
[b]Institut Polytechnique LaSalle Beauvais, Rue Pierre Waguet - BP 30313 - 60026 Beauvais Cedex, France.
[c] Sustainable Production - Environmental & Social Impacts, The New Zealand Institute for Plant & Food Research Limited (Plant & Food Research), Palmerston North, 4442, New Zealand.
[d]Soil and Earth Sciences, Institute of Natural Resources, Massey University, Palmerston North, 4442, New Zealand
[e]AgResearch, Grasslands, Palmerston North, 4442, New Zealand.

Abstract
We compared the microbial biomass, basal respiration, dehydrogenase activity, mineral-N (nitrogen) and hot-water extractable carbon (HWC) of the soil with and without charcoal as a biological and a chemical property. Using quantitative polymerase chain reaction (qPCR) we tested for the presence of microbial groups and genes associated with methane metabolism as indicators of any change in microbial diversity resulting from the addition of charcoal. As a soil physical property we analysed if the addition of charcoal increased soil water repellency.

Our preliminary analysis showed that the addition of charcoal resulted in no significant change to microbial biomass, basal respiration or HWC. The qPCR analysis showed that there was also no significant change to biodiversity. The soil in the orchard prior to the addition of charcoal was not hydrophobic; after the addition of charcoal this did not change.

Key Words
Basal respiration, microbial biomass, hot water carbon, qPCR, carbon sequestration.

Introduction
Biochar is a term reserved for the plant biomass derived materials contained within the black carbon. This definition includes chars and charcoal, and excludes fossil fuel products or geogenic carbon (Lehmann *et al*. 2006). Work on terra preta de índio (TP) soil, the fertile Amazonian Dark Earths, has served as a major inspiration for the use of biochar as a promising soil additive promoting crop growth and carbon storage (Glaser *et al*. 2002; Glaser and Woods 2004; Lehmann *et al*. 2006; Glaser 2007).The sequestering of carbon through the addition of charcoal to agricultural and horticultural soils is a strategy that has recently gained interest as a way to mitigate climate change. To assess the practical feasibility of this strategy the impact of the addition of charcoal on soil biophysical properties needs to be understood. As yet, only limited field trials have been conducted to investigate this. The objective of this study is to measure the effects of the addition of charcoal to soil in an integrated research apple orchard in Havelock North (Figure 1a), on a number of biophysical soil properties. The apple trees in the integrated orchard system were 12 yr old. The apple variety was Pacific Rose, and the rootstock variety was 'MM.106'. The tree spacing was 3.4 m within the rows and 4.5 m between the rows. A 0.5-m wide strip under the trees was kept bare by regular herbicide applications. The apple trees were drip-irrigated during the vegetative period. The irrigation, nutrient, and pest management followed the guidelines of integrated fruit production (Wiltshire 2003).

Methods
Charcoal was added at a rate of 2 kg/m^2 (20 t/ha), and mixed with the top 0.1 m of the soil (Figure 1b). This served as the soil-plus-charcoal treatment. The charcoal was added to three sampling sites within a single tree row. Three separate sampling sites in the same tree row, but without the addition of charcoal served as the control. The 6 sites had the same soil type and climate, and had received the same orchard management.

Figure 1a. Left. Havelock North integrated apple orchard. Figure 1b. Right. Mixing charcoal into the soil

We compared the microbial biomass according to the method of Höper (2006). Microbial respiration was determined by using basal respiration (Őhlinger *et al*. 1996), Dehydrogenase activity (Chandler and Brooks 1991) and microbial biodiversity of the soil with and without charcoal as biological soil properties.

Detecting microorganisms by polymerase chain reaction (PCR) amplification of Deoxyribonucleic acid (DNA) extracted from environmental samples has an advantage over culture techniques which requires recovery and growth of active organisms (Johnston and Aust 1994; Sivakumaran *et al*. 1997). DNA was purified from three samples of each soil type using PowerSoil DNA kit (MoBio Laboratories, Carlsbad, Ca, USA) following the maker's instructions. Microbial biodiversity was analysed using quantitative polymerase chain reaction (qPCR). Sixteen microlitre qPCR reactions were performed in triplicate on two separate plates on a LightCycler 480 (Roche Applied Science, Indianapolis, IN, USA) using 25 ng of DNA, 0.5 μM primers with LightCycler® 480 SYBR Green I Master (Roche Applied Science, Indianapolis, IN, USA). Cycling conditions included an initial hot start at 95 °C for 5 min, followed by 40 cycles of 95 °C for 10 s, 53 °C for 10 s and 72 °C for 30 s. Each qRT–PCR was ended by the addition of a dissociation curve analysis of the amplified product. This involved denaturation at 95 °C for 5 s, cooling to 65 °C for 1 minute and then gradual heating at 0.21 °C/s to a final temperature of 97 °C. Raw crossing points were converted to quantities representing relative expression levels using a modified comparative method (Pfaffl 2001) and with correction for different amplification efficiencies (Ramakers *et al*. 2003). Primers used in qPCR of 16S rRNA in Eubacteria, and sulfate-reducing bacterial groups Desulfovibrionaceae, Desulfobacteraceae and Desulfobulbus were 9/27f, 519f, 519r, 907r, DSVIB679r, DSBA355f and DSBb279f from Stubner (2004); primers for urease gene wereURE1F and URE2R from Koper *et al*. (2004); primers for type I and II methanogtroph 16S rRNA were taken from Chen *et al*. (2007) and for methane oxidases from Holmes *et al*. (1995). We tested for the presence of microbial groups and genes associated with methane metabolism.

Hot water extractable carbon (HWC) (Ghani *et al*. 2003) and mineral-N (nitrogen) content (Keeney and Nelson 1982) were compared as chemical soil properties.

As a soil physical property we analysed if the addition of charcoal caused the soil to become hydrophobic. (Roy and McGill 2002).

Data was analysed using 95% confidence intervals.

Results
Biological properties

Addition of charcoal had no significant impact on basal respiration or microbial biomass (Figure 2a & b).

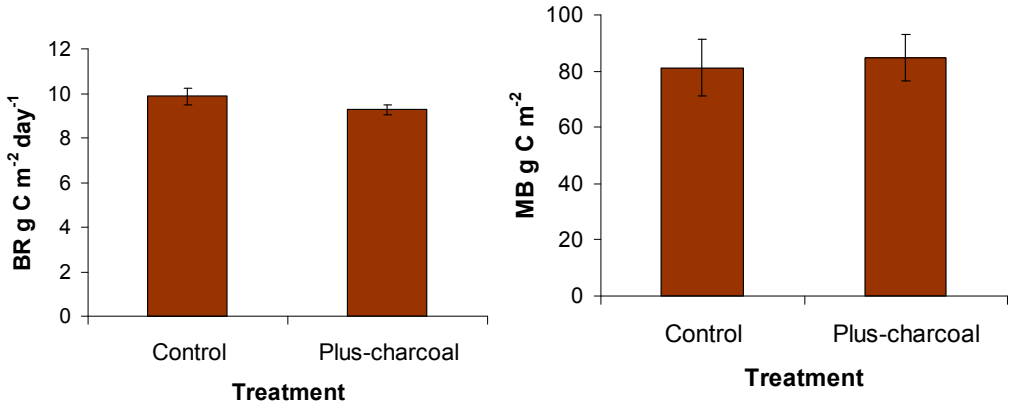

Figure 2a. Left. Basal respiration measured in soil with and without the addition of charcoal. (Error bars are mean ± s.e., n = 9). Figure 2b. Right. Microbial biomass measured in soil with and with out the addition of charcoal. (Error bars are mean ± s.e., n = 9).

Following experimentation we found that dehydrogenase activity cannot be reliably quantified in soil if charcoal amendments have been added, since the charcoal interferes with the absorbance readings.

There was no significant change in population size of methanogens, methanotrophs, ammonia-oxidising bacteria, eubacteria, fungi, archaea, α-proteobacteria and β-proteobacteria resulting from the addition of charcoal to the soil.

Chemical properties

The hot water extractable carbon (HWC) content was significantly lower in the soil-plus-charcoal than in the control (Figure 3a).

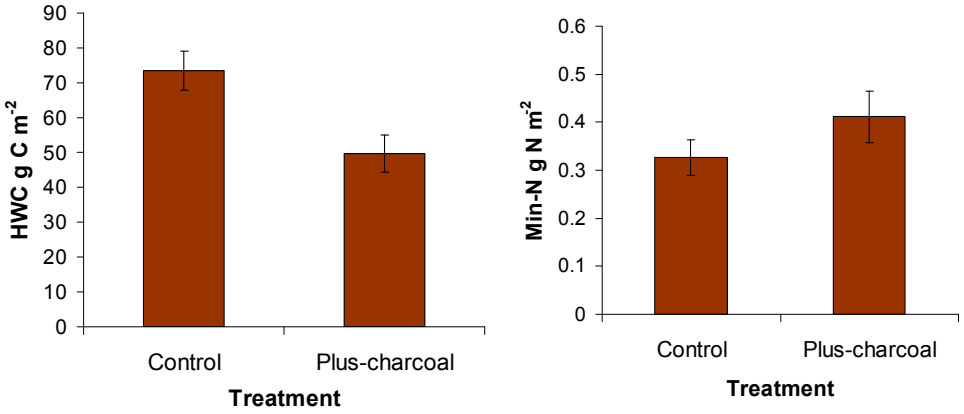

Figure 3a. Left. Hot water extractable carbon (HWC) content of soil with and with out the addition of charcoal (Error bars are mean ± s.e., n = 9). Figure 3b Right. Mineral-N (nitrogen) content of soil with and without the addition of charcoal. (Error bars are mean ± s.e., n = 6).

The addition of charcoal led to no significant change in mineral-N content (Figure 3b).

Physical properties

The soil in the orchard prior to the addition of charcoal was not hydrophobic; after the addition of charcoal this did not change. When testing for hydrophobicity it was noted that pure charcoal was slightly water repellent.

Conclusion

Most of the measured properties of the orchard soil were not significantly affected by the addition of charcoal during the five months of this trial. However, the difference in HWC content could be an early indicator of changes that may become more significant over a longer period of time. Comparing the N-

mineralisation rates of the two treatments would further indicate if changes are occurring. To properly assess what effect the addition of charcoal has on a soil's biophysical functions further trials and analysis are required.

Acknowledgements
Plant & Food Research: The Excellence Programme/summer studentship programme.

References

Chandler K, Brooks PC (1991) Is the dehydrogenase assay invalid as a method to estimate microbial activity in copper contaminated soils? *Soil Bio. Biochem.* **23** (10), 909–915.

Chen Y, Dumont MG, Cebron A, Murrell JC (2007) Identification of active methanotrophs in a landfill cover soil through detection of expression of 16S rRNA and functional genes. *Environ. Microbiol.* **9,** 2855-2869.

Ghani A, M Dexter, Perrot KW (2003) Hot-water extractable C in soils: A sensitive measurement for determining impacts of fertilisation, grazing and cultivation. *Soil Biol. Biochem*. **35**, 1231–1243.

Glaser B, Woods W (2004) Towards an understanding of amazon dark earths. In 'Amazon dark earths: explorations in space and time' (Eds B Glaser, W Woods) pp. 1–8. (Springer, Berlin)

Glaser B, Lehmann J, Zech W (2002) Ameliorating physical and chemical properties of highly weathered soils in the tropics with charcoal – a review. *Biol. Fert. Soils* **35,** 219–230.

Glaser B (2007) Prehistorically modified soils of central Amazonia: a model for sustainable agriculture in the twenty-first century. *Phil. Trans. R. Soc. B*. **362,** 187–196.

Holmes AJ, Costello A, Lidstrom ME, Murrell JC (1995) Evidence that particulate methane monooxygenase and ammonia monooxygenase may be evolutionarily related. *FEMS Microbiol. Lett*. **132**, 203-208.

Höper H (2006) Substrate-induced respiration. In 'Microbiological methods for assessing soil quality'. (Eds J Bloem *et al.)* pp. 84–92. (CAB International, Wallingford, UK).

Johnston CG, Aust SD (1994) Detection of *Phanerochaete chrysosporium* in soil by PCR and restriction enzyme analysis. *Appl. Environ. Microbiol*. **60,** 2350-2354.

Keeney DR, Nelson DW (1982) Nitrogen - Inorganic Forms. In 'Methods of Soil Analysis, Part 2. Chemical and Microbiological Properties', 2nd Edition (Eds Page AL, Miller RH, Keeney DR) pp. 643-709. (American Society of Agronomy, Inc. and Soil Science Society of America, Inc. Pubs., USA).

Koper TE, El-Skeikh AF, Norton JM, Klotz MG (2004) Urease-encoding genes in ammonia-oxidizing bacteria. *Appl. Environ. Microbiol.* **70,** 2342-2348.

Lehmann J, Gaunt J, Rondon M. (2006) Biochar sequestration in terrestrial ecosystems – a review. *Mitig. Adapt. Strat. Global Change* **11,** 403–427.

Őhlinger R, Beck T, Heilmann B, Beese F (1996) Soil respiration. In 'Methods in Soil Biology'. (Eds F Schinner *et al.)* pp. 93-110. (Springer-Verlag, Berlin).

Pfaffl MW (2001) A new mathematical model for relative quantification in real-time RT–PCR. *Nucleic Acids Res.* **29,** 2002–2007.

Ramakers C, Ruijter JM, Lekanne Deprez RH, Moorman AFM (2003) Assumption-free analysis of quantitative realtime polymerase chain reaction (PCR) data. *Neurosci Lett* **339,** 62–66.

Roy JL, McGill WB (2002) Assessing soil water repellency using the molarity of ethanol droplet (MED) test. *Soil Sci.* **167,** 83-97.

Sivakumaran S, Lockhart PJ, Jarvis BDW (1997) Identification of soil bacteria expressing a symbiotic plasmid from *Rhizobium leguminosarum* biovar *trifolii*. *Canadian Journal of Microbiology* **43,** 164-177.

Stubner S (2004) Quantification of Gram-negative sulphate-reducing bacteria in rice field soil by 16S rRNA gene-targeted real-time PCR. *J. Microbiol. Meth.* **57,** 219-2230.

Wiltshire JW (2003) Integrated fruit production in the New Zealand pipfruit industry. Primary Industry Council/Kellogg Rural Leadership Programme, Lincoln University, Christchurch, New Zealand.

Charge properties and potassium fixation by clay from Thai Vertisols

Natthapol Chittamart[A], Anchalee Suddhiprakarn[A,*], Irb Kheoruenromne[A], Robert J. Gilkes[B]

[A] Department of Soil Science, Faculty of Agriculture, Kasetsart University, Bangkok 10900, Thailand.
[B] School of Earth and Environment, University of Western Australia, 35 Stirling Highway, Crawley, WA 6009, Australia.
*Corresponding author. Email agrals@ku.ac.th

Abstract
Potassium fixation by soil clays dominated by smectite was examined in order to relate clay mineralogy and charge properties (total CEC and tetrahedral CEC) of clays from Thai Vertisols to K fixation capacity. Clays from representative Thai Vertisols were analysed for mineralogical properties including total CEC, tetrahedral CEC, and K fixation capacity by wet and dry procedures. The results show that beidellite is the dominant smectite species and has high total CEC. Tetrahedral CEC is poorly related to total CEC. Poor statistical relationships between both CEC values and K fixation are observed and reflect the uniformity of the soil clay mineralogy. Kaolinite, illite and vermiculite are associated clay minerals in the clay fraction. Vermiculite contributes to the K fixation by upland soil clays. K fixation by beidellite in Thai Vertiosols is small with most K remaining exchangeable with NH_4^+, a little K being fixed. Potassium fixation by dry-wet cycles was more in soil clays from upland Vertisols than lowland Vertisols reflecting the presence of vermiculite.

Key Words
Charge properties, potassium fixation, Thai Vertisols

Introduction
Fixation and release of K by 2:1 layer silicates are very important processes influencing the availability of K to plants. Stage of weathering, types, and amounts of primary and secondary K-bearing minerals have been suggested as important factors affecting K equilibrium in soil. The magnitude of K-release and fixation appears to be directly related to the clay mineralogy. Illite is the source of K-released (Dowdy and Hutcheson 1963). Smectite in most Vertisols is Fe-rich, tetrahedally high-charge beidellite. Beidellite and vermiculite are known to have more capacity to fix K than other clay minerals. Total charge and the distribution of the charge between the tetrahedral and octahedral sheets are also important properties that contribute to K fixation by 2:1 layer silicates. Vertisols are the important soils in Thailand being used for various field crops and they receive large K fertilizer applications. This study aimed at (i) determining charge properties of clays obtained from representative Thai Vertisols (ii) determining the effects of amount of added K and wetting-drying cycles on K fixation by soil clays and (iii) relating charge properties of soil clays to K-fixation by these soils.

Methods
The clay fraction (< 2 μm) which is dominated by smectite (> 60%) were extracted from representative Thai Vertisols which were categorized into lowland (Ban Mi (Bm1, Bm2), Wattana (Wa), Lop Buri (Lb1, Lb2), Chong Khae (Ck)) and upland ((Buri Ram (Br), Chai Badan (Cd1, Cd2), Wang Chomphu (Wc1, Wc2), Lop Buri (Lb3), Samo Thod (Sat1, Sat2)). Kaolinite, illite, and vermiculite are associated with smectite in these soils. The Greene-Kelly test was employed to identify the location of charge and species of smectite, which is beidellite (Chittamart *et al.* 2010). The chemical composition of the Ca-saturated clay fraction was determined by X-ray fluorescence (XRF) and used for calculation of structural formulae. Total CEC of Na-saturated clay was measured by the silver thiourea method (Rayment and Higginson 1992). Tetrahedral CEC was measured by the silver thiourea method after saturating the clay with 3 M LiCl and heating at 300°C overnight in order to neutralize octahedral charge (Lim and Jackson 1986). Potassium fixation was determined for soil clay following the method proposed by Bouabid *et al.* (1991). Four milliliters of KCl solutions containing three levels of K (K1 = 3.32 mg, K2 = 9.96 mg, K3 = 19.92 mg) were added to 500 mg of Na-saturated clay. The suspensions were shaken for 16 h at room temperature and exchangeable K was extracted three times with 10 ml of 1 M NH_4OAc at pH 7.0. The amount of K not displaced by NH_4 was assumed to be fixed. To study the effects of wetting and drying in the presence of K, 250 mg Na-saturated clay were incubated three times with 20 ml of 1 M KCl solution and subjected to wetting in 20 ml of DI water and drying at 60 °C. Twenty five wetting and drying cycles were performed. After reaction, samples were washed several times with distilled water until chloride free, and then saturated with Ca^{2+} in 0.5 M $CaCl_2$ solution. Oriented specimens were prepared, treated with glycerol and then analyzed by XRD.

Results

Clay Mineralogy

Clay fractions of these soils are dominated by smectite as indicated by the expansion after Mg-saturation and glycerol treatment. Kaolinite is present in small amounts in all clay fractions. Vermiculite occurs in small amounts (< 5-20 %) in the clay fraction of upland Vertisols which developed on residuum of andesite and basalt (Chai Badan (Cd2), Samo Thod (Sat1, Sat2)). Quartz occurs in all clay fractions and is dominant in the silt fraction of these soils. Results of the Greene-Kelly test indicate that all smectite behaved as beidellite indicated with re-expansion after Li-saturation, heating at 300 °C and glycerol solvation. The Greene-Kelly test also indicates that charge originates mainly in the tetrahedral sheet.

Chemical composition

The chemical composition of clay was corrected for relative percentages of mineral impurities determined by XRD and the structural formula of smectite was calculated. These data show that the beidellite has a quite constant chemical composition. Calcium, Na and K are allocated as exchangeable cations in calculated structural formulas (Laird 1994). Plot of major elements from tetrahedral and octahedral sheets $[Al^{VI}/(Al^{VI}+Fe^{VI}]$ versus $[Al^{IV}/(Al^{IV}+Mg^{VI}])$ (Figure 1.1) shows that all the samples have an iron rich beidellite composition. The structural formulas show that negative charges mostly originated in the tetrahedral sheet and thus confirm the result of the Greene-Kelly test. Beidellite in these Thai Vertisols has a high Fe content and low Mg content in the octahedral sheet. Therefore, the oxidation state of iron in the beidellite structure will affect fixation and release of interlayer K^+ and NH_4^+ (Barshad and Kishk 1970). This mechanism may be important for lowland Thai Vertisols which are used for paddy rice cultivation. Long waterlogging during rice cultivation practices may induce structural Fe reduction and the change in layer charge may increase K fixation capacity of these soils (Khaled and Stucki 1991).

Charge properties and K fixation

The total CEC refers to the total charge originating from interlayer, edge, and surface charged sites. The CEC values of these clay fractions are mostly very high (44.6-106.6 cmol/kg) reflecting high smectite content. Tetrahedral CEC values ranges from 14-50 cmol/kg based on the CEC of Li-treated and heated clays. The relationship between total CEC and tetrahedral CEC (R^2=0.24) (Figure 1.2) is poor as the clays have a quite uniform composition. The variation of CEC values of these clay fractions partly reflects the presence of associated minerals. High proportions of kaolinite and illite which have lower CEC than smectite reduce CEC values (both total CEC and tetrahedral CEC) of clay samples. However the tetrahedral CEC tends to increase with increasing total CEC indicating that charge is mostly located in the tetrahedral layer of smectite structure that can be confirmed by Greene-Kelly test. In fact, ideal beidellite with tetrahedral charge > 50% is rarely found in soils. The determination of charge by CEC determination contributes error to the identification soil smectite species because of the effect of impurities. The combination of the Greene-Kelly test, layer charge measurement, CEC measurement and chemical analysis is recommended for detailed identification of soil smectite.

There is no relationship between K-fixed and total CEC or tetrahedral CEC because K was almost completely exchanged by NH_4^+ (Figure 1.3). Potassium fixation capacity by clays is quite different for lowland and upland Vertisols. Clays from lowland Vertisols shows the amount of K fixed increased with increasing of quantity of K added (K1< K2< K3). Similar results were found by Bouabid *et al.* (1991) using clay minerals from soils of Morocco in which smectitic soil clays and vermuculitic soil clays fixed much more K than soil clays with mixed mineralogy and clays from Thai Vertisols. Lowland Vertisols have average fixed-K values of 1.69, 2.60, and 4.05 cmol K/kg for K1, K2, and K3 levels of added K respectively (Figure 1.4). For upland Vertisols, clays have average fixed-K values of 1.64, 4.52, and 3.39 cmol K/kg for K1, K2, and K3 treatments respectively. The differences in amount and K fixation capacity between lowland and upland Vertisols reflect the differences in mineral assemblage. Most sorbed K could be exchanged by NH^{4+} indicating that the smectites do not extensively fix K.

In nature, the presence of highly hydrated cations like Ca, Mg competes and would further reduce fixation of K in these soils. Clays from upland Vertisols have higher fixed-K values than clays from lowland Vertisols, reflecting the presence of vermiculite especially in Sat1, Sat2, Cd2 and Wc2 soils along with the soils developed under drier condition (Figure 1.5).

The effect of wetting and drying cycles on K-fixation as indicated by XRD shows that for lowland soil smectite reflections do not collapse to 10 Å (Figure 1.6) after wash with $CaCl_2$ solution indicating that K was exchanged by Ca and not fixed. This behavior indicates that beidellite in these soils does not fix K. In contrast, beidellite in upland soil clays associated with vermiculite shows 10 Å peak after wetting-drying

cycles, washing with $CaCl_2$ and solvating with glycol. Wet-dry cycles may have altered smectite to illite (Figure 1.7).

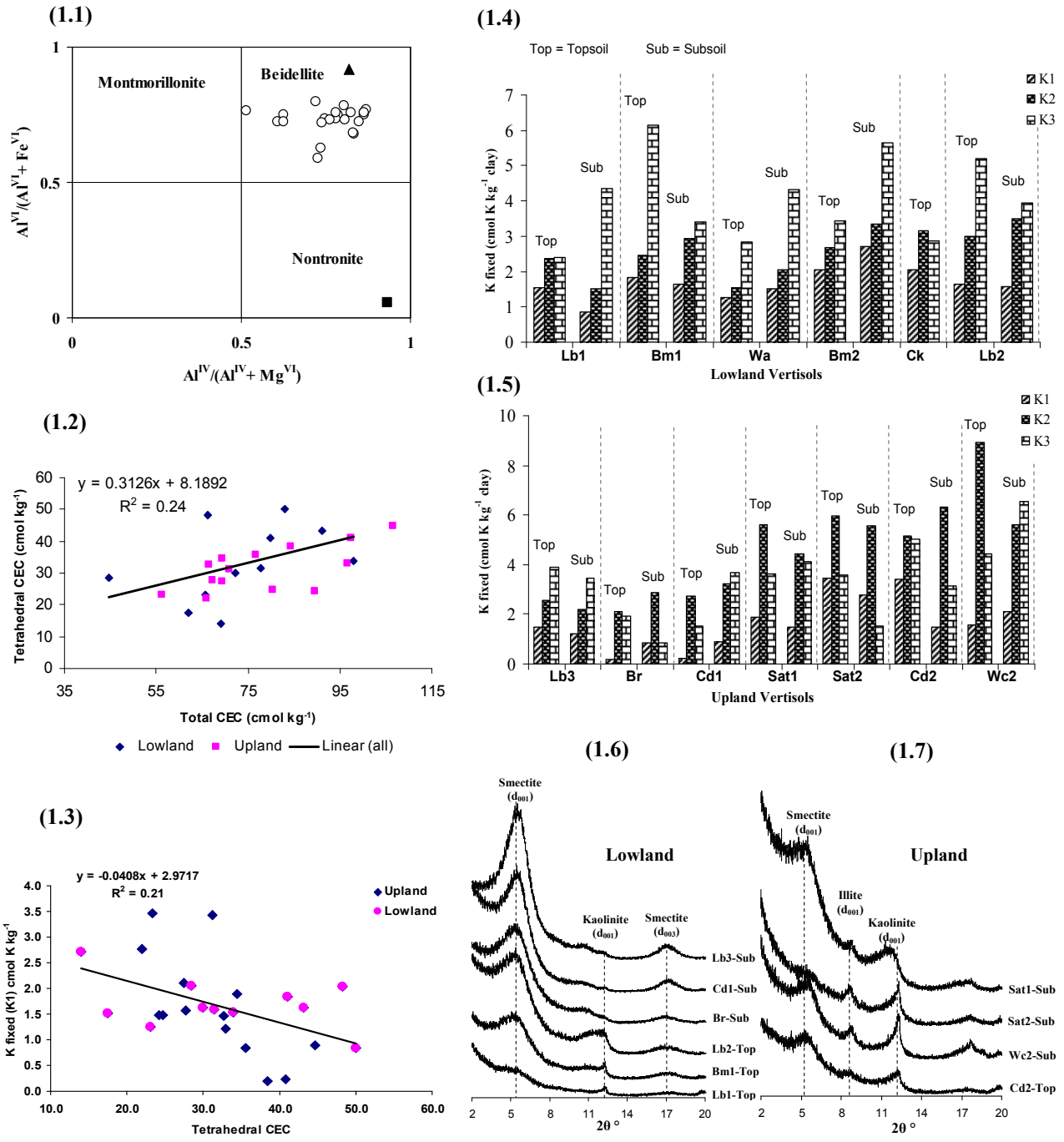

Figure (1.1) Plot of major elements calculated from structural formula in tetrahedral and octahedral sheets showing beidellite composition, (1.2) Relationship between tetrahedral CEC and total CEC, (1.3) Relationship of K fixation and tetrahedral CEC, (1.4, 1.5) K fixed for the three levels of K added (K1, K2, K3) of lowland soil clays and upland soil clays respectively, (1.6, 1.7) XRD pattern showing effect of wetting and drying on K fixation by smectite from lowland and upland Vertisols respectively, (Ca and glycerol saturated samples).

Conclusion

Clay in Thai Vertisols is dominated by beidellite. Beidellite in these soils has a high capacity to retain and exchange cations but does not fix substantial amount of K. The magnitude and location of charge may affect K fixation in smectite, but this study shows that total CEC and tetrahedral CEC have no relationship with K fixation.

Acknowledgments
The authors acknowledge the kind support of this work by The Royal Golden Jubilee Ph.D. Program of The Thailand Research Fund.

References
Barshad I, Kishk FM (1970) Factors affecting potassium fixation and cation exchange capacities of soil vermiculite clays. *Clays Clay Miner.* **18**, 127-137.
Bouabid R, Badraoui M, Bloom PR (1991) Potassium fixation and charge characteristics of soil clays. *Soil Sci Soc. Am. J.* **55**, 1493-1498.
Chittamart N, Suddhiprakarn A, Kheoruenromne I, Gilkes RJ (2010) Layer charge characteristics of smectite in Thai Vertisols. *Clays Clay Miner*. (In press).
Dowdy RH, Hutcheson TB (1963) Effect of exchangeable potassium level and drying on release and fixation of potassium by soils as related to clay mineralogy. *Soil Sci. Soc. Am. J.* **27**, 31-34.
Khaled EM, Stucki JW (1991) Iron oxidation state effects on cation fixation in smectites. *Soil Sci. Soc. Am. J.* **55**, 550-554.
Laird DA (1994) Evaluation of the structural formula and alkylammonium methods of determining layer charge. In 'CMS Workshop Lectures, Vol. 6, Layer charge characteristics of 2:1 silicate clay minerals' (Ed. Mermut AR), pp. 80-103. (The Clay Mineral Society: Boulder, Colorado, USA).
Lim LL, Jackson ML (1986) Reactions of expandable phyllosilicates with lithium and heating. *Clays Clay Miner.* **34**, 346-352.
Rayment GE, Higginson FR (1992) 'Australian Laboratory Handbook of Soil and Water Chemical Methods: Australian Soil and Land Survey Handbook'. (Inkata Press: Melbourne, Australia).

Charge properties of kaolinite in acidic soils from Thailand

Khwunta Khawmee[A], Anchalee Suddhiprakarn[A], Irb Kheoruenromne[A] and Balwant Singh[B]

[A]Department of Soil Science, Faculty of Agriculture, Kasetsart University, Bangkok 10900, Thailand,
Email g5181048@ku.ac.th; agrals@ku.ac.th, Irbs@ku.ac.th
[B]Faculty of Agriculture, food and Natural Resources, The University of Sydney, NSW 2006, Australia,
Email Balwant.Singh@sydney.edu.au

Abstract
Oxisols and Ultisols of Thailand, generally have kaolinite as the dominant clay mineral. Surface charge properties of kaolinite in these soils have a major influence on chemical and physical properties of the soils yet a limited research has been done to determine the nature of the charge on soil kaolinites, especially in Thai soils. The objective of this study was to evaluate charge properties of kaolinite from highly weathered soils of Thailand. All soils exhibited an acid reaction and clay mineralogy was dominated by kaolinite. The pH in 1:1 H_2O, organic matter and cation exchangeable capacity (CEC) of Ultisols and Oxisols ranged from 4.3-5.1 and 4.4-5.6, 2.5-19.2 and 3.6-26.5 g/kg, 1.94-4.81 and 2.61-19.89 $cmol_c$/kg, respectively.

The width at half height (WHH) of kaolinite in Ultisols and Oxisols ranged from 0.22-0.66 and 0.5-1.22 $^o2\theta$ respectively. There was an increase in the CEC of soil with increasing WHH of kaolinite suggesting that surface charge increase with decreasing crystallinity of kaolinite. Charge properties of kaolinite will be investigated by measuring the extent of permanent structural charge by cesium adsorption, and variable charge will be quantified by simultaneous proton titration and background electrolyte (LiCl) adsorption measurements. The research should provide a better understanding of kaolinite properties in soils and help in improving the productivity of kaolinite dominated soils in Thailand.

Key Words
Permanent charge, Variable charge, Acidic soils, Highly weathered soils

Introduction
Oxisols and Ultisols are highly weathered soils of the Tropics (Beinroth *et al.* 2000; West and Beinroth 2000). A large majority of Thai soils are highly weathered and clay fraction is often dominated by kaolinite (Wongvisitrangsi 1986; Yoothong *et al.* 1997). Surface charge properties of kaolinite are not only important for adsorption reactions but they also affect the dissolution behaviour of kaolinites (Chorover and Sposito 1995a). Limited research on the charge properties of soil kaolin from Thailand shows that the surface charge density of the Thai kaolins range from 0.16 to 0.99 C m^{-2} in comparison to 0.18 C m^{-2} for the Georgia kaolinite (Kanket *et al.* 2005). However, a little is known about the exact nature of the charge in kaolinite of Thai soils. This study aims to contribute towards an understanding of the surface charge properties of kaolinites in highly weathered soils of Thailand by measuring permanent and variable charges of kaolinite.

Methods
Five Ultisols and five Oxisols soil profiles were chosen for the study, and samples from three horizons of each of these profiles were taken for this study. Soils were air-dried, ground and passed through 2 mm sieve for various laboratory analyses. Soil pH was determined in 1:1 soil:solution ratio with distilled water. Organic carbon (OC) was determined by the Walkley-Black method (Nelson and Sommers 1996). Cation exchangeable cations were determined by displacing these with 1 M NH_4OAc at pH 7 solution and cation exchange capacity (CEC) was taken to be equivalent to the sum of exchangeable cations present in the leachate. Extractable acidity (EA) was determined by barium chloridetriethanolamine solution buffer at pH 8.2 (Thomas 1982). Particle size analysis was determined by the International pipette method (Gee and Bauder 1986).

Kaolinite in the clay fraction of soils was concentrated by dissolving iron oxides. CEC will be measured using 0.01 M silver thiourea (AgTU) solution at pH 4.7 to displace exchangeable cations (Rayment and Higginson 1992). Surface area of kaolinite will be measured using the N_2-BET method (Aylmore *et al.* 1970). Permanent and variable charges, and point of zero charge of soil kaolinites will be determined using the procedures described by Chorover and Sposito (1995b) and Phillips and Sheehan (2005).

Results and discussion

Important soil chemical and physical properties of the soils used in the study are given in Table 1. Soil pH of both Oxisols and Ultisols is highly acidic, with mean values of 4.7 and 4.9, respectively. Clay content in the Oxisols was significantly higher (709 g/kg) than the Ultisols (285 g/kg), and this is reflected in the corresponding CEC values of these soils with relatively higher CEC for Oxisols (mean = 10.7 $cmol_c/kg$) than the Ultisols (mean = 2.92 $cmol_c/kg$) These values are similar to those for the red Oxisols (mean 9.50 $cmol_c/kg$) and the red Ultisols (mean = 3.00 $cmol_c/kg$) in Thail soils (Trakoonyingcharoen *et al*. 2006). In general lower CEC values for both Oxisols and Ultisols indicated the dominance of kaolinite mineral in the clay fraction of these soils.

The clay fraction of the studied soils was dominated by kaolinite in both Oxisols and Ultisols (Figure 1). The WHH of soil kaolinite varied considerately and were generally higher of the Oxisols (mean = 0.73 $^o2\theta$) than the Ultisols (mean = 0.49 $^o2\theta$) (Table 1; Figure 1) suggesting that an increase in the CEC of soil with increasing WHH of kaolinite similar to Singh and Gilkes (1992) found that a general trend for CEC to increase with decreasing crystal size of soil kaolins. Permanent and variable charges, and point of zero charge are currently being determined using the procedures outlined by Chorover and Sposito (1995b) and Phillips and Sheehan (2005), and this data will be presented at the conference.

Table 1. Chemical and physical properties of highly weathered soils from Thailand.

Soil type	Soil Properties											WHH * 001 ($^o2\theta$)
	pH (H_2O)	OC (g/kg)	Sand (------g/kg--------)	Silt	Clay	Extractable bases				EA*	CEC	
						Ca	Mg	Na	K	($cmol_c/kg$)		
Ultisols												
Minimum	4.3	1.45	498	66	176	0.09	0.04	0.07	0.02	1.7	1.94	0.22
Maximum	5.1	11.14	758	173	415	0.38	0.16	0.66	0.07	11.5	4.81	0.66
Mean	4.7	3.42	613	102	285	0.27	0.08	0.31	0.03	4.8	2.92	0.49
Median	4.7	2.78	604	98	259	0.25	0.08	0.29	0.03	3.6	2.69	0.54
SD	0.3	2.45	66	29	65	0.10	0.04	0.17	0.01	3.4	0.79	0.15
Oxisols												
Minimum	4.4	2.09	33	50	512	0.03	0.03	0.06	0.02	7.4	2.61	0.50
Maximum	5.6	15.37	333	422	868	3.77	1.26	3.20	0.25	22.4	19.89	1.22
Mean	4.9	5.58	112	179	709	0.95	0.38	0.41	0.07	13.4	10.70	0.73
Median	4.8	4.18	82	149	737	0.43	0.17	0.19	0.04	13.3	9.75	0.58
SD	0.4	3.80	92	118	123	1.30	0.43	0.71	0.06	4.1	4.39	0.26

* EA = Extractable acidity; WHH = Width at half height

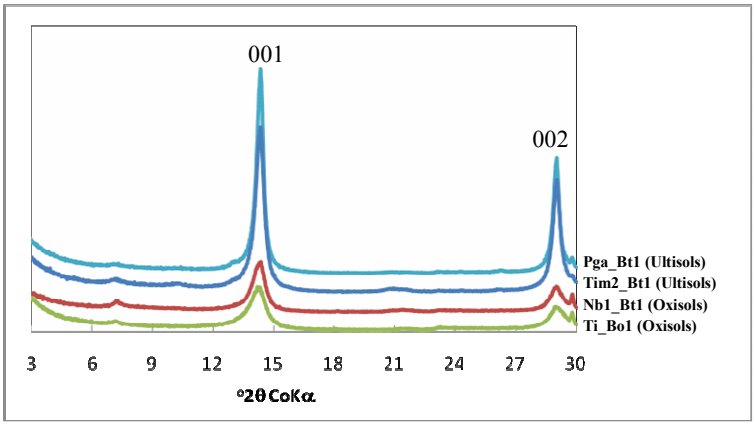

Figure 1. XRD patterns of the oriented specimens of some Oxisols and Ultisols from Thailand showing varying width at half height for the basal reflection of kaolinite.

Conclusions

Mineralogical and surface charge properties of kaolinite in Oxisols and Ultisols from Thailand were investigated to understand their influence on chemical and physical properties of these soils. The preliminary results indicate that the negative surface charge on kaolinite in these soils increases with decreasing crystallinity of kaolinite.

Acknowledgments
The authors are grateful to The Royal Golden Jubilee Ph.D. Program under the Thailand Research Fund for financial support.

References

Aylmore LAG, Sills ID, Quirk JP (1970) Surface area of homoionic illite and montmorillonite clay minerals as measured by the sorption of nitrogen and carbon dioxide. *Clays and Clay Minerals* **18,** 91-96.

Beinroth FH, Eswaran H, Uehara G, Reich PF (2000) Oxisols. In 'Handbook of Soil Science'. (Ed. LP Wilding) Vol. E, pp. 373–392. (CRC Press, Boca, Raton, London, New York, Washington, DC).

Chorover J, Sposito G (1995a) Dissolution behavior of kaolinitic tropical soils. *Geochimica et Cosmochimica Acta* **59(15),** 3109-3121.

Chorover J, Sposito G (1995b) Surface charge characteristic of kaolinitic tropical soils. *Geochimica et Cosmochimica Acta* **59(5),** 875-884.

Gee GW, Bauder JW (1986) Particle–sized analysis In 'Methods of Soil Analysis, Part I. Physical and Mineralogical Methods'. (Ed A Kulte) pp. 383-411. (Amer. Soc. Agron. Inc., Madison, Wisconsin, USA.).

Kanket W, Suddhiprakarn A, Kheoruenromne I, and Gilkes RJ (2005) Chemical and crystallographic properties of kaolin from Ultisols in Thailand. *Clays and Clay Minerals* **53,** 478-489.

Nelson DW, Sommers LE (1996) Total carbon, organic carbon, and organic matter. In 'Methods of Soil Analysis, Part III -Chemical Methods' (Eds DL Sparks, AL.Page, PA Helmke, RH Loeppert) pp. 961-1010. (SSSA Book Series., Madison, Wisconsin).

Phillips IR, Sheehan KJ (2005) Importance of surface charge characteristics when selecting soils for wastewater re-use. *Australian Journal of Soil Research* **43**, 915-927.

Rayment GE, Higginson BR (1992) Australian Laboratory Handbook of Soil and Water Chemical Methods: Australian Soil and Land Survey Handbook. Inkata, Melbourne, Australia.

Singh B, Gilkes RJ (1992) Properties of soil kaolins from southwestern Australia. *Journal of Soil Science* **43**, 645-667.

Thomas GW (1982) Exchangeable cations In 'Methods of Soil Analysis, Part II. Chemical and Microbiological Properties'. (Ed CA Black) pp. 159-165. (ASA and SSSA. Inc., Madison, Wisconsin).

Trakoonyingcharoen P, Kheoruenromne I, Suddhiprakarn A, Gilkes RJ (2006) Properties of kaolins in red Oxisols and red Ultisols in Thailand. *Applied Clay Science* **32**, 25-39.

West LT, Beinroth FH (2000) Ultisols. In 'Handbook of Soil Science'. (Ed LP Wilding) Vol. E, pp. 358-372. (CRC Press, Boca, Raton, London, New York, Washington, DC).

Wongvisitrangsi C (1986) A Study on Physical, Chemical, Mineralogical Properties and Morphology of Selected Red and Yellow Soils in Southeast Coast and Peninsular Thailand. M.S. Thesis, Kasetsart University, Bangkok. 293 p. (in Thai with English abstract).

Yoothong K, Moncharoen L, Vijarnson P, Eswaran H (1997) Clay mineralogy of Thai soils. *Applied Clay Science* **11,** 357-371.

Chemistry and clay mineralogy of Thai Natraqualfs

Chutharmard Kaewmano[A], Irb Kheoruenromne[A,*], Anchalee Suddhiprakarn[A] and Robert J. Gilkes[B]

[A]Department of Soil Science, Faculty of Agriculture, Kasetsart University, Bangkok 10900, Thailand. Email irbs@ku.ac.th
[B]School of Earth and Environment, Faculty of Natural and Agricultural Science, University of Western Australia, WA, Australia.

Abstract
Thai Natraqualfs including saline-sodic and sodic soils from eight sites on alluvium or wash over residuum derived from clastic sedimentary rock under a tropical savanna climate were investigated. They have a large variation in EC values ranging from 0.3 - 60.5 dS/m with variable ESP values ranging from 0.1-31.5% and SAR values $\leq$ 13. Kaolinite is the dominant mineral in the clay fraction with small amounts of smectite and a trace of illite. Transmission electron microscope (TEM) micrographs of kaolinite show a variety of crystal morphologies including euhedral, subhedral and anhedral platy crystals. Anhedral crystals are abundant in saline-sodic soils and a high proportion of euhedral crystals occur in sodic soils. The median size of kaolinite crystal ranges from 43-69 nm. Morphology and size of kaolinite crystals for these Natraqualfs are statistically related to electrical conductivity and soil pH. Decreasing kaolinite crystal size is associated with increasing soil salinity and exchangeable Na.

Key Words
Salt affected soils, salinity, sodicity, kaolinite morphology

Introduction
Salt affected soils are problem soils in Thailand, particularly in the Northeast Plateau basin where salt bearing rocks are common. The soils usually support lowland rice cultivation which is variously affected by salinity. Generally, kaolinite is the dominant clay mineral with a trace of smectite (Suddhiprakarn and Kheoruenromne 1998; Wongpokhom *et al.* 2008). Knowledge of the mineralogy of these soils will be useful in making predictions about soil behavior and responses to management.

Methods
Soil sampling
The study sites were located on the Northeast Plateau, Thailand. Eight representative salt affected soils under a tropical savanna climate were selected. Methods of study included detailed profile description and sampling by genetic horizon according to standard field study methods (Soil Survey Division Staff 1993; Kheoruenromne 2009). Bulk soil samples were air-dried, gently crushed and then passed through a 2-mm sieve. The resultant <2 mm samples were used for laboratory analysis.

Laboratory analyses
The particle size distribution was determined by a combination of sieve and pipette analysis. Soil pH was measured in water and in 1M KCl using 1:1 soil:liquid. Organic carbon was determined by the Walkley and Black method. Extractable bases were measured by 1 M NH_4OAc at pH 7.0 extraction. Cation exchange capacity was measured by saturating the exchange sites and displacing it with 1M NH_4OAc at pH 7.0. Extractable acidity was measured by barium chloride-triethanolamine pH 8.2 extraction. Base saturation percentage was calculated by sum of bases extracted by NH_4OAc pH 7.0 divided by the CEC based on the sum of cations and multiplied by 100. Sodium adsorption ratio was calculated by dividing the molar concentration of the monovalent cation Na^+ by the square root of the molar concentration of the divalent cations Ca^{2+} and Mg^{2+}. Exchangeable sodium percentage was obtained by dividing the exchangeable sodium by the CEC at pH 7.0 and multiplying by 100. Electrical conductivity was determined by the saturation extract method at 25^{o}C.
Soil mineralogy was identified by X ray diffraction (XRD) analysis using monochromatized CuKα radiation with a Philips PW-3020 diffractometer (50 kV, 20 mA). Clay fractions were scanned from 4 to 45° 2θ, using a step size of 0.02° 2θ and a scan speed of 0.04° 2θ/s. Relative proportions of various minerals were calculated by comparing the XRD peak intensities with the intensities for standard minerals (Brown and Brindley 1980). For analytical transmission electron microscopy, representative clay samples were prepared as dispersed samples. One milliliter of clay suspension was transferred into the 10-mL test tube, mixed well with 9 mL of deionized water. A drop of the suspension was deposited on a carbon-coated Cu grid and examined using a Jeol 2000 FX II electron microscope operated at 80 kV.

Results

General soil characteristics

These soils have been formed on alluvium or wash over residuum derived from clastic sedimentary rock on flat to gently undulating terrain (slope ranges 1-2 %) under annual rainfall ranging from 907-1237 mm y^{-1} and temperature of 26-30^{o}C. Land uses at the time of sampling were paddy rice/left idle and a plantation of *Eucalyptus sp*. All soils are deep and the common profile development features of the soils are Apng/Apg - Btg/Btng - 2Btg/2Btng indicating a high stage of profile development. Clay accumulation in subsoils and accumulations of soluble salts in both surface and subsoils indicate the argillic-natric horizon. The soils have low chroma ($\leq$2) and are mottled indicating poorly drainage and a long period of water saturation. Therefore, these soils can be classified as Natraqualfs according to USDA Soil Taxonomy (Soil Survey Staff 2006).

Physico-chemical properties

Particle size distribution results show that soil texture varies from loamy sand to clay. Most soils are fine to medium textured (clay to clay loam) with the coarser textured horizons being due to depositional grading of sediments. The increases in clay size particle at some depths in subsoils where clay coatings can clearly be observed are due to clay illuviation and lessivage. Soil pH in water is in a range of very strongly acid to slightly alkaline (pH 4.9-7.7). The high pH values are largely due to the hydrolysis of sodium carbonate as occurs in sodic soils. The low pH values of soils are consistent with the pH values of tropical soils that experience leaching (van Wambeke 1992). The pH values measured in KCl are smaller than those measured in water indicating that the minerals have a net negative charge. Their organic matter contents decrease with depth ranging from very low to medium (0.35-22.01 g/kg). The soils have very low to high CEC values, ranging from 0.65–29.47 $cmol_{/kg}$ and the variation in CEC closely reflects the clay content and mineralogy. The sum of exchangeable bases of these soils is very low to high and Na is the dominant exchangeable base. The extractable acidity of the soils ranges from medium to high indicating highly leaching conditions (Buol *et al.* 2003). All soils have high base saturation percentage of more than 35 percent.

Soil salinity and sodicity

There is a large variation in the EC values of these soils from very low to very high (Figure 1a). The highest EC values in the surface of some soils are due to a salt patch at the surface. A low surface EC and increasing EC with depth may be due to these soils being at intermediate stage of salt leaching (desalinization). All soils have low SAR values (SAR $\leq$ 13), whereas the ESP values vary substantially ranging from 0.1-31.5%. According to the criteria for classifying salt affected soils (Soil Survey Staff 2006), there are two groups of salt affected soils consisting of saline-sodic soils (Pedons 1-4) and sodic soils (Pedons 5-8) (Figure 1b).

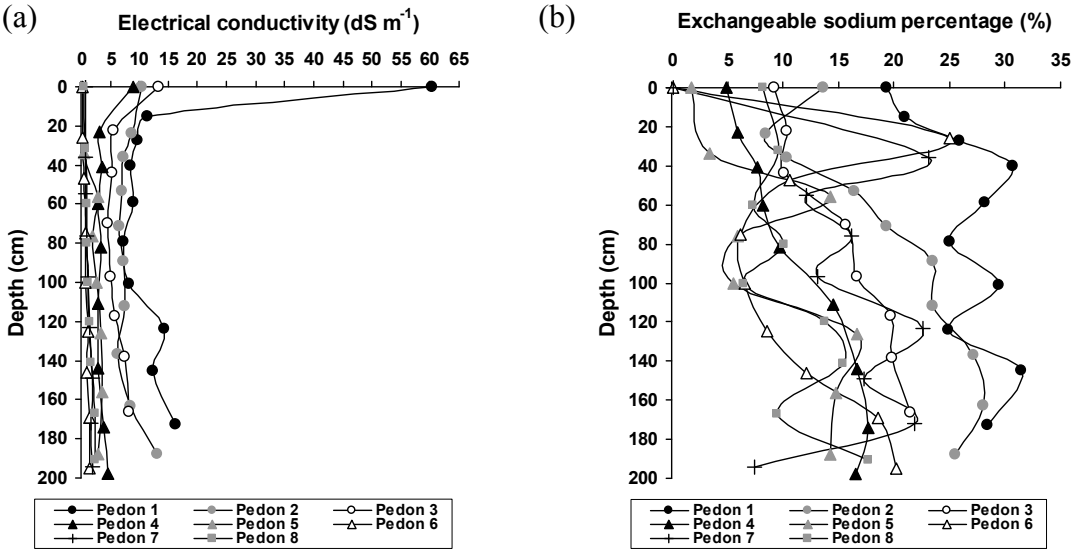

Figure 1. Depth function diagram for electrical conductivity (a) and exchangeable sodium percentage (b) of the soil profiles.

Clay mineralogy

Kaolinite is a dominant mineral in the clay fraction of these salt affected soils with small amounts of smectite and a trace of illite. All soils have kaolinitic mineralogy (Soil Survey Staff 2006). Most soils have

experienced leaching of Si and basic cations in the tropical climate with high rainfall under a former pedogenic regime prior to salinization. The small amount of quartz in the clay fraction may be inherited from sandstone and siltstone. Halite is a dominant salt mineral in these salt affected soils.

The morphology of kaolinite from electron micrographs for these soils includes anhedral, subhedral and euhedral platy crystals (Figure 2) and most crystals are subhedral. Anhedral crystals are most abundant in saline-sodic soils and show a strong negative relationship with soil pH in KCl (R^2 = -0.82) and a positive relationship with EC (R^2 = 0.57) (Figure 3), whereas, sodic soils have higher proportions of euhedral kaolinite crystals. The abundance of euhedral crystals in these soils has a negative relationship with EC (R^2 = -0.45) and a strong positive relationship with soil pH in KCl (R^2 = 0.95).

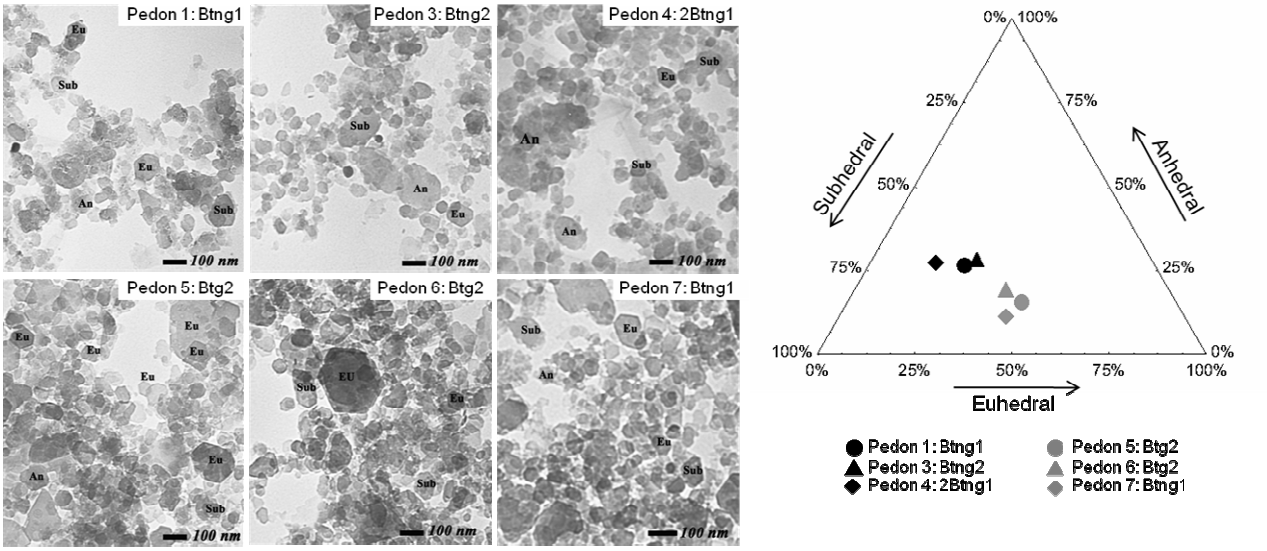

Figure 2. Transmission electron microscope (TEM) micrographs of kaolinite from representative salt affected soils showing the wide ranges of crystal morphology and size. Various morphologies are indicated in the Figure: Eu=euhedral crystal, Sub=subhedral crystal and An=anhedral crystal. The triangle graph shows the relative abundance of crystal shapes for kaolinite (0 plane faces=Anhedral, 1-3 faces=Subhedral, 4-6 faces=Euhedral).

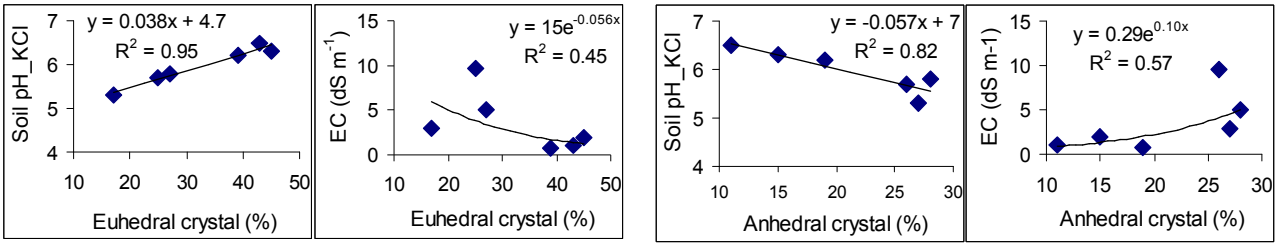

Figure 3. The relationships between percentage of kaolinite crystal morphologies determined by TEM and some chemical properties of representative salt affected soils.

The median size of kaolinite crystals ranges from 43-69 nm with the standard deviation in size ranging from 13-25 nm and furthermore the smaller kaolinite crystals are more abundant in saline-sodic soils (Figure 4). Generally, kaolinite crystals in these salt affected soils are smaller than for Thai soils investigated by Trakoonyingcharoen *et al.* (2006) with values of median size from 58-124 nm. Kaolinite crystal size shows a negative relationship with EC and exchangeable Na for these salt affected soils (Figure 5).

Conclusion

Thai Natraqualfs under a tropical savanna climate are saline-sodic and sodic soils. The clay fraction is predominantly kaolinite. Kaolinite morphology includes anhedral, subhedral and euhedral crystals. Smaller kaolinite crystals are more abundant in saline-sodic soils. Anhedral crystals are abundant in saline-sodic soils but sodic soils have higher proportions of euhedral crystals. Morphology and size of kaolinite crystals in these salt affected soils are statistically related to salinity and pH.

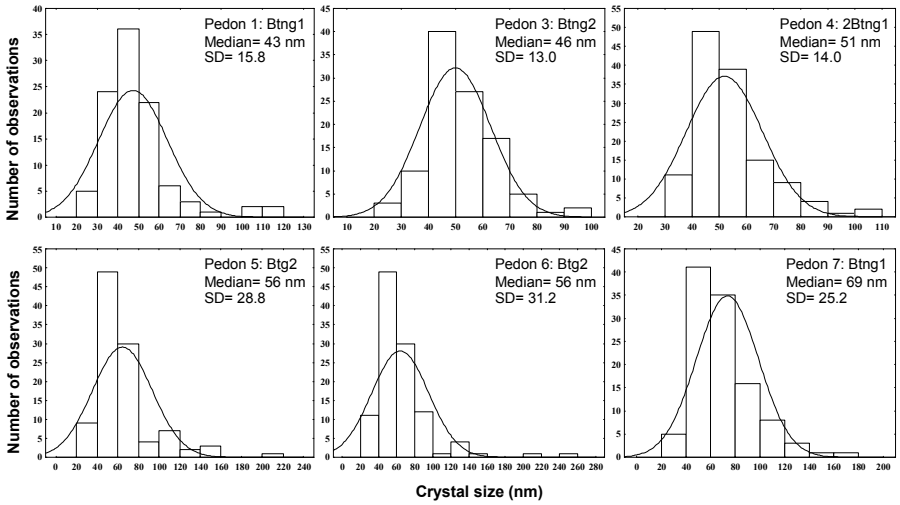

Figure 4. Histograms showing the size distribution of kaolinite crystals from representative salt affected soils.

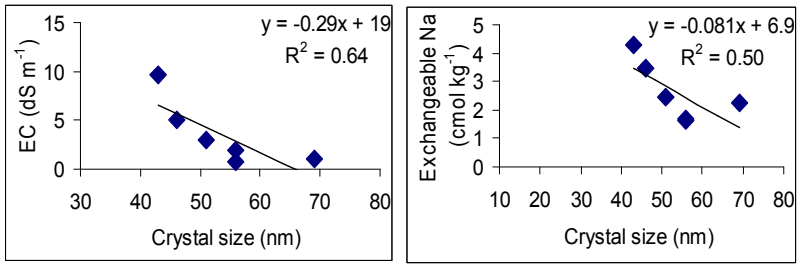

Figure 5. Relationships between kaolinite crystal size observed from TEM and some chemical properties.

Acknowledgments

The authors are grateful to The Royal Golden Jubilee Ph.D. Program of The Thailand Research Fund for financial support and Soil Mineralogy Group of The University of Western Australia for laboratory facilities.

References

Brown G, Brindley GW (1980) X-ray diffraction procedures for clay mineral identification. In 'Crystal Structures of Clay Minerals and Their X-ray Identification'. Mineralogical Society Monograph. No. 5. (Eds GW Brindley, G Brown), pp. 305-359. (Spottiswoode Ballantyne Ltd.: London).

Buol SW, Southard RJ, Graham RC, McDaniel PA (2003) 'Soil Genesis and Classification.' (Iowa State University Press: New Jersey).

Kheoruenromne I (2009) 'Soil Survey Laboratory Manual.' (Department of Soil Science, Faculty of Agriculture, Kasetsart University: Bangkok) (in Thai).

Soil Survey Division Staff (1993) 'Soil Survey Manual.' (United States Department of Agricluture: Washington, DC).

Soil Survey Staff (2006) 'Soil Taxonomy: a basic system of soil classification for making and interpreting soil survey.' (United States Department of Agriculture: Washington, DC).

Suddhiprakarn A, Kheoruenromne I (1998) Mineralogy and micromorphology of salt affected soils in Central Plain, Thailand. *Thai Journal of Agrcultural Science* **31**, 3-20.

Trakoonyingcharoen P, Kheoruenromne I, Suddhiprakarn A, Gilkes RJ (2006) Properties of kaolins in red Oxisols and red Ultisols in Thailand. *Applied Clay Science* **32**, 25-39.

van Wambeke A (1992) 'Soils of the Tropics: Properties and Appraisal'. (McGraw-Hill: New York)

Wongpokhom N, Kheoruenromne I, Suddhiprakarn A, Gilkes RJ (2008) Micromorphological properties of salt affected soils in Northeast Thailand. *Geoderma* **144**, 158-170.

Clay and oxide mineralogy of different limestone soils in Southeast Asia

Karl Stahr[1], Ulrich Schuler[3], Volker Häring[1], Gerd Clemens[2], Ludger Herrmann[1] und Mehdi Zarei[1]

1 Institut of Soil Science and Land Evaluation, Hohenheim University, D-70593 Stuttgart
2 Bundesanstalt für Geowissenschaften und Rohstoffe, Stilleweg, D-30655 Hannover
3 The Uplands Program, Vietnamese-German Center, Technical Universität Hanoi, 1 Dai Co Viet, Hanoi, Vietnam
Email of corresponding author: kstahr@uni-hohenheim.de

Abstract
Limestone areas in the tropics are rare. However in South Asia they occur frequently. Soils derived from Palaeozoic and Mesozoic limestones in North Laos and Thailand, Vietnam were sampled. Dominant soils were Alisols and Acrisols in Thailand, Acrisols with few Luvisols in Laos and Luvisols with Alisols in Vietnam. The clay minerals show a sequence from illite to vermiculite and kaolinite. In strongly weathered profiles gibbsite is abundant while goethite and hematite occur sporadically. Chemical fertility is endangered in all areas, particularly in very weathered profiles of Thailand and the erosion problem is highest in Vietnam. Both are consequences of soil development and current land use.

Introduction
Limestone areas in Southeast Asia are characterized by unique landforms consisting of limestone towers with carstic depressions in between. Due to the deep and rugged slopes this areas is mostly inhabited by the socially disadvantaged groups like ethnic minorities. Fallow based farming systems without chemical fertilizer and pesticide applications are still prevailing in these areas. However recently a change from long time fallow system to short time fallow based farming systems including the application of agrochemicals is observed. This development is problematic as limestone areas are generally carstified and therefore are often characterized by high subsurface discharge. Tracer tests revealed very high transport velocities in the carstic underground, excluding significant degradation of agrochemicals. Downstream this affects the functionally of agrosystems and quality of human drinking water supply. On the other hand in areas with recent clearing of forest, high rates of erosion occur, which made sustainable agriculture impossible. The limestone soils are barriers between the surface and carstic underground. They play therefore a very important role in the ecosystems of these areas. This paper aims to highlight soil formation in limestone areas in three countries of Southeast Asia. The following questions will be addressed.

Which factors are influencing soil formation, how can differences can be explained and how vulnerable are these soils to chemical and physical soil degradation.

Materials
Three carstic areas in Northern Thailand, Laos and Northern Vietnam have been selected.

Table 1. Research sites

Research area	Bor Krai	Huay Sang	Muong Lum
Country	Thailand	Laos PDR	Vietnam
Province	Mae Hong Son	Bokeo	Son La
District	Pang Ma Pha	Pha Udom	Yen Chau
Elevation [m asl]	550 - 1020	415 - 575	700 - 1300
Annual mean temperature [°C/a]	19.8 [a]	25.6 [b]	19.7 [c]
Mean annual precipitation [mm/a]	1197 [a]	1153 [b]	1427 [c]
Age of limestone	Permian	Carboniferous-Permian	Triassic
Ethnic group	Black Lahu	Hmong, Khamu	Black Thai, Hmong
Farming system	Subsistence	Subsistence	Subsistence, commercial
Main crops	Upland rice, maize	Paddy rice, maize	Paddy rice, maize, cassava

[a] Bor Krai – 770 m asl
[b] Chiang Rai – 394 m asl, 143 km WSW of Huay Sang, period 1971-2005
[c] Muong Lum – 780 m asl

They contain limestones of different ages the Carboniferous to Permian limestone of Laos being the oldest, then the Permian in Thailand and Triassic limestone in Vietnam. This limestone and the whole area has undergone cretaceous and tertiary orogeny as well as tectonic movements. This movements continued at

least partially through the Pleistocene. However the age of the landscape is not well known. Intensive carstic phenomena have changed the land surface up to the decameter scale, thereby exposing limestone rocks with deep carstic depressions filled with residual material from limestone dissolution. All other carstic phenomena like dollines, underground rivers and dry valleys occur. All the research areas are placed in the outer tropics. The climate is subhumid tropical climate with marked dry humid phases. The mean temperature is about 20 degrees in the high mountain areas of Thailand and Vietnam. The farming system was shifting cultivation for subsistence but is moving in all areas towards more intensive landuse and more market orientation. There are hughe clearcuts and consequent tremendous erosion especially under upland rice and sweet corn cultivation. Beside other soils in the Thai area of Bor Krai Alisols and Acrisols are dominant. The development in the high altitudes also reaches the Ferralsol stage. In Laos Acrisols are the dominant soils, but under conditions were secondary lime is involved Luvisols are found. In the case of the Vietnamese area Alisols seem to be the most dominant soils. However in all areas the residues from limestone are rather thick covering the limestone in a thickness of several meters. A few meters away one can find places were the limestone crops out. That means the subsurface relief of the limestone is very rough (Figure 1-3).

Methods

The soils have been described according the FAO guide lines (2006) and the World Reference Base of Soil Resources (WRB 2006). The particle size, pH, carbon, nitrogen, CEC and carbonates have been analysed using the Institutes Standard Procedures (Schlichting *et al.* 1995). Bulk mineralogy was analysed using X-ray diffraction of powders specimens. The clay mineralogy was analysed after separating clay fraction and using oriented samples for X-ray diffraction with pretreatments of magnesium-, glycerol-, potassium-, saturation and heating to 50°C, 400°C und 600°C as well as ambient conditions. The qualitative analyses were done using standard minerals and a modified Rietveld analysis. The scanning electromicrographs are from natural aggregates of sand size, which have been coated with gold. The same sample have been also used for EDX-analysis.

Results

A relatively wide range of minerals has been obseverd in the bulk of the soil as well as in the clay fraction. A very clear but simple observation is that quartz was only found in the bulk soil but not in the clay fraction. This is a clear sign that we have no significant physical weathering. In temperate regions, we do find through physical cryoclastic weathering regularly in the topsoils also quartz in the clay fraction. Beside this the oxides, hematite and goethite as well as gibbsite are identified in several samples. The clay minerals are represented by illite, illite-vermiculite mixed layer, vermiculite, kaolinite and some chlorite.

Table 2. Clay minerals in three representative soils from limestone in Northern Thailand.

Soil	**Alisol**				**Acrisol**				**Ferralsol**	
Slope (%)	1.7				3.5				34.4	
Horizon	Ah (N=1)		Bt3 (N=1)		Ah1 (N=1)		Bt2 (N=1)		Bo4 (N=1)	
Depth (cm)	0-17		56-76		0-20		62-86		150-160	
Skeleton (%)	2-5		0-2		0		0		0	
Sand (%)	15		13		8		7		3	
Silt (%)	44		26		44		13		16	
Clay (%)	41		61		48		79		82	
Mineralogy:	Bulk	Clay	Bulk	Clay	Bulk	Clay	Bulk	Clay	Bulk	Clay
	(%)									
Gibbsite	0	0	0	0	36	18	37	20	58	45
Goethite	0	4	13	5	0	0	0	0	0	0
Hematite	8	5	8	5	19	15	18	13	14	22
Ilite	13	36	17	38	0	6	0	5	0	0
Illite/Vermiculite	0	26	0	22	0	0	0	0	0	0
Kaolinite	24	24	27	24	31	50	36	52	14	22
Quartz	54	0	48	0	12	0	5	0	4	0
Vermiculite	0	5	0	6	3	11	3	10	0	0
Chlorite	0	0	0	0	0	0	0	0	9	11

There is a clear tendency of mineral development when comparing the three Thai soils given in Table 2. The primary illite is not found in the Ferralsol and only in traces in the Acrisol and but it is abundant in the Alisol. Also the expanding clay minerals have their maximum in the Alisol and are reduced in Acrisols as well as Ferralsols. There is a tendency of desilification or ferralitisation, which is observed in the increasing kaolinite content from Alisols to the other soils. The tendency of desilification is further confirmed by the

existence of gibbsite in the Acrisols and Ferralsols. Through the formation of iron and aluminium oxide cements, we find gibbsite as well as hematite in higher quantities in bulk soil, than in the separated clay fractions, especially in the Acrisol. Also rubification has its highest values in the Acrisol, and goethite is no detectable in Thai Acrisol and Ferralsols.

The findings of profiles from Laos and Vietnam confirm the results found in Thailand. With no exception an illitic clays mineral was found in the clay fraction in all soils. On the other hand the occurrence of gibbsite is only in very small amounts and could not be quantified. Also hematite was not found in samples from the two research sites but goethite was found in high quantities. Consistent with this finding is that in some of the Laostick profiles calcium carbonate could was present. The scanning electron microscope shows the presence of predominant kaolinite and gibbsite and especially kaolinite is not well crystallised having no idiomorphic shapes. The gibbsite crystals are very abundant however, they are extremely small and seem to cover all fragments and aggregates. This phenomenon, however, confirms the pedogenic origin and formation of these crystals insitu.

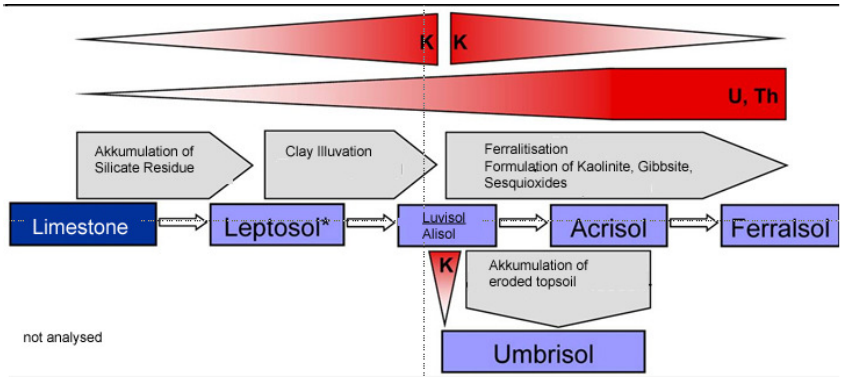

Figure 1. Mayor processes governing soil formation on limestone in SE-Asia

Discussion

Soil development especially the differentiation of clay minerals and oxides in the three analysed areas are different. Already the occurence of Ferralsols in Thailand points to the more advantaged development. This is confirmed through the overall presence of gibbsite and also by the occurrence of some chlorite. Both minerals are mainly absent in the other two areas. The major directions of soil formation and mineral formation are shown in (Figure 1). The development is in the beginning a formation of residual clays, which also gathers potassium. This improving the plant nutrition status of Luvisols and Acrisols. In the second phase of desilification and extreme base depletion the clay minerals are formed into kaolinite and finally gibbsite. This further development stage forms the aggregates and thereby the physical constitution of the soils, while the first process improves the nutrient situation of the soils. The ecological consequence is that in the areas analysed in Laos and Vietnam plant nutrition is still in an acceptable situation with exchange capacity and especially potassium nutrition at an acceptable level. However in this area the erosion problem is terrible. On the other hand the poor soils in Thailand, which have undergone rubification and strong decalcification have formed very stable aggregates and have a very good infiltration. Therefore these soils are more stable under cultivation. Sustainable landuse needs a management which stabilises the soil structure in Vietnam and Laos while in the North Thailand case especially the chemical situation has to be improved by specific fertilizer application.

Acknowledgement

The founding by the German Research Foundation through SFB 564 is thankfully acknowledged.

References

Schuler U, Choocharoen C, Elstner P, Neef A, Stahr K, Zarei M, Herrmann L (2006) Soil mapping for land use planning in a karst area of northern Thailand: Integrating local and scientific knowledge. *J. Plant Nutrition and Soil Science* **169,** 444-452.

Tien PC, An LD, Bach LD, Bac DD, Vongdara B, Phengthavongsa B, Danh T, Dy ND, Dung HT, Hai TQ, Khuc V, Kun SC, Long PD, Ly MN, My NQ, Ngan PK, Ngoc N, Ratanavong N, Quoc NK, Quyen NV, Aphaymani SD, Thanh TD, Tri TV, Truyen MT, Xay TS (1991) Geology of Cambodia, Laos and Vietnam. Explanatory note to the Geological map of Cambodia, Laos and Vietnam at 1:1,000.000 scale 2nd edition, pp. 158 (Geological Survey of Vietnam, Hanoi, Vietnam).

Clay minerals in Luvisols formed from acid glacial till of the Drawsko Lake District (North Poland)

Jacek Dlugosz, Miroslaw Kobierski and Iwona Zielinska

Department of Soil Science and Soil Protection, University of Technology and Life Sciences, Bydgoszcz, Poland,
email: jacekd@utp.edu.pl

Abstract
Preliminary investigations of Luvisols formed from acid glacial till of the Drawsko Lake District and soils developed from them concentrated on the assays of composition of clay minerals of the clay fraction and fine clay fraction of glacial till. Effects of pedogenic processes on the rate and direction of their transformation was also studied. Mineralogical composition of the clay fraction was assessed by X-ray diffraction. The soils under study revealed a very diversified mineralogical composition of clay fraction of a profile and inter-profile nature. The profile distribution of swelling minerals suggested a significant influence of the fallowing process. One of the indices for inter-profile differentiation was the occurrence of vermiculite minerals in some of the profiles.

Key words
Clay minerals, glacial till, Luvisols, mixed layers minerals.

Introduction
Glacial till of the Drawsko Lake District was deposited over the youngest stage of the Vistulian (Weichselian) glaciation. It's the most characteristic feature is acidic reaction, which increased in the soil horizons. In consequence it intensified the transformation of clay minerals (Righi and Elsass 1996, Righi *et al.* 1997). That is why the objective of the investigations pursued within the framework of the project no. N 305 053134 granted by the Polish Ministry of Science and Higher Education is an assessment of the composition of clay minerals of the clay and fine clay fractions of glacial till and soils formed from it. Another aspect of the study is an evaluation of the pedogenic processes on the rate and direction of their transformations.

Methods
The Drawsko Lake District is a mesoregion of 1861 km^2 surface belonging to the Central European Lowland, the South Baltic Lake District sub-province, and the West Pomeranian Lake District macroregion. It is an area with a very diversified relief where the main elements are glacial and fluvioglacial forms formed during the Pomeranian stage of the Vistula (Weichselian) glaciations. The evidence of that phenomenon is the occurrence of ground moraine, outwash plain, stagnation deposits, kames, kameic terraces, and dead-ice moraines. However, the main formation covering the Lake District is glacial till. That is why the basic objective of this monograph are soils formed from glacial till of the Pomeranian stage localized on the western area of the Drawskie Lake (Klysz 2001). The objective of the research are Luvisols formed from the Pomeranian stage glacial till localized in the south part of the Drawskie Lake District between Zlocieniec and Czaplinek (Figure 2). In general you find sandy loam and loam, rather acidic (pH in 1 M KCl between 3.76–7.42). More data on the soils under study have been published in: Soils of the Drawskie Lake District formed from glacial till (Dlugosz *et al.* 2009)

The clay fraction samples (< 2 μm) for mineralogical investigations were separated by the Beckman centrifuge after dispersion with Na-ionite (Amberlite 120). Prior separation of the samples were prepared according to Jackson that was used to get rid of peptising components ($CaCO_3$, organic matter and free iron oxide). Mineralogical composition of the clay fraction was assessed by X-ray diffraction using the HZG – 4 instrument with a Cu Kα lamp and nickel filter. As for this analysis, samples of specific fractions were saturated with Mg^{2+} ions (Mg), then solvated with ethylene glycol (Mg+EG), and K^+ ions. Next, the samples were heated at 300°C and 550°C. These were oriented preparations obtained from a water suspension by sedimentation.

Results

Diffractometric analysis of the mineralogical composition of the clay fraction of the soils under study revealed a significant differentiation in profiles and among the investigated profiles. Illite (reflexes at 1.0, 0.500, and 0.334 nm) was the only mineral identified in all the samples, however, its percentage in fraction from various horizons was different. Its clear domination was observed in the case of the clay fraction of the surface horizons, where mixed-layer minerals of the illite/smectite type and chlorites were found in high concentrations, too (reflexes at 1.4, 0.72, 0.483, 0.356 nm) (Figure 1).

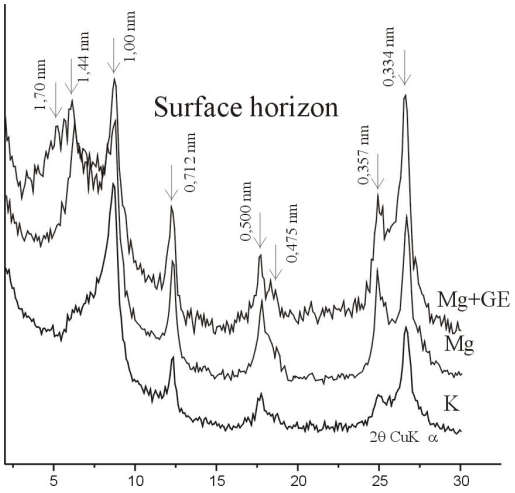

Figure 1. Diffractogram of clay fraction from surface horizon

These minerals occurred also in the eluvial horizons, what probably indicated that they are present in the coarse clay fraction. Smectite minerals dominated in the illuvial horizons. It was probably caused by the illuvial process enriching them in the fine clay fraction (Figure 2). Similar results were reported by Allen and Fanning (1983) and Długosz (2002). A confirmation of such relationship between the amount of fine clay fraction and the percentage of swelling minerals could come from the transition EB horizons, where the clay fraction shows a higher content of these minerals. They are mainly mixed-layer minerals of the illite/smectite type.

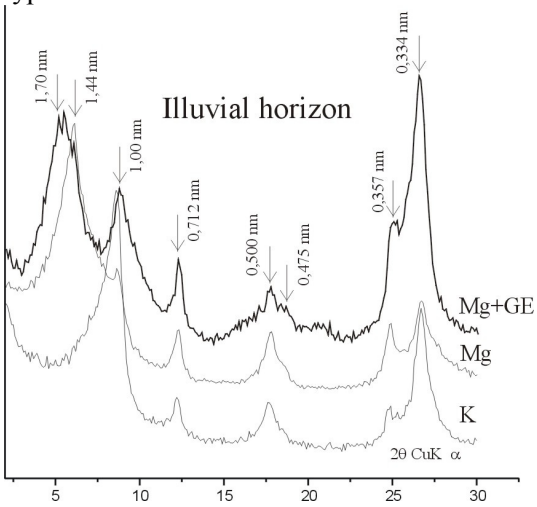

Figure 2. **Diffractogram of clay fraction from illuvial horizon**

Clay fraction of the glacial till showed the highest diversity. The profile studies revealed both the fraction of the illite-smectite-chlorite composition and the illite-vermiculite one (Figure 3). Vermiculite in these soil profile replaced probably chlorite minerals. These results indicated a different set of minerals as compared with that described for the glacial till of that area (Dlugosz 2002).

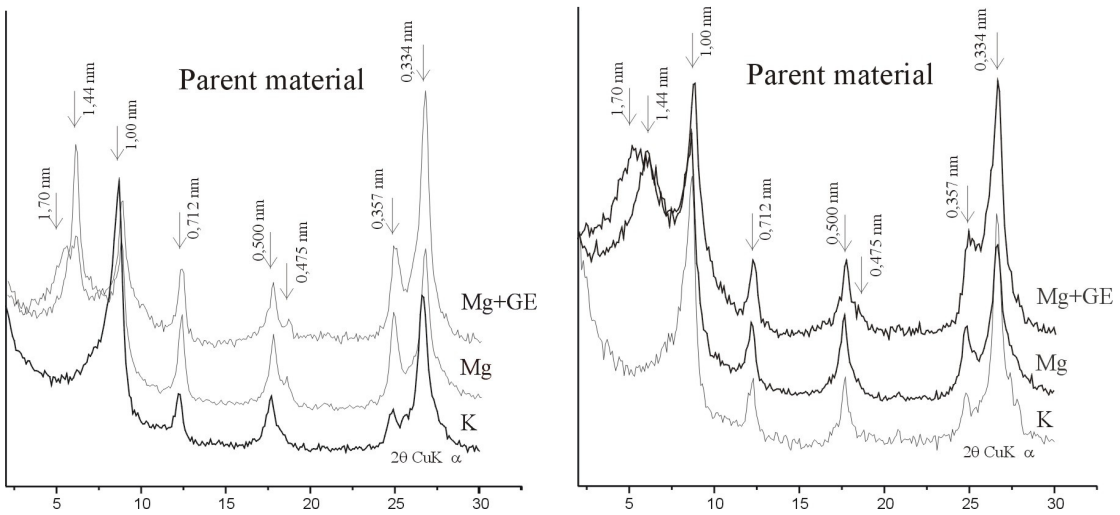

Figure 3. Diffractograms of clay fraction from parent material (glacial till)

Conclusion

The soils under study were characterized by significantly different mineralogical composition of the clay fraction. It was both of the profile and inter-profile nature. The distribution of the swelling minerals indicated a considerable effect of the fallowing process on their distribution. The occurrence of vermiculite minerals in some profiles suggested a inter-profile diversification. The investigations need further profound studies to learn more about the area and processes occurring there.

References

Allen BL, Fanning DS (1983) Composition and soil Genesis. In 'Pedogenesis and taxonomy. I Concepts interactions'. pp. 141-192 (Elsevier: Amsterdam, Oxford, New York)

Dlugosz J (2002) Differentiation of the composition of clay minerals in fine clay fraction (< 0.2 μm) of Alfisols formed from glacial till. (UTLS: The Bydgoszcz)

Dlugosz J, Kobierski M, Bartkowiak A (2009) Soils of the drawskie lake district formed from glacial till. In 'Soils of chosen landscapes'. (Ed B. Bieniek) pp. 37-50. (UWM: The Olsztyn)

Kłysz P (2001) Pomeranian phase of the last glaciation in the Drawskie Lakeland. *Polish. Geogr. Rev*. **73(**1-2), 3-24.

Righi D, Elsass F (1996) Characterization of soil clay minerals: Decomposition of X-ray diffraction diagrams and high-resolution electron microscopy. *Clay and Clay Miner*. **44**, 791-800.

Righi D, Raisanen ML, Gillot F (1997) Clay mineral transformations in podzolized tills in central Finland. *Clay Miner*. **32**, 532-534.

Determining impact of physical property for handling characteristics of bauxite ores

Naoko Zwingmann[A], Geoffrey Carter [A], Nobuo Tezuka [A], Robert Hart [B], Arie van Riessen [B], and Vladimir Golovanevskiy [A],

[A]Rio Tinto Centre for Materials and Sensing in Mining, Curtin University of Technology, Bentley, WA, Australia, Email N.Zwingmann@curtin.edu.au, G.Carter@curtin.edu.au, N.Tezuka@curtin.edu.au, V.Golovanevskiy@curtin.edu.au
[B]Applied Physics, Curtin University of Technology, Bentley, WA, Australia, Email R.D. hart@curtin.edu.au, A.vanRiessen@curtin.edu.au

Abstract
Within the bauxite/alumina industry wet and sticky ore classification has been elusive to pin point outside of full scale plant operations. By investing in plant modification and processing methods, operations groups have mitigated some of the problems arising from these ores. An initial investigation using SEM, TEM, optical microscopy methods, XRD, XRF and other physical methods has compared bauxite samples from the Weipa region of Queensland. The samples being investigated were classified as either wet and sticky or non-wet and sticky by operations groups. This investigation is a compare and contrast between these coarse classifications using a diverse range of techniques. Very few differences between the ores have been found, suggesting the problem is caused by quite subtle difference between the ores.

Key Words
Bauxite, problematic handling ore.

Introduction
As economic drivers dictate the exploitation of previously overlooked or the extension of existing ore bodies, the possibility of encountering problems in the handleability of ores increases. Often these ores are below the water table and are colloquially termed “wet and sticky” due to the prevalence for adhesive material building up on processing plant. This obviously reduces through put, increases wear and reduces service life of the plant, thus adding the cost of processing. Fortescue Metals Group recently reported problems with “wet and sticky” ores and high alumina content as being partially responsible for up to $400M in cost overruns at its Cloudbreak iron ore mine in Western Australia (West Australian, Thursday 30/4/09).

Significant intellectual investment has been made in learning how to mitigate such handling difficulties through processing plants. However as knowledge has advanced it may now be possible to develop greater understanding of the physics/mineralogy/chemistry behind why one ore may exhibit “wet and sticky” traits and why another does not. With such knowledge greater empowerment is offered to process managers in the control of such issues not withstanding the ability to make advanced decisions on the suitability of ore bodies for mining or even how much investment in processing plant is required.

A number of characteristics may play a part in the “wet and sticky” phenomena such as particle shape, size, mineralogy and chemistry of the major minerals in the bauxite. However mineralogical composition and the properties of those minerals can vary significantly within small areas of deposits (Sadlier and Gilkes 1976). This is particularly true for the ultra-fine clay minerals for example kaolin clays (kaolinite, halloysite) and iron oxides whose small size suggest they will make a large contribution to key properties such as, surface area and surface charge.

Methods
Samples
Four samples from the Weipa region of Queensland, the samples were classified as WS (wet and sticky) or NWS (non-wet and sticky) by the operations group. As received samples were cone-and-quartered to take representative samples this was achieved with out any pre-treatment such as sieving.

Techniques
The appearance of the as received samples was recorded using optical microscopy. Optical microscopy was conducted using an Olympus Stereo Microscope SZ60 magnification range: ×10 -×63 with Lumenera

Infinity Lite camera. The colour of the sample were determined by comparison with the Munsell® Soil Colour Charts (Munsell Colour Co. 2000) for the samples in the, as received, dried and powdered (ring-milled) states; comparisons were made on a white ceramic tile under daylight. Particle size distribution was determined using Endecotts calibrated sieves and sieve shaker. The bulk chemistry of the samples was determined by XRF of fusion beads developed using 12:22 flux with 1:10 sample to flux ratios using a Philips PW1404 Spectrometer. X-ray Diffraction of randomly oriented powder specimens was carried out using a Bruker D8 Advanced instrument using a LynXeye detector for a 2θ range of 5 to 80 degrees with a 0.02 degrees step size. Radiation was copper K_α with an accelerating voltage of 40kV and current of 40mA. Samples were prepared using a ring mill for 2.5 minutes. Patterns were analysed using EVA software. Scanning electron microscopy was carried out using Zeiss Evo 40XVP. Samples were prepared by platinum/palladium coating (thickness: 2nm). Stokes' law was used to separate the Clay (<2 μm) fraction from the remainder of the sample (Brindley and Brown 1980). The morphology of the minerals in the clay fraction was investigated by JEOL 2011 transmission electron microscope (TEM) operating at 200kV with an Oxford Instruments EDS.

Results

The Bauxites investigated are relatively uniform size ball shape materials (Figure 1) described as pisoliths after Taylor *et al.* (2008). The WS samples (Figure 1a) were wet and the surface of the pisoliths was coated with muddy materials, the texture of this "muddy material" is clearer in Figure 1c. The alternative NWS sample, both as received (Figure 1b) and dried (Figure 1d) show the surface of the pisoliths appears to be smooth. Table 1 summarises the colour of the bauxites which are red to light red in Munsell® Soil Colour classification (Munsell Colour Co. 2000).

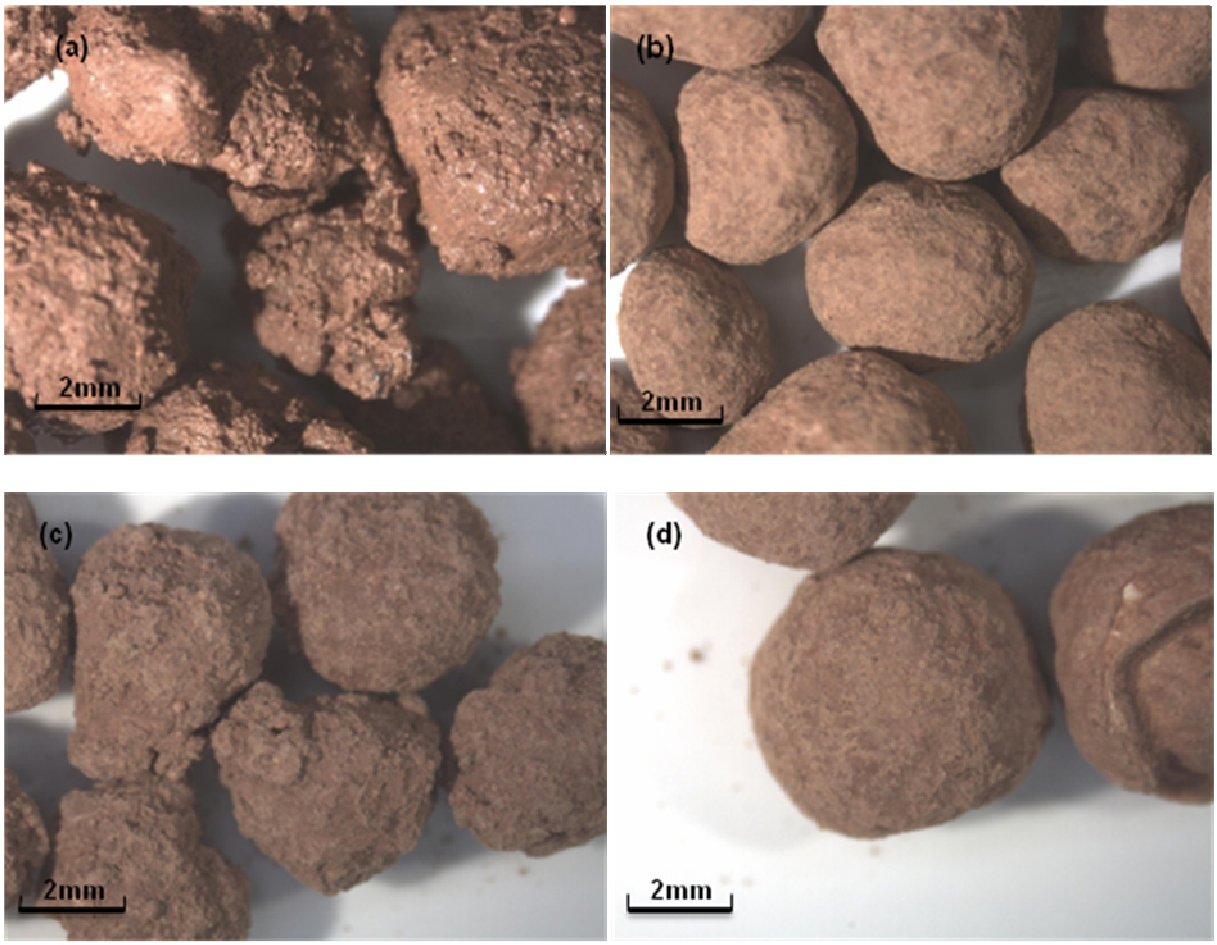

Figure 1. Appearance of bauxites; WS as received (a), NWS as received (b), WS dried (c) and NWS dried (d). Comparing to NWS bauxites, the surface of the WS bauxites is rough and covered with fine and large particles. The coating on the surface is clearer when bauxites is dried.

Table 1. The colour of WS (wet and sticky) and NWS (non wet and sticky) bauxites for "as received", "dried and "ring milled" sample.

	as received		dried		ring milled	
Sample Name	Munsell	colour	Munsell	colour	Munsell	colour
WS 1	10R4.5/6	red	2.5R5.5/6	red - light red	2.5YR5/6	red
WS 2	2.5YR4/6	red	2.5YR6/6	light red	2.5YR5/6	red
NWS 1	2.5YR5/8	red	2.5YR5/6	red	2.5YR5/8	red
NWS 2	2.5YR4/6	red	2.5YR6/6	light red	2.5YR5/6	red

XRD indicated that both types of bauxites contain gibbsite, boehmite, kaolin, hematite, and anatase. Quartz was detected in one of the NWS bauxites when analysing the whole sample. Additional goethite peaks became detectable for the <63µm sample for both type of bauxites. In addition the <63µm sample also has higher boehmite/gibbsite ratio across the sample set. Thus the mineralogy of WS and NWS bauxites are very similar.

The WS bauxites were found to have a pH of 6.3 while NWS, had pH 6.0 (solid: deionised water=1:5). Macroscopic particle size distributions of dried samples are presented in Figure 2.

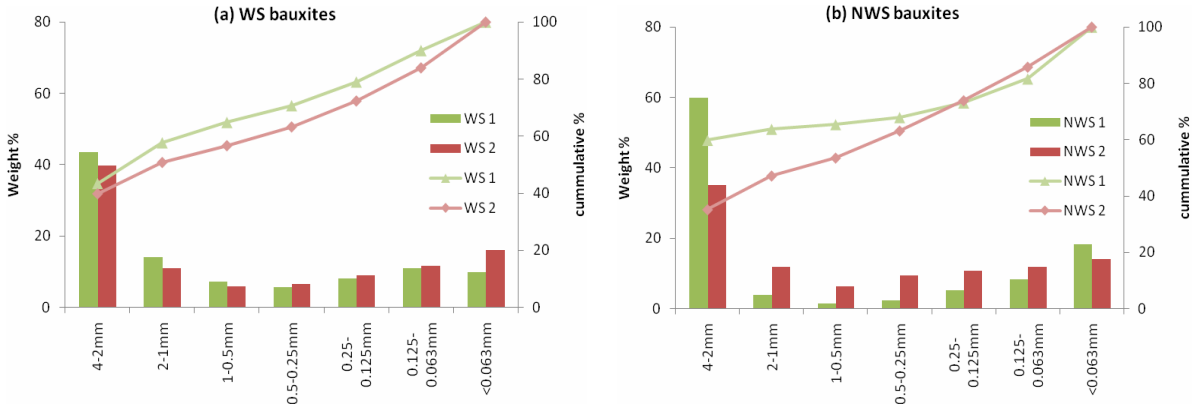

Figure 2. Macroscopic particle size distribution of dried WS (a) and NWS (b) bauxites. More than 40wt% of WS is larger than 2mm (granule size) particles. One of NWS is similar to WS, but 60wt% of NWS 1 is larger than 2mm and it contains very little coarse sand size (1-0.5mm) particles.

Table 2 shows the chemical compositions of bauxites as developed using WD-XRF. WS bauxites have slightly higher LOI at 1000°C, higher Al_2O_3 and TiO_2 while NWS bauxites have more SiO_2 and Fe_2O_3.

Table 2. Chemical composition of WS and NWS bauxites (mean values).

Sample	Al_2O_3	SiO_2	Fe_2O_3	TiO_2	K_2O	Na_2O	MgO	CaO	BaO
UNITS	%	%	%	%	%	%	%	%	%
WS mean	56.6	4.12	12.5	3.22	0.003	0.02	0.02	0.01	0.002
NWS mean	55.2	5.73	13.8	2.90	0.007	0.02	0.03	-0.01	0.002

Sample	V_2O_5	Cr_2O_3	MnO	ZrO_2	P_2O_5	SO_3	LOI_{1000}	Sum
UNITS	%	%	%	%	%	%	%	%
WS mean	0.034	0.023	0.03	0.121	0.058	0.05	23.3	100.0
NWS mean	0.038	0.030	0.02	0.118	0.062	0.05	21.9	100.0

Figure 3 (a) and (b) show SEM secondary electron micrographs for both the WS and NWS respectively. These micrographs are of the <63µm cut of samples after dry-sieving. WS samples tended to be covered by fine components adding complexity to EM examination, whilst NWS often show well crystallised surface which may be gibbsite.

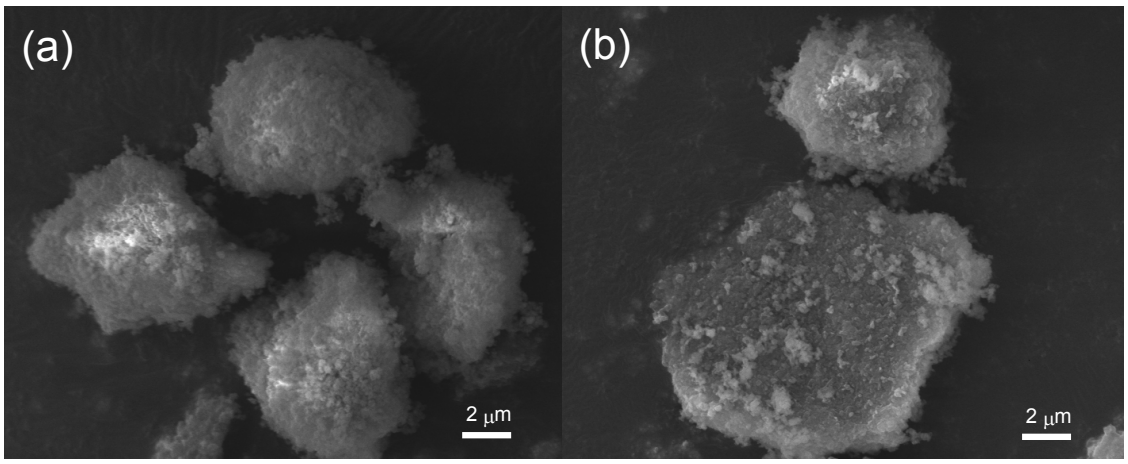

Figure 3. SEM secondary electron images of WS (a) and NWS (b) bauxites. The surfaces are covered with fibrous and fine particles.

TEM observation of the clay size fraction shows that the WS and NWS are similar, however, individual rectangular shaped crystals can be observed more clearly in WS (Figure 4 a) than in NWS samples (Figure 4 b).

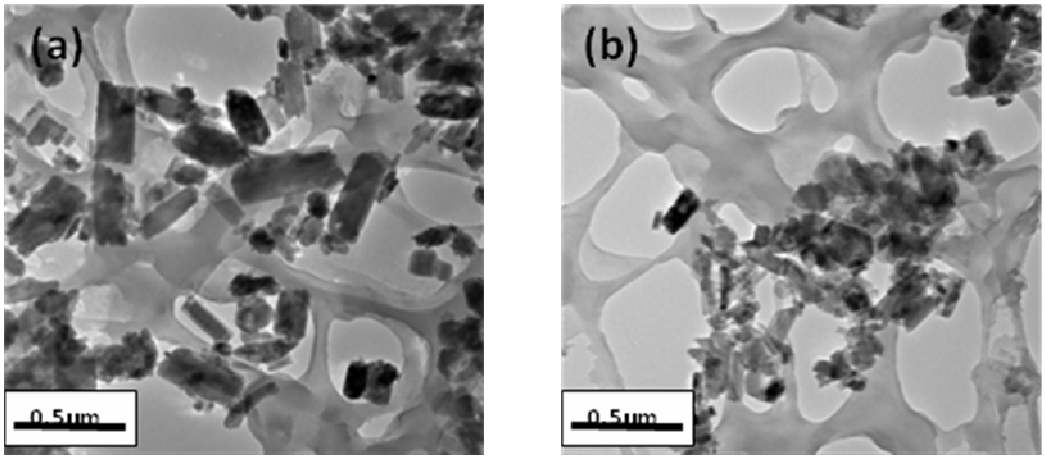

Figure 4. TEM images of WS (a) and NWS (b) bauxites of the clay size (<2μm) fraction.

Conclusion

At this stage, few differences in properties other than handleability between the WS and NWS bauxites were determined. This suggests that the properties are determined by quite subtle difference between the ores and that more detailed investigation and/or additional properties which might be related to handling problems is required.

Acknowledgement

The authors would like to thank Ms. Elaine Miller (Curtin University) for her assistance. We would like to thank Rio Tinto Technology and Innovation as well as Rio Tinto Alumina for their support for this work.

References

Brindley GW, Brown G (1980) 'Crystal structures of clay minerals and their X-ray identification'. Mineralogical Society Monograph No.5. (Mineralogical Society: London)

Munsell Colour Co. (2000) 'Munsell® Soil Colour Charts – Year 2000 revised washable edition'.

Sadlier S B, Gilkes R J (1976) Development of bauxite in relation to parent material near Jarrahdale, Western Australia. *Journal of the Geological Society of Australia* **23,** 333-344.

Taylor G, Eggleton RA, Foster LD, Tilley DB, Le Gleuher M, Morgan CM (2008) Nature of the Weipa Bauxite deposit, northern Australia. *Australian Journal of Earth Sciences* **55**, S45-S70.

Development of Halloysite/Smectite Mixed Layer Mineral in Paleudult of Java Island

Mohammad Nurcholis

Department of Soil Science, Univ. Pembangunan Nasional "Veteran" Yogyakarta
Jl. Lingkar Utara Condongcatur Yogyakarta Indonesia, 55283
Personal communication: M Nurcholis nurch2003@yahoo.com

Abstract
This study was initiated to investigate the development of unique kaolin/smectite mixed layer minerals in the Paleudult of Java Island. The present study was aimed to identify the kaolin minerals and to understand the development of the kaolin/smectite mixed layer. Clay fraction samples were collected from the Paleudult profile. Selective dissolutions using dithionite citrate bicarbonate, NaOH, and Na-citrate treatments were conducted on the clay fraction. The result showed that free iron oxide content increased with the depth. Halloysite which showed a 7.6 Å peak on the X-ray diffraction (XRD) was confirmed by the hot NaOH extraction. SiO_2/Al_2O_3 molar ratio from the hot-citrate extracts provided the halloysitic property only in the upper horizons. However, the peaks of 10-14 Å on the XRD collapse at 300^oC following the hot citrate treatment suggesting that crystallinity of the halloysite mineral is weak. This halloysite mineral developed well in the upper horizons. The development of halloysite/smectite mixed layer is proposed in the four stages.

Key Words
Halloysite, development of halloysite/smectite mixed layer.

Introduction

Smectite minerals are found in several acidic soils such as Red-yellow Podzolic Soils in Java Island. The formation of smectite minerals in this area might be resulted from ejected materials from activities of several volcanoes in the past. These materials were then deposited in the sea and further weathering processes resulting smectite minerals. Geological processes might lead an uplift of the sea floor to be terrestrial and then developed soils. McDaniel (1995) reported the presence of beidellite in the E horizon in Spodosols that developed on volcanic ash in Northern Idaho.

Hydroxyl-Al interlayered vermiculite mineral was found in some Ultisols in Indonesia (Goenadi and Tan 1988; Supriyo *et al.* 1992). They described that this minerals showed 14.02 Å peak on the XRD on the Mg^{2+}-saturated clay and glycerol solvation, and the peak was gradually collapsed for K^+-saturated clay and following subsequent heating treatments. Rich (1960) mentioned the interlayering process of aluminum in the interlayer space of expansible 2:1 minerals. Transition of smectite to chlorite that resulted from geothermal alteration was reported by Robinson and de Zamora (1999). Kaolin/smectite mixed layer was identified in the clay fraction of the Paleudult developed on dacitic-andesitic tuffs from Jasinga Subdistrict Bogor Regency West Java Province Indonesia (Nurholis and Tokashiki 1998).

The objectives of the study were: (i) to identify the kaolin minerals in the kaolin/smectite mixed layer minerals, and (ii) to understand the development of this kaolin/smectite mixed layer minerals in the soil profile of the Paleudult.

Materails and Methods

The studied soils were the Paleudult, developed from volcanic materials, at Jasinga subdistrict, Bogor regency, West Java province. Five soil samples were collected from each horizon that developed in the soil profile. Soil texture was analyzed using mechanical analysis after oxidizing the organic matter using H_2O_2. The coarse and fine sand, silt and clay fractions were separated and collected for mineralogical studies. The fine sand fraction was then analyzed the primary mineral composition using XRD. The clay fraction was then pretreated using dihionite citrate bicarbonate (DCB) using Mehra and Jackson (1960) method. Formamide treatment was conducted to identify the kinds of kaolin minerals. Successive dissolutions were done to identify the properties and kinds of mineral that compose the clay specimens. Hot NaOH treatment was done on the DCB pretreated clay to extract kaolin mineral (Tokashiki *et al.* 1986). The extractable Si and Al elements were then determined using an inductively couple plasma spectrophotometer (ICPS). Sodium citrate treatment (Tamura 1958) was conducted on the residual clay after NaOH-DCB treatment. In

the same way, the extractable Si and Al were then determined using ICPS. The residual clays were then analysed mineralogical properties using XRD.

Results

Lithologic discontinuity

Table 1 shows the primary minerals identified using XRD for fine sand and silt fractions. Integrated intensity of feldspar and amphibole increased with the depth, except feldspar decreased in B3 horizon, on the contrary quartz decreased with the depth. Based on the Goldich stability series, amphibole is more stable than feldspar. Feldspar was only detected in the A horizon. Feldspar was still detected in the 2B horizon. Anatase was detected in the silt fraction in all horizons and it showed increase with the depth. Free iron oxides slightly increased from the surface horizon to B3 horizon, and slightly increased in 2B horizon. According to the results it can be stated that the soil profile exhibited lithologic discontinuities, as there was a different in the mineralogical composition in the fine sand fraction.

Table 1. The primary minerals identified using XRD of the fine sand and silt fractions

Horizon	Fine sand			Silt		
	Feldspar	Amphibole	Quartz	Feldspar	Quartz	Antase
	Integrated intensity fraction*					
A	0.07		0.93	0.07	0.89	0.10
Bl	0.12	0.05	0.83		0.89	0.11
B2	0.23	0.05	0.72		0.86	0.14
B3	0.07	0.19	0.72		0.86	0.14
2B			1.00	0.12	0.71	0.17

*relative value among the detectable minerals

Halloysite/smectite miexed layers

Figure 1 shows the XRD pattern of the clay fraction of the soil A horizon as a representative result for five clay samples. The Mg saturated clay showed 15.9 Å and 7.6 Å peaks. NaOH treatment resulted in a collapse of the 7.6 Å peak. Glycerol solvation resulted in swelling the peak of 15.9 Å to 19.64 Å, whereas the 7.6 Å peak changed from a relatively sharp peak to a broad peak. K saturated clay showed a change in the 15.9 Å peak of the Mg saturated clay to a broading of the 12.1 Å peak accompanied with a continuous form between 7.6 Å and 12.1 Å. Formamide solvation resulted in a shift of the 7.6 Å peak to 9.72 Å. Accordingly, it is suggested that the 7.6 Å peak is halloysite.

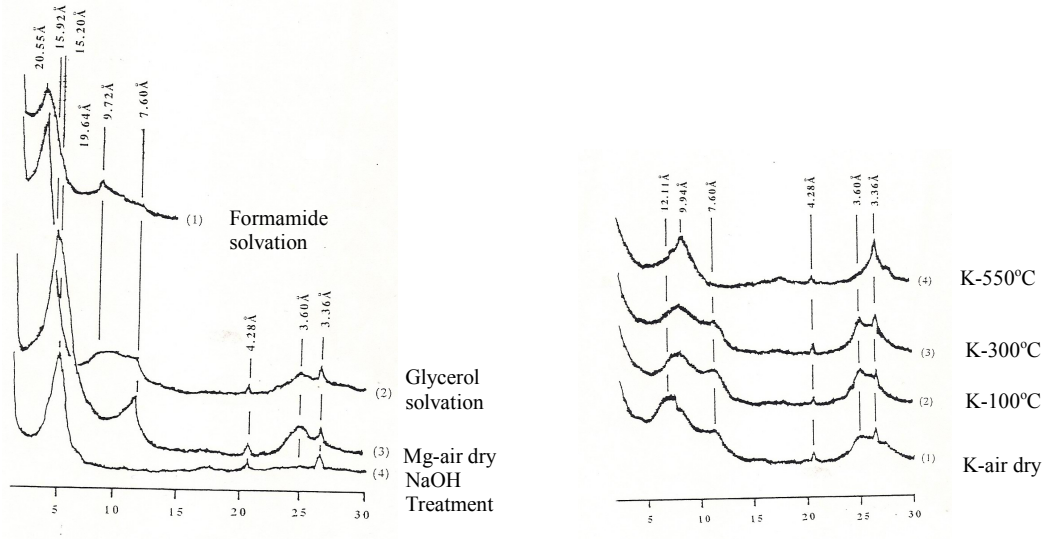

Figure 1. The XRD pattern of the clay fraction of the soil at A horizon

Development of the halloysite/smectite mixed layers

Table 2 shows the results of the successive dissolution using hot NaOH and hot citrate extraction. The hot-NaOH extraction resulted in the SiO_2/Al_2O_3 molar ratio of 2.29 for the A horizon and increased from A to B2 horizon and then decreased for the following B3 and 2B horizons. According to Tan and Troth (1982), the extracted material is kaolin minerals, and for the present study is halloysite. Prolonged hot-citrate extraction

was successfully used to identify the interlayer materials in hydroxyl-Al interlayered vermiculite (Nurcholis 2003). The hot citrate extractable SiO_2 and Al_2O_3 resulted in the SiO_2/Al_2O_3 molar ratio of 2.83 for the A horizon, and the highest value was for the B2 horizon. The value of the SiO_2/Al_2O_3 molar ratio resulting from the hot citrate extraction is too high for halloysite. It is probably that prolonged hot citrate extraction also caused the destruction of the crystals of whole minerals. The lithologic discontinuity in the studied soil profile might also contribute to the variation in materials.

Table 2. Dissolution of silica and alumina and silica/alumina molar ratio by the NaOH treatment for the DCB pretreated clays

Horizon	NaOH extraction on the DCB pretreated clay			Hot-citrate extraction on the NaOH-DCB pretreated clay		
	Al_2O_3 mg/g	SiO_2	SiO_2/Al_2O_3 molar ratio	Al_2O_3 mg/g	SiO_2	SiO_2/Al_2O_3 molar ratio
A	58.75	79.37	2.29	1.93	3.22	2.83
Bl	67.71	90.91	2.28	1.49	2.08	2.36
B2	62.62	96.09	2.60	1.81	3.70	3.46
B3	67.17	96.09	2.43	1.54	2.95	3.25
2B	61.06	72.71	2.01	1.62	2.98	3.31

Conclusion

According to the results, it is possible to propose a mechanism of the development of halloysite/smectite mixed layer in four stages, as follows: the first stage is designated with the deposition of quaternary volcanic ash under the sea environment and it was diagenetically altered to smectite minerals. The second stage is gradual transgression of the sea, weathering and soil genesis processes. The third stage is Al-OH growth in the interlayer space of smectite mineral as hydroxyl-interlayered smectite. And the fourth stage is an inversion of a portion of the Si tetrahedral sheets of smectite mineral and halloysite which are then separated as free forms, and there is an arrangement of halloysite-smectite layers.

References

Goenadi DH, Tan KH (1988) Differences in clay mineralogy and oxidic ratio of selected LAC soils in temperate and tropical regions. *Soil science* **146**, 151-159.

McDaniel PA, Falen AL, Tice KR (1995) Beridelite in E horizon of Northern Idaho Spodosols formed in volcanic ash. *Clays and Clay Minerals* **43**, 525-532.

Mehra OP, Jackson ML (1960) Iron oxide removal from soils and clays by a dithionite citrate system buffered with sodium bicarbonate. *Clays and clay Minerals* **7**, 317-327.

Nurcholis M, Tokashiki Y (1998) Characterization of kaolin/smectite mixed layer mineral in Paleudult of Java Island. *Clay Science* **10**, 291-302.

Nurcholis M (2003) Identification of interlayer materials in the Hydroxy Interlayered Vermiculite. In 'Proceedings International conference on Mineral and energy Resources Management'. (Eds Sutarto) pp. 127—134. (UPNVY Press)

Rich CI (1960) Aluminum in interlayer of vermiculite. *Soil Science Society of America Proceeding* **24**, 26-32.

Robinson D, de Zamora AS (1999) The smectite to chlorite transition in the Chipilapa geothermal system, El Salvador. *American Mineralogist* **84**, 607-619.

Supriyo H, Matsue N, Yoshinaga N (1992) Chemistry and mineralogy of some soils from Indonesia. *Soil Science and Plant Nutrition* **38**, 217-225.

Tamura T (1958) Iderntification of clay minerals from acid soils. *Journal of Soil Science* **9,** 141-147.

Tan KH, Troth PS (1982) Silica-sesquioxides ratios as aids in characterization of some temperate and tropical region. *Soil Science society of America Journal* **46,** 1109-1114.

Tokashiki Y, Dixon JB, Golden DC (1986) Manganese oxide analysis in soils by combined X-ray diffraction and selective dissolution methods. *Soil Science society of America Journal* **50**, 1079-1084.

Effect of earthworms on nutrients dynamics in soil and growth of crop

Srinithi Mayilswami[A] and Brian Reid[B]

[A]School of Environmental Sciences, University of East Anglia, Norwich, NR4 7TJ, UK

Abstract
Effects of earthworms especially with Lumbricus terrestris on nutrients dynamics and on plant growth were studied in the laboratory. Soil was amended with varied levels of compost and earthworms were introduced: 60.9 g soil alone, 60.9 g soil + 20.78 g compost (60:40), 60.9 g soil + 41.57 g compost alone (80:20) and 41.57 g compost alone. The ion chromatography data showed there was significant variation in the nutrient status mainly nitrite, nitrate, ammonium and phosphate between the treatments (with worms) and control (devoid of worms). The significant variation in nitrite concentration was observed in treatment containing 60.9 g soil+ 20.78 g compost which was around 6.32 (mg/kg). Phosphate concentration was predominant in treatment having 41.57 g compost alone with 23.855 mg/kg concentration. The amount of ammonium varied slightly, though major concentration around 6.90 mg/kg was observed in treatment with 41.57 g compost alone. The difference in nutrient status appeared to be due to the variations in nutrient cycling probably ascribable to the earthworm's activities.

Pot experiment showed that the mustard plant growth was stimulated by earthworms digging capacity. The germination percentage, shoot length, root length and fresh biomass were determined. The variation between treatments and controls were measured. The average germination percentage in treatment containing 60.9 g soil + 20.78 g compost was 75.83 which was more significant, also accounts 8.51 cm and 3.5 cm shoot length and root length respectively. The total fresh biomass was measured to be 1.96 g more suggestive compared to controls. These modifications emerged due to the active participation of earthworms in stirring of soil.

Keywords
Bioremediation; soil; earthworm; nutrient; plant growth.

Introduction

Earthworms activities are deciding factors of soil fertility, its effect can be measured by various factors accordingly with time and space (climate, edaphic characters, and organic inputs). Earthworms exhibit Dilosphere concept to take part in soil function, which is a combination of earthworms, physical structures, whole microbial and invertebrate community. Earthworms induce microbial activities which inturn promotes organic matter processing and nutrient cycling.

Earthworm modify atmosphere apart from nutrient availability. Root feeding and dispersion of seed are some of the direct effects on plant growth by earthworms. Some of the indirect effects are alteration in soil properties, circulation of microbes and dissemination of microbes antipathetic to the root pathogens. Earthworms also help in breakdown of seed dormancy by gut passage and control the dispersion of organic matter which affects root foraging. It's also proved that effect of earthworm increases the nutrient composition in plant tissues (Stefan Scheu 2002). In the current study we investigated the role of earthworm in promoting nutrient status and plant growth.

Methods

Measurement of nutrients
Soil extraction with water is theoretically appropriate for nitrate that is very soluble, but for the inorganic forms of N not applicable. Therefore 0.5 mol/L potassium sulphate solution which enables solubility of calcium sulphate or potassium chloride for extraction of ammonium ions are recommended (Marc Pansu *et al*. 2006). Due to high sensitivity of IC apparatus extractions were carried out using Milli Q water.

Measurement of nutrients in soil
A 4 g soil was taken in centrifuge tubes from each treatments and 40 ml of Milli Q water was added. The tubes were placed in the mechanical shaker for overnight to ensure the solubility of ions. The tubes were placed in centrifuge and rotated for 15 min to get clear supernatant. The supernatant is collected and filtered using the millex filter and 10 ml from filtrate was taken to IC for measurement of nitrite (NO_2) and nitrate (NO_3).

Pot culture
Simultaneously mustard (white) seed were sown in the treatment beakers to examine the efficiency of plant growth with and without earthworms. Twenty seeds were placed in each beaker. To have clear idea of germination, the seeds were placed over the wet moisture filter paper over the soil surface and watered continuously for 15 days. The germination percentage; average shoot, root length and biomass were measured.

Results and Discussion
The initial characteristics of the soil and compost were calculated before the experiment started and given in Table 1. After 15 days the seeds in each treatment were germinated, the parameters like germination %, biomass, shoot and root length were calculated and presented in Table 2.

Table1. Initial characteristics of soil and compost:

Sl. No.	Characteristics	Soil	Compost
1.	pH	5.5	6

Only ph of the soil and compost was calculated.

Table2. Effect of earthworms and compost on growth of mustard

Sl. No.	Treatments	Without earthworms				With earthworms			
		Germination (%)	Biomass (g)	Shoot length (cm)	Root length (cm)	Germination (%)	Biomass (g)	Shoot length (cm)	Root length (cm)
1.	Soil alone	41.67	1.22	6.15	2.10	61.67	1.75	8.11	3.08
2.	Compost alone	54.17	1.66	7.25	2.51	60.83	1.91	7.98	2.92
3.	Soil + compost at 60:40 ratio	55.00	1.65	8.12	3.10	75.83	1.96	8.51	3.50
4.	Soil + compost at 80:20 ratio	58.33	1.92	7.61	2.72	65.00	1.92	8.32	3.30

Table3. Nutrients concentration in soil as affected by earthworms and compost

Sl. No.	Treatments	Without earthworms(mg/kg)				With earthworms(mg/kg)			
		Nitrite NO_2	Nitrate NO_3	Ammonium NH_4	Phosphate PO_4	NO_2	NO_3	NH_4	PO_4
1.	Soil alone	0.4999	17.51	0.416	1.0847	2.4218	19.543	5.27	3.623
2.	Compost alone	NA	NA	1.405	23.7133	0.9123	39.831	6.905	23.855
3.	Soil + compost at 60:40 ratio	0.4969	71.755	1.0991	9.723	6.327	4.734	4.668	12.116
4.	Soil + compost at 80:20 ratio	0.3235	102.492	1.506	11.85	0.816	28.012	0.728	7.843

The results from an Ion chromatography was calculated and given in Table 3. In total the ion chromatography calculated the value for many ions namely Fluoride, Chloride, Nitrite, Bromide, Nitrate, Sulphate, Oxalate, Phosphate, Sodium, Ammonium, Potassium, Magnesium and Calcium. Since the present experiment was concentrated on nitrite, nitrate, ammonium and phosphate only those values are recorded.

According to Lee 1985, the burrowing capacity of earthworms can be modified by the number of earthworms and other agricultural practices undertaken in the land area managed to reach more than 100 square metres. The digging capacity of earthworms play vital role in nutrient cycling and enriching the soil. In the present study the varied result may be due to the minor population of earthworm in each treatment. Due to the space constraint only two earthworms were accommodated in each treatment. Even though *L.terrestrics* is surface feeders which prefer organic matter to a greater extent and influence the nutrient status. Experiment conducted by Barley and Jennings (1959) with *A.caliginosa* species resulted in 129 ppm of nitrate and ammonium in 50 days where as treatments without earthworms resulted only 105 ppm (Edwards *et al*. 1977). The present study resulted in related solution with increased in quantity of ammonium, but the concentration of nitrite was not increased in treatments. This may be due to time constraint since the experiment was ran only about one month where as the previous experiment was extended upto 50 days. But remarkable variation was absorbed in nitrate concentration, which was increased in all treatments.

Conclusion

Earthworms are now greatly relied for increase in crop yield in the intensive agriculture system. Commercial production of earthworms started to gain popularity nowadays due to various studies which proved the efficiency of earthworms. From the current experiment, it is concluded that earthworm plays vital role in altering the nutrient composition in soil and promote plant growth. The earthworm activities clearly accelerate the nutrient release and sequential uptake of nutrients.

Acknowledgement
The authors are greatly indebted to the University Of East Anglia for providing CEEC Lab and equipments to complete this experiment successfully. Finally we thank all the lab technicians for their immense support and guidance rendered to finish this project.

References

Lavelle P (1988) Earthworm activities and the soil system. *Biol Fertil Soils* **6**, 237-251.
Syres JK, Springett JA (1984) Earthworms and soil fertility. Department of Soil Science, Massey University, and Ministry of Agriculture and Fisheries, Palmerston North, New Zealand, *Plant and Soil* **76**, 93-104.
Stefan Scheu (2002) Effects of earthworms on plant growth: patterns and perspectives. The 7th International Symposium on Earthworm Ecology, Cardiff, Wales, Submitted September 6.
Marc Pansu, Jacques Gautheyrou (2006) Handbook of soil analysis, mineralogical, organic and inorganic methods. Springer-Verlag Berlin Heidelberg, pp 597-598
Edwards CA, Lofty JR (1977) Biology of Earthworms. Chapman and Hall. A Halsted Press Book.
Lunt HA, Jacobson GM (1944) The chemical composition of earthworm casts. *Soil science* **58**, 367-376
Laverack MS (1963) The physiology of earthworms, Pergamon press
Spider GA, Gagnon D, Nason GE, Packee EC, Lousier JD (1986) Effects and importance of indigenous earthworms on decomposition and nutrient cycling in coastal forest ecosystem, pp.983-989.
Haimi J, Einbork ME (1991) Effects of endogeic earthworms on soil processes and plant growth in coniferous forest soil. *Biol Fertil Soils* **13**, 6-10.
Edwards CA, Lofty JR (1976) Effects of earthworm inoculation upon the root growth of direct drilled cereals. *Journal of applied ecology* **17**, 533-543.
Atlavinyte O, Bagdonaviciene Z, Budaviciene (1968) The effect of Lumbricidae on the barley crops in various soils. *Pedobiologia* **8**, 415-423.
Graft O, Makeschin F (1971) Crop yield of ryegrass influenced by the excretions of three earthworm species. *Pedobiologia* **20**, 176-180.
Barley KP, Jenings JP (1959) Earthworms and soil fertility: The influence of earthworms on the available nitrogen. *Australian journal of Agricultural research* **10**(3), 364- 370.
Bhadauria T, Ramakrishnan PS (1991) Population dynamics of earthworms and their activities in forest ecosystems of north east India. *Journal of Tropical Ecology* **7**, 305-318,

Effect of exhaustive cropping on potassium depletion and clay mineral transformations

Ghorbanali Roushani[A]

[A]Department of Soil and Water, Golestan Agricultural Research Center, Gorgan, Iran, Email gh_roshani@yahoo.com

Abstract
Identification of various clay minerals and their changes in the clay fraction of soil samples of 3 types of Indian soils before and after depletion of K by exhaustive cropping by growing Sudan grass (*Sorghum vulgare)* was done on the basis of strongest XRD peaks from basal planes. Sudan grass was grown in clay pots containing 5 kg of three types of soils from India and potassium was applied at the rate of 0, 50, 100, and 200 mg /kg before starting the experiment and after each of the first three cuttings. Seven cutting of Sudan grass were taken over a period totalling 280 days, each time the forage was grown for 4-6 weeks. It has been observed that, permanent removal of K from Illite-dominating soils leads to the degradation of Illite with its transformation to expandable or non-expandable minerals and decrease in Illite content was high in Vertisol (46%), medium in Alfisol (33%) and low in Inceptisol (14%)**.** There was a decrease in intensity of peak at 10 Å resulting in degradation of illite due to permanent removal of potassium ions by plants from inter-layers of clay lattice. This proved the formation of vermiculite, chlorite and smectite.

Key Words
K exhaustion, K depletion, clay mineralogy, and exhaustive cropping.

Introduction

The clay fraction was analyzed for semi-quantitative composition by X-ray diffraction following the method of Gjems (1967). Intensive cropping of soils without application of K-fertilizers may lead to a degradation of Illite as has been shown by Boguslawski and Lieres (1981) in a soil derived from loess. Ross *et al.* (1985) conducted a six-year field manure application experiment and found the transformation of vermiculite to pedogenic mica by fixation of potassium and ammonium. Potassium fixation caused a marked increase in the 1.0 nm peak at the expense of the 1.4 nm peak due to collapse of vermiculite layers to form pedogenic mica.

Mutscher and Tran Vu (1988) reported that biological depletion of potassium decreases the K concentration in the soil solution and induces the release of inter-layer potassium (K_i). Due to the massive decrease of the K concentration directly near active roots, easily releasable K_i takes part in the K supply even if the potassium concentration of the bulk soil solution and the average contents of exchangeable K are still high. Permanent removal of K from Illite-containing soils leads to the degradation of Illite and transformation of smectite and interstratified minerals. On natural habitats such K removal from the surface soil layer may be brought about by leaching. In cultivated soils large amounts of K are removed from the soil clays by plants. If the resulting K deficit in the soil is not balanced by K fertilizer application a degradation of clay minerals, especially Illite, will proceed. Thus, the growing plant seemed to be very effective in promoting the alteration clay minerals.

Tributh *et al*. (1987) studied the effect of potassium removal by crops on transformation of illitic clay minerals in soils from long-term field experiments and exhaustive cropping pot experiments. X-ray diffraction analysis of soil samples revealed that cropping without K fertilizer application had led to a substantial decrease in illitic content and to an increase of smectite and interstratified Illite / smectite minerals.

Materials and methods

Effect of continuous and exhaustive cropping on clay mineral changes due to K depletion was studied by X-ray diffraction analysis. Soils were dispersed and fractionated to separate clay fraction according to Jackson (1956). The mineralogy of the clay fraction is conveniently assessed separately, following pretreatment and separation of the fractions using the methods of particle-size analysis. This study was carried out on 3 types of Indian soils, namely Inceptisol (Delhi), Alfisol (Bangalore), and Vertisol (Bhopal), before and after high and moderate K exhaustion by Sudan grass to examine the effect of continuous exhaustive cropping on clay mineral changes due to K depletion. Sudan grass crop was grown in properly sealed 8-kg capacity clay pots

containing 5 kg of three types of soils, namely Alfisol, Vertisol, and Inceptisol from India and placed randomly in greenhouse and seven cuttings of biomass were harvested periodically. Measured quantity of deionized water was applied to the pots depending on the amount of evapo-transpiration which was calculated by daily weighing method. Twenty seeds of Sudan grass (*Sorghum vulgare* var. sudanensis) were sown in each pot. After 12 days of sowing, thinning was done to retain eight healthy plants per pot to ensure enough dry matter production and potassium removal from the soil. In order to study the effect of different levels of K exhaustion on potassium dynamics, pots were divided into four sets, receiving different potassium doses as fertilizer. Before sowing the crop, optimum doses of nitrogen (50 mg /kg), phosphorous (30 mg /kg), copper (2 mg /kg), manganese (5 mg /kg), iron (10 mg /kg), and zinc (5 mg /kg) were applied as basal and these nutrients were also supplied at the same rate after 1st, 2nd, and 3rd cutting. Potassium was applied at the rate of 0, 50, 100, and 200 mg /kg before starting the experiment and after each of the first three cuttings. Urea, di-ammonium phosphate and potassium chloride served as source of N and P, and K respectively, while the micronutrients were applied in their sulphate form. Treatment combinations were:

Type of soils (Inceptisol, Vertisol, and Alfisol)	: 3
Potassium treatments	: 4
Total number of treatments	: $3 \times 4 = 12$
Replication	: 6
Total number of pots	: 72

Sudan grass was harvested 7 times (totally 280 days) at a height of about three centimeters above soil level at 4-6 weeks intervals. After each cutting, small quantity of representative soil sample was also collected from each pot with a tube auger. After air drying, the soil samples were crushed using a wooden mortar and pestle and passed through a 2 mm round hole sieve and kept for chemical analysis. A 30 g of soil sample was treated chemically to remove cementing materials like carbonate, organic matter, free iron oxide and free silica by following the various pretreatments as outlined by Jackson (1967). Sand fraction was separated by wet-sieving (300 mesh) of the dispersed soil and dry weight of that was calculated. The upper 10 cm mixture of silt + clay was siphoned off at 8 h intervals for separation of clay from mixture. Silt fraction was dried and weighed and finally each fraction was expressed as a percentage of the total to obtain particle size distribution. The clay suspension (in NaCl) containing sufficient clay to give 10 mL of 2 % clay, was washed first with distilled water to remove excess of NaCl and was then saturated with Mg and K using normal solution of $MgCl_2$ and KCl by repeated centrifugation. The Mg and K saturated clays were then made electrolyte free using distilled water and alcohol, and were stored as 2 % clay suspension. Parallel oriented-aggregate clay specimens were prepared by taking 2 mL of the 2 % suspension on 2.5 cm x 4.0 cm glass slides, in duplicate, on a level surface and air dried These slides were then subjected to X-ray diffraction analysis by using Cu-K_α radiation and Ni filter in a X-ray diffractometer (Philips PW 1710). The different treatments given to the clay specimen prior to analysis as follows: (i) K-saturated air dried, (ii) K-saturated heated to 550°C, (iii) Mg saturated and (iv) Mg-saturated glycerol solvated.

From the X-ray diffractograms, the Ɵ values were obtained, which were used in calculating "d-spacing", and were used in characterizing the soil clays, into its component clay minerals. X-ray profile was fitted using automated powder diffractometery software package and peak area was calculated from the fitted profile. A semi-quantitative estimation of the minerals was done by following the procedure as described by Jackson (1956). For semi-quantitative estimation, the peak size of the first order basal reflection is determined. The peak area is divided by a factor for each clay mineral to give the corrected intensity (Table 1). After measuring the peak area of any particular mineral and division of area by its own correction factor, all the areas were added up and made up to 100. The amount of conversion coefficient will be 100 / sum of peak areas, and with multiplication of peak area of the mineral into conversion coefficient, the per cent of that mineral can be obtained. After correction of area, the amounts of minerals were estimated in proportion to their corrected area.

Results and discussions

Quantitative analysis of clay minerals in soil is more difficult to carry out than qualitative analysis. The reflections of mixed-layer minerals are usually found between those of the pure compounds and this further complicates the interpretation of data. X-ray diffraction analysis was carried out on soil clay samples subjected to the following treatments: (a) K-saturated and air dried; (b) K-saturated and heated at 550°C; (c) Mg-saturated and air dried, and (d) Mg-saturated and glycerol solvated. To obtain glycerol solvated samples,

Table 1. Correction factor for peak intensity.

Mineral	Factor
Illite	1
Pyrophillite	1
Kaolinite	1
Chlorite	1
Vermiculite	3
Montmorillonite	4
Mixed layer minerals	2

the Mg-saturated clay samples were sprayed with 10% glycerol solution in ethanol. These pre-treatments are necessary for distinguishing the various clay minerals present in a clay sample. The X-ray diffractogram of the samples obtained after various pretreatments are presented in this chapter and the c-spacing [d (00l)] representing prominent reflections of the clay mineral present in each soil are described below:

X-ray diffractogram of Inceptisol clay (Mg-saturated and glycerol solvated) showed four peaks at 19, 14.4, 10, and 7.1 Å, which indicated the presence of smectite, vermiculite, and kaolinite in the clay. The peak of 7.1 Å suggested the presence of kaolinite which was confirmed by the diffractogram of the same sample obtained after pretreatment of K-saturated and heated at 550°C. The clay samples which have been separated from the original Inceptisol and from the same soil after exhausting the soil K to high level by Sudan grass were subjected to this type of analysis.

Vertisol clay contained predominantly smectite as shown by a broad peak in the X-ray diffractogram of Mg-saturated and air-dried sample at 14.9 Å, and Mg-saturated and glycerol solvated sample at 17.6 Å. This peak shifted to 12.5 Å on K-saturation (air dried). The other peak in Mg-saturated and glycerol solvated sample at 10.1 and 7.1 Å showed the presence of Illite and kaolinite as confirmed from the diffractogram of the same sample treated with K and heated at 550°C. The general patterns shown by clay sample from highly K exhausted Vertisol was almost same with the original soil but the differences in the semi-quantitative estimates are presented in Table 2.

The clay from Alfisol exhibited three peaks at 13.6, 10.2 and 7.1 Å with Mg-saturated and glycerol solvated clay which indicated the presence of vermiculite, Illite, and kaolinite in the sample. The decrease in Illite content due to K depletion was high in Vertisol (46%), medium in Alfisol (33%) and low in Inceptisol (14%). It is evident from the data presented in Table 2 that permanent removal of K from Illite-dominant soils leads to the degradation of Illite. From the semi-quantitative analysis it is confirmed that percentage of Illite decreased due to its exhaustion by plant uptake of K. Although there was an increase in percentage of kaolinite, vermiculite and smectite, it is not certain that the Illite has transformed to kaolinite, vermiculite and smectite. Increase in the calculated value of percentage of kaolinite might be due to the fact that intensity of x-ray diffraction depends on the mass fractions of a crystalline component among the total crystalline materials. Since the percentage of Illite decreased due to its apparent weathering the calculated mass fractions of the other minerals can be expected to increase. So keeping in mind the short duration of the K release a portion of Illite might have transformed to vermiculite only.

Table 2. Semi-quantitative estimation of clay minerals in clay fraction of different soils (%).

Soil	Mineral			
	Kaolinite	Illite	Smectite	Vermiculite
Iceptisol (Delhi)	9	66	16	10
- moderately Exhausted	11	61	17	11
- Highly Exhausted	12	57	18	13
Vertisol (Bhopal)	4	43	47	5
- moderately Exhausted	10	34	50	7
- Highly Exhausted	13	23	56	8
Alfisol (Bangalore)	91	9	-	-
- moderately Exhausted	93	8	-	-
- Highly Exhausted	94	6	-	-

This however needs to be verified by another set of corroborative evidences. In intensively cultivated soils, large amounts of K are removed from the soil and if this results in K deficit in the soil in the absence of K fertilizer application, a degradation of clay minerals, especially Illite, is a distinct possibility. Therefore in

intensively cropped soils having Illite as the main clay mineral, K fertilizer application is not only a question of plant nutrition, but also of clay conservation. In all Indian soils after exhaustive cropping there was a decrease in intensity of peak at 10 Å indicating strongly of degradation of Illite due to permanent removal of K ions by plants from inter-layers of clay lattice.

References

Boguslawski, E Von, Lieres A Von (1981) Biological and Chemical proof for potassium impoverishment and its consequence for soil fertility. *Landw Forsch sonderh* **38,** 722-729.

Gjems O (1967) 'Studies on Clay Minerals and Clay Mineral Formation in Soil Profiles in Scandinavia, Middlelser fra Det Norske Skrgforsko Kesen. No. 91, Bird 21'. (Vollbeek: Norway).

Jackson ML (1956) 'Soil Chemical Analysis'. (Advanced course, privately published: Madison, WI).

Jackson ML (1967) 'Soil Chemical Analysis'. 'University of Wisconsin: Madison, Wisconsin, USA).

Mutscher H, Tran Vu T (1988). Studies on the release of interlayer potassium of an illitic dystric cambisol and its effect on the potassium studies of the soil. II. Rates of release of inter-layer potassium and their relation to the intensity factor. *Beitrag Zur Tropischen Land wirtschaft and veterinarmedizin* **26,** 107-115.

Ross GJ, Hoyt PB, Neilsen GR (1985) Soil chemical and mineralogical changes due to acidification in Okahagen apple orchards. *Canadian Journal of Soil Science* **65,** 347-55.

Tributh HB, Boguslawski EV, Lieres AV, Steffens D, Mengel K (1987) Effect of Potassium removal by crops on transformation of illitic clay minerals. *Soil Science* **143,** 404-409.

Effect of the natural clay mineral illite on the enhanced growth of cherry tomato (*Lycopersicon esculentum Mill*) in the glass house

Seok-Eon Lee[A], Hong-Ki Kim[A], Seok-Soon Han[A], Hee-Jung Kim[A], Sang-Moon Kwon[A], Moon-Soon Lee[B], Sun-Hee Woo[C], Jong-Soon Choi[D], Jai-Jung Kim[A] and Keun-Yook Chung[A,E]

[A]Department of Agricultural Chemistry, Chungbuk National University, Cheongju 361-763, Korea.
[B]Department of Industrial Plant, Chungbuk National University, Cheongju 361-763, Korea.
[C]Department of Crop Science, Chungbuk National University, Cheongju 361-763, Korea.
[D]Proteomics Team, Korea Basic Science Institute, Daejeon 305-333, Korea.
[E]Corresponding author. Email kychung@cbnu.ac.kr

Abstract
This study was performed to explore the effect of the natural clay mineral illite on the improvement of soil quality and plant growth. Cherry tomato was used as a model vegetable crop. The experiment was performed during two months in the glass house of the Chungbuk National University. Seedlings were pre-cultivated in the bed soil normally used for horticultural purpose. Of the seedlings cultured, the healthy and regular sized ones were selected and cultivated in pots with 7 cm diameter and 10 cm height. They were treated with two forms of illite, particulate (PA) and powder (PW), at the following application rates: standard application [P1(PA1, PW1), 1:30(w/w)], two times[P2(PA2, PW2), 1:15(w/w)], and four times[P4(PA4, PW4), 1:7.5(w/w)] application. Untreated (P0) soil was used as a control in the experiment. At four weeks of cultivation, growth length was greater in pots treated with P1 and P2 application of illite than in P0. At ten weeks of cultivation, growth lengths increased as the application rate increased with P0, P1, P2, and to P4 applications of illite, compared to the P0 at four weeks of cultivation. Their growth length was a little greater for the application of PW illite than for the PA illite. Based on analysis of leaf and stem parts of cherry tomato, the amounts of K, Ca, and Mg, correspondingly increased, as the application rate increased from P0, P1, P2, to P4 application. At the same application rate, amounts taken up in the respective two parts were a little higher for the application of PW illite than on the PA illite. Amounts of K were relatively evenly distributed leaf and stem, whereas, the amounts of Ca and Mg were higher in the leaf than in the stem. Consequently, it appears that the illite treatment, especially, the PW form of illite, enhanced the growth of cherry tomato in the glass house during the ten weeks of the experiment.

Key Words
Clay mineral, illite, soil conditioner, cherry tomato, growth, cations, K, Ca and Mg uptake.

Introduction
Illite is a 2:1 type of sheet clay mineral and is called illite, since it is originally discovered in the deep sediment of Illinois State in USA. It is well known that illite is in large reserved and distributed in Quebec of Canada, Illinois and Pennsylvania of USA, China, and Australia. In Korea, good quality of illite is reported occur as a massive amount in the Yeongdong area of Chungbuk province. It is frequently proposed that Illite can be utilized practically on a small scale in various fields, such as environmental, medical, cosmetic, architectural, and agricultural industries. Since the specific surface area of illite is relatively large, it can absorb the malodor, toxic chemicals, and heavy metals. In addition, it can improve soil quality and help the plant growth for agricultural purposes. However, very little information is available to support such reports. Therefore, in this study, explore growth of cherry tomato in the glass house as affected by forms and concentrations of illite.

Materials and Methods
Materials
Two forms of Illite, particulate and powder, which are produced in Yeongdong of Chungbuk province, in Korea were used as soil conditioners in this study. The cherry tomato(*Lycopersicon esculentum Mill*), was selected and cultivated as the target plant.

Cultivation and treatment
The seedlings of Cherry tomato were pre-cultivated in a 36 plug pot box with dimensions of 25cm X 25cm for two weeks packed with bed soil used for horticultural purposes. Then, the healthy seedlings were selected and transferred to cup pot with dimension of 7cm in diameter and 10 cm in height. Before they are

transferred, the particulate and powder forms of illite were mixed well in the cup pot as standard concentration (P1), two times (P2), and four times (P4) standard concentrations (Table 2).

Plant extraction
Plant extraction for the K, Ca, and Mg measurement were performed according to the plant analytical method (NAAS 2000).

Instrumental analysis
ICP (PerkinElmer, USA) was used for the analyses of K, Ca, and Mg.

Experimental Design and Data analysis
Seventy pots with 2 forms and 3 levels of illite including the control and 10 replications were arranged in a randomized block design. Data analysis was performed by Duncan's multiple test using SAS at a significance level of 0.05.

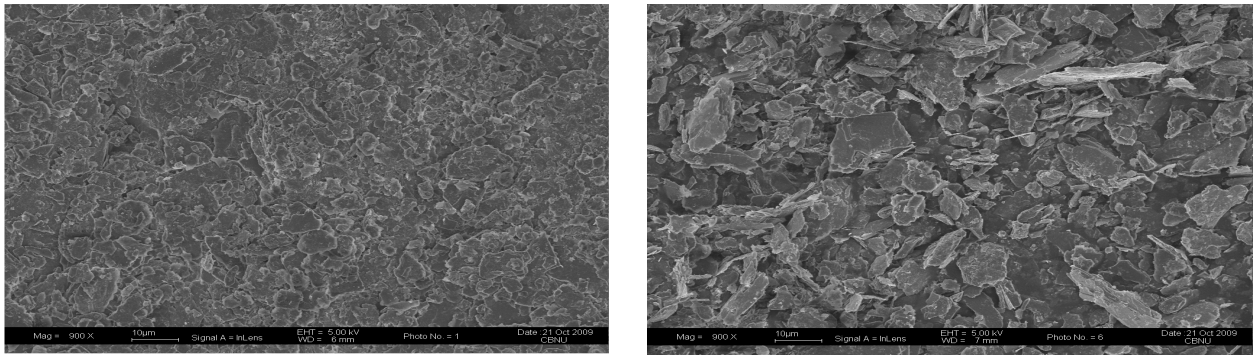

SEM of particulate Illite SEM of powder Illite

Figure 1. Scanning electron microscope (SEM) photograph of particulate and powder forms of illite.

Table 1. Physical and chemical properties of particulate and powder forms of illite.

Class	pH	O.M	Exch. Cations($cmol_c/kg$)			EC
		(%)	K	Ca	Mg	(dS/m)
Particulate Illite	7.13	0.34	0.12	1.13	0.49	0.10
Powder Illite	7.14	0.52	0.45	1.55	0.69	0.13

Table 2. Application rate of particulate and powder forms of illite used in the study.

	Standard application P1(PA1, PW1) w/w	Two times applications P2(PA2, PW2) w/w	Four times application P4(PA4, PW4) w/w
Illite treatment	1:30	1:15	1:7.5

Results

Figures 2 and 3 showed the growth length of cherry tomato in the pots treated with the PA and PW illite and in untreated pots (control, P0). The growth lengths of cherry tomato were greater in the pots treated with both PA and PW illite than for P0. The growth lengths of cherry tomato treated with the PA illite were 10%, 16%, and 12% greater than that of P0, respectively. Growth lengths of cherry tomato treated with PW illite were 11%, 17%, and 15% greater than that of P0, respectively. Growth length was a little greater with PW illite than with PA illite.

Figures 4, 5, and 6 demonstrate the amounts of K, Ca, and Mg in the leaf and stem of cherry tomato as affected by the applications of PA and PW forms of illite. The results shown in the figures 4, 5, and 6, indicate that the amount of K, Ca, and Mg in the two parts of cherry tomato, leaf and stem were higher on applications of both PA and PW forms of illite than for the P0 treatment. The amounts of K were relatively evenly distributed in the two plant parts, but amounts of Ca and Mg were larger in the leaf than in stem.

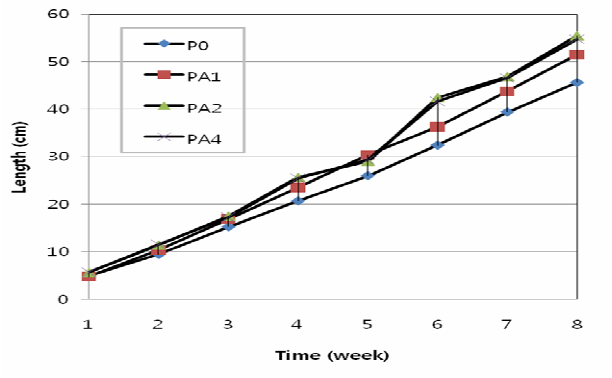

Figure 2. Growth of cherry tomatotreated with particulate illite as a function of time (week).

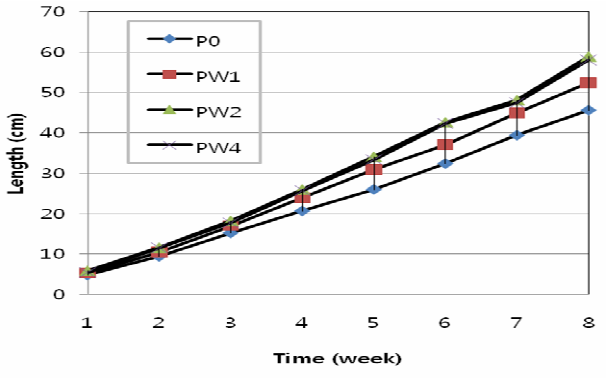

Figure 3. Growth of cherry tomato treated with powder illite as a function of time (week).

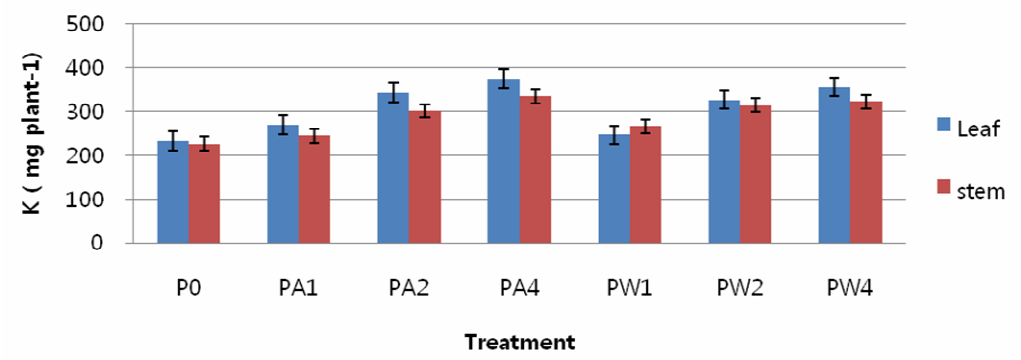

Figure 4. Amount of K in the leaf and stem as affected by the application rate of PA and PW illite.

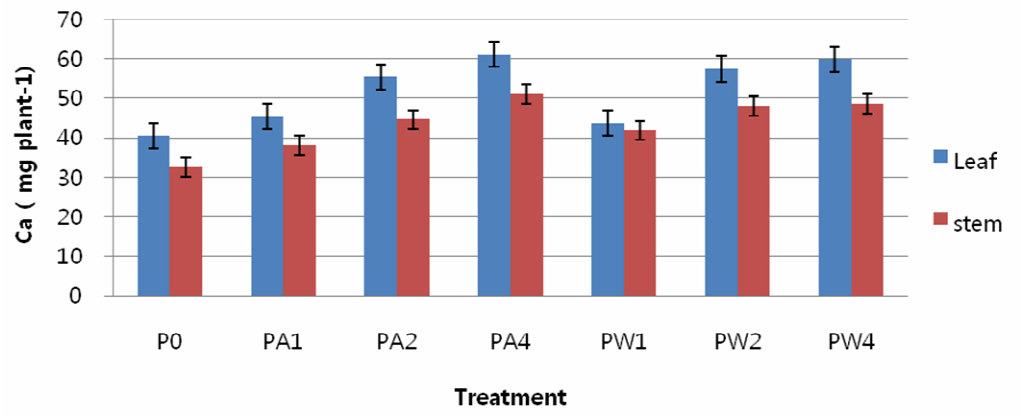

Figure 5. Amount of Ca in the leaf and stem as affected by the application rate of PA and PW illite.

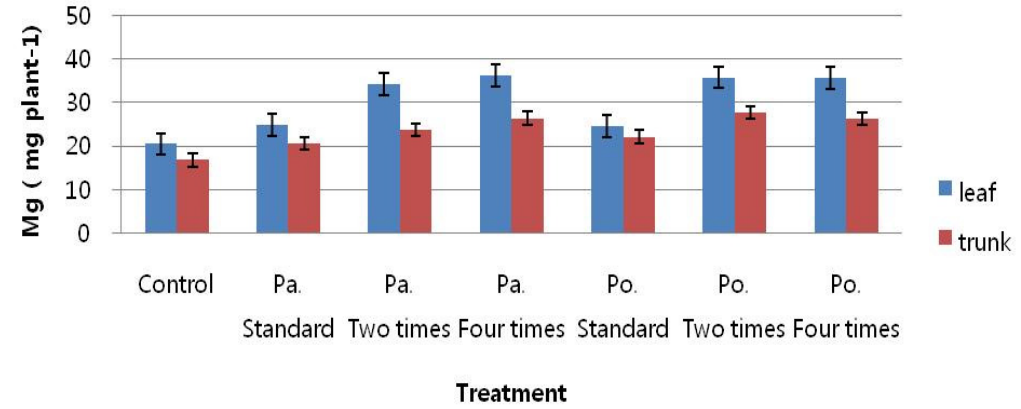

Figure 6. Amount of Mg in the leaf and stem as affected by the application rate of PA and PW illite.

Conclusion

This study showed that the growth length of cherry tomato was increased by the application of particulate (PA) and powder (PW) forms of illite. It demonstrated that the growth length of cherry tomato was 11-14% greater on the application of PA illite and 12-15% greater on the application of PW illite relative to the P0 for the three application rates (P1, P2, and P4) of illite during the ten weeks of cultivation. Their growth length was a little greater due the application of PW illite than PA illite. Under the same three application rates (P1, P2, and P4) of illite, the plant analysis for the leaf of cherry tomato showed that the amount of K was 10-36% on the application of the PA illite and 7-36% on the application of PW illite greater than values of P0. The increased in Ca was 8-26% on application of PA illite, 9-28% on application of PW illite relative to P0. Mg was 14-40% higher on application of PA illite and 18-44% on the application of PW relative to P0. For the stem of cherry tomato, the amount of K was 4-22% greater on application of the PA illite and 6-26% greater on application of PW illite relative to P0, that that of Ca was 5-26% on the application of PA illite, 7-29% on the application of PW illite relative to P0. The increase in Mg was 10-26% on application of PA illite and 10-33% on the application of PW illite relative to P0. The amount of K in the leaf on the application of PA and PW illite was similar to that of K in the stem, whereas, the amounts of Ca and Mg in the leaf were higher than in the stem on the applications of PA and PW forms of illite. The uptake amounts of cations were a little greater on the application of PW illite than for PA illite. Consequently, it appears that illite stimulates the growth of cherry tomato through the uptake of K, Ca, and Mg included in the natural clay mineral illite.

References

Choi JS, Cho SW, Kim TS, Cho K, Han SS, Kim HK, Woo SH, Chung KY (2008) Proteome analysis of greenhouse-cultured lettuce with the natural soil mineral conditioner illite. *Soil Biology and biochemistry* **40,** 1370-1378

Lee SS, Han SS, Choi GS, Ahn HJ, Kim HK, Chung KY, Woo SH, Lee CW (2005) Effect of the treatment and concentration of the natural soil mineral applied as the soil conditioner on the growth of lettuce in the glass house. In 'Proceedings of the Korean Society of Agriculture and Environment'.

Tisdale SL, Nelson WL, Beaton JD (1985) 'Soil Fertility and Fertilizers' 4th edn. (Macmillan Publishing)

Sparks DL (1995) 'Environmental Soil Chemistry'. (Academic Press: San Diego).

Sheng XF, He LY (2006) Solubilization of potassium-bearing minerals by a wild-type strain of *Bacillus edaphicus* and its mutants and increased potassium uptake by wheat. *Can. J. Microbiol.* **52,** 66-72.

Ministry of Agriculture and Forestry (2005) 'Agriculture and Forestry Statistical Year Book'. (Gwacheon: Korea).

Kang BK, Jeong IM, Kim JJ, Hong SD, Min KB (1997) Chemical characteristics of plastic film house soils in Chungbuk area. *J. Korean Soc.Soil Sci. Fert*. **30,** 265-271

Effect of the Natural Clay Mineral Illite on the Enhanced Growth of Red Pepper (*Capsicum Annuum L.*) in the Glass House

Sang-Moon Kwon[A] , Hee-Jung Kim[A] , Hong-Ki Kim[A], Seok-Eon Lee[A], Seok-Soon Han[A], Moon-Soon Lee[B], Sun-Hee Woo[C], Jong-Soon Choi[D], Keun-Yook Chung [A], **Jai-Joung Kim [A, *]**

[A]Department of Agricultural Chemistry, Chungbuk National University, Cheongju 361-763, Korea, *Corresponding Author (jjkim@cbnu.ac.kr, (O)82-43-261-3383, (F) 82-43-271-5921
[B]Department of Industrial Plant, Chungbuk National University, Cheongju 361-763, Korea
[C]Department of Crop Science, Chungbuk National University, Cheongju 361-763, Korea
[D]Proteomics Team, Korea Basic Science Institute, Daejeon 305-333, Korea

Abstract
This study was performed to explore the effect of the natural clay mineral illite on the improvement of soil quality and plant growth. Red pepper (***Capsicum Annuum L.***) was used as a model vegetable crop. The experiment was performed during ten weeks in the glass house of the Chungbuk National University. Its seedlings were pre-cultivated in soil normally used for horticultural purpose. Of the seedlings cultured, the healthy and regular size plant were selected and cultivated in pots 7 cm in diameter and 7 cm in height. They were treated with two forms of illite, particulate (PA) and powder (PW), at the following application rates: standard application [P1(PA1, PW1), 1:30(w/w)], two times[P2(PA2, PW2), 1:15(w/w)], and four times[P4(PA4, PW4), 1:7.5(w/w)] of standard application. Untreatment (P0) was used as a control pot. After the four weeks of cultivation, their length was greater in pots treated with P1, P2, and P4 of illite than the P0. At ten weeks of cultivation, their lengths were correspondingly increased as the application rate was increased ranging from P0, P1, P2, and to P4. Their growth length was a little greater for the application of powder illite (PW) than the particulate illite (PA). Based on plant analysis for the leaf, stem, and fruit parts of red pepper, the uptake of K, Ca, and Mg correspondingly increased, as the application rate was increased ranging from P0, P1, P2 to P4. At the same application rate, their amounts taken up in the respective parts were higher for the application of PW illite than for PA. K was relatively evenly distributed in the three plant parts: leaf, stem, and fruit, whereas, the amounts of Ca and Mg were higher in the leaf than in the stem and fruit. Consequently, it appears that illite treatment, especially, PW form of illite, enhance the growth of red pepper in the glass house during the whole ten weeks of experiment.

Key Words
Natural clay mineral, illite, soil conditioner, red pepper, growth, cations, K, Ca, Mg uptake

Introduction
Light, temperature, air, water, and nutrients are essential for the growth of vegetable crops in agriculture. Among these things, water and nutrient are taken up through the plant root. It is well known that the soil function as providing the plant with the water, nutrient, and space to which the root can be extended. For a long time, a great attention has paid to the conservation of soil quality. Traditionally, until recently, the soil quality has been in large evaluated using parameters, such as, crop productivity, soil color, organic matter, soil texture, soil hardness, and irrigation. However, soil quality in modern agriculture to a large extent depends on the use of external agricultural resources, such as, fertilizer, pesticide, and manure for the increased crop productivity. As a result, the crop productivity has been greatly increased, whereas, the agricultural ecology in terms of sustainable agriculture have been adversely affected. The proper soil conditioning and management for the improvement of soil quality is essential to maintain the proper function of plant root and increase the crop productivity of soil. Inorganic mineral materials are frequently used for soil conditioning and improvement, such as bentonite, zeolite, illite, perlite, vermiculite, limestone, and dolomite. Of those materials, it is reported that illite enhance the growth of vegetable crops (Choo 2001). However, scanty information is available to scientifically support such research. Therefore, this study was performed to explore the stimulatory effect of illite on the growth of red pepper (Imperial) through the measurement of plant size and the plant analysis for major cations (K, Ca, and Mg).

Materials and Methods
- *Materials*
Two forms of illite, such as particulate and powder, which are produced in the area of Yeongdong of Chungbuk province, Korea, were used as soil conditioner in this study. The red pepper (*Capsicum Annuum*

L, was cultivated as the target plant for ten weeks.

- *Cultivation and treatment*

The seedlings of red pepper were pre-cultivated in the box with dimension of 60cm X 30cm for two weeks packed with bed soil used for horticultural purpose. Then, the healthy seedlings were selected and transplanted to cup pot with dimension of 7cm in diameter and 7 cm in height. Before they are transplanted, the particulate and powder forms of illite were mixed well in the cup pot as standard concentration, two times and four times of standard concentrations (Table 2).

- *Plant extraction*

Plant extraction for the K, Ca, and Mg measurement were performed according to the plant analytical method (NAAS 2000).

- *Instrumental analysis*

ICP (Perkin Elmer, USA) was used for the analyses of K, Ca, and Mg.

- *Experimental Design & Data analysis*

Seventy pots with 2 forms and 3 levels of illite including the control and 10 replications were arranged by randomized block design. Data analysis was performed by Duncan's multiple test of SAS at the significance level 0.05.

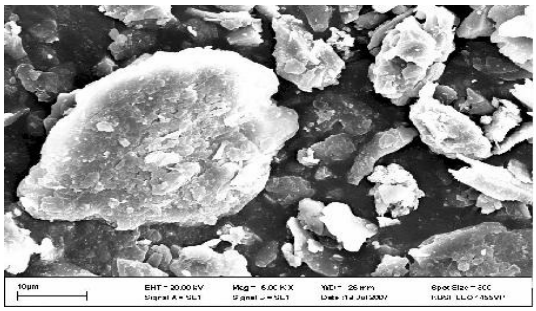

SEM of particulate illite

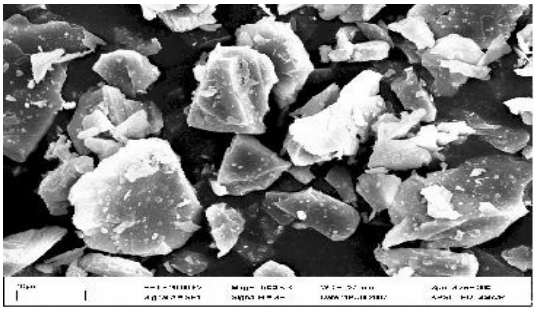

SEM of powder illite

Figure 1. Scanning electron microscope(SEM) images of particulate and powder forms of illite.

Table 1. Chemical properties of particulate and powder forms of illite.

Class	pH	O.M (%)	Exch. Cations($cmol^+/kg$)			EC (dS/m)
			K	Ca	Mg	
Particulate illite(PA)	7.13	0.34	0.12	1.13	0.49	0.10
Powder illite(PW)	7.14	0.52	0.45	1.55	0.69	0.13

Table 2. Application rate of particulate (PA) and powder (PW) forms of illite used in the study.

	Standard application P1(PA1, PW1) (w/w)	Two times application P2(PA2, PW2) (w/w)	Four times application P4(PA4, PW4) (w/w)
Illite treatment	1:30	1:15	1:7.5

Results

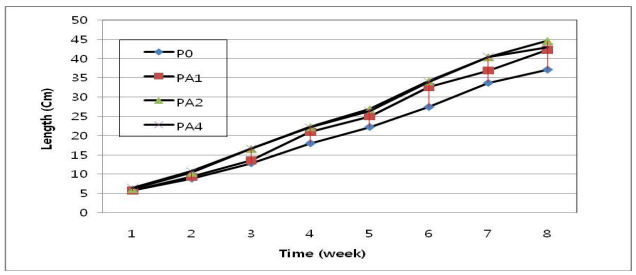

Figure 2. Growth of red pepper treated by particulate (PW) illite as a function of time.

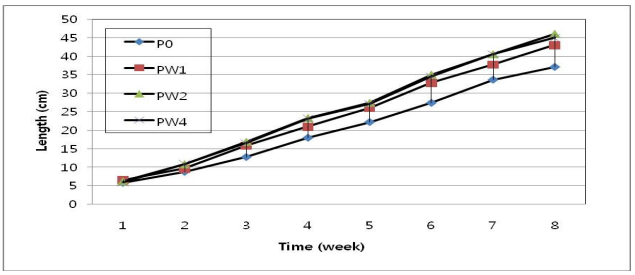

Figure 3. Growth of red pepper treated by powder (PA) illite as a function of time.

Figures 2 and 3 showed the growth of red pepper in the pots treated with the particulate and powder forms, respectively. The length of red peppers were greater in the pots treated with both particulate and powder

forms of illite than plants in untreated pots. The growth length of red pepper treated with the PA illite were 12.2%, 16.7%, and 13.6% greater than that of untreated one(control), respectively. Also, the growth length of red pepper treated with PW illite were 12.4%, 19.0%, and 15.8% greater than that of untreated one (control), respectively. Their growth length was a little better for the PW application than on the PA one.

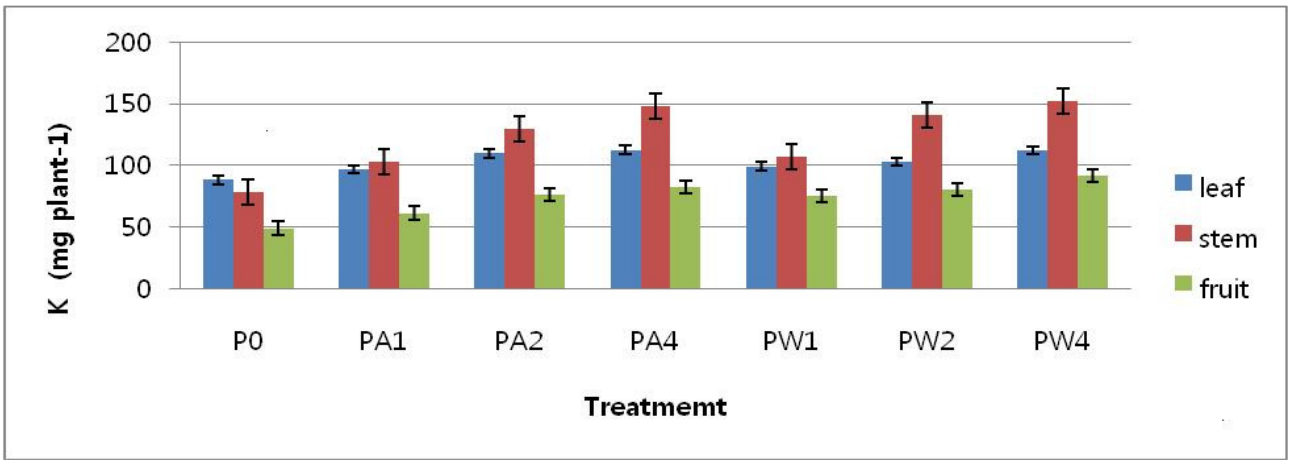

Figure 4. Amount of K in the leaf, stem, and fruit as affected by the application rate of particulate(PA) and powder(PW) forms of illite.

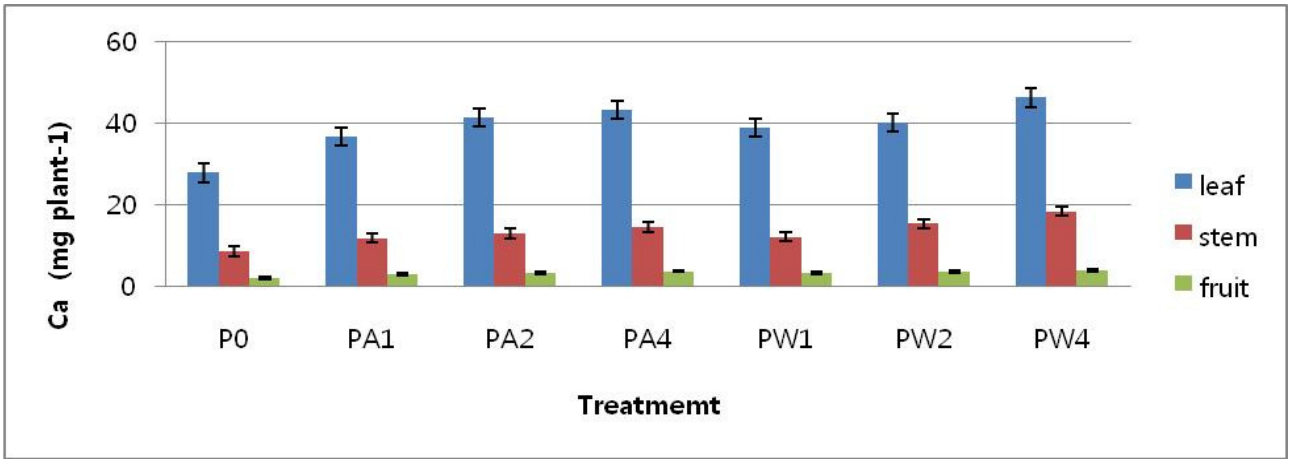

Figure 5. Amount of Ca in the leaf, stem, and fruit as affected by the application rate of particulate (PA) and powder (PW) forms of illite.

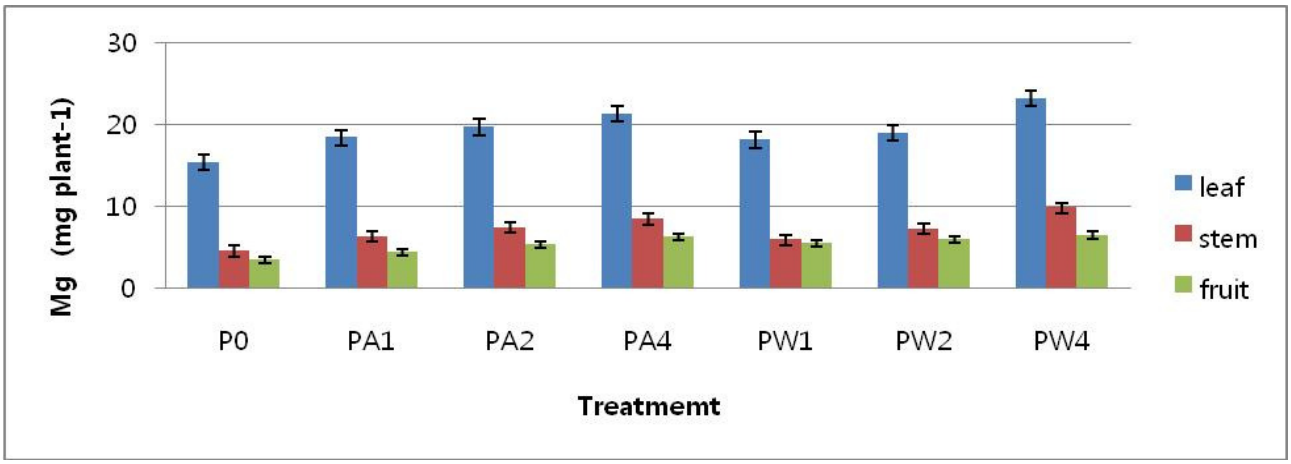

Figure 6. Amount of Mg in the leaf, stem, and fruit as affected by the application rate of particulate (PA) and powder (PW) forms of illite.

Figures 4, 5, and 6 demonstrate the amount of K, Ca, and Mg in the leaf, stem, and fruit of red pepper as affected by the applications of particulate(PA) and powder(PW) forms of illite. The amount of K, Ca, and Mg in the three parts of red pepper were higher on the applications of both forms of illite than on the non

application, respectively. They showed that as the application rate was increased, the uptake amounts of K, Ca, and Mg were correspondingly increased. In addition, on the all the applications of illite including control, the amount of K were relatively evenly distributed in three parts, but, those of Ca and Mg were more abundant in the leaf than in stem and fruit.

Conclusion

This study showed that the growth length of red pepper was increased by the application of PA and PW forms of illite relative to nil application (P0). It demonstrated that the growth length of red pepper was 12-17% greater for the application of PA illite and 12-19% greater for the application of PW illite than on the nontreatment under the range of three different application rates (P1, P2, and P4) of illite during the whole ten weeks of cultivation. Their growth length was a little greater for the application of PW illite than for the PA. Under the three different application rates (P1, P2, and P4) of illite, the plant analysis for the red pepper showed that the amount of K was 19-46% for the application of the PA illite and 21-48% for the application of PW illite greater than for the non application. The content of Ca was 24-45% for the application of PA illite, 28-53% for the application of PW illite greater than for the nil treatment. The content of Mg was 16-46% for the application of PA illite and 15-54% for the application of PW illite than for the nil treatment. The amounts of cations were a little greater for the application of PW illite than on the PA one. Consequently, it appears that the illite stimulated the growth of red pepper through the uptake of K, Ca, and Mg included in illite.

References

Ministry of Agriculture and Forestry (2005) Agriculture and forestry statistical year book, Gwacheon, Korea.

Kang BK, Jeong IM, Kim JJ, Hong SD, Min KB (1997) Chemical characteristics of plastic Film house soils in Chungbuk area. *J. Korean Soc. Soil Sci. Fert*. **30**, 265-271.

Park BG, Jeon TH, Kim YH, Ho QS (1994) Status of farmers' application rates of chemical fertilizer and farm manure for major crops. *J. Korean Soc. Soil Sci. Fert*. **27**, 238-246.

Jung BG, Choi JW, Yun ES, Yoon JH, Kim Y.H. and Jung, G.B. (1998) Chemical properties of the horticultural soils in the plastic film houses in Korea. *J. Korean Soc. Soil Sci. Fert*. **31**, 9-15.

Moreno-Caselles J, Moral R, Perez-Murcia MD, Perez-Espinosa A, Paredes C, Agullo E (2005) Fe, Cu, Mn, and Zn input and availability incalcareous soils amended with the solid phase pigslurry. *Commun. Soil Sci. Plant Anal*. **36**, 525-534.

Solan JJ, Dowdy RH, Dolan MS (1998) Recovery of biosolids applied heavy metals 16 years after application, *J. Environ. Qual*. **27**, 1312-1317.

Enhancing the solubility of insoluble phosphorus compounds by phosphate solubilizing bacteria

Jinhee Park[AB], Nanthi Bolan[AB], Megharaj Mallavarapu[AB] and Ravi Naidu[AB]

[A]Centre for Environmental Risk Assessment and Remediation, University of South Australia, Mawson Lakes, SA, Australia, Email parjy014@students.unisa.edu.au
[B]Cooperative Research Centre for Contamination Assessment and Remediation of the Environment, Adelaide, SA, Australia

Abstract
Phosphorus (P) is one of the major nutrients for plant growth, and also can be used for metal immobilizing amendment in soil. However, the uptake of P by plants is limited due to its strong adsorption onto soil particles and low solubility of phosphate compounds in soil solution. The objective of this research was to isolate phosphate solubilizing bacteria (PSB) from various soils and evaluate their potential for P solubilization from insoluble P compounds. Nineteen PSB were isolated from various soil samples and six strains solubilized more than 250 mg/L of P from tricalcium phosphate amended National Botanical Research Institute's Phosphate (NBRIP) medium. Direct inoculation of PSB to rock phosphate increased the citric acid solubility of rock phosphate indicating that the isolated PSB strain was effective for P solubilization in soil.

Key Words
Phosphate solubilizing bacteria, Phosphorus, Rock phosphate

Introduction
Phosphorus (P) is one of the major nutrients required for plant growth but most of the P compounds are not readily soluble in soil, hence P is not easily accessible for plant growth. Insoluble phosphate compounds such as rock phosphate are cheaper than soluble P fertilizer, but the solubility of these compounds is a limiting factor for their use as a source of P. Insoluble phosphate compounds can be solubilized by organic acids, phosphatase enzymes and complexing agents produced by plants and microorganisms (Duponnois *et al*. 2005). For example, phosphate solubilizing bacteria (PSB) have been shown to enhance the solubilization of insoluble P compounds through the release of organic acids and phosphatase enzymes (Sahu and Jana 2000). Therefore, PSB have been widely used as inoculants to increase crop yield by solubilizing insoluble P in soils (Sundara *et al*. 2002; Dey *et al*. 2004). The objective of this research was to isolate PSB from various soils and evaluate their potential for P solubilization from insoluble P compounds.

Methods
Isolation of PSB from various soils
Soils used for PSB isolation were locally collected from P amended and Pb contaminated sites. To extract bacteria from soil, 0.5 g of soil was mixed with 50 mL of autoclaved 0.2 % NaCl solution (soil: solution = 1: 100) and shaken for 16 hours (Illmer and Schinner 1992). Suitable dilutions were inoculated using the NBRIP growth agar medium containing (per L) glucose, 10 g; $Ca_3(PO_4)_2$, 5 g; $MgCl_2 \cdot 6H_2O$, 5 g; $MgSO_4 \cdot 7H_2O$, 0.25 g; KCl, 0.2 g and $(NH_4)_2SO_4$, 0.1 g, agar 1.5 % (Nautiyala 1999). The pH of the agar medium was adjusted to 7.0 before autoclaving. Tricalcium phosphate was autoclaved separately. Then, the other sterile ingredients were aseptically mixed after autoclaving. The soil solution (0.1 mL NaCl extract) was spread on the NBRIP agar medium and incubated for 14 days at 25 □. The colonies with clear halo were considered as PSB (Nautiyala 1999) and these colonies were picked up and further purified by re-streaking on an agar plate. The halo and colony diameters were measured after 14 days of the incubation of plates at 25 °C.

Identification of PSB
Crude DNA was extracted from bacterial strains, CS2-B1 and SM1-B1 and almost complete 16S rRNA genes were amplified. Successful amplification of DNA fragment was confirmed by running 5 µL of the PCR reaction on a 1 % agarose gel. The sequencing of 16S rRNA was conducted at the Flinders DNA Sequencing Facility (Adelaide). Acquired 16S rRNA sequence were assessed through the Greengenes website. The 16S rRNA sequences from the isolate were aligned and bootstrapped neighbor-joining relationships were estimated with MEGA version 4.1 (Kumar *et al*. 2008).

Analysis of P solubilization, phosphatase activity and organic acid
The isolated bacteria were cultured in 250 mL Erlenmeyer flask containing 100 mL of tricalcium phosphate-based NBRIP medium and incubated for 14 days. A separate broth medium inoculated with sterile water was served as a control. The PSB culture was harvested by centrifugation at 4000 rpm for 10 minutes followed by filtration with 0.45 μm syringe filter. Phosphorus concentration of the filtrate was measured by spectrophotometer using phosphomolybdate method (Murphy and Riley 1962).
The acid phosphatase activity in the culture media used for P solubilizaiton experiment was measured by following the method based on hydrolysis of ρ-nitrophenyl phosphate (Tabatabai and Bremner 1969). pH and organic acid content of the filtrate were measured using pH meter and ion chromatography (IC, ICS-2000, Dionex), respectively.

Phosphorus solubility after incubation of rock phosphate with PSB
To test the effect of PSB on P solubilization of rock phosphate, 0.2 mL of bacterial suspension (SM1-B1, ca. $1.0X10^9$ CFU/mL) was added to 2 g of rock phosphate in sterile 50 mL tube, 0.8 mL of water was added into the tube and incubated for 7, 14 and 28 days at 25 ℃. Control sample was prepared by adding same amount of sterile water instead of bacterial inoculation. After incubation, samples were analyzed for bacterial population by plate counting method, water- and citric acid-extractable P concentration by phosphomolybdate method using ascorbic acid as the reducing agent (Murphy and Riley 1962).

Results
Isolation of PSB from various soils
Most of the bacteria isolated from P amended soil showed halo formation on NBRIP medium indicating that they are PSB, but only one bacterium showed halo formation from Pb contaminated soils. Among 19 different bacterial strains, CS2-B1, NCPR-B3, JRP-B1, SSP-B1, and TSP-B4 solubilized more than 300 mg/L of P from insoluble tricalcium phosphate and SM1-B1 showed the highest P solubilization among those isolated from Pb contaminated soils (Table 1). In control, 6.6 mg/L of P was solubilized without PSB. Acid phosphatase acivity produced by the isolated bacteria ranged from 0.0034 mM to 0.1420 mM as measured by p-nitrophenol production (Table 1). The PSB strains isolated from P amended soils showed relatively higher acid phosphatase activity compared to the PSB from non-amended soils and Pb contaminated soils. Phosphatase enzymes are produced mostly by microorganisms and play a key role in the solubilization of organic P compounds (Rodríguez and Fraga 1999; Jakobsen *et al*. 2005). The total amount of organic acid produced by the isolated bacteria ranged from 20 mg/L to 112 mg/L (Table 1). The PSB strains isolated from P amended soils produced more organic acid than PSB from Pb contaminated soils and there was a strong relationship between amount of organic acid produced and the extent of P solubilizaiton. The most commonly produced organic acids by the nineteen isolated bacteria were acetic, pyruvic, fumaric and citric acids.

Identification of PSB
The two bacterial strains which showed the highest P solubilization capacity, CS2-B1 and SM1-B1 were putatively identified as *Pantoea sp*. and *Enterobacter cloacae,* respectively and the obtained sequence deposited in the Genbank with accession number GQ414734 and GQ414735, respectively. Phylogenetic tree in Figure 1 based on16S rRNA sequence showed the relationship between isolated bacteria in this research and published PSB.

Table 2. Isolated PSB and their characterization in NBRIP broth medium.

Bacterial strains	Source soil	Halo formation on solid medium	pH	Solubilized P (mg/L)	Acid phosphatase activity (ρ-nitrophenol (mM))	Organic acid (mg/L)*
Control	No bacteria	-	7.10	6.6	0.0144	49
CS1-B1	Control soil1	Yes (3 mm)	7.60	14.9	0.0147	248
CS1-B2	Control soil1	No	6.87	5.7	0.0102	181
CS1-B3	Control soil1	Yes (3 mm)	6.84	5.2	0.0134	125
CS2-B1	Control soil2	Yes (2 mm)	5.68	479.2	0.1420	601
CS2-B2	Control soil2	Yes (2 mm)	6.73	30.1	0.0105	333
NCPR-B1	NCPR	Yes (2 mm)	5.26	281.8	0.0112	204
NCPR-B2	NCPR	Yes (0.5 mm)	6.83	8.2	0.0131	124
NCPR-B3	NCPR	Yes (2 mm)	4.37	387.0	0.1104	1026
SSP-B1	SSP	Yes (2 mm)	4.53	380.5	0.1198	1112
JRP-B1	JRP	Yes (3 mm)	5.20	493.0	0.0034	791
DAP-B1	DAP	Yes (2 mm)	4.66	248.3	0.0837	347
TSP-B1	TSP	Yes (1 mm)	4.64	259.9	0.1286	263
TSP-B2	TSP	Yes (2 mm)	4.75	273.2	0.1286	598
TSP-B3	TSP	Yes (1 mm)	4.86	216.8	0.0824	401
TSP-B4	TSP	Yes (3 mm)	5.1	336.2	0.1045	778
SR-B1	Shooting range	No	6.96	6.6	0.0173	36
SR-B2	Shooting range	No	5.78	40.6	0.0082	44
SM1-B1	Smelter1	Yes (3 mm)	4.60	293.1	0.1401	314
SM2-B1	Smelter2	No	5.46	31.0	0.0073	20

*Organic acid was sum of lactic acid, acetic acid, propionic acid, pyruvic acid, malonic acid, maleic acid, tartaric acid, oxalic acid, succinic acid, fumaric acid, citric acid and trans-aconitic acid.

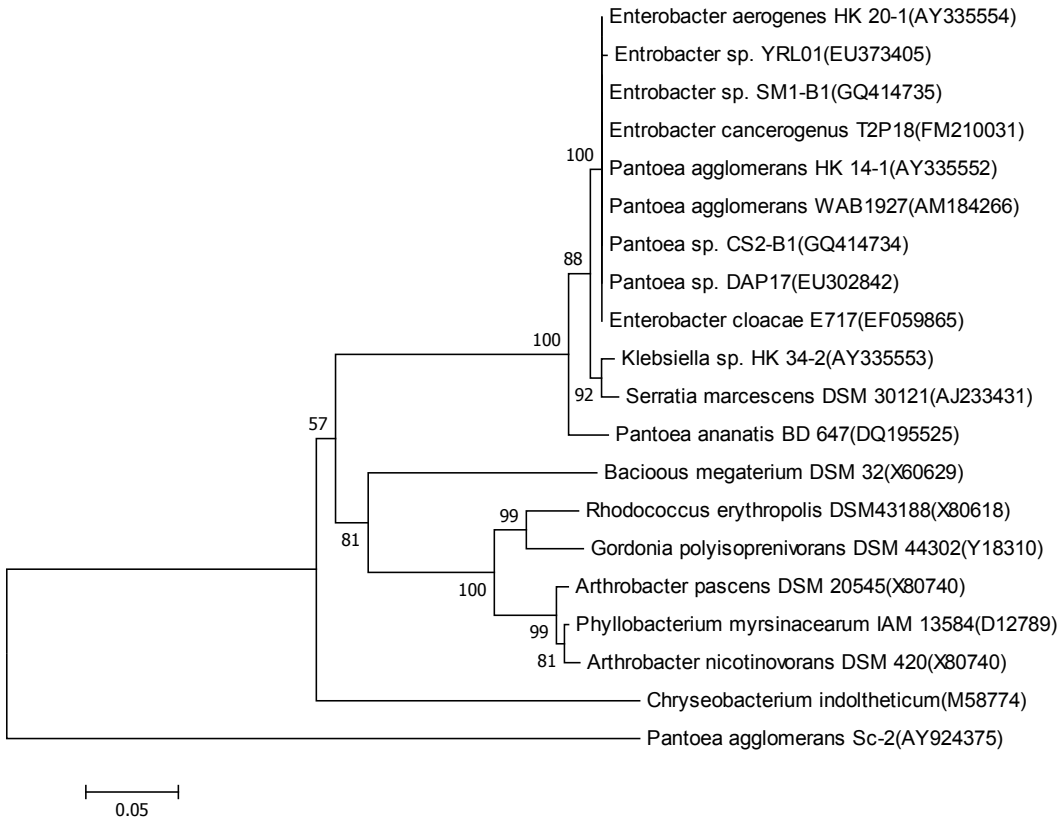

Figure 1. Phylogenetic tree based on16S rRNA sequence that shows the relationships between isolated PSB in this research and other published PSB isolates (accession numbers are given in parentheses). The tree was clustered with the neighbour-joining method using MEGA 4.1 package. Bootstrap values based on 1000 replications were listed as percentages at the nodes. The scale bar indicates 0.05 substitutions per nucleotide position.

Phosphorus solubility after incubation of rock phosphate with PSB

Phosphate solubilizing bacterial inoculation increased the concentration of citric acid-soluble P by 70 - 100 times compared to the control treatment (Figure 2). Citric acid-soluble P increased with incubation period and PSB inoculation achieved 0.93 % (w/w) citric acid-soluble P (9.3 % of total P) compared to 0.013 % (w/w) for control (0.13 % total P) at days 28.

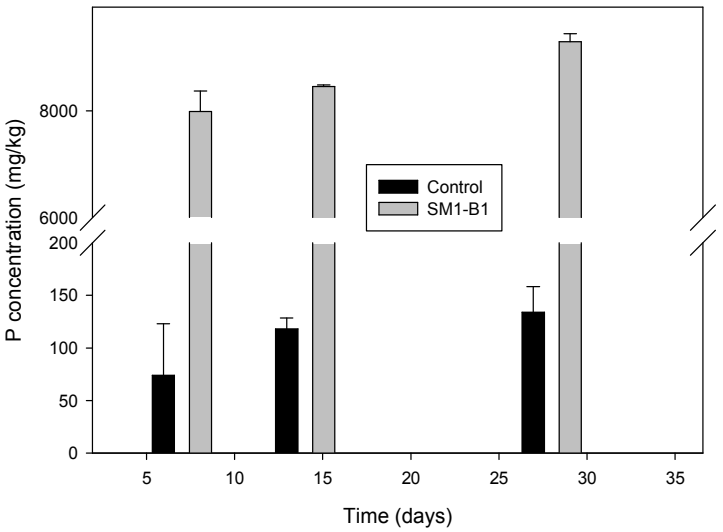

Figure 2. Citric acid extractable P concentration after incubation of rock phosphate with PSB.

Conclusion

Six PSB strains isolated from Pb contaminated and P amended soils solubilized more than 250 mg/L of P from tricalcium phosphate amended NBRIP medium. Direct inoculation of PSB to rock phosphate increased the solubilization of rock phosphate as shown by an increase in citric acid solubility.

References

Dey R, Pal KK, Bhatt DM, Chauhan SM (2004) Growth promotion and yield enhancement of peanut (*Arachis hypogaea* L.) by application of plant growth-promoting rhizobacteria. *Microbiological Research* **159,** 371-394.

Duponnois R, Colombet A, Hien V, Thioulouse J (2005) The mycorrhizal fungus *Glomus intraradices* and rock phosphate amendment influence plant growth and microbial activity in the rhizosphere of *Acacia holosericea*. *Soil Biology & Biochemistry* **37,** 1460-1468.

Illmer P, Schinner F (1992) Solubilization of inorganic phosphates by microorganisms isolated from forest soils. *Soil Biology and Biochemistry* **24,** 389-395.

Jakobsen I, Leggett ME, Richardson AE (2005) Rhizosphere microorganisms and plant phosphorus uptake. In 'Phosphorus: Agriculture and the Environment'. (Eds JT Sims, AN Sharpley) pp. 437-494. (Agronomy: USA)

Kumar S, Nei M, Dudley J, Tamura K (2008) MEGA: A biologist-centric software for evolutionary analysis of DNA and protein sequences. *Briefing in Bioinformatics* **9**, 299-306.

Murphy J, Riley JP (1962) A modified single solution method for the determination of phosphate in natural waters. *Analytica Chimica Acta* **27,** 31-36.

Nautiyala CS (1999) An efficient microbiological growth medium for screening phosphate solubilizing microorganisms. *FEMS Microbiology Letters* **170,** 265-270.

Rodríguez H, Fraga R (1999) Phosphate solubilizing bacteria and their role in plant growth promotion. *Biotechnology Advances* **17**, 319-339.

Sahu SN, Jana BB (2000) Enhancement of the fertilizer value of rock phosphate engineered through phosphate-solubilizing bacteria. *Ecological Engineering* **15,** 27-39.

Sundara B, Natarajan V, Hari K (2002) Influence of phosphorus solubilizing bacteria on the changes in soil available phosphorus and sugarcane and sugar yields. *Field Crops Research* **77,** 43-49.

Tabatabai MA, Bremner JM (1969) Use of p-nitrophenyl phosphate for assay of soil phosphatase activity. *Soil Biology and Biochemistry* **1**, 301-307.

Genesis of the quartz in Spanish Mediterranean soils. An advance

Rocío Márquez[A], Juan Manuel Martín-García[B], Gabriel Delgado[B], Jaume Bech[C] and Rafael Delgado[B]

[A]Centro de Instrumentación Científica, Universidad de Granada, Granada, Spain, Email semfarma@ugr.es
[B]Facultad de Farmacia, Universidad de Granada, Granada, Spain, Email jmmartingarcia@ugr.es, gdelgado@ugr.es, rdelgado@ugr.es
[C]Facultad de Biología, Universidad de Barcelona, Barcelona, Spain, Email jbech@ub.edu

Abstract
The quartz grains of the light fine sand fraction of five Mediterranean soils from Granada province have been classified in 13 morphotypes with genetic associations, by means of a morphoscopic study with a scanning electron microscope (SEM) and image analysis (IA). A factorial analysis of the soil variables (physical, chemical, physico-chemical and mineralogical characters) and the morphoscopic characteristics of the quartz grains, has defined a system with six components (80.1% of the explained variance). This statistical analysis has allowed to distinguish morphotypes with neoformation traits from others that are without them.

Key Words
Quartz, Mediterranean soils, quartz grain morphotypes, SEM, multivariate statistical analysis.

Introduction

Quartz (SiO_2) is one of the most abundant constituent minerals of soils. The quartz is concentrated in the sand and silt fractions, both inherited from the parent rock by physical disintegration and/or dissolution, and by eolian contributions. It can be also neoformed. The low temperature polymorph of the quartz (α-quartz) is the most frequent in the superficial environments. Quartz is considered chemically stable, in Mediterranean soils (Delgado *et al.* 1990; Martin-García 1994; White *et al.* 1996). However, different papers (some of our Investigation Group; Delgado *et al.* 2003; Martin-García *et al.* 2004) have shown that the alteration, dissolution, transport and deposition processes, including regrowing, can impose marks in the surface of the quartz grains and changes in their chemical composition. The objective of this work is to elucidate the genesis of this mineral in the soil environment of five representative Mediterranean soils from the Granada province (south of Spain): Typic Calcixeroll *Sierra Elvira* (P1), Humic Distroxerept *Sierra Nevada* (P2), Inceptic Haploxeralf *Sierra Nevada* (SR-2), Typic Haploxeralf the *Llano de la Perdiz* (P3) and Fluventic Haploxeroll *Vega de Granada* (P4).

Methods

Description, analysis and soil classification
The macromorphologic field description of the soils and the analysis of the main physical, chemical, physico-chemical and mineralogical features of the soil horizons, granulometric fractions and soil solution samples (that have allowed to establish the soil classification – Soil Survey Staff 2006 –) have been carried out following the usual methods (Márquez 2010).

Quartz study
Morphoscopy of quartz grains of the light fine sand fraction (gravimetrically separated with bromoform – ρ = 2.82 g/cm^3 – in order to concentrate the quartz particles – ρ = 2.65 g/cm^3 –) has been studied by scanning electron microscopy (SEM) and energy dispersive X-ray analysis (EDX). The classification of quartz grains in morphotypes has been carried out with the application of a heuristic method (using morphologic, crystallographic, mineralogical and weathering features). The analysis of the SEM images (SEM-IA) has been carried out with the program Image'J (National Institutes of Health 2008).

Statistical study
A factorial analysis has been carried out using the obtained results by means of the statistical package SPSS 15.0. Previously, the test Kolmogorov–Smirnov was applied to the data population. Some variables were transformated.

Results

Site description of soils is shown in Table 1. The morphoscopic study of the quartz grains allowed classifying them in 13 morphotypes and 6 sub-morphotypes, with genetic sense, some of which are showed

in the Figure 1. Thereby, morphotypes with quartz grains predominantly showing mechanical marks (Figure 1A, 1C), with some surface weathering marks (Figure 1B) or with some neoformation features can be distinguished. This classification has been confirmed by means of image analysis and statistical study (Márquez *et al.* 2009).

The adjustment of a factorial analysis to the variables of the studied soils and the morphologic variables of the analyzed quartz grains allowed to define the system for six components that explain 80,1% of the total variance (Table 2). The first component (28.4% of the variance) contains mainly the forming factors of the soil variables (climatic and topographic variables) and general chemical characters of soils (pH, exchangeable cations, i.e). The second component (18.0% of the variance) is a Mediterranean pedoevolution factor in which weathering variables are included (redness indexes, clay content, free forms, mineralogy of the clay fraction, phyllosilicate content, etc). The third component (10.9% of the variance) includes mainly the variables related with the silt granulometric fraction. The fourth component (8.7% of the variance) contains the variables related with the fine sand fraction and the morphotypes M2 and M6; these quartz grains haven't neoformation features. The fifth component (7.8% of the variance) is mainly a factor related with the soil organic matter. Finally, the sixth component (6.3% of the variance) contains the variables related with the soil solution (mmol/L of Si^{4+}, i.e) and the morphotype M7; this morphotype contain quartz grains with certain traits of mineral neoformation.

Table 1. General information on the soil site.

Soil	Typic Calcixeroll	Humic Distroxerept	Inceptic Haploxeralf	Typic Haploxeralf	Fluventic Haploxeroll
Horizon sequence	Ah, Bw, BCk, 2CBk, 2Ck1, 2Ck2, 3Ck	Ah1, Ah2, Ah3, AC, C	Ap, AB, Bt, BCt1, BCt2	A, AB, Bt, Btg, BCtg	Ap, C, 2Cg, 3C1, 4C2
Parent material	Slope deposits from sandstone and marls	Slope deposits from mica-schits and quartzites	Slope deposits from mica-schits and quartzites	Formación Alhambra's conglomerates	Aluvial sediments
Elevation (m)	760	2420	1410	1020	600
Physiographic location/Slope (%)	Lower slope/37	Upper slope/49	Middle slope/23	Upper slope/15	Flood plain/2
Vegetation	Holm oaks and scrubs (thymus)	Thyme field	Scrubs (thymus)	Scrub (thymus) and reforested pines	Poplar plantation
Moisture regime	Xeric	Xeric	Xeric	Xeric	Xeric
Temperature regime	Thermic	Cryic	Mesic	Thermic	Thermic

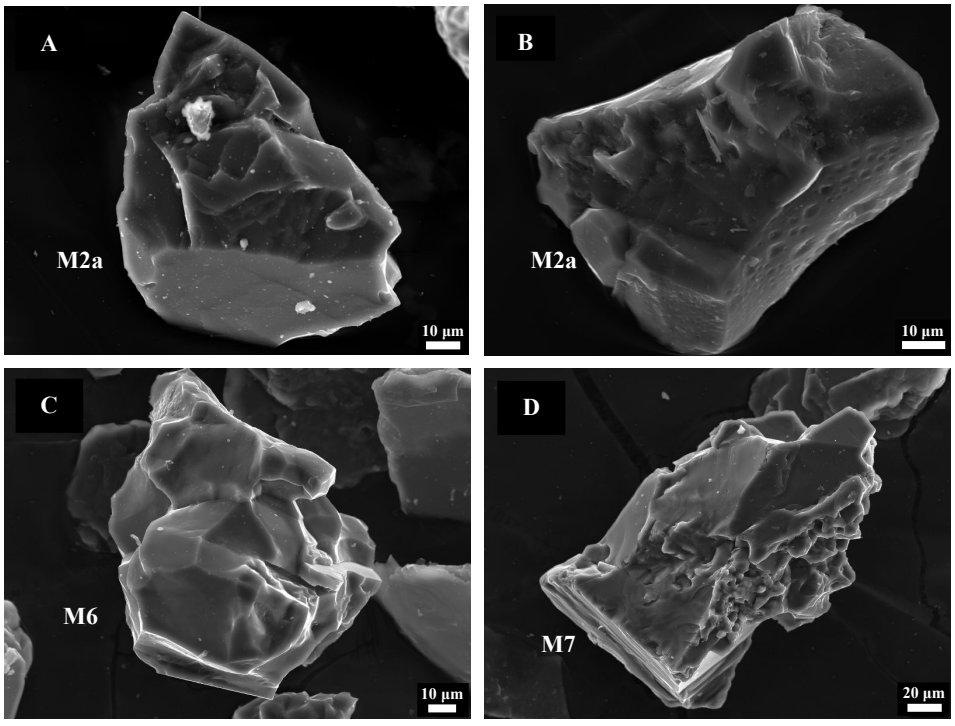

Figure 1. SEM images of some quartz grains morphotypes and submorphotypes. A: submorphotype M2a; B: submorphotype M2a with surface weathering marks (etch-pits); C: morphotype M6; D: morphotype M7.

Table 2. Factorial analysis. Rotate component matrix.

Variables	Components					
	1	2	3	4	5	6
Elevation (m)	-xx					
Slope (m)					x	
RI (wet)		xxx				
RI (dry)		xxxx				
T (ºC)	xxxx					
[1]P (m)	xxxx					
ETP (m)	xxxx					
Ex (m)	-xxxx					
[1]Df (m)	-xx					
ETR (mm)	xxx					
Silt (%)			xx			
Clay (%)		xxx				
Coarse sand (%)	-x					
Fine sand (%)				xxx		
W (-33kPa) (%)			x			
W (-1500kPa) (%)		xx				
Available water (mm/cm)			xxx			
Organic carbon (%)					xxxx	
Nitrogen (%)					xxxx	
pH(H_2O)	xxxx					
pH(KCl)	xxxx					
Ca^{2+} (cmol(+)/kg)	xxx					
Mg^{2+} (cmol(+)/kg)		xxx				
Na^{+} (cmol(+)/kg)			xx			
Total bases (cmol(+)/kg)	xxx					
Saturation (%)	xxxx					
Fe_2O_3 (%)		xxx				
Al_2O_3 (%)	-xx					
SiO_2 (%)		xxx				
Total free forms (%)		xxx				
CS Quartz	-x					
CS Potassium feldspar	-xx					
CS Clay minerals	-xx					
[2]CS Chlorite	-xxx					
CS Goethite	-xx					
LFS Quartz				xx		
LFS Potassium feldspar				xx		
LFS Plagioclase				xx		
LFS Clay minerals	-xx					
S Quartz			xx			
S Plagioclase	x					
S Clay minerals			xxx			
S Chlorite			xxxx			
S Goethite			x			
S Haematite			x			
[2]C Quartz		xxxx				
C Clay minerals		xxxx				
[2]C Goethite		xxxx				
Chlorite		xxx				
Illite		xxx				
[2]Kaolinite		xxxx				
Smectite	xxx					
SS EC (mS/cm)	x					xx
SS pH	xxx					
SS K^{+} (mmol/L)						xx
SS Ca^{2+} (mmol/L)						xxx
[3]SS Mg^{2+} (mmol/L)						xxx
SS Si^{4+} (mmol/L)						xxx
SS Fe^{3+} (µmmol/L)					xxx	
[4]SS Al^{3+} (µmmol/L)					x	
[3] SS Li^{+} (µmmol/L)	xx					
[4] SS Mn^{2+} (µmmol/L)	-x					
SS Sr^{2+} (µmmol/L)						xxxx
SS Ba^{2+} (µmmol/L)						xxxx
Morphotype M2 (%)				x		
Submorphot. M2a (%)				xxx		
Morphotype M6 (%)				xxx		
Morphotype M7 (%)						x

RI, redness index; T, annual temperature; P, rainfall; ETP, evapotranspiration; Ex, water excess; Df, water deficit; ETR, real evapotranspiration; W, water content; CS, coarse sand; LFS, light fine sand; S, silt; C, clay; SS, soil solution; EC, electric conductivity.
Data transformated: [1]Opposite variable; [2]2*arcsen[√(variable/100)]; [3]√variable; [4]ln(variable+1).
Factorial analysis. Extraction method, principal components; Rotation method, Varimax with Kaiser.
Factor loadings. x, ≥0.6-<0.7; xx, ≥0.7-<0.8; xxx, ≥0.8-<0.9; xxxx, ≥0.9-1

Conclusion

In the Mediterranean soils studied, the quartz grains of the light fine sand have been classified in 13 morphotypes and 6 submorphotypes with genetic associations. Among others, morphotypes composed by quartz grains that only show surface mechanical marks, morphotypes with grains with surface weathering marks or morphotypes with quartz grains showing traits of neoformation, have been recognized. Morphotypes with neoformation traits (M7) have been distinguished from other that are without them (M2 y M6) by means factory analysis. The existence of these morphotypes in the studied soils questions the paradigm of quartz inalterability in Mediterranean environments, making necessary a bigger study of these problems.

Acknowledgements

This study was supported by the Spanish Ministry of Science and Innovation project no CGL2009–10671 "Revisión del Paradigma de la Inalterabilidad del Cuarzo en Suelos Mediterráneos".

References

Delgado R, Párraga J, Huertas F, Linares J (1990) Genèse d'un sol fersiallitique de la Formation Alhambra (Granada, Espagne). *Science du Sol* **28,** 53-70.

Delgado R, Martín-García JM, Oyonarte C, Delgado G (2003) Genesis of the *terrae rossae* of the Sierra Gádor. *European Journal of Soil Science* **54,** 1-16.

Márquez R, Martín-García JM, Delgado G, Pérez-Lomas AL, Delgado R (2009) SEM-IA of morphotypes of Quartz grains in Mediterranean soils. In 'XXIV Congress of the Spanish Microscopy Society and XLIV Annual Meeting of the Portuguese Microscopy'.

Márquez R (2010) Génesis del mineral cuarzo en suelos mediterráneos. Tesis Doctoral, Universidad de Granada.

Martín-García JM (1994) La génesis de Suelos Rojos en el macizo de Sierra Nevada. Tesis Doctoral, Universidad de Granada.

Martin-García JM, Aranda V, Gámiz E, Bech J, Delgado R (2004) Are Mediterranean mountains Entisols weackly developed? The case of Orthents from Sierra Nevada (Southern Spain). *Geoderma* **118,** 115-131.

National Institutes of Health (2008) 'Image J Image Processing and Análisis in Java'. http://rsb.info.nih.gov/ij/

Soil Survey Staff (2006) 'Keys to soil taxonomy', 10th ed. (NRCS, USDA: Washington, DC).

White AF, Blum AE, Schulz MS, Bullen TD, Harden JW, Peterson ML (1996) Chemical weathering of a soil chronosequence on granitic alluvium 1. Reaction rates based on changes in soil mineralogy. *Geochimica et Cosmochimica Acta* **60,** 2533-2550.

Impact of clay mineralogy on stabilisation of organic matter in the clay fraction of a Neo-Luvisol and a Cambisol

Laurent Caner[A] Fabien Hubert[A] Christophe Moni[B] and Claire Chenu[B]

[A]Université de Poitiers, CNRS/INSU FRE 3114 HYDRASA, 40 avenue du Recteur Pineau, 86022 Poitiers cedex, France. Email laurent.caner@univ-poitiers.fr; Email fhubert@etu.univ-poitiers.fr
[B]AgroParisTech - BioEMCo - Bâtiment EGER - 78850 Thiverval Grignon, France. Email chenu@grignon.inra.fr

Abstract
This study was focused on the identification and quantification of the clay mineral assemblage of the clay fraction of two surface soil samples from a Neo-Luvisol on loess deposit in the Parisian basin (France), and a Cambisol on ancient ferrallitic soil in south-west France in relation to their organic carbon content. The two soil samples exhibit contrasted mineralogy. In order to better characterize the clay mineralogy the < 2 µm fraction was subsequently fractionated in sub-micronic fractions. The < 0.04 µm fraction of the Neo-Luvisol is rich is smectite both as discrete and mixed layers while in the Cambisol, kaolinite is the dominant species. However the carbon content is larger in the < 0.04 µm fraction of the Cambisol compared to the Neo-Luvisol. In the 0.2 – 2 µm fraction organic carbon content is larger for the Neo-Luvisol. These preliminary results support the hypothesis that in the Cambisol the poorly crystallised kaolinite exhibits a large specific surface area that allow important organic matter sorption, and that in the Neo-Luvisol smectite favours, in addition to sorption, organic matter stabilisation within micro-aggretates that leads to larger content in organic carbon of the < 2 µm fraction.

Key Words
Clay mineralogy, XRD profile fitting, organic matter, particle size fractionation, smectite

Introduction

The "clay fraction" of soils is commonly dominated by clay minerals which control to a large extent important soil chemical and physical properties (Dixon & Weed 1989). An accurate determination of soil clay mineralogy is required to better understand their role on soil properties. Several factors impede their precise identification: first, soil clay mineral assemblages are often mixtures of clay species with a variety of particle sizes, crystal-chemistries and mineralogy; second, soil clay minerals are often mixed layers with variable compositions (Righi & Elsass 1996). Mixed layer identification is performed from the comparison of experimental peak positions with those calculated using decomposition and Newmod simulation for mixed layers. Such a combination of XRD pattern decomposition and Newmod calculations has been successfully applied for several purposes in soil science. However, this dual procedure allows only an approximate characterisation of the mixed layers as the identification relies essentially on peak position. Consistently, profile fitting which allows fitting the complete reflection profiles including asymmetries results in a more reliable identification of mixed layers (Drits 2003). Profile fitting calculates a complete XRD pattern from a structure model optimized for each clay species present (Drits & Sakharov 1976; Drits 1997; Sakharov *et al.* 1999a, b). This method can be applied to mixed layers with more than two layer types and different layer stacking sequences and also provides quantitative phase analysis of complex clay assemblages (Drits 2003). This method used in burial diagenesis context has been applied to soil samples developed on loess deposits by Hubert *et al.* (2009).

Methods

Soil profiles

Two soil samples were used in this study: profile 1 is a "Neo-Luvisol" developed on loess deposits from the Closeaux Field Experiment, at the Station of the INRA de Versailles (France) and profile 2 a "Cambisol" developed on a relic of an ancient ferralitic soil was sampled at the experimental site of the ORE ACBB (INRA de Lusignan, France). This study was focused on the surface horizons (L1) of these two profiles studied in details by Moni (2008), Hubert (2008) and Hubert *et al*. (2009).

Particle size fractionation and X-ray diffraction

Soil samples were air dried and sieved at 2 mm to remove coarse fragments. 100 g of the fine earth were dispersed in osmosed water and disaggregated using agitation with glass balls. The < 50 µm fraction was

separated by wet sieving and dispersed using ultrasonic treatment. The < 2 µm clay fraction was isolated from the silt one (2-50 µm) by repeated siphoning. An aliquot (1g) of the <2 µm fraction was sequentially fractionated into three sub-fractions (2-0.2 µm; 0.2-0.04 µm and <0.04 µm) according to the procedure employed by (Laird *et al.* 1991) using a Biofuge stratos centrifuge. Two dispersion procedures without destruction of organic matter were employed: 1) a dispersion using molar NaCl solution and washed until chloride-free and 2) dispersion into osmosed water. Between each centrifugation step, the sample was sonified in osmosed water (30 s at ~150 W for 40 ml). The particle-size fractions were collected using repeated centrifugation until the supernatant becomes clear (8 to 10 steps). The different fractions were flocculated and saturated four times with $CaCl_2$ (0.5 M), dialysed in osmosed water until chloride-free, freeze-dried and then weighted.
Oriented preparations for quantitative XRD analysis were obtained by pipetting the Ca-saturated suspensions on a glass slide (sample length: 3 cm, sample density: 3 mg cm^{-2}) and drying at room temperature (AD). XRD patterns were obtained using a Panalytical X'pert Pro diffractometer equipped with an X'celerator detector ($CuK_{\alpha 1+2}$) in air-dried state (AD) at room humidity conditions (~35% RH) and following vapour ethylene glycol (EG). Diffraction data was recorded in a scanning mode and converted to a step pattern (step of 0.017°2θ from 2.5 to 35°2θ, using a 200 s counting time per step). Organic carbon content of the different particle-size fractions were determined by dry combustion (NF ISO 10694).

X-ray diffraction profile modelling method
XRD patterns were modelled, in both AD and EG states, using the Sybilla© software developed by Chevron™ (Aplin *et al.* 2006) and using the algorithm developed by Drits & Sakharov (1976) and used recently on soil samples by Hubert *et al.* (2009). The modelling allows the direct comparison between experimental and calculated XRD profiles, the latter being the sum of all elementary contributions which have been identified. Details on the modelling procedure are given in Hubert *et al.* (2009). For each mixed layer, the number, nature, proportion and stacking sequences of the different layer types were considered as adjustable parameters. Optimization was performed using a trial-and-error approach without automatic refinement of the parameters. To ensure the reliability of the modelling, both AD and EG patterns of a given sample were fitted with a unique set of structural parameters. The relative proportions of the different clay species in these complex assemblages were also optimized with Sybilla©. The multi-specimen approach requires these proportions to be similar in both AD and EG states.

Results
Particle size distribution and organic carbon repartition
The percentages are based on gravimetric recoveries of each fraction that were > 92.9 % and have been normalised to 100% (Table 1). Particle-size fractionation shows that the dominant fraction of Neo-Luvisol is 0.2-2 µm for both dispersion methods. For the Cambisol the dominant fraction is 0.2-2 µm with water dispersion whereas Na dispersion results in approximate same proportion for the 3 fractions. For both profiles Na dispersion induces a doubling of the < 0.4 µm fraction proportion principally at the expense of the 0.2 -2 µm one.

Table 1. Sub-micronic particle size distribution of the two soil samples with both dispersion technique.

	Dispersion method	< 0.04 µm (%)	0.04 - 0.2µm (%)	0.2 - 2 µm (%)
Neo-Luvisol	water	8	36	56
	NaCl	15	38	47
Cambisol	water	17	39	44
	NaCl	35	33	32

Organic carbon measurements highlights that the richest fraction is the 0.2 – 2 µm fraction for the Neo-Luvsiol and the < 0.04 µm for the Cambisol with the both dispersion method (Table 2). Taking into account the mass percentage of the different fraction in both samples the 0.2 - 2µm fraction contains the larger amounts in organic carbon (Table 2). The < 0.04 µm fraction of the Cambisol is richer in organic carbon compared to the Neo-Luvisol one with respectively 44.9 g/kg and 35.0 g/kg.

Table 2. Organic carbon content and proportion of total carbon in the particle size fractions.

	Dispersion	< 0.04 µm		0.04-0.2µm		0.2-2 µm	
		C org. (g/kg)	% C tot (%)	C org. (g/kg)	% C tot (%)	C org. (g/kg)	% C tot (%)
Neo-Luvisol	water	32.5	8	23.8	24	44.7	69
	NaCl	35.0	16	32.5	36	35.6	49
Cambisol	water	45.4	23	27.7	33	32.9	44
	NaCl	44.9	46	31.2	30	26.3	24

Identification of the clay mineral assemblage

A qualitative description of the X-ray diffraction patterns of the different particle size fractions (Figure 1) show that the two samples present contrasted clay mineralogy. The clay minerals assemblage of the Neo-Luvisol is composed of kaolinite, illite mica, smectites and mixed layers illite/smectite with broad peaks displacing following ethylene glycol solvation (not shown). By contrast, the clay mineral assemblage of the Cambisol is composed of kaolinite, illite, chlorite in addition to low amounts of mixed layers containing expandable layers. In both samples quartz and feldspars are present. The average trend with decrease in particle size is an increase in swelling minerals particularly for the Neo-Luvisol. Na dispersion also induces an increase in swelling minerals in the 0.04 – 0.2 µm and < 0.04 µm fraction of the Neo-Luvisol.

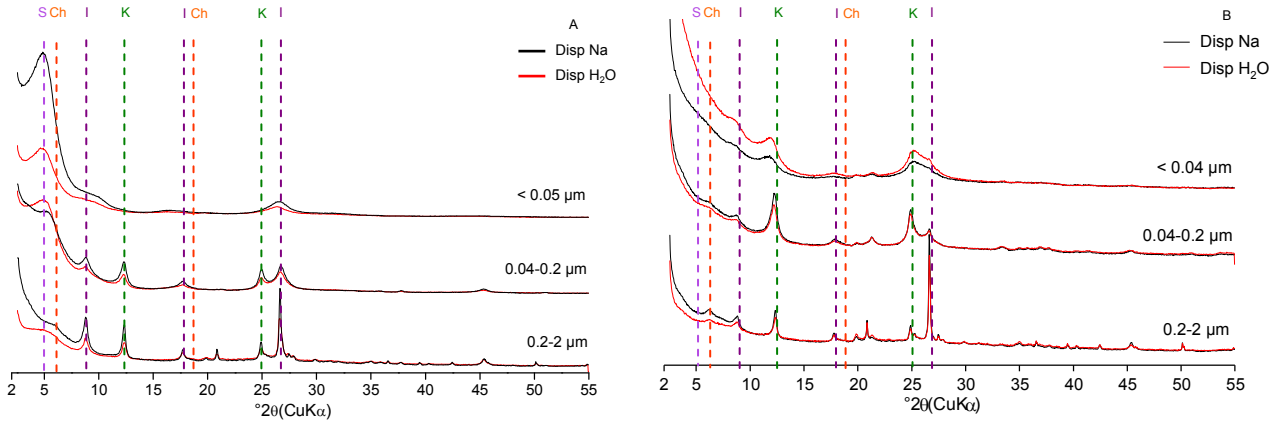

Figure 1. X-ray diffraction patterns of the particle-size fraction of the surface horizon of the Neo-Luvisol (A) and of the Cambisol (B) following EG solvation (red line: dispersion with water, black line: dispersion with NaCl).

XRD profile modeling were performed on the <0.05 µm which presents the most contrasted clay mineralogy and organic carbon content. The clay mineral assemblage of the L1 horizon of the Neo-Luvisol is composed of discrete smectite, two random-ordered mixed layers illite/smectites: one rich in illite (R0 90/10) and one rich in smectite (R0 65/35), and a random-ordered kaolinite/smectite mixed layers. The proposed mineral assemblage closely reproduces the experimental patterns in the EG state, and provides an acceptable fit in AD state (not shown). The optimum XRD patterns fits of <0.05 µm fraction of the Cambisol in AD and EG states were obtained with three mixed layer clays dominated by kaolinite, illite and smectite layers, respectively. The first interstratified corresponds to kaolinite-illite (R0 77/23) not commonly described in soils samples. The second clay mineral is a smectite-rich randomly interstratified illite-smectite (R0, 30/70) and the third clay type corresponds to illite-rich mixed layer clay containing three components: illite (75%), smectite (17%) and chlorite (8%) layers. The employed clay mineral assemblage provides good quality of the fit in EG state and an acceptable one in AD state (not shown).

Conclusion

The two soil profiles present contrasted clay mineralogy especially in the < 0.04 µm fraction. However the < 0.04 µm fraction of the Cambisol on palaeo-oxisol which is dominated by kaolinite minerals has larger content in organic carbon than the same fraction of the Neo-Luvisol rich in smectitic minerals. These results supports the hypothesis that in the Cambisol the poorly crystallised kaolinite minerals exhibit a large surface area that allows sorption of larger quantity of organic matter than in the Cambisol.

By contrast, the 0.2 – 2 µm fraction of the Neo-Luvisol is richer in organic matter most probably due to the impact of smectite on micro-aggregation that allows physical protection of carbon which is not observed in

the Cambisol. However to complete these preliminary results we have to check the role of iron oxides in both samples by estimating their amounts by chemical dissolution.

References

Aplin AC, Matenaar IF, McCarty DK, van der Pluijm BA (2006) Influence of mechanical compaction and clay mineral diagenesis on the microfabric and pore-scale properties of deep-water Gulf of Mexico mudstones. *Clays and Clay Minerals* **54,** 500-514.

Dixon JB, Weed SB (1989). Minerals in Soil Environments. Soil Science Society of America Inc. USA., Madison.

Drits VA (1997) Mixed-layer minerals. In 'EMU notes in Mineralogy, Volume 1' (Ed. Merlino S), pp. 153-190. Eötvös University Press, Budapest.

Drits VA (2003) Structural and chemical heterogeneity of layer silicates and clay minerals. *Clay Minerals*, **38,** 403-432.

Drits VA, Sakharov BA (1976) X-ray structural analysis of mixed-layer minerals. Nauka. (In Russian).

Hubert F (2008) Modélisation des diffractogrammes de minéraux argileux en assemblages complexes dans deux sols de climat tempéré. Implications minéralogique et pédologique. PhD Thesis, University of Poitiers, France.

Hubert F, Caner L, Meunier A, Lanson B (2009) Advances in characterization of soil clay mineralogy using X-ray diffraction: from decomposition to profile fitting. *European Journal of Soil Science* (In press).

Moni C (2008) Stabilisation physique et physico-chimique de la matière organique dans les horizons profonds du sol, Université Pierre et Marie Curie, Paris.

Righi D, Elsass F (1996) Characterization of soil clay minerals: Decomposition of X-ray diffraction diagrams and high-resolution electron microscopy. *Clays and Clay Minerals*, **44,** 791-800.

Sakharov BA, Lindgreen H, Salyn AL, Drits VA (1999) Determination of illite-smectite structures using multispecimen XRD profile fitting. *Clays and Clays Minerals*, **47,** 555-566.

Minerals and carbon stabilization: towards a new perspective of mineral-organic interactions in soils

Markus Kleber[A]

[A]Department of Crop and Soil Science, 3017 Agricultural and Life Science Building, Oregon State University, Corvallis OR 97331, Email markus.kleber@oregonstate.edu

Abstract
Classical models based on adsorption mechanisms are questioned as the only mechanisms involved in C stabilization in soils. An alternate three-dimensional functional view of carbon turnover dynamics at the microscale has gained ground in recent years. According to this view, soil consists of a multitude of largely independent microreactors formed around microbial cells, cell colonies and fungal hyphae. Mineral particles are conceptualised as components for the construction of small microstructures which are built around microbiota. This view is supported by abundant evidence that substantial parts of mineral surfaces are not covered by organic matter. In this alternate view, minerals may play an ecological function in relation to microbiota. Several experiments have pointed to the active role played by minerals in the functioning and structure of microbiota and their communities. As a result of differences in formation and breakdown processes, each particular type of mineral in soils can show great variation in its shape and size, kinetic and thermodynamic stability, abundance and extent of reactive surfaces. Hence each type is not constant in its ability to provide reactive surfaces and to serve as physical barriers or as suppliers of dissolved cations, which in turn may act as complexing and/or precipitating agents.

Key Words
OM mineralisation, carbon NEXAFS, microreactors, microhabitats, spatial, condensation nuclei.

The paradigm of mineral control: are minerals just adsorbents for organic C?
Significant debate surrounds the question whether the abundance of certain mineral phases might serve to predict the mean residence time of organic matter in soils. Iron oxides from identical soils, for example, may be positively correlated with carbon content in clay subfractions (Kahle *et al.* 2003) but negatively (Kahle *et al.* 2002b) with carbon contents of whole clay fractions. This raises the question if classical stabilization models based on adsorption mechanisms are capable of representing the whole breadth of the mineral-organic interactions involved in C stabilization. While minerals differ widely in the nature and extent of surface reactivity, long-term protection of organic molecules by sorptive interactions appears to be limited to those organic materials directly bonded to the protecting mineral surface (Kleber *et al.* 2005). Kalbitz *et al.* (2003) showed that sorption of soluble OM to subsoil material (Bw horizon) reduced OM mineralisation to 20% to 30% compared to mineralization in soil solution, but a detailed mechanistic understanding of why sorption to soil minerals reduces decomposition rates is lacking and is complicated by artefacts in the experiments.

A new perspective: minerals as rate controlling constituents of micro-bioreactors
Initiated largely by the work of Chenu and collaborators (Chenu and Plante 2006; Chenu and Stotzky 2002) and seconded by recent imaging and X-ray spectroscopic work (Lehmann *et al.* 2007; Lehmann *et al.* 2008; Wan *et al.* 2007), an alternate functional view of carbon turnover dynamics at the microscale has gained ground over the last years. In this view, the two-dimensional concept of soil as a system composed of adsorbent (mineral surface) and adsorbate (soil organic matter) has been extended to a three-dimensional view of soil consisting of a multitude of largely independent microreactors formed around microbial cells, cell colonies and fungal hyphae. Figure 1 illustrates how microbial cells might act as condensation nuclei for soil microstructures, effectively inverting purported causal relationships by suggesting that rather than viewing organics as adsorbates on mineral adsorbents, a better representation of observational evidence would be to conceptualise mineral particles as components for the construction of small microstructures which are built around microbial cells or cell colonies (Spectrum 1 in Figure 1 is archetypical for microbial cells). This view is supported by abundant evidence that substantial parts of mineral surfaces are not covered by organic matter (Arnarson and Keil 2001; Kahle *et al.* 2002a; Mayer and Xing 2001; Ransom *et al.* 1998). This fact is difficult to reconcile with a chromatographic view of soil, where the mineral matrix is conceptualized as an adsorbent and soil organic matter as an adsorbate that is dissolved and/or suspended in the soil solution.

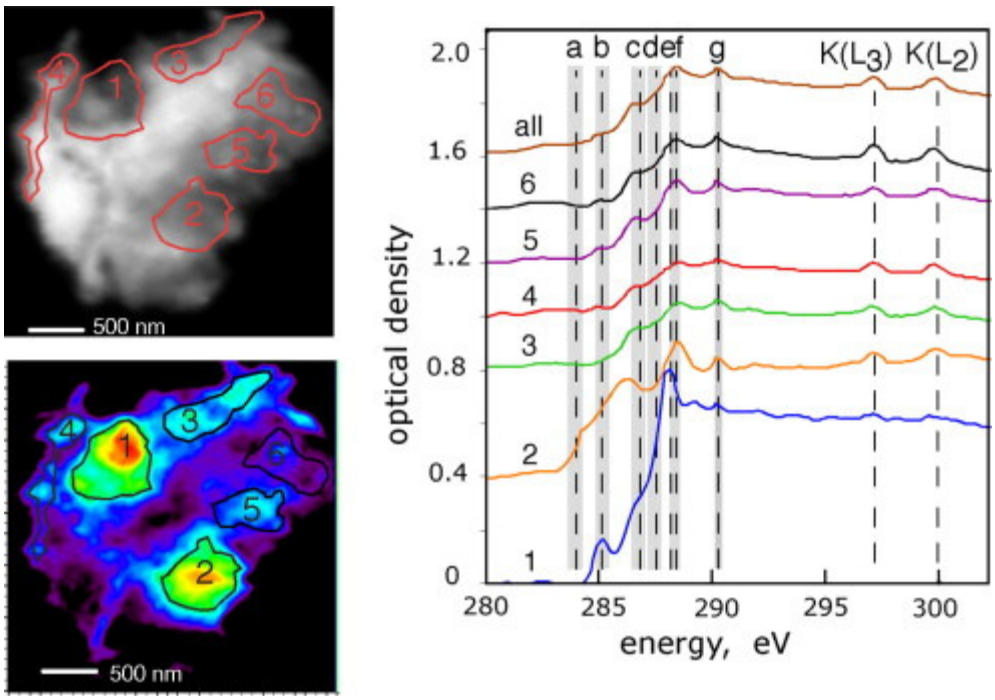

Figure 1. Variations of organic matter composition in close proximity to mineral surfaces within a microaggregate. Carbon NEXAFS spectra obtained within selected areas (regions numbered 1 through 6), and for the whole sample. Spectral features identified by the vertical dashed lines correspond to C in (a) quinonic, (b) aromatic, (c) phenolic, (d) aliphatic, (e) peptidic, (f) carboxylic, and (g) carbonate/carbonyl functional groups. The shaded gray bands indicate energy ranges attributed to each functional group. The peaks at the higher energies result from small amounts of K^+, and correspond to its L_3 and L_2 edges. Figure adopted from Wan *et al.* (2007).

The new view of minerals as building blocks of microbial microreactors raises the question whether minerals simply have structural roles ("bricks") in such microstructures, or whether they have any ecological function, for example, serving as nutrient sources or as alternate electron acceptors at times when oxygen is scarce. Historic knowledge about the role of the microbiota in weathering processes (Barker *et al.* 1998) together with more recent publications on microbial-mineral interactions leave little doubt that the microbiota actively interact with mineral surfaces for a number of purposes. One well known process is the reduction of structural Fe(III) by bacteria on the surface of smectite clay minerals (Kostka *et al.* 2002). The presence of smectite has also been shown to be a key stimulus to the rapid growth of biofilms in a laboratory setting (Alimova *et al.* 2006), with evidence that the microbiota actively create composite organo-clays (Alimova *et al.* 2009). In another recent example, altering the mineral composition of soil caused a shift in microbial community structure (Carson *et al.* 2007), prompting Kotani-Tanoi *et al.* (2007) and Carson *et al.* (2009) to state that the structure of bacterial communities in soil is influenced by the mineral substrates in their microhabitat and that minerals in soil play a greater role in bacterial ecology than simply providing an inert matrix for bacterial growth.

Outlook

Evidence is accumulating that the role of the mineral matrix in carbon stabilization needs to be viewed in a new light. In the past, the effect of mineralogy on SOM turnover has typically been viewed as a matter of variations in surface reactivity. But differences in mineralogy are not just differences in surface chemistry. As minerals are either weathered into fragments or crystallize from solution, they vary in shape and size, kinetic and thermodynamic stability, abundance and extent of reactive surfaces. Consequently, differently sized specimens of the identical mineral can not be considered constant in their ability to provide reactive surfaces, their ability to serve as physical barriers or as suppliers of dissolved cations, which in turn may act as complexing and/or precipitating agents. It appears that scientific progress will require us to add spatial complexity to the classical sorbent-sorbate model of mineral-organic interactions.

References

Alimova A, Katz A, Steiner N, Rudolph E, Wei H, Steiner JC, Gottlieb P (2009) Bacteria-clay interactions: structural changes in smectite induced during biofilm formation. *Clays and Clay*

Minerals **57**, 205-212.
Alimova A, Roberts M, Katz A, Rudolph E, Steiner JC, Alfano RR, Gottlieb P (2006) Effects of smectite clay on biofilm formation by microorganisms. *Biofilms* **3**, 47-54.
Arnarson TS, Keil RG (2001) Organic-mineral interactions in marine sediments studied using density fractionation and X-ray photoelectron spectroscopy. *Organic Geochemistry* **32**, 1401-1415.
Barker WW, Welch SA, Chu S, Banfield JF (1998) Experimental observations of the effects of bacteria on aluminosilicate weathering. *American Mineralogist* **83**, 1551-1563.
Carson JK, Campbell L, Rooney D, Clipson N, Gleeson DB (2009) Minerals in soil select distinct bacterial communities in their microhabitats. *Fems Microbiology Ecology* **67**, 381-388.
Carson JK, Rooney D, Gleeson DB, Clipson N (2007) Altering the mineral composition of soil causes a shift in microbial community structure. *Fems Microbiology Ecology* **61**, 414-423.
Chenu C, Plante AF (2006) Clay-sized organo-mineral complexes in a cultivation chronosequence: revisiting the concept of the 'primary organo-mineral complex'. *European Journal of Soil Science* **57**, 596-607.
Chenu C, Stotzky G (2002) Interactions between Microorganisms and Soil Particles: An Overview. In 'Interactions between Soil Particles and Microorganisms'. (Eds PM Huang, J-M Bollag, N Senesi). (John Wiley & Sons.
Kahle M, Kleber M, Jahn R (2002a) Carbon storage in loess derived surface soils from Central Germany: Influence of mineral phase variables. *Journal of Plant Nutrition and Soil Science* **165**, 141-149.
Kahle M, Kleber M, Jahn R (2002b) Predicting carbon content in illitic clay fractions from surface area, cation exchange capacity and dithionite-extractable iron. *European Journal of Soil Science* **53**, 639-644.
Kahle M, Kleber M, Torn MS, Jahn R (2003) Carbon storage in coarse and fine clay fractions of illitic soils. *Soil Science Society of America Journal* **67**, 1732-1739.
Kalbitz K, Schmerwitz J, Schwesig D, Matzner E (2003) Biodegradation of soil-derived dissolved organic matter as related to its properties. *Geoderma* **113**, 273-291.
Kleber M, Mikutta R, Torn MS, Jahn R (2005) Poorly crystalline mineral phases protect organic matter in acid subsoil horizons. *European Journal of Soil Science* **56**, 717-725.
Kostka JE, Dalton DD, Skelton H, Dollhopf S, Stucki JW (2002) Growth of iron(III)-reducing bacteria on clay minerals as the sole electron acceptor and comparison of growth yields on a variety of oxidized iron forms. *Applied and Environmental Microbiology* **68**, 6256-6262.
Kotani-Tanoi T, Nishiyama M, Otsuka S, Senoo K (2007) Single particle analysis reveals that bacterial community structures are semi-specific to the type of soil particle. *Soil Science and Plant Nutrition* **53**, 740-743.
Lehmann J, Kinyangi J, Solomon D (2007) Organic matter stabilization in soil microaggregates: implications from spatial heterogeneity of organic carbon contents and carbon forms. *Biogeochemistry* **85**, 45-57.
Lehmann J, Solomon D, Kinyangi J, Dathe L, Wirick S, Jacobsen C (2008) Spatial complexity of soil organic matter forms at nanometre scales. *Nature Geoscience* **1**, 238-242.
Mayer LM, Xing B (2001) Organic matter - surface area relationships in acid soils. *Soil Science Society of America Journal* **65**, 250-258.
Ransom B, Dongsom K, Kastner M, Wainwright S (1998) Organic matter preservation on continental slopes: Importance of mineralogy and surface area. *Geochimica et Cosmochimica Acta* **62**, 1329-1345.
Wan J, Tyliszczak T, Tokunaga TK (2007) Organic carbon distribution, speciation, and elemental correlations within soil microaggregates: Applications of STXM and NEXAFS spectroscopy. *Geochimica et Cosmochimica Acta* **71**, 5439-5449.

Occurrence and environmental significance of sideronatrite and other mineral precipitates in Acid Sulfate Soils

Rob Fitzpatrick[A,B] Paul Shand[A], Mark Raven[A] and Stuart McClure [A,B]

[A] CSIRO Land and Water, Urrbrae, South Australia, Australia
[B] Earth and Environmental Sciences, The University of Adelaide, South Australia, Australia
Email addresses: rob.fitzpatrick@csiro.au; paul.shand@csiro.au; mark.raven@csiro.au; stuart.mcclure@csiro.au

Abstract
This study documents the first occurrence of metavoltine in Australia and the widespread occurrences of sideronatrite and tamarugite in Acid Sulfate Soils (ASS). We interpret the occurrence of these soluble salts to represent changing surface and ground water tables, which are linked to the lowering of water levels in the River Murray and Lower Lakes where capillary action, combined with subsurface evaporation, has concentrated Fe-Al-Na-Mg sulfates, especially in summer or during dry periods. During winter rainfall wet/drying events in the sandy sulfuric materials on exposed beaches, soluble white sulfate-containing evaporite minerals comprising pickeringite-halotrichite, redingtonite, hexahydrite and epsomite precipitate as micron thick layers on the soil surface. Sideronatrite and tamarugite precipitate within yellowish-green friable 2 to 5 mm thick crusts on the soil surface. Sideronatrite (large platelets) is derived from the oxidation and dissolution of the sulfide framboids in sulfuric materials (< pH 2.5). Surrounding some of the crusts where water temporarily leaches and ponds, sideronatrite dissolves and re-precipitates as schwertmannite within orange coloured patches. These mineral precipitates play important roles in the transient storage of components (Fe, Al, Na, Ca, Mg, Cl, Sr and SO_4), which may also dissolve to contribute to the formation of saline monosulfidic black ooze in wetter soils (e.g. adjacent to the lakes). These salts are likely to form if water levels decrease and have the potential to become a problem during re-flooding if not managed properly. Salt efflorescences also have potential for aerial transport and to be dissolved in water. There is a need to prevent stock from ingesting these salts (similar to Epsom salts) because this is likely to lead to scouring in sheep and cattle. Magnesium salts are toxic when ingested in high levels.

Key Words
Sulfuric materials, salt efflorescences, iron oxyhydroxysulfates; sulfate-containing evaporite minerals

Introduction

Acidification occurs if the amount of acidity produced exceeds the pH buffering capacity (the overall neutralizing capacity) of the soil. For sulfuric materials, the products of the chemical reactions can: (i) remain as dissolved constituents of soil pore waters, (ii) form a range of secondary minerals in the form of salt efflorescences comprising sulfate-rich salts that accumulate due to evaporation (e.g. epsomite and hexahydrite), (iii) undergo a series of hydrolysis reactions and precipitate new minerals such as iron oxyhydroxides and iron oxyhydroxysulfates (e.g. jarosite, natrojarosite, schwertmannite and sideronatrite) and (iv) accelerate the weathering or dissolution of minerals in soils and sediments. The hydroxysulfate minerals formed are important to recognize because they store acidity and metals that can subsequently generate poor water quality. Several studies have shown that dissolution of salt accumulations along stream banks during a rainstorm temporarily lowers pH and increases metal loads in streams (e.g. Fitzpatrick *et al.* 2009a,b). Such water quality impacts can have damaging effects on aquatic ecosystems and can complicate efforts to remediate acid drainage. Rainfall and rewetting events can also flush salts, leading to pulses of contaminated water flowing into streams or wetlands. Such flushes mean that these various products or minerals may or may not be present at a given site on a given day, depending on weather conditions.

Results and Discussion

Lake Alexandrina, Lake Albert and adjacent tributaries (Finniss River and Currency Creek)

Due to the extreme drought conditions in south-eastern Australia that commenced in about 2006, water levels have declined in Lake Alexandrina, Lake Albert and the River Murray system, especially in the section below Blanchetown (Lock 1) (e.g. Lake Alexandrina shown in Figure 1a; Fitzpatrick *et al.* 2008a; 2009a,b). The reducing hypersulfidic material once covered by water has became exposed to oxygen at the river and lake margins (Figures 1a and 2), and in adjacent wetlands. With continued lowering of water levels, the hypersulfidic material has became progressively oxidised to greater depths in the soil profile (Figure 1).

The spatial variation of the following soil features caused by receding water levels due to current extreme drought conditions is described in Figure 2: (i) monosulfidic material in the subaqueous soils, (ii) the prominent bright yellow mineral, sideronatrite, with a pH ranging between 1.3 to 1.6 on the soil surface, which overlies black hypersulfidic material in the soil pit (see close-up views in Figure 1) and (iii) brownish-orange coatings of the mineral schwertmannite, which forms from sideronatrite (dissolves in rainwater and re-precipitates as schwertmannite).

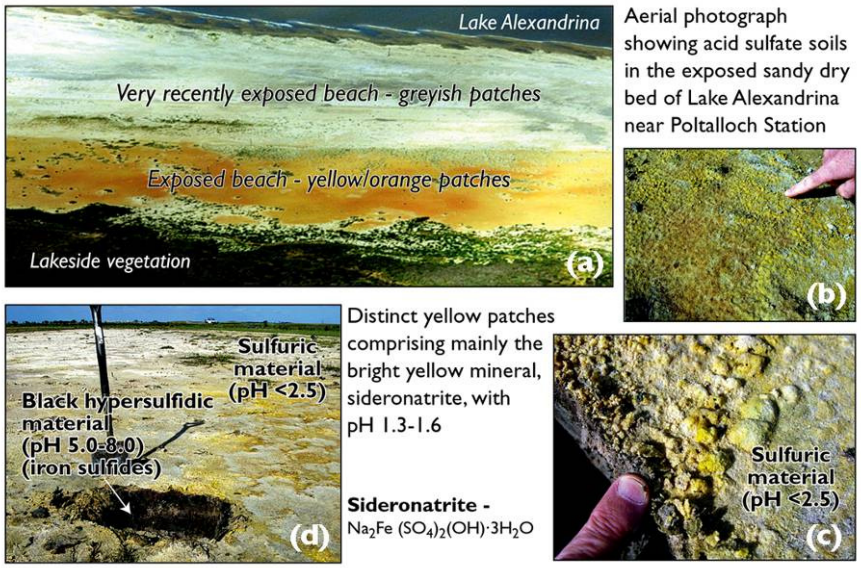

Figure 1. (a) Aerial photograph showing of sandy dry lake-bed of Lake Alexandrina with surface crusts comprising coloured salt efflorescences: (i) bright yellowish coloured on slightly elevated surfaces as seen in the close-up photographic views [(b) and (c)] and (ii) orange patches occurring on the edges of lightly elevated surfaces [(b)]. (d) Soil pit with black hypersulfidic material (iron sulfides) at depth overlain by sulfuric material with distinct yellow patches of the bright yellow mineral, sideronatrite, with a pH ranging between 1.3 to 1.6 (from Fitzpatrick *et al.* 2008a,c; 2009b).

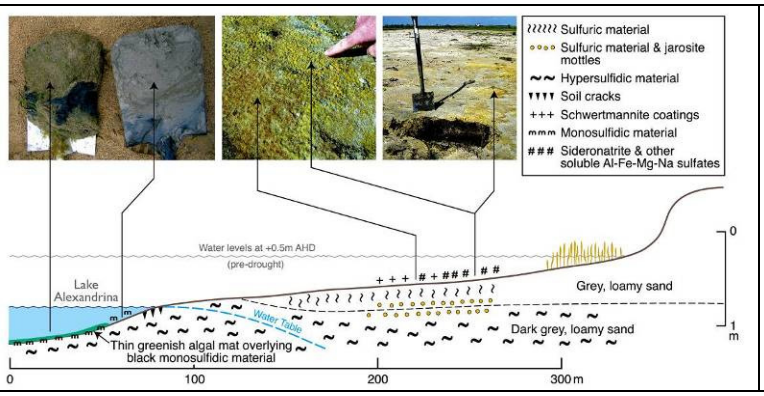

Figure 2. Descriptive soil-regolith model of Lake Alexandrina to elevated land near Poltalloch Station. (from Fitzpatrick *et al.* 2009a, b).

NOTE: The water table pattern is exaggerated because of the inflated vertical scale necessary to display all soil features.

The widespread occurrences of bright yellowish-green surface efflorescences can be observed at a range of scales from landscape (Figure 1a) to soil profile (Figures 1d & 2) scales and may be present as either finely dispersed powder in sand or as a 2 to 5 mm thick, sandy friable crust (Figure 1c). These surface efflorescences contain mainly precipitates of the minerals sideronatrite ($[Na_2Fe(SO_4)_2.OH\cdot 3H_2O]$), tamarugite($[Na_2Al(SO_4)_2.OH\cdot 3H_2O$) and alunogen ($[Al_2(SO_4)_3\cdot 17H_2O]$). Sideronatrite occurs as rosettes and platelets (Figure 3) within sulfuric material (pH 0.8 to 1.6) on the soil surface. Sideronatrite is derived from the oxidation and dissolution of pyrite framboids, which occur mainly in the form of spheroidal aggregates of pyrite crystals (Figure 4). Sideronatrite in the yellowish-green crusts dissolves and re-precipitates as schwertmannite (Figure 1 and 2) in immediately adjacent zones where the pH is slightly higher, to display distinct orange patches or areas on the soil surface and diffuse orange mottles to a depth of 2 to 10 cm.

These minerals not only form seasonally during summer heat and high evaporative conditions in soils exposed by drought, but also during: (i) the winter rainfall cyclic wetting and drying events and (ii) the cyclic rewetting of the sulfidic materials due to lake level changes associated with seiching, which is likely to be an important acidity transfer mechanism from ASS to lake water. Seiching has a tidal effect, and occurs when wind blows shallow lake water onshore. Typical water level variations in Lake Alexandrina during seiching can be tens of centimetres according to wind strength and direction, and may advance the waterline many tens of metres inland (i.e. up the beach) due to the shallow bathymetric gradient. The rewetting of sideronatrite by rainwater and seiching causes mineral dissolution and the resultant mobilisation of acid, iron, sulfate and sodium ions to immediately adjacent, temporary ponded areas, where orange coloured

schwertmannite rapidly crystallises. This process has also been simulated in the laboratory by adding rainwater to both natural samples of the sideronatrite-rich crusts and synthetically prepared sideronatrite. A remarkably similar dissolution and precipitation mechanism was previously observed by Fitzpatrick *et al*. (2000) in sandy sulfuric materials in eroded river banks in the Mount Lofty Ranges. This was the first identification of the formation of sideronatrite from oxidation of sulfide framboids in sandy sulfuric materials. They also observed dissolution of sideronatrite (and tamarugite) in sulfuric materials on eroded stream banks and the subsequent formation of schwertmannite in immediately adjacent stream waters.

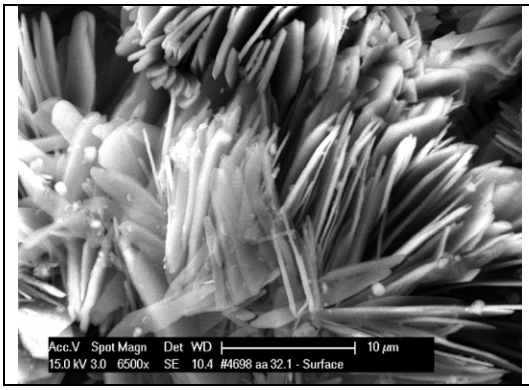

Figure 3. Scanning electron micrograph, of bladed sideronatrite crystals [Na_2 $Fe^{3+}(SO_4)_2(OH)\cdot 3(H_2O)$]. Sample as sub-sampled from Lake Alexandrina sample AA 32.1, 0-0.05 cm – from Fitzpatrick *et al.* 2008c). The image was taken in the secondary electron imaging mode, using a Phillips XL30 SEM, at a magnification of 6.50 kX. The approximate composition as analysed by Energy Dispersive X-ray analysis is illustrated in Fitzpatrick *et al.* 2008c.

In addition, a wide range of highly soluble whitish coloured sulfate-containing evaporite minerals in sulfuric materials were identified in Lake Albert and Lake Alexandrina (i.e. pickeringite-halotrichite and redingtonite together with hexahydrite and epsomite – Figure 4) that crystallise in micron thick layers on the exposed sandy soil surfaces during the winter rainfall cyclic wetting and drying events.

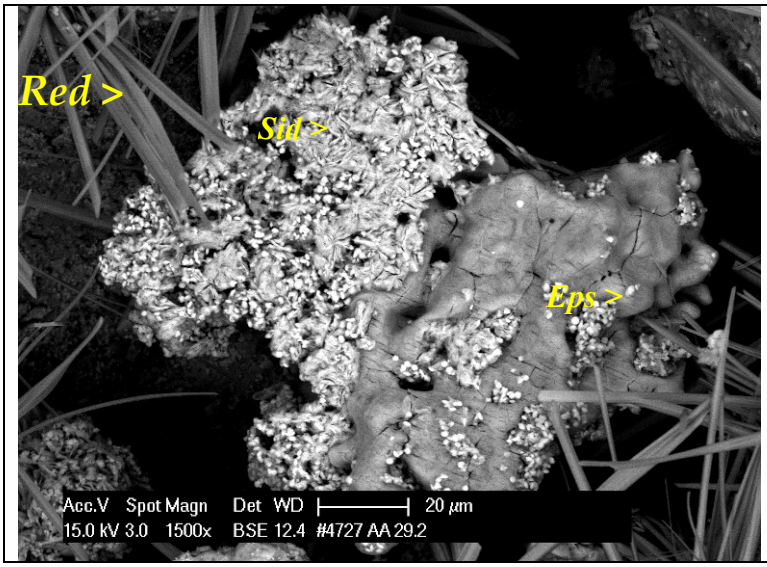

Figure 4. Scanning electron micrograph, of bladed sideronatrite crystals [$Na_2Fe^{3+}(SO_4)_2(OH)\cdot 3H_2O$] mixed with fine grained pyrite crystals (Pyr) [FeS_2], redingtonite (Red) [$(Fe^{2+}$, Mg, Ni) $(Cr, Al)_2(SO_4)_4\cdot 22H_2O$], and epsomite (Eps) [$MgSO_4\cdot 7H_2O$] infiltrating the conglomerate. Sample as sub-sampled from Lake Alexandrina; sample AA 29.2, 0-0.2 cm. The image was taken in the BSE imaging mode, using a Phillips XL30 SEM, at a magnification of 1.5kX (from Fitzpatrick *et al.* 2008c).

Main River Channel and adjacent wetlands for River Murray, Loddon River and Burnt Creek (Victoria)

A number of distinctive bight yellow oxyhydroxysulfate minerals have been identified in several wetlands adjacent to the River Murray as a consequence of sulfide oxidation and formation of sulfuric material, which developed after drainage of the soils as watertable levels dropped below 40 cm in June 2007 to below 90 cm in November 2007. In these wetlands, the presence of such key "indicator minerals" proved particularly useful in the field identification of sulfuric materials. In fact, it was these prominent features, which originally led CSIRO to first discover the presence of sulfuric materials in the Swanport wetland near Murray Bridge in June 2007 (Fitzpatrick *et al.* 2008b). In these surface soils salt efflorescences comprised salts with a yellowish (natrojarosite) or golden mineral determined to be the rare mineral metavoltine ($Na_6K_2FeFe_6(SO_4)_{12}O_2.18H_2O$), which formed botryoidal encrustations on the edges of cracks as an alteration product of weathered pyrite. This discovery documented the first occurrence of metavoltine in Australia and possibly the first ever occurrence associated with ASS. White crystals of alunogen ($Al_2(SO_4)_3$ $17H_2O$), hexahydrite and gypsum were also identified, having formed as a result of acidic (pH < 2.5), sulfate-bearing solutions that reacted with layer silicates in the soils. These localised solutions were rich in ferrous and ferric iron and also contained dissolved potassium and sodium. Metavoltine and alunogen are the last minerals to form in areas of intense evaporation.

Sideronatrite was also identified in salt efflorescences on surface layers in Lake Bonney (Fitzpatrick *et al.* 2008d) and Nelwart Lagoon (situated close to Renmark in SA Riverland; Shand *et al.* 2009) as they dried out and sulfuric materials gradually formed. These minerals also included natrojarosite and tamarugite together with a number of Mg and Na sulfate minerals, particularly where groundwater discharges were present. Bright yellowish green surface efflorescences were also identified in Burnt Creek and comprised sideronatrite, which formed as an alteration product of weathered pyrite. In addition, the minerals, hexahydrite, epsomite [$MgSO_4.7H_2O$], gypsum and halite were also present (Thomas *et al.* 2009).

Conclusions

Soil-surface salt accumulations are unique in the region, which results from a combination of the characteristic Mediterranean type climate, hydrogeology, saline seepages, and salt crusting formed above sulfidic materials. These salt efflorescences are often dominated by the widespread occurrences of sideronatrite and tamarugite together with a large number of soluble minerals, including halite, gypsum, thenardite (Na_2SO_4), hexahydrite and epsomite, and range in morphology from thin, powdery, very transient efflorescences to thicker, more persistent, soil-cementing crusts. The salt crusts form by the upward wicking of Na, Mg, Cl and SO_4 containing groundwaters and their subsequent surface evaporation. These Fe/Al oxyhydroxysulfate and oxyhydroxide minerals are indicators of very acidic soil conditions (i.e. the presence or former presence of oxidised pyrite), and as such their presence provides important environmental indicators of ASS (e.g. Fitzpatrick and Self 1997).

References

Fitzpatrick RW, Grealish G, Shand P, Simpson SL, Merry RH, Raven MD (2009a) Acid Sulfate Soil Assessment in Finniss River, Currency Creek, Black Swamp and Goolwa Channel, South Australia. CSIRO Land and Water Science Report 26/09. CSIRO, Adelaide, 213 pp. http://www.clw.csiro.au/publications/science/2009/sr26-09.pdf

Fitzpatrick RW, Raven M, Self PG, McClure S, Merry RH, Skwarnecki M (2000) Sideronatrite in acid sulfate soils in the Mt. Lofty Ranges: First occurrence, genesis and environmental significance. In 'New Horizons for a New Century' (Eds. Adams JA, Metherell AK), pp. 109-110. Australian and New Zealand Second Joint Soils Conference Volume 2: Oral Papers. December 2000, Lincoln University, NZ Society of Soil Science.

Fitzpatrick RW, Self PG (1997) Iron oxyhydroxides, sulfides and oxyhydroxysulfates as indicators of acid sulphate surface weathering environment. In 'Soils and Environment: Soil Processes from Mineral to Landscape Scale' (Eds. Auerswald K, Stanjek H, Bigham JM), pp. 227-240. Advances in GeoEcology 30. Catena Verlag, Reiskirchen, Germany.

Fitzpatrick RW, Shand P, Merry RH, (2009b) Acid Sulfate Soils. In 'Natural History of the Riverland and Murraylands' (Ed Jennings JT), pp. 65-111 (Royal Society of South Australia (Inc.) Adelaide, South Australia).

Fitzpatrick RW, Shand P, Marvanek S, Merry RH, Thomas M, Simpson SL, Raven MD, McClure S (2008a) Acid sulfate soils in subaqueous, waterlogged and drained soil environments in Lake Albert, Lake Alexandrina and River Murray below Blanchetown (Lock 1): properties, distribution, genesis, risks and management. Prepared for Department of Environment and Heritage, SA. CSIRO Land and Water Science Report 46/08. CSIRO, Adelaide, 167. pp. http://www.clw.csiro.au/publications/science/2008/sr46-08.pdf

Fitzpatrick RW, Shand P, Thomas M, Merry RH, Raven MD, Simpson SL (2008b) Acid sulfate soils in subaqueous, waterlogged and drained soil environments of nine wetlands below Blanchetown (Lock 1), South Australia: properties, genesis, risks and management. Prepared for South Australian Murray-Darling Basin Natural Resources Management Board. CSIRO Land and Water Science Report 42/08. CSIRO, Adelaide, 122. pp. http://www.clw.csiro.au/publications/science/2008/sr42-08.pdf

Fitzpatrick RW, Shand P, Merry RH, Thomas B, Marvanek S, Creeper N, Thomas M, Raven MD, Simpson, SL, McClure S, Jayalath N (2008c) Acid sulfate soils in the Coorong, Lake Alexandrina and Lake Albert: properties, distribution, genesis, risks and management of subaqueous, waterlogged and drained soil environments. Prepared for Department of Water, Environment, Heritage and Arts. CSIRO Land and Water Science Report 52/08. CSIRO, Adelaide, 167. pp. http://www.clw.csiro.au/publications/science/2008/sr52-08.pdf

Fitzpatrick RW, Shand P, Merry RH, Raven MD (2008d) Acid sulfate soil materials and salt efflorescences in subaqueous and wetland soil environments at Lake Bonney, SA: Properties, risks and management. Consultancy Report for South Australian Murray-Darling Basin Natural Resources Management Board. CSIRO, Adelaide, 130. pp http://www.clw.csiro.au/publications/science/2008/sr21-08.pdf

Shand P, Merry RH, Fitzpatrick, RW and Thomas M (2009) Acid sulfate soil assessment of disconnected wetlands between Lock 1 and Lock 5, River Murray, South Australia. CSIRO: Water for a Healthy Country National Research Flagship.

Thomas BP, Merry RH, Creeper NL, Fitzpatrick RW, Shand P, Raven MD, Jayalath N (2009) Acid Sulfate Soil Assessment of the Lower Loddon River and Burnt Creek, Central Victoria. CSIRO Land & Water Science Report CLW 18/09. http://www.clw.csiro.au/publications/science/2009/sr18-09.pdf

Phosphate sorption to organic matter/ferrihydrite systems as affected by aging time

Fiona R. Kizewski[A], Dean Hesterberg[B], James Martin[A]

[A] Department of Chemistry, North Carolina State University, Box 8240 Raleigh, NC USA 27695
[B] Department of Soil Science, North Carolina State University, Box 7619 Raleigh, NC USA 27695 Email: jrkizews@ncsu.edu,

Abstract
It's been hypothesized that organic matter (OM) can complex iron (Fe) from oxides minerals, which provide sorption sites for phosphate (PO_4) via the formation of Fe-PO_4-OM ternary complexes. To elucidate such mechanism, the coordination structure of Fe was examined, as well as PO_4 sorption capacity and crystallinity of ferrihydrite as it aged with OM. Stock suspensions containing 1 g ferrihydrite/kg and 0 to 3.1 g OM/kg were created at pH 6.8. PO_4 sorption capacities were measured as they have aged for 1, 7, 21, 40, and 55 days. After aging for 55 days, all systems had a 20% to 50% decrease of PO_4 sorption capacity. Extended X-ray absorption fine structure (EXAFS) analyses on selected aged peat/ferrihydrite samples showed no evidence of Fe(III)-OM complexation. With the same amounts of Fe(III) and peat, mixtures of Fe(III)-peat complexes and ferrihydrite provided higher PO_4 sorption capacity per unit Fe than ferrihydrite only. Indicated by HCl extractable Fe, ferrihydrite crystallinity increased during aging. For ferrihydrite itself, crystallization was the main cause for its decreased PO_4 sorption capacity. It is very likely that the continuous competition between OM and PO_4 resulted in the decreased PO_4 sorption capacity as ferrihydrite aged with OM.

Key Words
Ferrihydrite, phosphate, organic matter, EXAFS, iron, DOC.

Introduction

As an important soil component, soil organic matter (OM) has been extensively studied for its role on phosphate sorption to oxide minerals. Many studies have found that OM has instantaneous inhibitory effect on phosphate sorption to oxide mineral, although the mechanism is under debate (Antelo, Arce *et al.* 2007; Hiradate and Uchida 2004; Kreller, Gibson *et al.* 2003). With longer time, however, the scenario is different. After the studied soils and PO_4 have equilibrated for 7 days in calcium acetate background electrolyte, organic matter did not alter the soils' PO_4 sorption capacity (Borggaard, Jorgensen *et al.* 1990). When PO_4 was added to Fe- or Al-oxide/humic acid (HA) mixtures, the system's PO_4 sorption capacity was lower than the mineral itself after equilibration for three days. However, as longer equilibration time (up to 28 days) was given, the mineral/HA systems had about the same PO_4 sorption capacities as the mineral itself (Borggaard, Raben-Lange *et al.* 2005). While the change of PO_4 sorption to oxide minerals appears to be a kinetic issue since PO_4 sorption can take scores of days before reach equilibration (Bolan, Barrow *et al.* 1985), Gerke and Mt (1993) proposed that the increased PO_4 sorption to Fe-oxide/humic mixtures involved a change of sorption mechanism. In this study, PO_4 sorption capacities of mixture of poorly crystalline Fe-oxide and humic substances first decreased (pH 7), then increased by 15% after aging for 56 days, parallel with increased Fe-humic complexes. The author hypothesized that Fe from oxide was complexed by humic substances. These complexes provided more sorption sites for PO_4 via the formation of PO_4-Fe-OM ternary complexes, resulting in the increased PO_4 sorption capacity.

Although the published results support the ternary complexation mechanism, molecular understanding of such mechanism remains little. Direct evidence for such Fe-PO_4-OM complexes has yet to be found. Applying the technique of EXAFS and other analytical methods, this study aims to explore how OM affects PO_4 sorption to ferrihydrite as they age and elucidate the underlying mechanisms. The specific objectives were: 1) determine any change of PO_4 sorption capacity of ferrihydrite/OM systems as they age; 2) determine if Fe(III) from ferrihydrite is complexed by OM and how the Fe-OM complexation contributes to the change of the system's PO_4 sorption capacity, if any. The findings of this study add to the very much needed understanding of the long term effect of organic matter on PO_4 sorption on oxide minerals.

Methods

Pahokee peat (PP) and Pahokee peat humic acid (PPHA) were purchased from International Humic Substance Society and were hydrated prior to use. Stock suspensions containing 1 g ferrihydrite/kg and 80 mg DOC from PPHA, or 0~3.1 g peat/g of ferrihydrite were prepared in 0.05 M KCl at pH 6.8. These stock

suspensions were shaken at 0.5 s^{-1} in a water-bathed shaker at 25°C for aging. For each system when it had aged for 1, 7, 21, 40 and 55 days, KH_2PO_4 solution was added to 30 g of subsample. After equilibration for 42 hours, the adsorbed PO_4 was determined by the difference between added PO_4 and dissolved PO_4 in the supernatants.

To mimic the formation of Fe(III)-peat complex (Fe-peat), $FeCl_3$ solution was added to peat suspension (at pH 2.5) prior to addition of ferrihydrite. These Fe-peat/peat/ferrihydrite mixtures had the same amounts of peat and total Fe(III) as those in system of 1 g peat/g, but differed in the percentage of Fe(III) that was complexed with peat out of total Fe(III), ranging from 0 to 20%. These systems did not age. PO_4 sorption capacities of these systems were determined by 8-point sorption isotherm experiments.
For EXAFS analysis, stock ferrihydrite and peat/ferrihydrite suspensions with peat input as 3.1, 6.2, and 12.5 g/g were prepared with different aging time. Stock Fe-peat/peat/ferrihydrite systems (no aging) were also created with total peat and Fe(III) the same as those in system 3.1 g/g. The percentages of Fe-peat out of total Fe(III) were 0%, 50%, and 100%. All these suspensions were first centrifuged and the solids were mounted to sample holders for EXAFS data collection at beamline X-11B of National Synchrotron Light Source (NSLS) at the Brookhaven National Lab (Upton NY).
* DOC=dissolved organic carbon from Pahokee peat humic acid

Results
Figure 1 shows the change of PO_4 sorption capacities of OM/ferrihydrite systems as they aged. For ferrihydrite or system A, there was an approximately 20% decrease of PO_4 sorption capacity after aging for 55 days. PO_4 sorption capacity decreased by 38% and 56% when peat input was 1 and 3.1 g/g, respectively. Regardless of the amount of OM, all systems showed decreasing PO_4 sorption capacities during aging. The decrease is greater with higher OM. For the same aging time, more OM resulted in lower PO_4 sorption capacity, which indicates the competition between OM and PO_4 for sorption sites on ferrihydrite surface.

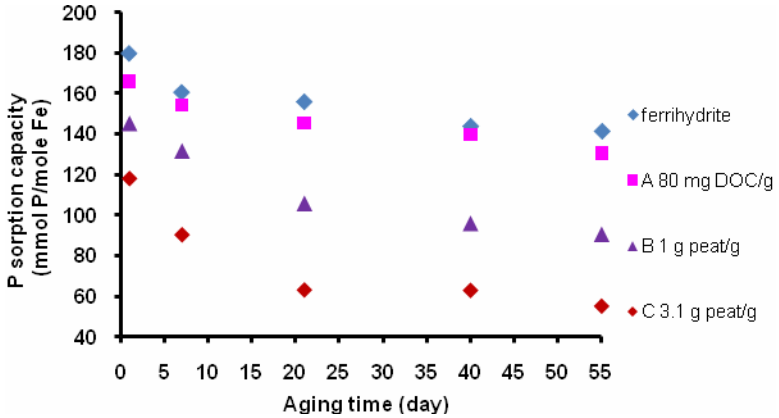

Figure 1. Change of PO_4 sorption capacities of OM/ferrihydrite systems as they aged for 55 days.

The systems presented in Figure 2 have the same Fe(III) and peat as those in system of 1g peat/g, but different amounts of Fe(III) that is complexed with peat. When all Fe(III) was in the form of ferrihydrite (0% Fe-peat), the system's PO_4 sorption capacity was the lowest as 125 mmol P/mole Fe. The system's PO_4 sorption capacity increased as Fe(III)-peat complexes increased, reaching the maximum capacity of 166 mmol/mole when 10% of total Fe(III) was complexed with peat. More Fe(III)-peat complexes did not further increase the system's PO_4 sorption capacity. These results suggest that if Fe(III) from ferrihydrite were complexed by peat, the PO_4 sorption capacities of these peat/ferrihydrite systems would have increased.

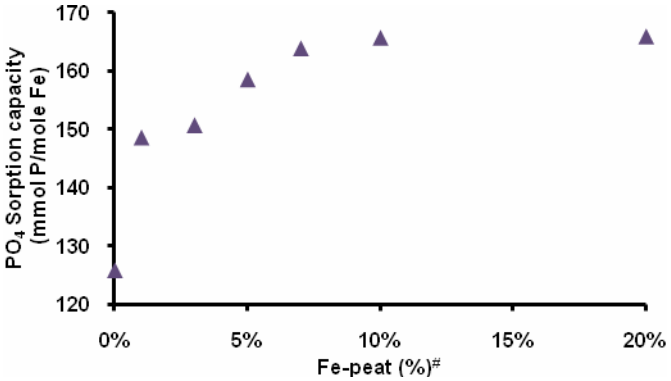

Figure 2. PO_4 sorption capacity of Fe-peat/peat/ferrihydrite systems increased as Fe(III)-peat complexes increased. Total peat and Fe(III) in these systems are equal to those in system B (1 g peat/g ferrihydrite).
Fe-peat (%) denotes the percentage of total Fe(III) that is complexed with peat.

Figure 3 displays the Fe K-edge EXAFS spectra of peat/ferrihydrite systems that have aged for 1 day. Essentially these spectra show no structural difference of Fe, regardless of the amount of peat present with ferrihydrite.

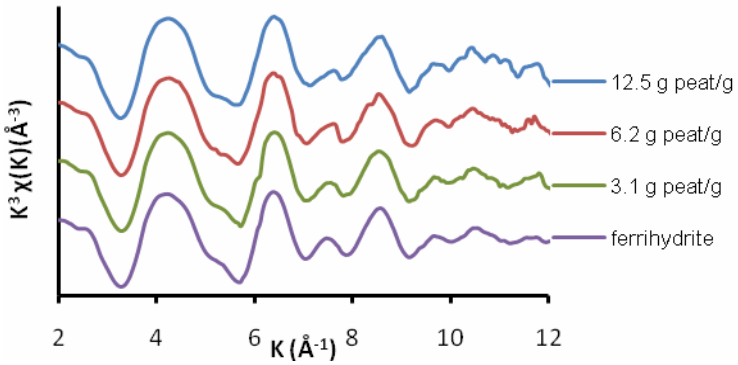

Figure 3. Fe K-edge EXAFS spectra of ferrihydrite/peat systems that have aged for 1 day.

The systems displayed in Figure 4A have the same amounts of total Fe(III) and peat as those in the systems displayed in Figure 4B (3.1 g peat/g), but different amounts of Fe(III)-peat complexes. Fe(III)-peat complexation illustrates distinct spectral features from Fe(III) in ferrihydrite (from bottom to top), as highlighted by the vertical bars. The spectral features of Fe(III)-peat complexation are absent in the spectra displayed in Figure 4B, which are essentially the same to each other, regardless of aging time. EXAFS analyses provided no evidence to show Fe(III)-peat complexation during aging.

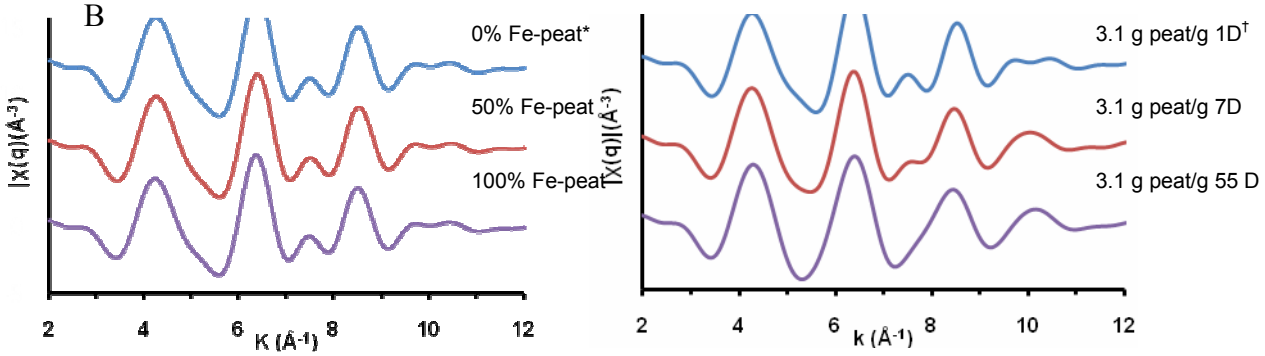

* peat-Fe denotes Fe(III) that is complexed with peat. †D denotes aging time in days.

Figure 4. (A) Fourier-filtered ($R+\Delta R$=1-3.5 Å) EXAFS spectra of Fe-peat/peat/ferrihydrite systems (total Fe(III) and peat are equal to those in 3.1g peat/g); (B) Fourier-filtered ($R+\Delta R$=1-3.5 Å) EXAFS spectra of peat/ferrihydrite systems (3.1 g/g) that have aged for 1, 7 and 55 D. Vertical bars highlight the change or no change of spectral features.

As an indication of crystallinity (Cornell and Schneider 1989), 0.4 M HCl extractable Fe from ferrihydrite decreased by 10% after aging for 55 days (data not shown), although the change of crystallinity was not detected by x-ray diffraction (XRD). B.E.T. surface area of ferrihydrite decreased from 330 to150 m^2/g after aging for 55 days. No crystallization was detected by XRD in all OM/ferrihydrite systems.

Conclusions

Crystallization of ferrihydrite caused its decreased PO_4 sorption capacity by 20% after aging for 55 days. We did not find increasing PO_4 sorption capacity as ferrihydrite aged with OM as reported in the literature. On the contrary, these OM/ferrihydrite systems had a 20% to 50% decrease of PO_4 sorption capacity after aging for 55 days. EXAFS analyses of peat/ferrihydrite systems that have aged for different time did not show any change of Fe coordination structure as induced by the amount of peat or aging time. On the other hand, Fe(III)-peat complexation did contribute to higher PO_4 sorption capacity than the same amount of Fe(III) in the form of ferrihydrite. The competition between organic matter and PO_4 appeared to be responsible for the decreasing PO_4 sorption capacity as ferrihydrite aged with organic matter.

Acknowledgement

This work was supported by the USDA-CSREES NRI Grant No.2005-35107-16253. Beamline X-11B (National Synchrotron Light Source, Brookhaven National Laboratory) is supported by DOE's Divisions of Materials Science and Chemical Sciences.

References

Antelo J, Arce F, Avena M, Fiol S, Lopez R, Macias F, Kq (2007) Adsorption of a soil humic acid at the surface of goethite and its competitive interaction with phosphate. *Geoderma* **138**(1-2), 12-19.

Bolan NS, Barrow NJ, Posner AM (1985) Describing the effect of time on sorption of phosphate by iron and aluminum hydroxides. *Journal of Soil Science* **36**(2), 187-197.

Borggaard OK, Jorgensen SS, Moberg JP, Rabenlange B, Eb (1990) Influence of organic-matter on phosphate adsorption by aluminum and iron-oxides in sandy soils. *Journal of Soil Science* **41**(3), 443-449.

Borggaard OK, Raben-Lange B, Gimsing AL, Strobel BW, Bj (2005) Influence of humic substances on phosphate adsorption by aluminium and iron oxides. *Geoderma* 127(3-4), 270-279.

Cornell RM, Schneider W (1989) Formation of goethite from ferrihydrite at physiological ph under the influence of cysteine. *Polyhedron* **8**(2), 149-155.

Gerke J, Mt (1993) Phosphate adsorption by humic/fe-oxide mixtures aged at ph-4 and ph-7 and by poorly ordered fe-oxide. *Geoderma* **59**(1-4), 279-288.

Hiradate S, Uchida N (2004) Effects of soil organic matter on pH-dependent phosphate sorption by soils. *Soil Science and Plant Nutrition* **50**(5), 665-675.

Kreller DI, Gibson G, Novak W, Van Loon GW, Horton JH, Zm (2003) Competitive adsorption of phosphate and carboxylate with natural organic matter on hydrous iron oxides as investigated by chemical force microscopy. *Colloids and Surfaces a-Physicochemical and Engineering Aspects* **212**(2-3), 249-264.

Quantifying microstructural stability of South-Brazilian soils by the application of rheological techniques and zeta potential measurements

Wibke Markgraf[a], Cornelia Bellmann[b], Anja Caspari[b], Rainer Horn[a]

[A]Christian-Albrechts-University zu Kiel, Institute for Plant Nutrition and Soil Science, Hermann-Rodewald-Str. 2, D-24118 Kiel, Germany, Email w.markgraf@soils.uni-kiel.de
[B]Leibniz-Institute of Polymere Research Dresden e.V., Hohe Strasse 6, D-01069 Dresden, Germany

Abstract
Rheological and zeta potential measurements were performed with South-Brazilian soils, a kaolinitic, Fe-oxide-rich Oxisol, and a smectitic Vertisol, respectively. Hence, a low active clay and a high active clay system were compared. Furthermore, the phenomenon of pseudosand was investigated. Stiffness degradation was measured by conducting amplitude sweep tests with a rotational rheometer in oscillatory mode. By using loss factor tan δ(γ), elasticity and viscosity of substrates can be defined in detail and calculated. Zeta potential measurements show a clear trend of agglomeration for Oxisols, whilst Vertisol suspensions remain stable over a wide range of pH 10…2; the isoelectric point (IEP) is reached at pH 2 in case of the Oxisol. A synopsis of rheological and zeta potential results may explain both pseudosand effects due to Fe-oxides and microstructural stability deriving from physicochemical properties i.e. texture, clay mineralogy, and CEC.

Key Words
Rheology, zeta potential, microstructural stability, Fe-oxides, pseudosand, IEP

Introduction
Amplitude sweep tests with controlled shear deformation have been conducted on homogenised substrates deriving from kaolinitic, Fe-oxide-rich Brazilian Oxisol and a smectitic Vertisol in order to (semi-)quantify stiffness degradation. The influence of Fe-oxides, and clay minerals on micromechanical shear behaviour under oscillation has been tested under saturated and pre-drained conditions. From collected data, which include parameters as G' (storage modulus), G" (loss modulus), loss factor tan d results, which indicates the dissipation of elasticity in a viscoelastic substance (=soil). Furthermore, rheological findings were complemented by zeta potential measurements, with the intention to investigate agglomeration behaviour.

Material and Methods
South-Brazilian soils, in detail an Oxisol (S. Ângelo, natural forest) and a Vertisol (Santana do Livramento, pasture) were investigated; rheological findings are presented by Markgraf and Horn (2007) in detail. Analyses i.e. texture, CEC, pH, and C_t, were conducted according to standard methods as described in van Reeuwijk (2002). Iron oxides were extracted by Na-dithionite according to Mehra and Jackson (1960). The Oxisol is dominated by a kaolinitic clay fraction, whereas the Vertisol shows a smectitic clay mineralogy and a typical, high content of Mg^{2+} and Ca^{2+} in a ratio of 1:2.5 (Table 1).

Table 1. Physicochemical properties of the investigated soil material.

	Sand	Silt	Clay	Na	Mg	Ca	pH	C_t
		(%)			($mmol_c/kg$)		($-log_{H+}$)	(%)
Oxisol	6	25	69	1.5	17	41	4.4	6.6
Vertisol	3	32	65	2.7	157	396	5.5	3.4

Rheological measurements
Markgraf *et al*. (2006) give a detailed description of amplitude sweep tests, including a theoretical background of rheology and its application. A parallel-plate-rheometer, MCR 300 (Anton Paar Company, Stuttgart, Germany), was used. During all tests a constant temperature of 20°C was maintained, regulated by a Peltier unit. Amplitude sweep tests (AST) under oscillatory conditions were conducted, with controlled shear deformation (CSD) γ = 0.0001… 100%, an angular frequency ω = π/s (f = 0.5 Hz), and 30 measuring points, which led to an average test duration of 16 minutes. A plate distance of 4 mm was pre-set according to a plate radius of the rotating bob of 25 mm and the given texture (>2 μm). The tests were controlled by the

software US 200 (Anton Paar Company, Stuttgart, Germany).
In Figure 1 three stages of stiffness degradation are given. Loss factor tan δ includes both elastic and viscous parts; it furthermore is the ratio of elasticity (=storage modulus G') and viscosity (=loss modulus G") (Markgraf and Horn 2009). If tan δ=G"/G'=1 substances are creeping or yielding; considering stress-strain relationships of soils on a particle-to-particle scale, at this stage a microstructural breakdown occurs. Hence, values <tan δ=1 indicate an elastic or stiff character, whilst a viscous behaviour predominates at values >tan δ=1.

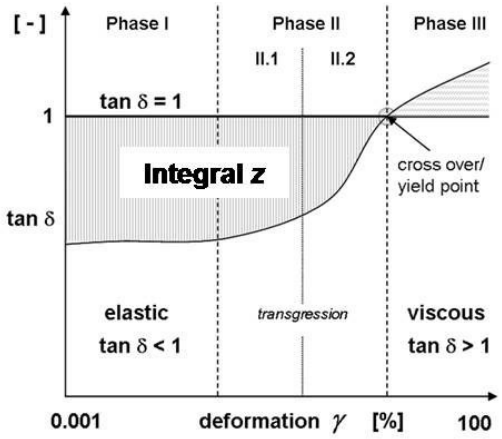

Figure 1. Idealized graph of conducted amplitude sweep test, loss factor tan δ (γ). Values below tan δ=1 (Phases I and II.1) indicate a elastic or pseudo-elastic behaviour; a yield point is given at the intersection of the graph with the tan δ=1-line (Phase II.2); viscous behaviour is given in Phase III tan δ>1, resulting in a microstructural, irreversible breakdown.

Electrokinetic investigation
Electrophoresis measurements were performed with a Zetasizer Nano ZS by Malvern Instruments Ltd., UK equipped with a 633nm He/Ne laser. By using the M3-PALS technology the electrophoretic velocity of the particles in an applied electric field of 40 V was determined. The M3-PALS technique (Minor *et al*. 1997) was developed to perform measurements at any point within the measuring cell independent of the electroosmotic flow. This technique is a combination of the 'Mixed Mode Measurement' technique of Laser Doppler Velocimetry and the application of Phase Analysis Light Scattering. The zeta potential was calculated from the electrophoretic velocity (ν=v/E) by the Helmholtz Smoluchowski (v. Smoluchowski, 1921) equation (κa » 1):

$$\frac{v}{E} = \frac{\varepsilon\varepsilon_0}{\eta}\zeta$$

where κ is the Debye Hueckel length, a is the particle radius, v is the particle velocity, E is the electric field strength, ε is the relative and ε_0 is the absolute dielectric constant, η is the viscosity of the liquid, and ζ is the zeta potential.

Sample preparation
100 mg of the soil was inserted in 50 ml of the respective electrolyte solution and dispersed 5 min in an ultrasonic bath. After 30 minutes rest 10 ml have been transfused and refilled with 40 ml of the equal electrolyte solution which was used before.

Results
An ideal behaviour is demonstrated with the data on the untreated saturated and pre-drained Vertisol samples. A sliding shear behaviour predominates, which results from a smectitic clay mineralogy. If graphs of tan δ (γ) are compared, a smoother curve progression occurs in case of the smectitic Vertisol, either under saturated or pre-drained conditions; whilst graphs of the kaolinitic, Fe-oxide- rich Oxisol, as well as the Fed-leached modification, indicate frictional heat (=increase of tan δ at γ=0.01…1%), and a turbulent shear behavior. These findings can be related to the semi-quantitative classification of stiffness degradation in Markgraf and Horn (2009). Furthermore, by calculating integral z of both the Oxisol and Vertisol (including all treatments), $z_{Vertisol} > z_{Oxisol}$; this instant can be also referred to a higher degree of elasticity in Vertisols,

which is also responsible for a high shrinkage and swelling behaviour (HAC), whereas kaolinitic soils (LAC) tend to show a more rigid, stiff structure, which leads to the occurrence of frictional heat. Due to Na-dithionite treatment of the oxisol, strengthening effects are decreased noticeably. Kaolinite piles may function as single grains with regard to shear behaviour, if one assumes stable structural conditions of partially sharp-edged grains. In this case, a direct surface-to-surface or edge-to-edge contact can be assumed during AST. Aggregate formation and strengthening are strongly enhanced by the remobilization of iron and the conversion of ferrihydrite to hematite (Ohtsubo *et al.* 1991).

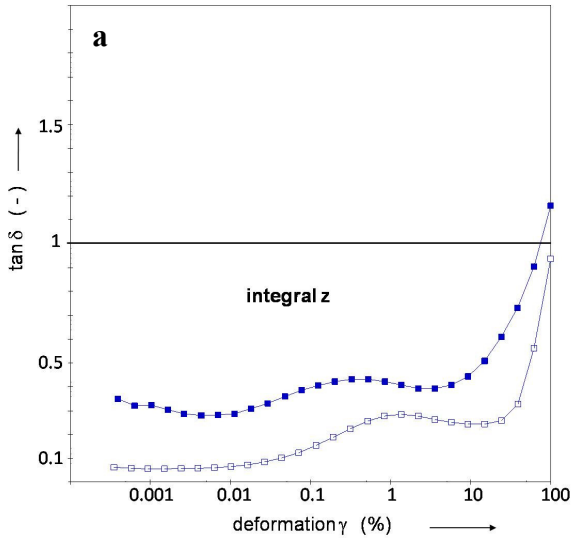

Figure 2a. Resulting graphs of conducted amplitude sweep tests with the kaolinitic, Fe-oxide-rich Oxisol (natural conditions, forest); Na-dithionite treated (filled squares) and untreated (blank squares) conditions.

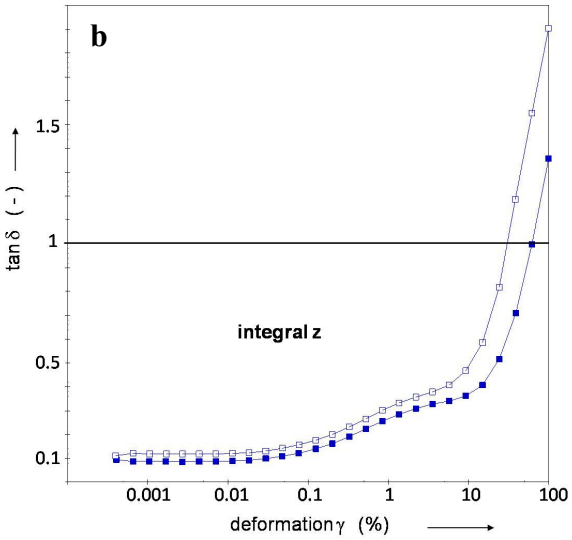

Figure 2b. Corresponding to Figure 1a resulting graphs of the investigated smectitic Vertisol are presented; saturated (blank squares) and pre-drained (filled squares) samples are compared.

Results of zeta potential measurements (Figures 3a and b) show a corresponding affinity to agglomeration in case of the oxisol (Figure 3a), which is strongly dependent on the pH. The isoelectric point is reached at a pH of ~2, wheras suspensions are stable from pH 10…5.5 at a zeta potential ζ of appr. -32 mV; a maximum particle size of 3000…4500 nm is reached at the IEP. In comparison, the smectitic Vertisol (Figure 3b) remains stable over the whole pH range from 10…2 at a corresponding zeta potential ζ of -30… -20 mV. At pH 2.5 a slight trend of agglomeration becomes obvious, as the particle size increases from >1500 to 4500 nm.

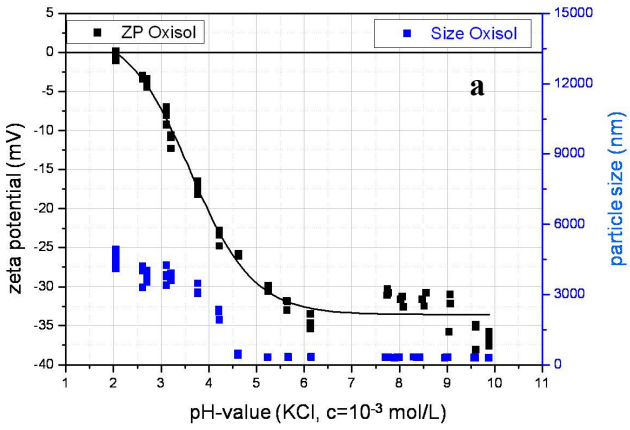

Figure 3a. Zeta potential and particle size measurements of the investigated Oxisol; suspensions remain stable in a range of pH 10…5.5; the IEP is reached at ~pH 2, whereas agglomeration is indicated at pH 4.5…<2.

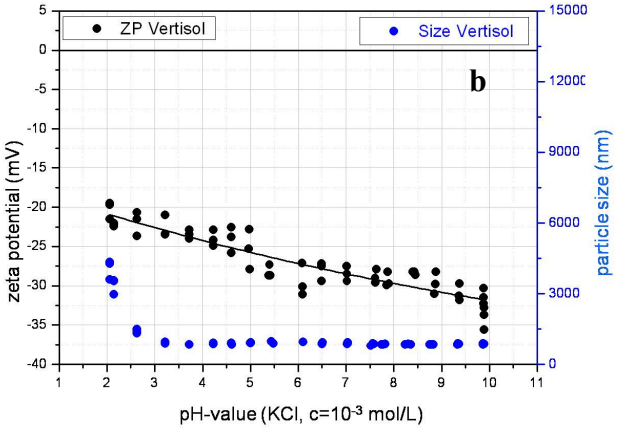

Figure 3b. Suspensions of the smectitic Vertisol remain stable over a range of pH 10…2; the IEP is not reached, and particle sizes indicate a trend of agglomeration at pH <2 only.

Conclusions

Rheological investigations as well as zeta potential measurements led to a reliable consistency. On one hand stiffness degradation could be (semi-) quantified by applying amplitude sweep tests, and be complemented by zeta potential results. Both methods showed a higher degree of agglomeration of the kaolinitic, Fe-oxide-rich Oxisol, indicating the phenomenon of 'pseudosand' in dependency of pH; furthermore, a stable, elastic structure was obvious for smectitic Vertisol samples. Hence, rheology may function as useful tool between the colloidal (particles <1µm) and micro scale (particles 1-250µm)), if structural effects need to be defined.

References

Markgraf W, Horn R, Peth S (2006). An approach to Rheometry in soil mechanics: Structural changes in bentonite, clayey and silty soils. *Soil and Tillage Research* **91**, 1-14.

Markgraf W, Horn R (2007) Scanning electron microscopy–energy dispersive scan analyses and rheological investigations of South-Brazilian soils. *Journal of the Soil Science Society of America* **71**, 851-59.

Markgraf W, Horn R (2009) Rheological Investigations in Soil Micro Mechanics: Measuring Stiffness Degradation and Structural Stability on a Particle Scale. In 'Progress in Management Engineering.' (Eds. Gragg, LP, Cassell, JM), Chapter 9 (Nova Science Publishers: Hauppauge).

Mehra OP, Jackson ML (1960) Iron oxide removal from soils and clays by a dithionite-citrate system buffered with sodium bicarbonate. In '7th National Conference on Clays and Clay Minerals.' (Ed. Swineford A), pp. 317-327. (Adlard & Son Ltd.: Washington, DC).

Minor M, van der Linde AJ, van Leeuwen HP, Lyklema J (1997) Dynamic aspects of electrophoresis and electroosmosis: A new fast method for measuring particle mobilities. *Journal of Colloid and Interface Science* **189**, 370-375

Ohtsubo YA, Yoshimura A, Wada SI, Yong RN (1991) Particle interaction and rheology of illite-iron oxide complexes. *Clays and Clay Minerals* **39**, 347-354.

van Reeuwijk LP (2002) 'Procedures for soil analysis' (International Soil Reference and Information Centre (ISRIC):Wageningen).

von Smoluchowski M (1921) 'Handbook of Electricity and Magnetism - Handbuch der Elektrizität und des Magnetismus', Volume II (Leipzig).

Relationships between mineralogical properties and carbon and nitrogen retention in upland soils of Thailand

Wittaya Jindaluang[A], Irb Kheoruenromne[A], Anchalee Suddhiprakarn[A], Bhupinder Pal Singh[B] and Balwant Singh[C]

[A]Department of Soil Science, Faculty of Agriculture, Kasetsart University, Bangkok, Thailand, Email g5181049@ku.ac.th, irbs@ku.ac.th, agrals@ku.ac.th
[B]Forest Science Centre, Industry and Investment NSW, Beecroft, NSW 2119, Australia, Email bp.singh@sf.nsw.gov.au
[C]Faculty of Agriculture, Food and Natural Resources, The University of Sydney, NSW 2006, Australia, Email Bawant.Singh@sydney.edu.au

Abstract
Soil organic matter (SOM) is both a source and a sink for C and it plays an important role in enhancing fertility, productivity and sustainability of agro-ecosystems. The C and N retention capacity of soil is known to be related with soil environmental conditions and soil properties including mineralogical properties. Specific surface area (SSA) and cation exchange capacity (CEC) of clay minerals have been shown to be positively related with C and N contents of soils. However, such relations are not well established and understood particularly for soils in Thailand. The objective of this study is to make a detailed assessment of the relationships between relevant soil properties and C and N retention mechanisms in mineralogically contrasting upland soils from Thailand. Several mineralogically contrasting soils were collected from four cropping systems (corn, sorghum, sugarcane and cassava) in Northeast plateau region of Thailand. Soils were characterized for important physical, chemical and mineralogical properties. Total C and N and CEC are being analysed in bulk soils, and particle-size (sand, silt and clay), and density-separated fractions of soils. The findings from this study will have implications for optimal management of SOM to enhance agricultural productivity and sustainability of upland soils in Thailand.

Key Words
Smectite, kaolinite, clay-organic interaction.

Introduction
SOM is an important source and sink for C and also contributes to improving fertility, productivity and sustainability of soils and agriculture production. Unfortunately, under tropical climate including Thailand, high temperature and rainfall and widespread adoption of cultivated land uses have accelerated decomposition rate of SOM. Soil organic matter can be increased by practices that return greater quantities of organic matter in soil. The content and type of clay mineralogy can also play an important role in retaining the added organic C and N in soil (Christensen 1992; Cheshire *et al.* 2000) through physical-chemical stabilization and formation of soil aggregates (Krull *et al.* 2003). Among phyllosilicates, smectites have been shown to be more intimately associated with retaining and increasing SOM than the other clay minerals (Wattel-Koekkoek *et al.* 2003), mainly due to their high SSA and CEC (Kaiser and Guggenberger 2003). In contrast, several studies have found that Fe and/or Al oxides can also have a large influence on the retention of organic C in soil and usually are better adsorbents for organic C than phyllosilicates (Chorover and Amistadi 2001; Kaiser *et al.* 2002). This study is being conducted to understand the role of soil mineralogical and other properties in the retention of C and N in soil. The findings from this study will be useful for devising management practices that helps in improving soil organic matter in mineralogically contrasting cropping soils in Thailand.

Methods
Top three horizons of eight smectitic soils from Central plain and Central highland regions, and four kaolinitic, two mixed and two siliceous soils from Northeast plateau region were collected from four cropping systems (corn, sorghum, sugarcane and cassava). The soils were characterized for important physical, chemical and mineralogical properties. Soil pH was measured in 1:1 soil:solution in H_2O and organic carbon was determined by the Walkley and Black method and organic matter was calculated from the organic values. Exchangeable cations and CEC were determined by 1 M NH_4OAc at pH 7.0. Clay minerals in the soil are being analysed by the X-ray diffraction (XRD) and quantitative mineralogy of the clay fraction will be done the Rietveld method. Particle-size fractionation is being done by the pipette method. Total C and N in soil fractions will be measured by dry combustion method using a Elementar Vario Max CNS analyser.

Results

Preliminary results obtained so far from this study are presented here. All smectitic soils selected for this study are classified as Vertisols. Local alluvium from alkaline rocks is the major parent materials of smectitic soils. All kaolinitic soils are highly weathered and highly developed soils from local alluvium and residuum derived from limestone. They are classified as Oxisols, Ultisols and Alfisols. Mixed soils were classified as Alfisols and Ultisols and parent materials are residuum and wash derived from sandstone. Siliceous soils were classified as Ultisols and Alfisols. They are residuum and wash derived from sandstone and granite. All soils represent ustic moisture regimes (Table 1).

Table 1. Parent material and classification of mineralogically contrasting upland soils of Thailand.

Soil series	Parent material	Classification
Smectitic soils		
Lop Buri (Lb)	Local alluvium derived from limestone	Typic Haplustert
Buri Ram (Br)	Local alluvium derived from limestone	Typic Haplustert
Chai Badan 1 (Cd1)	Local alluvium derived from lime producing rocks	Typic Haplustert
Chai Badan 2 (Cd2)	Local alluvium derived from weathered basalt	Typic Haplustert
Samo Thod 1 (Sat1)	Local alluvium on residuum derived from weathered andesite mixed with limestone	Typic chromustert
Samo Thod 2 (Sat2)	Local alluvium derived from limestone on residuum derived from weathered andesite	Typic chromustert
Wang Chomphu 1 (Wc1)	Local alluvium and wash over residuum derived from lime containing rock	Typic chromustert
Wang Chomphu 2 (Wc2)	Local alluvium on residuum derived from calcareous rock	Typic chromustert
Kaolinitic soils		
Pak Chong 1 (Pc1)	Local alluvium and residuum derived from weathered limestone	Typic Kandiustox
Pak Chong 2 (Pc2)	Mainly residuum derived from weathered limestone	Rhodic Kandiustox
Pak Chong 3 (Pc3)	Residuum derived from weathered limestone	Typic Paleustult
Loei (Lo)	Mixed wash and colluvium derived from limestone and metasedimentary rock	Typic Paleustalf
Mixed soils		
Sikhio (Si)	Residuum derived from weathered calcareous sandstone	Typic Rhodustalf
Borabu (Bb)	Wash over residuum derived from weathered sandstone	Typic Haplustult
Siliceous soils		
Chum Phung (Cpg)	Residuum and wash derived from weathered red sandstone	Typic Kandiustult
Chan Tuk (Cu)	Residuum derived from weathered granite	Arenic Haplustalf

Some chemical properties of the selected soils are shown in Table 2. All soils exhibit a wide range of chemical properties corresponding to their parent material properties. The mean OM content of the selected soils was highest (17.0 g/kg) in smectitic soils followed by kaolinitic soils (14.2 g/kg), mixed soils (7.4 g/kg), and siliceous soils (5.4 g/kg).

Table 2. Range and mean value of important chemical properties of soils.

Soil properties	Mineralogical group							
	Smectitic soils		Kaolinitic soils		Mixed soils		Siliceous soils	
	Range	Mean	Range	Mean	Range	Mean	Range	Mean
pH (1:1H_2O)	5.6-8.4	7.3	5.3-7.3	6.6	4.9-7.1	6.0	5.1-6.3	6.2
OM (g/kg)	5.3-30.3	17.0	6.1-34.1	14.2	1.9-9.8	7.4	1.1-13.6	5.4
Extractable bases ($cmol_+/kg$)								
Ca	18.2-132.2	45.0	3.7-12.3	9.0	0.6-21.3	6.6	0.2-4.4	1.6
Mg	1.6-16.7	7.2	0.5-2.4	1.3	0.2-0.9	0.6	0.1-0.6	0.3
Na	0.1-1.3	0.6	0.1-0.5	0.3	0.2-0.6	0.4	0.1-0.4	0.2
K	0.04-0.3	0.15	0.04-0.74	0.19	0.06-0.21	0.14	0.01-0.25	0.06
CEC (cmol/kg)	27.1-96.8	51.2	7.4-22.5	14.3	1.7-9.0	5.8	1.5-14.1	4.5

The correlation analysis (Table 3) suggests that OM content in all soils is significantly positively correlated with soil pH ($r = 0.41$, $P \leq 0.01$), extractable Ca ($r = 0.36$, $P \leq 0.05$) and CEC ($r = 0.51$, $P \leq 0.01$). At each soil level, a highly significant correlation was found between OM content and extractable K for smectitic ($r = 0.63$, $P \leq 0.01$), kaolinitic ($r = 0.91$, $P \leq 0.01$), and mixed soils ($r = 0.87$, $P \leq 0.05$), and between OM content and extractable Mg for kaolinitic ($r = 0.66$, $P \leq 0.05$) and mixed soils ($r = 0.83$, $P \leq 0.05$). Only

smectitic and siliceous soils showed a significant positive correlation between OM content and soil pH ($r = 0.39$, $P \leq 0.10$; $r = 0.73$, $P \leq 0.10$, respectively) and only mixed soils showed a positive correlation between OM content and CEC ($r = 0.88$, $P \leq 0.05$). These relationships are consistent with the results of many other studies; for example, some studies concluded that pH is an important regulator of C and N dynamics in soil (Kemmitt *et al* 2006; Li *et al.* 2007; Leifeld *et al* 2008). Extractable bases in soil have been shown to enhance binding between SOM and clay minerals through cation bridges (Dontsova and Bigham 2005), and soil CEC has been shown to be related with OM content through SSA depending on properties of mineral surfaces (Kahle *et al* 2002). Some studies have shown that the content of Fe and/or Al oxides can control OM content in soil (Chorover and Amistadi 2001; Kaiser *et al.* 2002). Clearly there is a need for detailed evaluation of the role of soil mineralogy in controlling C and N retention in these uplands soils from Thailand.

Table 3. Correlation coefficients between SOM and measured soil properties.

Soil	pH (1:1 H_2O)	Ca	Mg	Na	K	CEC
All soils (n = 48)	0.41***	0.36**	-0.00	-0.15	-0.16	0.51***
Smectitic soils (n = 24)	0.39*	0.28	0.33	-0.25	0.63***	0.28
Kaolinitic soils (n = 12)	-0.42	0.19	0.66**	-0.30	0.91***	0.43
Mixed soils (n =6)	0.62	0.65	0.83**	0.21	0.87**	0.88**
Siliceous soils (n =6)	0.73*	0.09	0.06	0.06	0.06	0.15

Correlations are significant at ***$P \leq 0.01$, **$P \leq 0.05$, *$P \leq 0.10$

We propose to employ size- and density-fractionation together with analysis of CEC, total C and N and mineral content and composition of relevant separated fractions to acquire greater understanding of mineral controls on soil organic matter storage in these soils. These results will be presented at the conference.

Conclusions

Preliminary results on relationships between mineralogical properties and C and N retention in Upland soils of Thailand show that smectitic soils tend to have higher OM content than other soils. All soils exhibited a wide range of relationships between OM content and some important chemical properties such as pH, extractable bases and CEC. However, to address the objective of this study, we propose to undertake further evaluation of the role of soil mineralogy in controlling C and N retention in these uplands soils from Thailand, by employing size- and density-fractionation together with analysis of CEC, total C and N and mineral composition of the relevant separated fractions.

Acknowledgments

The authors are grateful to The Royal Golden Jubilee Ph.D. Program under the Thailand Research Fund for financial support

References

Cheshire MV, Fraser AR, Hillier S, Dumat C, Staunton S (2000) The interactions between soil organic matter and soil clay minerals by selective removal and controlled addition of organic matter. *European Journal of Soil Science* **51**, 497-509.

Chorover J, Amistadi MK (2001) Reaction of forest floor organic matter at goethite, birnessite and smectite surfaces. *Geochimica et Cosmochimica Acta* **65**, 95-109.

Christensen BT (1992) Physical fractionation of soil and organic matter in primary particle size and density separates. *Advanced Soil Science* **20**, 1-90.

Dontsova KM, Bigham JM (2005) Anionic Polysaccharide adsorption by Clay Minerals. *Soil Science Society American Journal* **69**, 1026-1035.

Kahle M, Kleber M, Torn MS, Jahn R (2002) Predicting carbon content in illitic clay fracions from surface area, cation exchange capacity and dithionite-extractable iron. *European Journal of Soil Science* **53**, 639-644.

Kaiser K, Eusterhues K, Rumpel C, Guggenberger G, K**Ö**gel-Knabner I (2002) Stabilization of organic matter by soil minerals-investigations of density and particle-size fractions from two acid forest soils. *Journal of Plant Nutrition and Soil Science* **165**, 451-459.

Kaiser K, Guggenberger G (2003) Minerals surfaces and organic matter. *European Journal of Soil Science* **54**, 219-236.

Kammitt SJ, Wright D, Goulding KWT, Jones DL (2006) pH regulation of carbon and nitrogen dynamics in two agriculture soils. *Soil Biology and Biochemistry* **38**, 898-911.

Krull ES, Baldock JA, Skjemstad JO (2003) Importance of mechanisms and processes of the stabilisation of soil organic matter for modelling carbon turnover. *Functional Plant Biology* **30**, 207-222.

Leifeld J, Zimmermann M, Fuhrer J (2008) Simulating decomposition of labile soil organic carbon: Effects of pH. *Soil Biology and Biochemistry* **40**, 2948-2951.

Li X, Rengel Z, Mapfumo E, Bhupinderpal-Singh (2007) Increase in pH stimulates mineralization of native organic carbon and nitrogen in naturally salt-affected sandy soils. *Plant and Soil* **290***,* 269-282.

Wattel-Koekkoek EJW, Buurman P, van der Plicht J, Wattel E, van Breemen N (2003) Mean residence time of soil organic matter associated with kaolinite and smectite*. European Journal of Soil Science* **54**, 269-278.

Root-fungus symbiosis in agricultural crops selectively makes soil clays

J. M. Arocena[A], B. Velde[B] and S. J. Robertson[A]

[A]University of Northern British Columbia, Prince George, BC Canada V2N4Z9.
[B]UMR 8538 CNRS Ecole Normale Supérieure, 24 rue Lhomond 75231 Paris France.

Abstract
In addition to the mutual association of roots and fungi, mycorrhizas benefit the general ecosystem through the production of soil clays. X-ray diffraction analyses showed that the fungus *Glomus* when inoculated onto barley, canola and alfalfa produced various types of potassium-deficient minerals (e.g., smectites) and slightly altered biotite, the K-rich mineral in the experiment. Non-inoculated plants produced mixed layer minerals, illite and left no biotite intact. The presence of K-poor clay minerals and unaltered biotite in inoculated samples implies selective K-extraction from some biotite grains to benefit plant growth and at the same time leaving unaltered biotite for future extractions. Symbiosis between fungus and plant roots (or mycorrhiza) is more efficient than roots alone in producing soil clays through the selective and efficient extraction of potassium ions from biotite

Key Words
Arbuscular mycorrhizae, agricultural crops, PCR.

Introduction

Fungal-root symbioses (or mycorrhizas) are found with an estimated 95% of all plant species (Sylvia 1998). It is known that mutual benefits results when host plants provide carbon to fungus and the latter supplies plants with nutrients and water. The symbiosis is more than beneficial to plant and fungus because synthesis of new clay minerals is often reported in root-soil interface (rhizosphere). The uptake of potassium by plants, such as ryegrass, converts soil biotite (potassium-rich mica) into vermiculite, a high-charged clay mineral (Hinsinger *et al.* 2006). The removal of magnesium from chlorite (magnesium-rich mineral) leaves behind high-charged hydroxy inter-layered clays (HIC) (Arocena and Velde 2009). Negative charges associated with surfaces of these high-charged clays and HIC are effective adsorption sites to store cations (e.g., magnesium and potassium) and improve the natural fertility of soils. Although HIC and soil vermiculites are commonly observed in many rhizosphere soils, the identity of fungi associated with the formation of new clay minerals is limited to our work in spruce and fir forest ecosystems (Glowa *et al.* 2004). In the Canadian sub-boreal forests, the symbiosis between *Piloderma* (an ectomycorrhizal fungus) and white spruce roots transformed soil mica and chlorite to HIC with subsequent improvement in soil fertility arising from increased cation exchange capacity (CEC) and exchangeable potassium and magnesium (Glowa *et al.* 2004). The removal of potassium and magnesium through uptake by white spruce trees developed some negative charges in soil biotite and chlorite, hence the synthesis of HIC and other high-charged clays in mycorrhizal soils. The objective of the study was to investigate the transformation of biotite in the rhizosphere soils of barley (*Hordeum vulgare*), alfalfa (*Medicago sativa*), and canola (*Brassica napus*) to determine the role of arbuscular mycorrhizal (AM) associations (*Glomus* sp) in the formation of expanding clays in rhizosphere soils of common crop plants.

Materials and methods

Growth chamber experiment

We cultivated three common agricultural crops (i.e. barley, canola and alfalfa) in a growth chamber. The growth medium was composed of Ottawa sand (691 g) and biotite (9 g) with the essential nutrients (except K) provided to the plants through a modified Hoagland solution. One group of seedlings (IN) were inoculated with MycoApply Seed Inoculant (Fort Myers, Florida) and maintained in a growth chamber while the second group in another growth chamber was left uninoculated (NIN). The plants were grown to 100 days and then harvested. Each treatment was replicated three times.

DNA extraction and amplification

Total DNA was extracted from root samples of non-inoculated (NIN) and inoculated (IN) alfalfa, barley and canola using a 2X CTAB (hexadecyl trimethyl ammonium bromide) protocol for plants (Hillis *et al.* 1996). DNA was extracted from the seed inoculant using the Ultraclean Soil DNA kit (MoBio, Carlsbad, CA,

USA), following the manufacturer's recommended alternative protocol for increased yield. Fungal DNA was amplified by polymerase chain reaction (PCR) using the universal primer ITS1 (White *et al.* 1990) and the AM fungal-specific primer AM1 (Helgason *et al.* 1998). DNA fragment analysis followed runs on a CEQ^{TM} 8000 automated sequencer (Beckman-Coulter Inc.).

X-ray diffraction analyses

Clay fractions were separated from rhizosphere (*i.e.*, soils clinging to roots) and non-rhizosphere (*i.e.*, > 3 mm from roots) collected from IN and NIN samples. Calcium- and K-saturated oriented clay samples were analyzed using a Bruker D8 with GADDS® x-ray diffractometer. X-ray diffractograms were subjected to deconvolution analysis (Lanson 1997) to estimate the proportion of various secondary clay minerals from the transformation of biotite.

Results and discussion

Advanced analysis (Lanson 1999) of X-ray diffraction patterns of clay minerals collected from rhizosphere soils showed that various types of low-potassium clays were produced from the potassic high temperature mineral biotite in non-inoculated (NIN) and *Glomus*-inoculated (IN) barley, canola and alfalfa (Figure 1A-F). The biotite in non-planted soil (control treatment) retained its original structure with a sharp 1.0 nm peak. Soil clay minerals produced by the alteration of biotite by NIN plants were dominated by a mixed layer (ML) mineral (mixed layering of potassic, micaceous mineral and a low K mineral, smectite), and illite (Figure 1B, D, F). *Glomus*, a mycorrhizal fungus used to improve the yield in cultivated crops (Powell 1981), when inoculated to barley, canola and alfalfa produced several types of K-deficient minerals from the initial biotite which were not present in the NIN treatments. Calcium saturation of clays in the air dried state showed 1.42 nm spacing indicating the presence of aluminum hydroxyl-compounds instead of the normal hydrated (two water layer) state (1.52 nm) common for smectite (Figure 1A, C). Mixed layering of illite and low K minerals was indicated by reflections at 1.17-12.2 nm (Figure 1A-D) which were somewhat modified by glycol treatment.

Both inoculated and NIN alfalfa produced illite (Figure 1E, F) which indicates only minor destabilization of the biotite structure due to minimal removal of K showing that plant species is an important factor in plant-soil mineral breakdown. Electrical charges on the HIC result from the removal of K in biotite, and are commonly compensated by cations (e.g., Ca^{2+}, NH_4^+, Mg^{2+}, Al-OH) in the soil system many of which are essential to maintain vigorous growth of plants and organisms. Thus, synthesis of HIC in rhizosphere improves the long term fertility of soils. In Figure 1, one can easily see that the IN samples showed mineral phases with peaks of higher basal spacing (low 2θ position) indicating stronger loss of K than in NIN samples. However, the most K-rich mineral is biotite with a peak at near 10.2 °2θ Co radiation was still present in IN samples while in the NIN samples, all biotite appeared to have been altered.

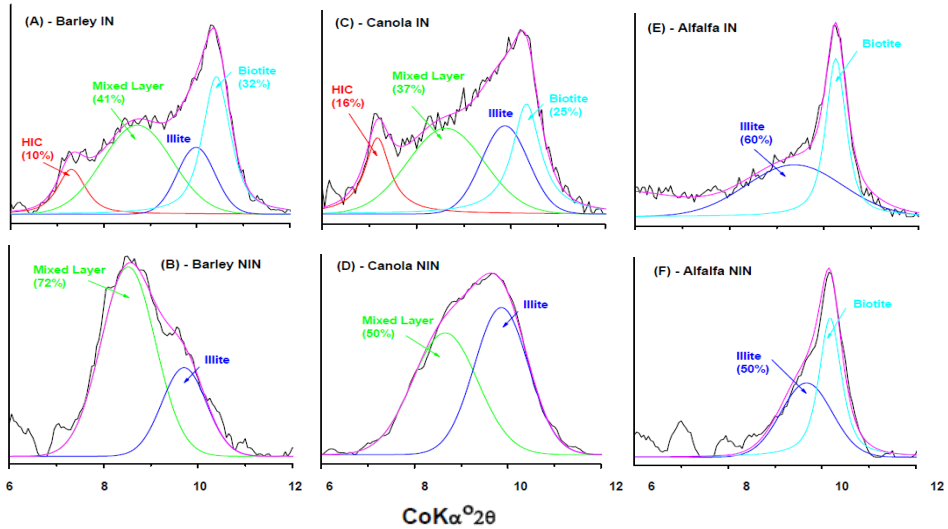

Figure 1. Biotite is transformed into several types of hydroxy-interlayered soil clays (HIC) in *Glomus*-inoculated (A, C, E) and non-inoculated rhizosphere soils of barley, canola and alfalfa (B, D, F). Position of the peaks to the left (lower angle) indicates more potassium extraction.

The presence of more K-poor minerals (*i.e*., smectites, HIC) in the IN than in NIN samples indicates a more efficient K-extraction process from individual biotite grains when *Glomus* and other organisms are present in the system (Figure 2). Overall, there were 57 fragments comprising the AM fungal communities ranging from approximately 95-700 bp in size. Of the 47 fragments in the IN group, only 7 were shared with the NIN group. Two DNA fragments were significantly associated with the IN group ($p=0.02$) whereas no fragments were specifically associated with the NIN group. In general, IN plants showed a greater diversity (i.e. richness of fragment sizes) of AM fungi than NIN plants. Differences in the functional attributes of different AM fungi colonizing a root system may increase resource acquisition and plant survival (Helgason and Fitter 2005). Most unique fragments were associated with alfalfa (IN); however, further analysis by plant could not be conducted due to small sample size (*i.e*., n=1 except for barley (NIN)).

Unaltered biotite in the IN samples suggests that there was a selective extraction of K from some biotite grains by mycorrhiza leaving others intact. In the NIN samples, no biotite is left intact and all material is altered but less in the extreme cases than in the IN samples. Thus, mycorrhiza selectively extracts K to immediately benefit plant growth and at the same time leave unaltered biotite for future extractions. Further in the NIN treatment, all biotite grains were transformed with the implication that much of the K released by root – mineral interaction can be lost from the plant growth system through leaching. It is interesting to note that the extent of alteration of the biotite grains is not only dependent on the mycorrhizal treatment, but also on the type of plant used. Overall alfalfa has less of an altering effect in both inoculated and non-inoculated experiments. Canola and barley have similar effects in the IN experiments but barley shows a greater effect (shift to lower spectral positions) than in the NIN experiment. This indicates, as one might expect, somewhat different responses of extraction efficiency depending upon plant type.

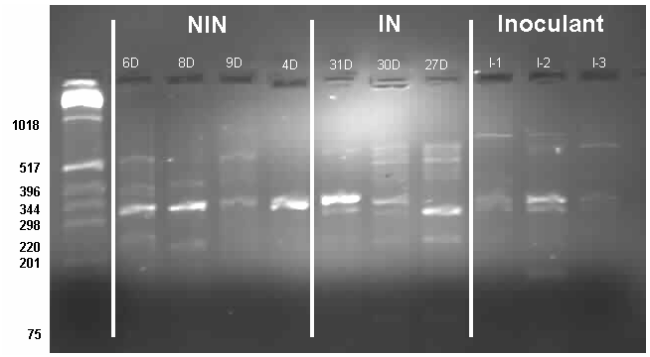

Figure 2. High resolution gel with 1 kb DNA ladder (lane 1) comparing PCR products of NIN, IN and inoculant samples. (NIN: 6D-alfalfa, 8D and 9D-barley, 4D-canola; IN: 31D-alfalfa, 30D-barley, 27D-canola).

Conclusion

We can conclude that the symbiotic plant–fungus system is more efficient through the selective extraction of K in some biotite grains, conserving K resources for future use in others. Our results provide useful information to the important role of fungus-root symbiosis in the maintenance of fertility and long term productivity of agricultural (and forest) soils.

Acknowledgements

We acknowledge the financial support from the Natural Sciences and Engineering Research Council, and the Canada Research Chair Program. We thank S. Brown, R. Miller and M. Thompson for assistance in the experiment and laboratory analyses.

References

Arocena JM, Velde B (2009) Transformation of chlorites by primary biological agents – a synthesis of X-ray diffraction studies *Geomicrobiology J.* **26**, 382-388.

Arocena, JM, Glowa KR, Massicotte HB, Lavkulich L (1999). Chemical and mineral composition of ectomycorrhizosphere soils of subalpine fir (*Abies lasiocarpa* (Hook.) Nutt.) in Ae horizon of Luvisol *Can. J. Soil Sci.* 79, 25-35.

Glowa KR, Arocena JM, Massicotte HB (2004). Properties of soils influenced by ectomycorrhizal fungi in hybrid spruce [*Picea glauca x engelmannii* (Moench.) Voss] *Can. J. Soil Sci.* **84**, 91-102.

Helgason T, Daniell TJ, Husband R, Fitter AH, Young JPW (1998) Ploughing up the wood-wide web? *Nature* **394,** 431.

Helgason T, Fitter A (2005). The ecology and evolution of the arbuscular mycorrhizal fungi. *Mycologist* **19,** 96-101.

Hinsinger P, Plassard C, Jaillard B (2006). Rhizosphere: A new frontier for soil biogeochemistry *J. Geochem. Explor.* **88**, 210-213

Lanson B (1997) Decomposition of experimental X-ray diffraction patterns (profile fitting) – A convenient way to study clays. *Clays Clay Miner.* **45**, 132-146

Powell CL (1981) Inoculation of barley with efficient mycorrhizal fungi stimulate seed yield. *Plant and Soil* **5**9, 487-489

Sylvia DM (1998). Principles and Applications of Soil Microbiology (Eds DM Sylvia, JJ Fuhrmann, PG Hartel, DA Zuberer) pp. 408-426 (Prentice Hall: New Jersey, USA).

White TJ, Bruns T, Lee S, Taylor J (1990) Amplification and direct sequencing of fungal ribosomal RNA genes for phylogenetics. In 'PCR Protocols: A Guide to Methods and Applications'. pp. 315-321. (Academic Press, Inc.).

Soil formation from ultrabasic rocks in bioclimatic conditions of mountainous tundra (the Polar Urals, Russia): Mineralogical aspects

Sofia Lessovaia[A], Yurii Polekhovsky[B], and Evgeniy Pogozhev[C]

[A]Faculty of Geography and Geoecology, St. Petersburg State University, St. Petersburg, Russia, Email lessovaia@yahoo.com
[B]Geology Faculty, St. Petersburg State University, St. Petersburg, Russia, Email yury1947@mail.ru
[C]Faculty of Soil Science, Moscow State University, Moscow, Russia, Email pogozhev@mail.ru

Abstract
Mineral associations of soils located in mountainous tundra derived from and underlain by ultrabasic rocks using the example of the Polar Urals were studied. Key plots are located on a flat summit and a slope of the Rai-Iz massif where ultrabasic rocks are represented by a dunite - harzburgite complex and the Rai-Iz massif, on a moraine ridge consisting mostly of basic material with admixtures of ultrabasic rocks.
The mineral association in all studied sola is a result of (i) disintegration of easy weathering ultrabasic rocks that are a source of olivine, pyroxenes, serpentine, talc, and chlorite; (ii) influence of allochthonous material enriched by quartz and feldspars; and (iii) pedogenic neoformation and decomposition of saponite; and (iv) development of iron (hydr)oxides in micro-cracks of olivine, pyroxenes, and serpentine and fragments of plant tissues. Clay minerals associations in sola are determined by resources of ultrabasic rocks even in case of mixture of ultrabasic and basic rocks when the latter are predominant. The acidic effect of moss and lichens seems to be a reason for selective decomposition of the most unstable minerals despite the pH value of bulk samples.

Key Words
Dunite-harzburgite complex, phyllosilicates, pedogenesis

Introduction
Weathering of ultrabasic rocks and mineral association of soils derived from ultrabasic rocks have extensively been studied and pedogenesis has been characterized in rather wide spectrum of bioclimatic conditions (Wildman *et al.* 1968; Ducloux *et al*. 1976; Wilson *et al.* 1984; Alexander 1988; Bulmer and Lavkulich 1994; Bonifacio *et al*. 1996; Caillaud *et al*. 2004; Gaudin *et al*. 2004). Nevertheless, soil formation from ultrabasic rocks in cold, humid climate as well as permafrost influence on the silicate matrix is not well known. In mountainous tundra permafrost affects rock disintegration and the increase in their dispersion which affects silicate sustainability.
The aim of the present work was to investigate silicate associations changes and transformation in soils derived from and underlain by ultrabasic rocks and to assess the relative importance of pedogenesis in bioclimatic conditions of mountainous tundra using the example of the Polar Urals.

Methods
The mineral compositions of the hard rocks and sola were studied in thin section by optical microscopy using Zeiss Axioplan 2 and Polam P-312 microscopes. The mineral association of clay size fraction (<1 μm) separated by sedimentation was studied. Ammonium hydroxide was used as a peptizing agent. The XRD patterns were obtained from oriented specimens using DRON-2 X-ray diffractometer, with CoKα radiation and a monochromator in the diffracted beam. Pretreatment of samples included saturation with Mg, ethylene glycol solvation, heating at 350ºC and 550ºC, and boiled for 2 h with 1 N HCl. A Rigaku-MiniFlex2 diffractometer (CuKα) was used for powder samples of rocks and fine earth.
Light and heavy fractions (specific weight < 2.9 and > 2.9, correspondently) of sand fractions were investigated by immersion method.
Bulk chemical composition was done by X-ray fluorescence analysis. Various forms of Fe and Al were also measured on the base of dithionite (Mehra and Jackson) and oxalate extractable procedures. The pH values were measured potentiometrically in the suspension with a soil: H_2O ratio of 1:2.5 (shaking for 2 h).

Results
Ultrabasic rocks represented by a dunite - harzburgite (peridotite with orthopyroxene) complex make up the Rai-Iz massif, the Polar Urals. Climate conditions are characterized by mean annual temperature -9.0 (ºC) and precipitation 800 (mm). Studied soils are represented by Haplic Regosol (Eutric) (Pit Y-01-07); Haplic Cryosols (Reductaquic) (Pit Y-02-07), and Stagnic Leptosol (Eutric) (Pit Y-04-07) (WRB 2006).

© 2010 19th World Congress of Soil Science, Soil Solutions for a Changing World
1 – 6 August 2010, Brisbane, Australia. Published on DVD.

Key plots are located: (i) on a flat summit at an altitude of 664m of the Rai-Iz massif, permafrost was at a depth of 30 cm (Pit Y-02-07); (ii) southern slope of the Rai-Iz massif covered by colluvial blocks of ultrabasic stones at an altitude of 300m (Pit Y-01-07); and (iii) the Rai-Iz massif at an altitude of 300m, on a moraine ridge consisting mostly of basic material with admixture of ultrabasic rocks (Pit Y-04-07).
In the studied sola crushed stones and gravels make up 70% of the total volume; they are mainly composed by basic (meta-gabbro amphibolites, Pit Y-04-07) and ultrabasic (serpentinous dunites (olivinite), Pit Y-01-07 and Y-02-07) rocks. Despite significant difference of their mineral association and chemical composition (Table), clay size fraction (<1 μm) of sola is characterized by the same phyllosilicate association: (i) inherited from ultrabasic rocks (talc, serpentine, and chlorite); (ii) mineral of smectite group (saponite) that is a result of pedogenesis; and (iii) illite as a trace, the origin of this mineral is not clear (Lessovaia and Polekhovsky 2009).

Table 1. Some properties of studied sola.

Horizon, depth	pH	Chemical composition of sola fine earth and rocks, % in ignited sample									Fe_2O_3d	Fe_2O_3o	Al_2O_3o
	H_2O	SiO_2	Al_2O_3	Fe_2O_3	CaO	MgO	K_2O	Na_2O	MnO	TiO_2	%		
Haplic Cryosols (Reductaquic), Pit Y-02-07													
Ah 0-4 cm	7.2	54.59	5.05	10.62	1.35	25.88	0.75	0.63	0.23	0.38	2.68	1.79	0.08
Bg 4-15 cm	7.0	56.00	5.70	11.25	1.43	22.57	0.86	0.96	0.20	0.42	4.05	2.57	0.11
Bgf 15-30 cm	8.0	65.92	8.66	7.10	1.44	13.23	1.35	1.20	0.07	0.65	1.53	0.66	0.11
R	–	44.52	0.72	12.87	0.85	40.34	0.10	trace	0.21	0.02	–	–	–
stones, surface of permafrost circle	–	44.40	0.90	13.39	0.89	39.86	0.05	trace	0.15	0.01	–	–	–
Haplic Regosol (Eutric), Pit Y-01-07													
A 0-2 cm	6.6	–	–	–	–	–	–	–	–	–	–	–	–
C1 2-10 cm	8.1	56.70	6.53	8.43	1.43	23.93	0.93	1.11	0.12	0.49	1.48	0.60	0.11
C2 10-25	8.3	55.76	6.24	8.71	1.50	25.13	0.84	0.77	0.16	0.46	1.48	0.58	0.09
25-52	8.4	57.23	6.67	8.50	1.43	23.54	0.93	0.74	0.12	0.50	1.28	0.53	0.10
C3 52-70 cm	8.6	55.12	6.16	8.85	1.36	26.04	0.82	0.71	0.15	0.43	1.82	0.56	0.10
R	–	49.20	3.83	9.46	0.96	32.43	3.01	0.37	0.13	0.25	–	–	–
Stagnic Leptosol (Eutric), Pit Y-04-07													
Ah 0-2 cm	7.1	53.22	6.82	10.99	2.77	23.56	0.70	0.71	0.22	0.44	1.90	1.10	0.21
Bwh 2-10 cm	7.1	53.57	7.01	11.22	2.76	22.77	0.68	0.74	0.23	0.45	2.37	1.17	0.26
BC 10-40 cm	7.6	59.06	8.49	10.03	2.04	17.39	1.00	0.87	0.17	0.56	1.66	0.78	0.22
BCg 40-60 cm	7.4	62.89	9.52	9.37	2.24	12.62	1.19	1.08	0.14	0.65	1.86	1.01	0.17
R	–	52.11	17.85	13.68	5.15	7.65	0.79	1.64	0.40	0.63	–	–	–

Notes: d – dithionite extractable; o - oxalate extractable; «–» - no data.

In light fraction quartz and feldspars that are not related with ultrabasic substrate are predominant even in case of Pit Y-02-07 whose location suggests that solum has been isolated from the influence of material that is outside of the Rai-Iz massif. Heavy fraction is enriched by pyroxenes that are usual for harzburgite but not for olivinite, though the latter were the source of stones in the solum. Therefore solum silicate matrix belongs to ultrabasic rocks as well as allochthonous substrates. The admixture of allochthonous material determines the silica abundance in the fine earth (<1mm), especially in the basal horizon. As a result the silica content is much higher than in rock (Table 1).
In Haplic Cryosols (Reductaquic) (Pit Y-02-07) besides fragments of more or less weathered ultrabasic rocks and minerals originated from ultrabasic rocks (olivine, pyroxenes, amphiboles, chlorites, and sometimes large particles of serpentine) that are frequent in thin sections of soil horizons, quartz and plagioclases are present. In this solum weathering and pedogenesis concerning mineral matrix, resulted in (i) the disintegration of rock fragments that led to their more similar sizes in the upper horizon; and (ii) iron (hydr)oxides development in micro-cracks of olivine, pyroxenes, and serpentine and fragments of plant tissues, frequently demonstrating preserved cellular texture, especially in the upper horizon.
Opposite to Haplic Cryosols (Reductaquic) (Pit Y-02-07) in Stagnic Leptosol (Eutric) (Pit Y-04-07) a solum mineral matrix is enriched by the presence of fragments of meta-gabbro amphibolites and amphiboles including hornblende, especially in a basic horizon (Figure). In meta-gabbro amphibolites high temperature regional metamorphism resulted in replacement of pyroxenes by amphiboles, sericitization of plagioclases, and replacement of some of the melanocratic minerals by quartz.
Thus meta-gabbro amphibolites are a possible source of plagioclases and quartz in solum on moraine ridge as well as in sola on ultrabasic substrate. The portion of minerals from basic rock including quartz decreases

in the upper horizons. Fragments of pyroxenes and serpentinite developed from olivinite are found in abundance in the upper horizons of Stagnic Leptosol (Eutric) (Pit Y-04-07). Thus, being a source of easily weathered minerals, ultrabasic rocks lead to soil formation on a matrix that is enriched in usual phyllosilicate association on ultrabasic rocks and is represented by serpentine, chlorite, and talc. The replacement of olivine in veins by serpentine, talc, and chlorites is identified in rock.
Iron (hydr)oxides formation is not so intensive in this solum as in Pit Y-02-07. Pyroxenes are more affected by this process than serpentines. According to chemical composition this solum is similar to sola on ultrabasic rocks that confirm the more significant influence of ultrabasic rocks than basic ones.
More pronounced disintegration and iron (hydr)oxides formation in Haplic Cryosols (Reductaquic) (Pit Y-02-07) could be explained by permafrost influence leading to increase of silicate dispersion with consequence transformation/ decomposition.

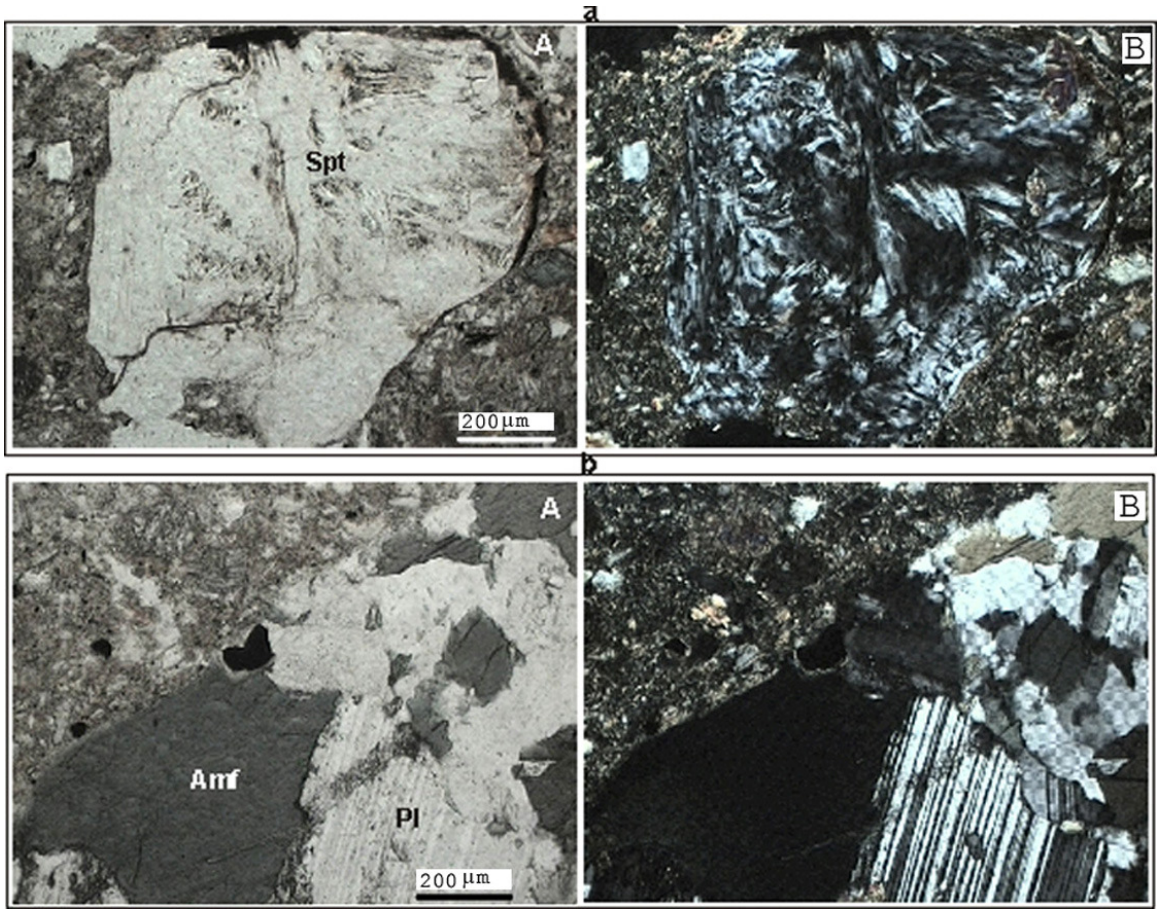

Figure 1. Thin section of horizon BC 10-40cm, Stagnic Leptosol (Eutric), Pit Y-04-07: **fragments of (a) serpentinite developed from olivinite and (b) part of meta-gabbro amphibolites. Spt – serpentine, Amf – amphibole, Pl – plagioclase. A: plain polars; B: crossed nicols.**

Dispersed olivine due to its extreme susceptibility to weathering is likely to be a source for iron (hydr) oxides. Iron removal from silicates matrix is reflected by increase of dithionite - and, especially oxalate extractable iron in the upper part of sola that is more remarkable in Haplic Cryosols (Reductaquic) (Pit Y-02-07), less intensive in Stagnic Leptosol (Eutric) (Pit Y-04-07), and the least in Haplic Regosol (Eutric) (Pit Y-01-07).
The rate of olivine dissolution significant rises simultaneously as pH decreases (Franke and Teschner-Steinhardt 1994). Although the studied sola are characterized by neutral – alkaline pH value, except horizon A, Pit Y-01-07, keeping by high amounts of exchangeable Mg, weakly films of Fe-Al-organo complexes on stones are present in Bwh horizon of Stagnic Leptosol (Eutric) (Pit Y-04-07) indicating the translocation of poorly crystalline iron and aluminum oxides. Moreover pedogenesis resulted in the decomposition of significant portion of pedogenic saponite in the upper horizons. Pedogenic saponite may be concentrated in the basal horizons and absent from more acidic upper horizons (Wilson and Berrow 1978).
In studied sola saponite decomposition appears to be most intensive in Pit Y-02-07, where the pH value is neutral. The instability of silicate matrix, especially saponite and olivine could be explained by the

decomposing acidic effects of moss and lichens despite neutral-alkaline conditions of the bulk samples. This effect is the strongest in the case of Pit Y-02-07, and decreases from Pit Y-04-07 to Pit Y-01-07, where the vegetation cover is almost absent.

Conclusion

The mineral association in studied sola of mountainous tundra is a result of (i) disintegration of easy weathering ultrabasic rocks that are a source of olivine, pyroxenes, serpentine, talc, and chlorite; (ii) influence of allochthonous material enriched by quartz and feldspars, and (iii) pedogenic neoformation and decomposition of saponite.

Clay minerals associations in sola are determined by resource of ultrabasic rocks even in case of mixture of ultrabasic and basic rocks when the latter are predominant.

The acidic effect of moss and lichens seems to be a reason of selective decomposition of the most unstable minerals despite the pH value of bulk samples. The silicate decomposition as a result of the acidic effect increases in Haplic Cryosols (Reductaquic) due to more pronounced rock disintegration.

Acknowledgments

This study was supported by the Russian Foundation for Basic Research. The authors are grateful to Dr. S.V. Goryachkin (Geography Institute, RAS, Russia) for his valuable help and consultations.

References

Alexander EB (1988) Morphology, fertility and classification of productive soils on serpentinised peridotite in California, USA *Geoderma* **41**, 337-351.

Bonifacio E, Zanini E, Boero V, Franchini-Angela M (1996) Pedogenesis in a soil catena on serpentinite in north-western Italy. *Geoderma* **75,** 33-51.

Bulmer CE, Lavkulich LM (1994) Pedogenic and geochemical processes of ultramafic soils along a climatic gradient in southwestern British Colombia. *Canadian Journal of Soil Science* **74**, 165-177.

Caillaud J, Proust D, Righi D, Martin F (2004) Fe-rich clays in the weathering profile developed from serpentine. *Clays and Clay Minerals* **52**, 779-791.

Duclox J, Meunier A, Velde B (1976) Smectite, chlorite and a regular interstratified chlorite-vermiculite in soils developed on a small serpentinite body. Massif Central, France. *Clay Minerals* **11**, 121-135.

Franke WA, Teschner-Steinhardt R (1994) An experimental approach to the sequence of the stability of rock-forming minerals towards chemical stability. *Catena* **21**, 279-290.

Gaudin A, Grauby O, Noack Y, Decarreau A, Petit S (2004) Accurate crystal chemistry of ferric smectites from the lateritic nickel ore of Murrin Murrin (Western Australia). I. XRD and multi-scale chemical approaches. *Clay Minerals* **39,** 301-315.

Lessovaia SN, Polekhovsky YuS (2009) Mineralogical composition of shallow soils on basic and ultrabasic rocks of East Fennoscandia and of the Ural Mountains, Russia. *Clays and Clay Minerals* **57**, 476-485.

Wildman WE, Jackson ML, Whittig LD (1968) Iron-rich montmorillonite formation in soils derived from serpentinite. *Soil Science Society of America Proceedings* **32,** 787-794.

Wilson MJ, Bain DC, Duthie DML (1984) The soil clays of Great Britain: II. Scotland. *Clay Minerals* **19**, 709-735.

Wilson MJ, Berrow ML (1978) The mineralogy and heavy metal content of some serpentine soils in north-east Scotland. *Chemie der Erde* **37,** 181-205.

World Reference Base for Soil Resources (2006) World Soil Resources Reports, 103, FAO, Rome, 145 pp.

Soil minerals recover after they are damaged by bushfires

Emielda Yusiharni[A, B] and Robert J. Gilkes[B]

[A]Department of Forestry, Faculty of Agriculture, University of Mataram, Lombok, Indonesia, Email yusihb01@student.uwa.edu.au
[B]School of Earth and Environment, The University of Western Australia, Perth, 6009, Australia, Email b.gilkes@cyllene.uwa.edu.au

Abstract
We studied the impact of bushfires on soil minerals and the recovery of minerals under wet conditions. Samples were taken shortly after a bushfire from under and adjacent to burnt logs. Kaolinite, goethite and gibbsite were dehydroxylated by the bushfire. Pure minerals were also investigated to determine how heating affects soil minerals and their recovery by rehydroxylation at 55 and 95°C. Rehydroxylation of heated gibbsite was extensive during hydrothermal treatment at 95°C and after 14 days had formed boehmite, bayerite and gibbsite. The process was much slower at lower temperatures. On heating metakaolinite formed from kaolinite and hematite formed from goethite. These minerals showed no change in XRD patterns after hydrothermal treatment but TGA weight loss did increase substantially for metakaolinite. SSA for all three dehydroxylated minerals increased substantially with period of hydrothermal treatment. These results suggest that dehydroxylated minerals and their partly rehydroxylated forms will exist in heated soils and may affect the chemical behaviour of soils.

.

Key Words
Reversion, rehydroxylation and dehydroxylation

Introduction

Australia has a history of severe forest and bushfires for diverse vegetation and fire regimes (FRA 2000). Fire was used as a powerful land-use tool by indigenous Australians to manage grasslands, forest and fauna (Gill and Moore 1990). The nature of the Australian environment, which is generally hot, dry and prone to drought and the volatile natural vegetation, causes Australian vegetation to be particularly vulnerable to fire.

Heating during a fire which burns litter and both fallen and standing timber may impose significant impacts on soil properties (Raison 1979). Increases in soil fertility and elevated plant nutrient concentrations in regrowth occurred after a single fire (Christensen 1994). These effects occur for both surface and lower soil horizons for high intensity fires. The effect of heating on soil mineralogy has not been extensively studied although modest (200-600°C) temperatures cause mineral transformations (Ketterings *et al.* 2000). Kaolinite decomposes at temperatures between 500°C and 700°C (Richardson 1972) losing lattice water. Metakaolinite forms in the temperature range from 450°C to 600°C. Gibbsite alters to an amorphous phase on heating at 200°C (Rooksby 1972), and goethite is transformed to hematite at ≈300 °C (Cornell and Schwertmann 1996). The persistence of the dehydroxylated compounds in heated soils is unknown and is the subject of this investigation.

Methods

We investigated how bushfire and laboratory heating of soil affects soil minerals and their recovery by rehydroxylation at 55 and 95°C.

Soil samples burnt in a forest fire

Samples were obtained from soils that had been heated under a burning log or litter. Samples were removed as a 1cm thick layer from under burnt Eucalyptus and grass tree (Xanthorrhoea pressii) logs from up-slope and down slope sites with a lateritic colluvium soil. Sampling took place shortly after a fire at Wundowie in the Darling Range, Western Australia in early March 2009. Samples were taken from a 10cm strip below a burnt log (0-10cm laterally) and 10-20cm and 20-30cm away from the log. The nomenclature for heated soil from under burnt Eucalyptus and grass tree logs from up-slope (US) and down slope (DS) sites at Wundowie bush fire site are as follow: DS Unburnt (unburnt soil 0-10cm depth from down slope), DS 0-10 cm (heated soil from down slope, 0-10cm from log), DS 10-20 cm (heated soil from down slope, 10-20cm from log), DS 20-30 cm (heated soil from down slope, 20-30cm from log), DS Unburnt (unburnt soil 0-10cm depth from Up slope), DS 0-10 cm (heated soil from up slope, 0-10cm from log), DS 10-20 cm (heated soil from up slope, 10-20cm from log), and DS 20-30 cm (heated soil from up slope, 20-30cm from log). The soils are very gravelly and were sieved to obtain the <2mm fraction for analysis.

Heated pure minerals
Gibbsite was obtained from Alcoa Alumina, Western Australia. Kaolinite from Mc Namee Pit, Bath, South Carolina, United States. Goethite from a lateritic Ni deposit, Koniambo, New Caledonia. The minerals were heated for 1 hour at temperatures above and below DTA dehydroxylation maxima. Gibbsite was heated at 250°C, 300°C and 350°C. Kaolinite at 500°C, 550°C and 600°C. Goethite at 250°C, 300 °C and 350°C. For the rehydroxylation experiment, 6.5g of the heated mineral was mixed with 26cm^3 of water then heated in closed containers in an oven for 0, 14, 70, and 200 days at two temperatures (55 and 95°C).

Analytical techniques
Materials were analyzed by XRD on a Philips PW3020 diffractometer, thermal gravimetric analysis (TGA) on a STA 6000 instrument (Perkin-Elmer, Norwalk, CT, USA), transmission electron microscopy (TEM) on a JEOL 3000 FEG electron microscope equipped with an Oxford Instruments INCA 200 Energy Dispersive Spectrometer (EDS). Specific surface area (SSA) was measured using a Micrometrics Gemini 2375 instrument with VacPrep 061 using a 5 point BET method with N_2 as the absorbate. The pH and EC of the materials was determined in a 1:5 deionised water extract. Forms of Fe, Al and Si were determined using the specific extractants: dithionite-citrate-bicarbonate, ammonium oxalate and sodium pyrophosphate (Rayment and Higginson 1992) and with analysis by an inductively coupled plasma with optical emission spectroscopy (ICP-OES) (Perkin-Elmer).

Results
Soil heated by forest fires
The XRD patterns of heated and unheated soil from the Wundowie bushfire show the effect of fire. The main crystalline compounds of unheated soil are quartz, gibbsite, kaolinite, and goethite. At the largest distance (20-30cm) from the burnt log, all the four minerals persisted and calcite occured as it is a common constituent of plant ash (Harper *et al.* 1982). Closer to the burnt log, gibbsite and goethite XRD intensities decreased as did the kaolinite intensity directly below the burnt log (0-10cm), these minerals had been dehydroxylated.

Table 1. Effect of heating on soil extractable Al, Fe and Si of 0-1cm depth soil at two distances from burnt grass tree (GT) and eucalyptus (EU) logs. DS: down slope, and US: up slope.

Samples	Oxalate			Na pyrophosphate			DCB		
	Al	Fe	Si	Al	Fe	Si	Al	Fe	Si
	mg/kg	mg/kg	mg/kg	mg/kg	mg/kg	mg/kg	mg/kg	mg/kg	mg/kg
GT DS Unburnt	**1353**	**452**	**110**	**1684**	**513**	**264**	**1161**	**3358**	**14**
GT DS 0-10cm	**7591**	**2373**	**2383**	**3617**	**620**	**356**	**5428**	**8467**	**941**
GT DS 10-20cm	**5199**	**1860**	**1128**	**3932**	**945**	**382**	**4116**	**10194**	**545**
GT DS 20-30cm	**4581**	**1574**	**1443**	**3137**	**651**	**371**	**3312**	**7337**	**607**
GT US Unburnt	**5153**	**2283**	**481**	**4593**	**1391**	**614**	**4751**	**17583**	**335**
GT US 0-10cm	**16958**	**4157**	**5230**	**9370**	**334**	**484**	**17230**	**9568**	**2093**
GT US 10-20cm	**15007**	**4288**	**2762**	**9276**	**1605**	**431**	**16842**	**24996**	**1701**
GT US 20-30cm	**10331**	**3011**	**2030**	**6948**	**1225**	**457**	**9672**	**17044**	**1109**
EU DS Unburnt	**2078**	**1035**	**194**	**1256**	**557**	**322**	**1686**	**7223**	**137**
EU DS 0-10cm	**12621**	**4068**	**5092**	**3493**	**522**	**354**	**4109**	**5678**	**802**
EU DS 10-20cm	**7045**	**2346**	**1640**	**3462**	**731**	**344**	**7123**	**16259**	**1082**
EU DS 20-30cm	**4112**	**1497**	**710**	**2750**	**613**	**436**	**4948**	**14287**	**637**
EU US Unburnt	**1260**	**748**	**1307**	**1461**	**706**	**210**	**3432**	**5468**	**265**
EU US 0-10cm	**8411**	**3291**	**1983**	**4617**	**964**	**299**	**6676**	**12515**	**921**
EU US 10-20cm	**5022**	**2090**	**1841**	**2756**	**711**	**363**	**3572**	**7955**	**849**
EU US 20-30cm	**4950**	**2105**	**1634**	**2859**	**740**	**360**	**5294**	**13901**	**1033**

Ash from bushfire considerably increased the pH and EC of all soil samples relative to the original. The increases in EC simply reflect the addition to the soil of soluble salts in plant ash (Harper *et al.* 1982). The extractable Al, Fe and Si values (Table 1) for GT DS, GT US, EU DS and EU US also increased substantially after the bushfire with values for the heated soil being considerably higher than for unburnt soil and the values are mostly higher directly under burnt logs. These poorly ordered soluble forms of Al, Fe and Si minerals had been formed by dehydroxylation of the parent crystalline minerals.

Dehydroxylation and rehydroxylation of pure minerals
Dehydroxylation of kaolinite, goethite and gibbsite caused slight to moderate increases in their specific surface area (SSA). All three minerals had lost most structural water during heating but had clearly aquired structural water (we define this as water lost at T>110^{o}C) during the rehydroxylation treatment (Figure 1). XRD indicated that the metakaolinite formed from kaolinite heated at 600^{o}C showed no change in structure for wet incubation times up to 200 days. Hematite formed from goethite at 350^{o}C also experienced no change in structure. XRD showed that rehydroxylation of heated gibbsite (initially boehmite and amorphous material) was extensive at 95^{o}C and after 14 days, additional boehmite (Bo), bayerite (Ba) and gibbsite (Gi) had formed (Figure 2). The process was much slower at 55^{o}C. TGA results for heated kaolinite and to a lesser extent for heated goethite showed considerable structural water was aquired during rehydroxylation with most water being lost over a range of temperatures rather than a specific temperature as occurred for the unheated mineral (Figure 1).

Gibbsite heated to 350^{o}C had a microporous, granular appearance, consistent with SSA results (Figure 3A). After incubation for 14 days at 95^{o}C complex intergrowths of hexagonal crystals had formed (Figure 3.B) which is consistent with XRD results (Figure 2) that show that boehmite, bayerite and gibbsite had formed.

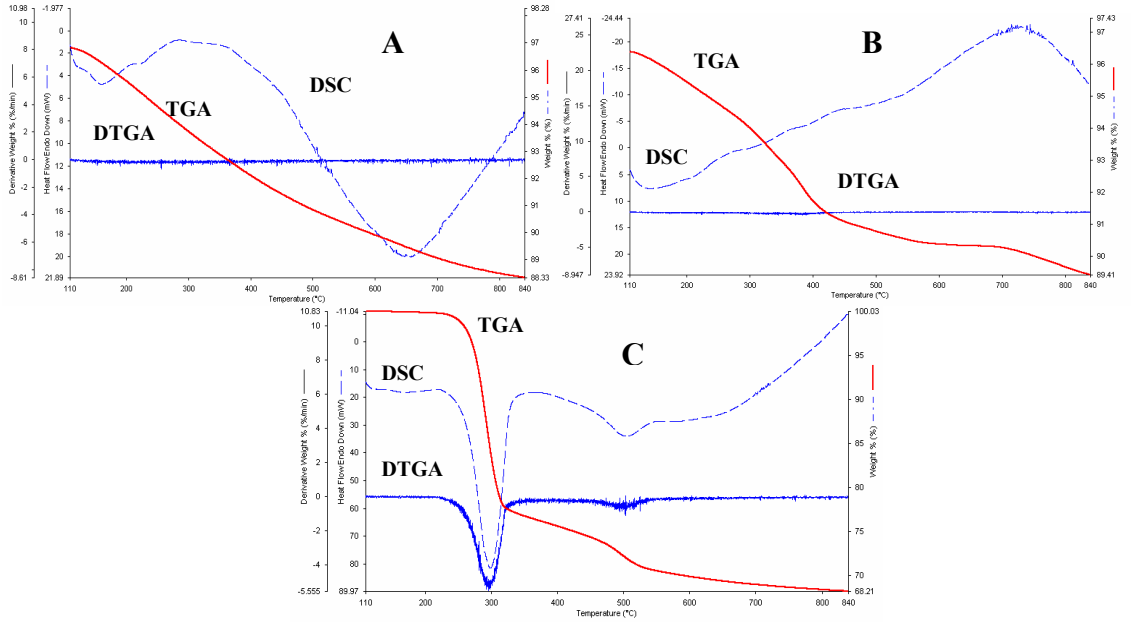

Figure 1. TGA results for rehydroxylated heated kaolinite (A), goethite (B) and gibbsite (C): 95^{o}C, 200 days, wet incubated at 55/95^{o}C, 0-200days.

Conclusion
Gibbsite, goethite and kaolinite are dehydroxylated by heating in bushfires. Laboratory dehydroxylation of kaolinite, goethite and gibbsite caused structural changes and slight to moderate increased in SSA. Rehydroxylation of 350^{o}C heated gibbsite was extensive during hydrothermal treatment at 95^{o}C and after 14 days boehmite, bayerite and gibbsite had formed, the process was slower at 55^{o}C. We propose that the process occurs in soils but at present remain unreported.

Metakaolinite and hematite showed no change in XRD patterns due to rehydroxylation but structural water content increased substantially for metakaolinite. These results suggest that dehydroxylated minerals and their rehydroxylated forms must be present in naturally heated soils and may exert significant effects on the chemical behavior of the soil.

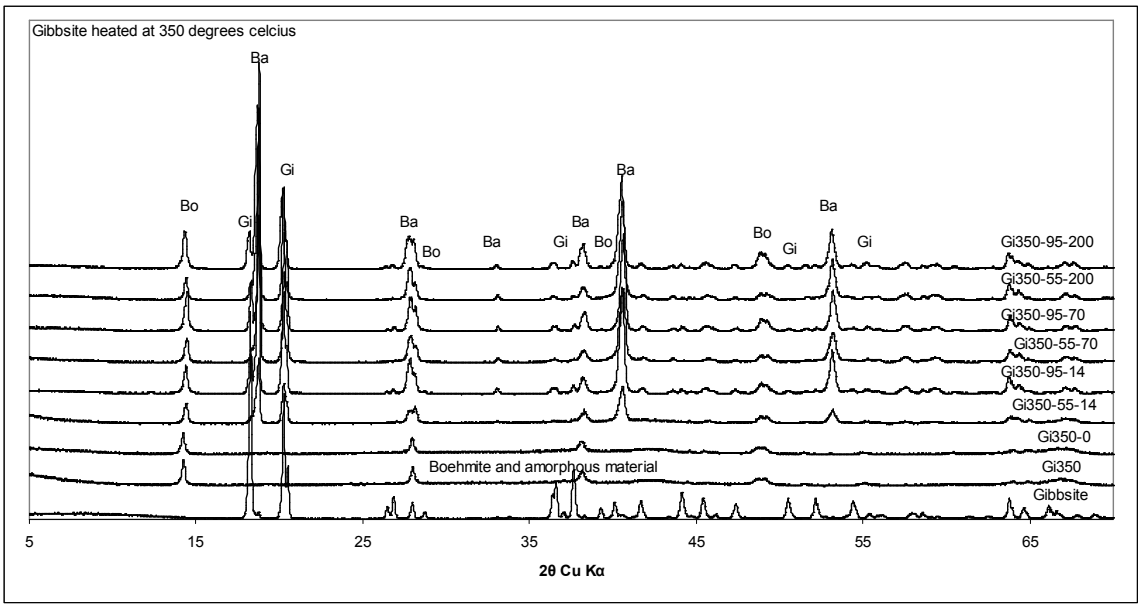

Figure 2. XRD patterns for heated gibbsite, wet incubated at 55/95°C, 0-200 days.

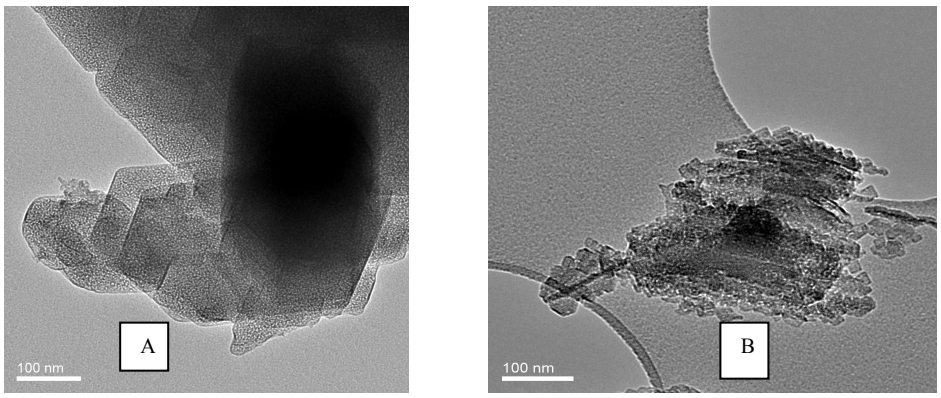

Figure 3. Electron micrographs of original gibbsite heated at 350°C (A), gibbsite dehydroxylated at 350°C then incubated for 14 days at 95°C (B).

References

Christensen NL (1994) The effects of fire on physical and chemical properties of soils in Mediterranean climate shrublands. In 'The role of fire in Mediterranean type ecosystems'. (Eds JM Moreno and WC Oechel), pp. 79-95. (Springer-Verlag Publishing; New York, USA)

Cornell RM, Schwertmann U (1996) The iron oxides: Structure, properties, reactions, occurence and uses. VCH Weinheim, Berlin.

FRA (2000) Global forest fire assessment. Forest Resources Assessment. Rome, Forestry Department, Food and Agriculture Organization of the United Nations.

Gill AM, Moore PHR (1990) Fire intensities in eucalypt forests of south eastern Australia. International Conference on Forest Fire Research, Coimbra, Portugal.

Harper RJ, Gilkes, RJ, Robson AD. (1982) Biocrystallization of quartz and calcium phosphates in plants- a re-examination of the evidence. *Aust. J. Agric. Res* **33**, 565-571.

Ketterings, QM, Bigham, JM (2000) Changes in soil mineralogy and texture caused by slash and burn fires in Sumatra Indonesia. *Soil Sci. Soc. Am. J.* **64**: 1108-1117.

Raison RJ (1979) Modification of the soil environment by vegetation fires, with particular reference to nitrogen transformations: a review. *Plant Soil* **51**: 73-108.

Rayment GE, Higginson L (1992) Australian laboratory handbook of soil and water chemical methods, Inkata Press, Melbourne

Richardson, HM (1972) Phase changes which occur on heating kaolin clays. The x-ray identification and crystal structures of clay minerals. (Ed G. Brown), pp. 132-142. (Miner. Soc Publishing; London)

Rooksby HP (1972) Oxides and hydroxides of aluminium and iron. The x-ray identification and crystal structures of clay minerals. (Ed G. Brown) (Miner. Soc Publishing; London)

Source and consumption of proton and its impacts on cation flux and soil acidification in a forested watershed of subtropical China

Jin-Ling Yang[A,B], Lai-Ming Huang[A,B], Gan-Lin Zhang[A,B]

[A] State Key Laboratory of Soil and Sustainable Agriculture, Institute of Soil Science, Chinese Academy of Sciences, Nanjing 210008, China, Email: glzhang@issas.ac.cn; jlyang@issas.ac.cn
[B] Graduate School of Chinese Academy of Sciences, Beijing 100049, China, Email: glzhang@issas.ac.cn; jlyang@issas.ac.cn

Abstract
To understand the impacts of H^+ from dry and wet deposition on soil acidification, the mass balance of elements of a forested watershed in subtropical China was studied. The studied watershed is located in south Anhui Province and in which the dry and wet deposition as well as runoff were monitored from Mar. 2007 to Feb. 2009. The physical and chemical properties of soil and rock were also determined. The results show that acid deposition bring in not only a mass of H^+ directly, but also nitrogen (N) and sulphur (S) that can produce abundant H^+ by secondary transformations and specific adsorptions in soil. As the discharge of H^+ by stream is very low, a large proportion of H^+ is consumed by soil (reaction). The rate of soil acidification is *c.a.* 1144 mol/ha/yr in the forest watershed besides the consumption of H^+ by mineral weathering. By comparison of the H^+ consumption by silicate mineral weathering and caion exchange, it shows that the loss of base cation can't be complemented by mineral weathering in this study area. So soil will be subject to acidification if the acid deposition continues.

Key Words
Watershed; Acid deposition; Nitrogen deposition; Sulphur deposition; Soil acidification.

Introduction
Soil nutrient losses and acidification caused by exterior source acid is one of the global environmental problems that human being is facing with. Acid precipitation can destroy forest, reduce crop output, even harm to animal and human being. Soil, as the hub of terrestrial ecosystems plays an important role in buffering the impacts of acid precipitation on environment (Miller and Watmough 2009). Because of this buffering capacity, the change of soil pH is not easily perceptible (Jönsson *et al.* 2003) in a short time, which protects the waters and ecosystems (Miller and Watmough 2009). However, permanent acid input will inevitably cause soil acidification and irreversible damages (Stevens *et al.* 2009).The objective of this study was to ascertain (1) the acid rain intensity and sources of H^+ in the subtropical forest watershed; (2) the effects of H^+ on soil and ecosystem; (3) soil acid buffering function and soil acidification trend in the granite area under the acid precipitation, which can provide a reasonable foundation for the management of soil resource and evaluation of soil environment risk.

Methods
The study area and sampling program
The study area, Fengxingzhuang (FXZ) watershed, has an area of 359 ha and is located in the southern Anhui Province in subtropical China. It is a forested watershed with the forest age of about 30 years old. The wet and dry precipitation as well as stream water was monitored from Mar. 2007 to Feb. 2009 in the FXZ watershed. The weather station and an automated sensing wet/dry precipitation collector were installed near the outlet of the watershed. An automatic stream water collector, ISCO6712, with a sensor to measure water level was installed indoors near the flume site. The flow volume (L/s) was automatically transformed by the instrument software based on the detected flow depth and the normative flume dimensions. Water samples (1000 ml each) were collected automatically by the instrument every week and with also extra samples during the rain events. Typical soil samples were collected on the top of mountain, hillside and piedmont respectively in the watershed. The fresh granite rock samples were also sampled from the watershed.

Chemical analysis
Water samples were analyzed as soon as possible when returning to the laboratory. Water pH, NH_4^+-N, NO_3^--N, K^+, Na^+, Ca^{2+}, Mg^{2+}, Cl^-, SO_4^{2-}, Si and Al were determined. Soil samples were tested with bulk density, grain size distribution, cation exchange capacity, exchangeable cations (K^+, Na^+, Ca^{2+}, Mg^{2+}), exchangeable

acidity, noncrystalline Fe and Al oxides, and free Fe and Al oxides. The total contents of K, Na, Ca, Mg, Fe, Al, Si of soil and rock samples were also determined.

Results and discussion

pH of wet precipitation and stream water and H^+ flux

The pH of wet precipitation, mainly rain, varies from 3.66 to 5.80 during the monitored period (Figure 1). The frequency of acid rain (pH<5.6) is 98% of the total rainfall events. However, pH of all stream samples in the watershed is higher than that of rain, which is from 6.44 to 7.68, with a mean of 6.93.

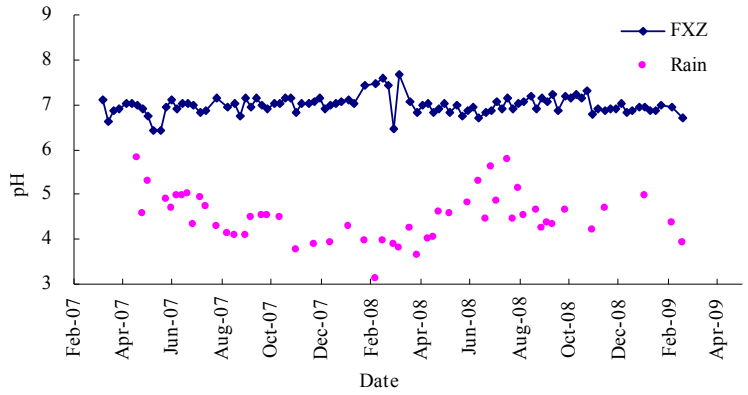

Figure 1. Dynamic changes of pH in rain and stream water from FXZ watershed during the monitored period from Mar. 2007 to Feb. 2009

The flux of H^+ by direct wet precipitation is 806 mol/ha/yr. The output of H^+ is very little, less than 1/ha/yr (Table 1). Both $SO_4^{2-}$and NO_3^- contents significantly correlates with H^+ content, which shows that the air pollution in the mountainous region of southern Anhui Province is characterized by a combination of NO_x pollution from local agricultural activities and distant SO_2 pollution transported by the atmosphere from modern industry.

Table 1. Input and output (mol/ha/yr) of some ions in wet precipitation, dry deposition and stream water

	H^+	NH_4^+	NO_3^-	S	K^+	Na^+	Ca^{2+}	Mg^{2+}	Al^{3+}	SiO_2
					mol /ha/yr					
Wet precipitation	806	670	527	628[a]	121	293	468	71	47	23
Dry deposition	ND	ND	ND	125[b]	73	45	160	63	154	ND
Stream	0.86	68	316	417	153	1510	849	262	5	1835
Net input/output	805	602	211	336	41	-1172	-221	-128	196	-1812

[a] S from wet precipitation as the form of SO_4^{2-}; [b] S from dry deposition as the form of SO_2; ND, not determined; – for net output of some elements

H^+ flux from nitrogen transformations

The content of NH_4^+ in the stream water is lower than that in wet precipitation, while the content of NO_3^- in the stream water is higher than that of wet precipitation. The total inorganic nitrogen content in the wet precipitation is higher than that in the stream water. The net input of total inorganic nitrogen is 813 mol/ha/yr in the watershed (Table 1). As for the undisturbed conifer ecosystems, the denitrification rates range from <0.01 to 0.45 g N/m^2/yr (Chen *et al.* 2000; Beier *et al*. 2001; Horvath *et al.* 2006), i.e. <7~321 mol N/ha/yr. So if taking the loss of denitrification into account, the net input of N is 492 mol/ha/yr. From this point, the forest watershed in subtropical China is still the sink of N at present.

Table 1 shows that NH_4^+ is the dominant form of inorganic nitrogen input, while NO_3^- is the dominant form of that input. The main reason is that soil colloids generally have negative charges, so easy to adsorb cations rather than anions (Zhu and Wen 1992). When NH_4^+ enters into soil, it can be adsorbed easily by soil colloids. Meanwhile the adsorbed NH_4^+ tends to be nitrified. Nitrogen transformation processes are extremely important in regulating the H^+ cycle. According to van Breemen *et al.* (1984), the actual acid-producing rate resulting from N transformations can thus be quantified by balancing the input of NH_4^+ (H^+ source) and NO_3^- (H^+ sink) verse the output on an annual basis.

$$H^+ \text{ production} = (NH_4^+{}_{(in)} - NH_4^+{}_{(out)}) - (NO_3^-{}_{(in)} - NO_3^-{}_{(out)}) \quad (1)$$

Where $_{(in)}$ denotes the input from wet precipitation and $_{(out)}$ denotes the output by stream water. Calculated from this formula, H^+ production rate due to N transformation is 391 mol/ha/yr in the watershed (Table 2).

Table 2. Mean annual H^+ fluxes (mol/ha/yr) of key H^+ production/consumption processes at the watershed

Source	H^+_{rain}	H^+_N	H^+_{SO2}	H^+_{SO4}	H^+_{BC}
H^+ production /consumption (mol/ha/yr)	805	391	250	-34	-1870

H_{rain}= net H^+ input from rainfall; H^+_N = net H^+ production/consumption due to nitrogen transformations; H^+_{SO2} = net H^+ production/consumption due to SO_2 transformations; H^+_{SO4} = net H^+ production/consumption due to SO_4^{2-} specific adsorption; BC= net H^+ production/consumption associated with base cation flux (weathering + ion exchange);– implies H^+ consumption.

H^+ flux from sulphur transformations

The input of SO_4^{2-} through wet precipitation is 581 mol/ha/yr, while SO_2 input as the major form of sulphur (S) in dry deposition is 125 mol/ha/yr. The output of SO_4^{2-} through stream water in the FXZ watershed is 417 mol/ha/yr, less than the input of S through wet and dry deposition, showing a net sink of S in the watershed (Table 1).The adsorption and transformation of SO_2 and SO_4^{2-} in soil also involves the production and consumption of H^+. SO_2 gets rapidly oxidized into SO_4^{2-} when enters into soil system and by which double molar of H^+ is produced for every molar of SO_4^{2-}. Because the dry deposition is mainly SO_2, the production of H^+ is about 250 mol/ha/yr by SO_2 transformation (Table 2).

The adsorption and transformation of SO_4^{2-} in soil is rather complex and involves a so-called specific adsorption mechanism by positively charged oxides colloids. The complexation and exchange of SO_4^{2-} on the surface of oxides has the following general ways (Parfitt 1980):

$$\left.\begin{matrix} M-OH_2 \\ M-OH \end{matrix}\right|^{+} + SO_4^{2-} \rightarrow \left.\begin{matrix} M-OH_2 \\ M-SO_4 \end{matrix}\right|^{0} + OH^-$$

$$M\left|\begin{matrix} -OH_2 \\ -OH \end{matrix}\right|^{0} + SO_4^{2-} \rightarrow M\left|\begin{matrix} -OH_2 \\ -SO_4 \end{matrix}\right|^{-} + OH^-$$

Therefore, when the input of hydrogen ion is relatively low, the complexation exchange of SO_4^{2-} with surface hydroxyl group leads to the release of hydroxyl which can buffer soil acidity by the reaction with H^+. Many studies showed that the apparent ratio of the OH^- release and the SO_4^{2-} adsorption is about 0.10~0.22 (Yu *et al*. 1996), not exactly following the 1:1 ratio. Taking the reality of the low soil oxide content of the area, the current study uses the OH^-/ SO_4^{2-} ratio of 0.10 for further calculation. It is estimated that the production of OH^- by the specific adsorption of SO_4^{2-} is about 34 mol/ha/yr, which in turn can consume 34 mol/ha/yr of H^+ in the watershed.

Flux of base cation and H^+ consumption

The content of K^+, Na^+, Ca^{2+}, Mg^{2+} in the stream water from the watershed are generally higher than that in wet precipitation, respectively. The net output of base cations are 1870 mol (p+)/ha/yr in the watershed (Table 1), which come from mineral weathering and cation exchange. Data in Table 2 shows there is a slight imbalance of H^+ with more consumption in soil than input, as dry deposition N is not measured currently. Generally dry deposition of N accounts for 25% to 30% that of wet deposition (Zeller *et al.* 2000). Of course, acid organic exudates in soil contribute a small amount of H^+ too (Forsius *et al.* 2005).

The molar ratio of total base elements (K, Na, Ca, Mg) to that of Si in the parent rock is averaged 0.204 in the watershed. If the rock is weathered completely, one can have such a hypothesis that release of base cations and the release of Si are proportional (1:5). As the hydrolysis of silicates is the predominant SiO_2 source, the release of base cations by silicates weathering can be estimated then. In the study, the net output of Si is 1812 mol/ha/yr (Table 2), so the base cation release in this way should be 362 mol/ha/yr (Table 3) that is about 19% of the net output of base cations. According to this proportion (19%), the H^+ consumption from weathering is about 268 mol/ha/yr to the total net input of H^+ is 1412 mol/ha/yr, while cation exchange is estimated about 1144 mol/ha/yr, accounting for 81% of total net input H^+. Weathering of primary minerals consumes directly H^+ and should not lead to soil acidification, while cation exchange would lead to soil acidification by exporting base cations. H^+ exchange will eventually lower the base cation saturation degree and the buffering capacity to acid addition. Accordingly, the soil acidification rate caused by direct and secondary H^+ addition is calculated as 1144 mol/ha/yr.

Table 3. SiO_2, base cation net output and H^+ consumption (mol (p+)/ha/yr) and the percentage (%) from rock weathering and cation exchange

SiO_2 net output	Base cation net output 1870		H^+ net consumption 1412	
1812	Contribution from silicate weathering 362 (19 %)	Contribution from cation exchange 1508 (81 %)	Contribution from silicate weathering 268 (19%)	Contribution from cation exchange 1144 (81%)

Conclusion

Although the studied forested watershed is far from urban environment, acid precipitation is frequent and has a strong acidity, as affected equally by long distance source of SO_2 and the local agricultural NO_x contribution. The watershed, as a typical forest ecosystem in subtropical China, is a net sink for both N and S. Atmospheric deposition adds H^+ to the forest ecosystem directly and through the transformation of the deposited ammonium and SO_2 indirectly. The transformation of ammonium contributes 27% of the total H^+ input, and the dry deposition of SO_2 contributes about 17%. The input of SO_4^{2-} is supposed to consume H^+ by its specific adsorption but the contribution is only 2.4%. The total net input of H^+ to the watershed by dry and wet deposition is 1412 mol/ha/yr. If the weathering of soil minerals is taken into consideration, the acidification rate of the soils would be about 1144 mol/ha/yr.

Acknowledgements

This study was supported by the National Natural Science Foundation of China (No. 40601040), the International Foundation of Science (C/4077-1) and Institute of Soil Science, Chinese Academy of Sciences Foundation of Science (ISSASIP0704).

References

Beier C, Rasmussen L, Pilegaard K, Ambus P, Mikkelsen TN, Jensen NO, Kjøller A, Priemé A, Ladekarl UL (2001) Fluxes of NO_3^-, NH_4^+, NO, NO_2 in an old Danish beech forest. *Water, Air and Soil Pollution*: **Focus 1**, 187-195.

Chen GX, Huang B, Xu H, Zhang Y, Huang GH, Yu KW, Hou AX, Du R, Han SJ, VanCleemput O (2000) Nitrous oxide emissions from terrestrial ecosystems in China. *Chemosphere—Global Change Science* **2**, 373-378.

Forsius M, Kleemola S, Starr M (2005) Proton budgets for a monitoring network of European forested catchments: impacts of nitrogen and sulphur deposition. *Ecological Indicators* **5**, 73-83.

Jönsson U, Rosengren U, Thelin G, Nihlgård B (2003) Acidification-induced chemical changes in coniferous forest soils in southern Sweden 1988–1999. *Environmental Pollution* **123**, 75-83.

Horvath L, Fuhrer E, Lajtha K (2006) Nitric oxide and nitrous oxide emission from Hungarian forest soils linked with atmospheric N-deposition. *Atmospheric Environment* **40**, 7786-7795.

Miller DE, Watmough SA (2009) Soil acidification and foliar nutrient status of Ontario's deciduous forest in 1986 and 2005. *Environmental Pollution* **157**, 664-672.

Parfitt RL (1980) Soils with variable charge. In 'Soils with Variable Change'. (Eds BKG Theng) pp. 167-194. (Lower Hutt, New Zealand Soc. Soil Sci.)

Stevens CJ, Dise NB, Gowing DJ (2009) Regional trends in soil acidification and exchangeable metal contents in relation to acid deposition rates. *Environmental Pollution* **157**, 313-319.

van Breemen N, Driscoll CT, Mulder J (1984) Acidic deposition and internal proton in acidification of soils and water. *Nature* **307**, 599-604.

Yu TR, Ji GL, Ding CP (1996) Electrochemistry of Variable Charge Soil. (Beijing: Science Press).

Zeller K, Harrington D, Riebau A, Donev E (2000) Annual wet and dry deposition of sulfur and nitrogen in the Snowy Range, Wyoming. *Atmospheric Environment* **34**, 1703-1711.

Zhu ZL, Wen QX (1992) Chinese Soil Nitrogen. (Jiangsu Science Press, Nanjing).

The Morphology and Composition of Pyrite in Sandy Podosols in The Swan Coastal Plain

Nattaporn Prakongkep[A], Robert J. Gilkes[A,] *, Balbir Singh[B] and Stephen Wong[B]

[A]School of Earth and Environment, University of Western Australia, 35 Stirling Highway, Crawley, WA 6009, Australia.
[B]Department of Environment and Conservation, 181-205 Davy Street, Booragoon, WA 6154, Australia.
*Corresponding author. Email bgilkes@cyllene.uwa.edu.au

Abstract
Seventeen very deep peaty sandy podosol profiles containing distinct A, E, B, coffee rock (spodic B horizon) and C horizons were investigated. Some profiles contain buried soils (Palaeopodosols) representing former levels of the water table. Electron microscopy showed that pyrite is present in these podosols. Synchrotron XRD confirmed the presence of pyrite. Two pyrite morphologies were present: discrete submicron single crystals and 10-20 μm framboids. Single crystals of pyrite occurred in all E, B, coffee rock and C horizons examined. X-ray spectra of single crystals and framboids have the pyrite atomic ratio of Fe: S ≈ 1: 2. Framboidal pyrite is present in coffee rock and B horizon. As individual pyrite crystals are very small (≤ 1 μm), they have high specific surface area and are thus potentially very reactive if profiles are aerated.

Key Words
Pyrite, acid sulphate soil, Podosols, Swan Coastal Plain

Introduction

The acid sulphate soils (ASS) contains iron sulphide, especially pyrite. The oxidation of pyrite is the primary cause of acidification of acid sulphate soils. Pyrite is generally stable under reducing conditions (below the watertable), however, when the soil is drained and pyrite exposed to the atmosphere acidity is produced due to pyrite oxidation. The release of oxidation products can affect water quality, aquatic life, agricultural production and causes corrosion of concrete and other infrastructure.
The Swan Coastal Plain comprises of a series of three major sand dunes including Quindalup, Spearwood and Bassendean dunes. The soils on the Swan Coastal Plain consist predominantly of former beach deposits, the highly leached Bassendean Sands with very little clay and no carbonates to provide acid buffering capacity. These very sandy soils are unable to buffer against very low intensity acidifying processes. The acidification of the soils is apparently caused by oxidation of pyrite in peat soils within swampy areas being dewatered for urban development which lower the watertable and exposes of the pyritic soil to oxidation.

Methods

The Swan Coastal Plain, which lies to the west of the Darling Fault, developed over a deep trough filled with sedimentary rocks and consists of a series of geomorphic entities oriented sub-parallel to the coastline. The generalised surface geology is largely reflected in the distribution of soils, and includes the Guildford Clay in the east, the Bassendean Dune System fringing the present coastline (McArthur 2004).
The plain is composed of sedimentary material of Cainozoic and Mesozoic age. Sediments in wetlands are commonly peaty. Seventeen Humic/ Alsilic aquic podosols in swales in the Bassendean Dunes have been investigated. The 85 samples include A horizon rich in decomposing organic matter (14 samples), a light coloured sandy albic E horizon (30 samples), brown B horizon (9 samples) and a dark spodic B horizon (coffee rock, 19 samples) over a sand C horizon (13 samples). Some profiles contain several E and B horizons which may be regarded as remnants of palaeopodosols that formed when the water table was at lower positions.

Soil samples were kept in a wet condition in a cool room until analyzed and novel preparation procedures were employed to limit microbial activity and oxidation. Physico-chemical properties of whole soils were determined. Studies of the fine fraction (non quartz sand fraction) used scanning electron microscopy (SEM; JEOL 6400), transmission electron microscopy (TEM; JEOL 3000) and energy-dispersive X-ray analysis (EDAX). A highly dilute suspension of the fine fraction was prepared in distilled water by dispersion using ultrasonic treatment. For synchrotron X-ray diffraction (XRD), powder samples of the fine fraction were placed in glass capillaries, and analysed over an angular range of 4 - 60° 2Theta. The wavelength was set at ~1.0Å to provide for adequate dispersion/resolution.

Results

Soil morphology and properties

These podosol profiles are ancient and represent an extreme stage of pedogenesis. The substantial annual rainfall (about 800 mm at present) and the very high sand content (>95%) of the parent material has resulted in highly leached podsolised soils. All studied soil profiles show the typical A horizon, bleached E horizon, brown B horizon, strong dark cemented B horizon (coffee rock) and C horizon typical of podosols.

- A horizon: the Ag horizon of all soils is rich in organic matter with sandy texture.
- E horizon: the Ag horizon is underlain by grey quartz sand which becomes increasingly bleached with depth.
- B horizon: below the bleached sand is the illuvial B horizon which is highly porous, (brownish gray to brownish black) but does not contain cemented material.
- coffee rock: coffee rock is the term used to define a material which has a dark colour (yellowish brown to black), high organic matter and is strongly cemented. There appears to be a reduced porosity within the coffee rock due to the precipitation of iron oxyhydroxide, organic matter and aluminosilicate organic complexes.
- C horizon: the pale yellow parent material consisting of dune sand.

The typical soil depth of A, E, coffee rock, B and C horizons is 0-20 cm, 20-200 cm, 200-300 cm, 300-350 cm and 350-400 cm, respectively. Soil texture is sand (A, E and C horizons), with some B and coffee rock horizons having a loamy sand texture due to the high organic matter and allophane contents. The sand grains of the Bassendean Dune System which is a beach dune deposit are characteristically well rounded and are well sorted due to prolonged transport and sorting by water and wind. Soil pH in 1:5 H_2O varies between pH 3.2 - pH 8.8 for the A horizon, pH 4.0 - pH 6.9 for E horizon, pH 4.2 - pH 6.0 for the B horizon, pH 3.7 - pH 6.6 for coffee rock and pH 4.1 - pH 6.4 for the C horizon. The pH of soil in pH 5.5 H_2O_2 solution is in the range pH 1.8 - pH 6.0. Delta pH (pH H_2O-pH H_2O_2) ranges from 0.01-4.39 units, high values being indicative of the presence of sulphide (Soil Survey Staff 2006). The organic carbon content is mostly low in the E and C horizons ranging between 0.02-1.2%. The organic carbon content of A, B, and coffee rock horizons is high (ranging from 0.05-3.6%). Some soil profiles have distinct deep sub-soil horizons (2E horizon and 2coffee rock) which indicate buried palaeopodosols. These wetlands on the Swan Coastal Plain are commonly peaty and the subsoils contain pyrite (Appleyard *et al*. 2006). The podosols are classified as Humic/ Alsilic aquic podosols and Typic Endoaquods respectively in the Australian (Isbell RF 2002) and US (Soil Survey Staff 2006) soil classifications.

Mineral properties

Synchrotron XRD patterns of fine fractions extracted from podosol horizons show that quartz is the dominant mineral of the fine fraction with minor amounts of feldspar, kaolin and in some samples gibbsite and lepidocrocite. Resistant mineral, including anatase and ilmenite are present in some horizons. Pyrite is present in most E, B and coffee rock horizons and elemental sulphur is a minor constituent in most samples and occurs in all horizons (Figure 4).

Morphology and composition of pyrite

The reducing chemical environment within saturated horizons of very sandy humus podosols on the Swan Coastal Plain provides a favorable condition for pyrite (FeS_2) formation. Pyrite is the only sulphide mineral present. Pyrite single crystals (0.5-1 µm diameter) are abundant in all horizons except for the A horizon (Figure 1), however pyrite framboids (10-20 µm diameter) only occur within organic rich soil materials (coffee rock and B horizons) (Figure 2). Thus this study indicates a close association between organic matter and framboidal pyrite. Framboid formation may have formed from the spherical grains of sulphur present in these podosols, which correspond in shape and size to framboids (Figure 3) (Graham and Ohmoto 1994). The abundance of iron, sulphur and organic material evidently play important roles in the formation of pyrite framboids in these soils. Several authors have concluded that the formation of framboids can be explained by sulphidation of metastable spherical grains of sulphur either in an inorganic way by oxidation of hydrogen sulphide (abiogenic activity), or in a metabolic way, by the action of microorganisms (biogenic activity) (Kribek 1975; Kortenski and Kostova 1996). Gong *et al*. 2008 reported that pyrite framboids are the pyritized remains of microbial colonies (probably sulphate-reducing bateria). On the other hand various morphological types of single crystals of pyrite e.g. euhedral cubic and octahedral and anhedral pyrite are generated in the sedimentary matrix due to chemical reactions (abiogenic activity) (Dharmasri *et al*. 2004). SEM and TEM of fine fractions of these sandy podosols show that the iron to sulphur ratio of single crystal and framboidal pyrite is always 1: 2 which is consistent with pyrite and not other iron sulphides (Figures 1 and 2).

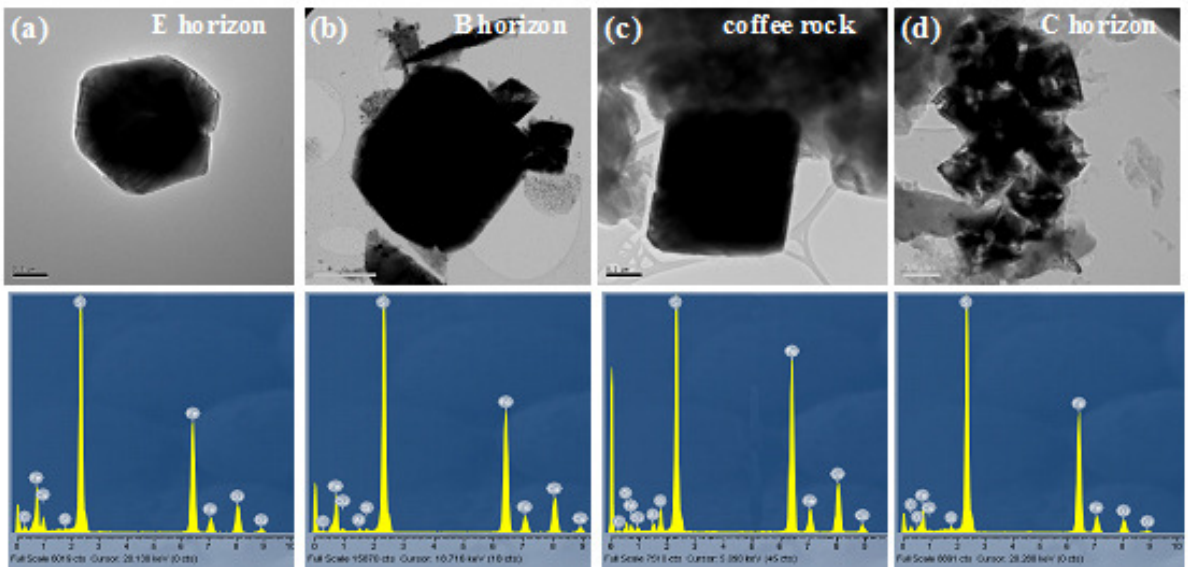

Figure 1. Transmission electron micrograph and x-ray spectra of pyrite crystals of diverse morphology from (a) E horizon (175-350 cm), (b) B horizon (350-600 cm), (c) coffee rock (225-400 cm) and (d) C horizon (250-350 cm); the atomic ratio of all particles is Fe: S ≈ 1: 2.

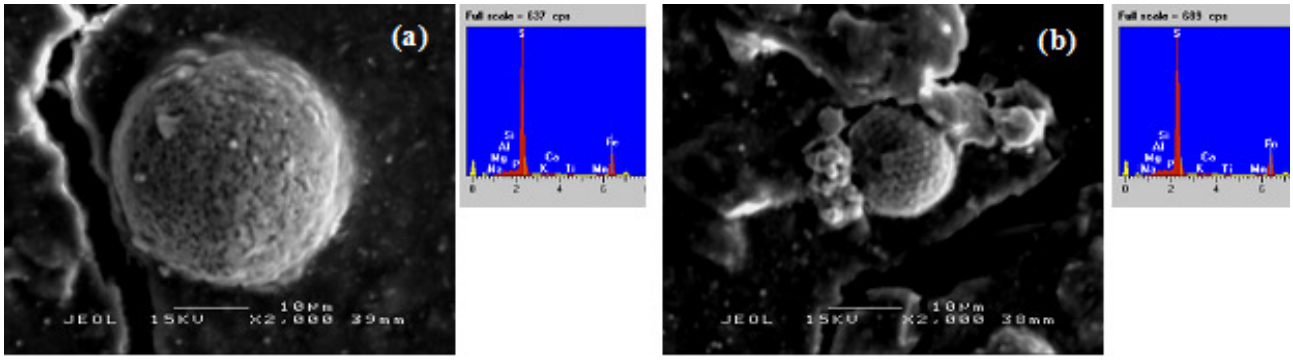

Figure 2 Backscattered electron image and x-ray spectra of pyrite particles in the fine fraction of (a) coffee rock (500-600 cm) and (b) B horizon (325-400 cm) deposited on a metal stub; the atomic ratio of all particles is Fe: S ≈ 1: 2.

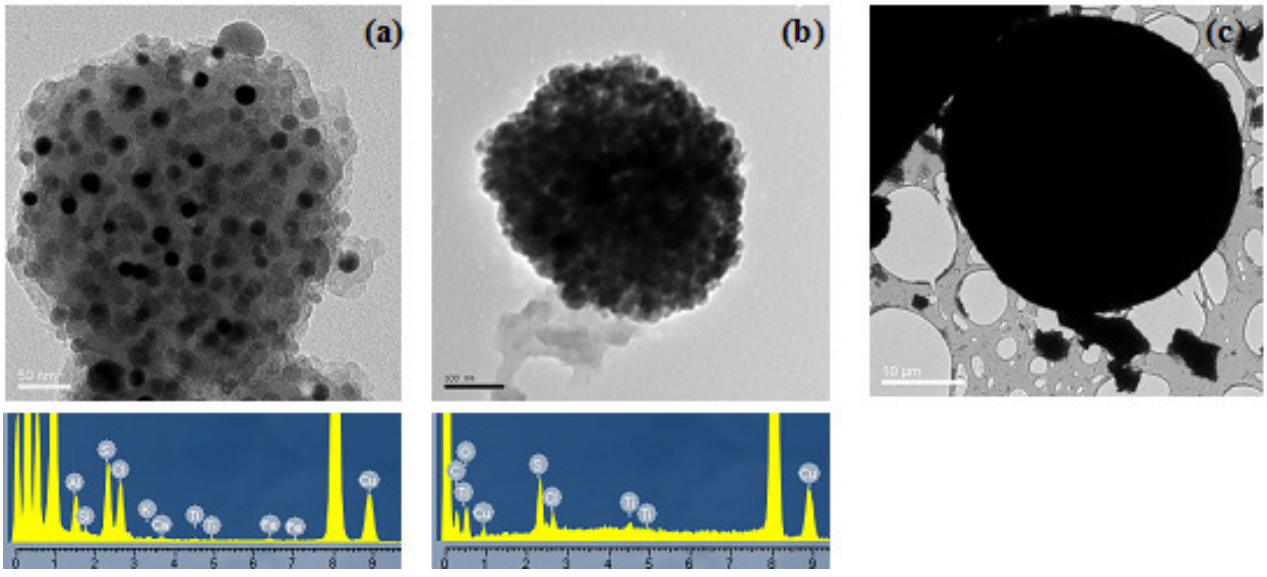

Figure 3 Transmission electron micrograph and X-ray spectra of (a, b) subspherical grains of sulphur from the B horizon (300-500 cm) and (c) framboidal pyrite from coffee rock (160-250 cm).

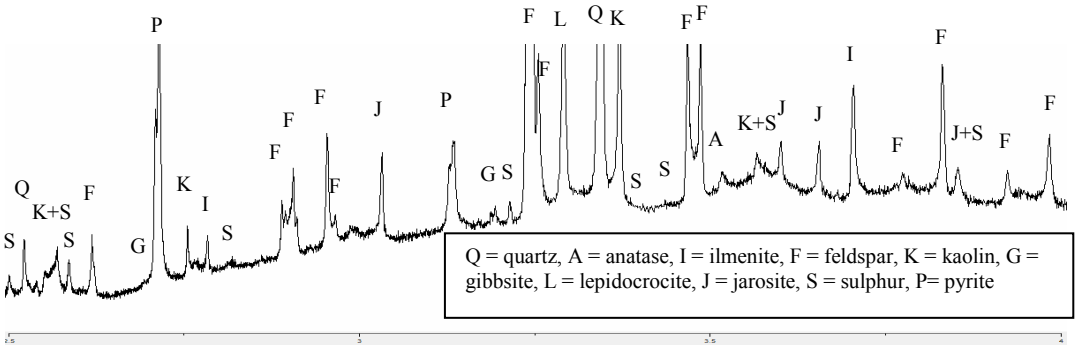

Figure 4. Synchrotron XRD pattern of the fine fraction of the E horizon of a podosol (200-325 cm) showing that pyrite and sulphur are present.

Conclusion

This research investigated 17 sandy podosols (85 samples) including A, E, B, coffee rock and C horizons from the Swan Coastal Plain. Some profiles contain palaeopodosols representing former levels of the water table. The studied soils are classified as Humic/ Alsilic aquic podosols (Australian Soil Classification, Isbell 2002) or Typic Endoaquods (Soil Survey Staff 2006). The studied acid sulphate soils on the Swan Coastal Plain are characterised by dark brown materials and pale leached sand which contains very little clay and no carbonate and is thus is unable to buffer changes in pH. The micrographs and XRD results provide unambiguous evidence for the occurrence of pyrite in these sandy podosols. Two pyrite morphologies occur: discrete submicron single euhedral crystals and 10-20 μm framboids. Single crystals of pyrite were present in all E, B, coffee rock and C horizons examined. Framboidal pyrite is present in coffee rock and B horizon materials. X-ray spectra of single crystals and framboids conform to the atomic ratio of pyrite Fe: S ≈ 1: 2. The grain size distribution and grain morphology of pyrite (euhedral single crystal or framboidal aggregate) provide information about the reactive pyrite surface area which affects oxidation rate and thus management. The rapid population growth of Perth with large numbers of developments requiring dewatering, and a prolonged period of low winter rainfall continue to induce acidification of groundwater.

Acknowledgments

We gratefully acknowledge assistance from the staff at the Centre of Microanalysis and Microscopy, University of Western Australia. We acknowledge the Australian Synchrotron for beam time. The Department of Environment and Conservation and Department of Water provided financial support for this research.

References

Appleyard SJ, Angeloni J, Wathins R (2006) Arsenic-rich groundwater in an urban area experiencing drought and increasing population density, Perth, Australia. *Applied Geochemistry* **21**, 83-97.

Dharmasri LC, Hudnall WH, Ferrell Jr RE (2004) Pyrite formation in Louisiana coastal marshes: scanning electron microscopy and X-ray diffraction evidence. *Soil Science* **169**, 624-631.

Gong YM, Shi GR, Weldon EA, Du YS, XU R (2008) Pyrite framboids interpreted as microbial colonies within the Permian *Zoophycos* spreiten from southeastern Australia. *Geol. Mag.* **145**, 95-103.

Graham UM, Ohmoto H (1994) Experimental study of formation mechnisms of hydrothermal pyrite. *Geochemica et Cosmochimica Acta* **58**, 2187-2202.

Isbell RF (2002) The Australian soil classification CSIRO Publishing, Australia.

Kortenski J, Kostova I (1996) Occurrence and morphology of pyrite in Bulgarian coals. *Int. J. Coal Geol.* **29**, 273-290.

Kribek B (1975) The origin of framboidal pyrite as a surface effect of sulphur grains. *Mineralium Deposita* **10**, 389-396.

McArthur WM (2004) Reference Soils of South-Western Australia. Department of Agriculture, Western Australia.

Renton JJ, Bird DS (1991) Association of coal macerals, sulfur, sulfur species and the iron disulphide minerals in three columns of the Pittsburgh coal. *Int. J. Coal Geol.* **17**, 21-50.

Soil Survey Staff (2006) Keys to Soil Taxonomy. United States Department of AgricultureNatural, Resources Conservation Service, USA.

Valley floor kaolinitic regolith in SW Australia that has been modified by groundwater under the present semi-arid climate

Georgina Holbeche[A], Robert Gilkes[A] and Richard George[B]

[A]School of Earth and Environment (M087), University of Western Australia, 35 Stirling Highway, Crawley, WA Australia Email holbeg01@student.uwa.edu.au (G. Holbeche), bob.gilkes@uwa.edu.au (B. Gilkes)
[B]Department of Agriculture and Food WA, Bunbury WA, Australia, Email rgeorge@agric.wa.gov.au

Abstract
The valley floor of the WA wheatbelt commonly consists of a diverse array of materials including alluvium, colluvium and residual lateritic regolith. The mineralogy is dominated by primary quartz and kaolinite; the ubiquitous product of intense weathering. Various amounts of iron oxides (goethite and hematite) and carbonates (calcite and dolomite) are also present. Scanning electron microscopy (SEM) was used to determine elemental distribution and thus identify processes such as impregnation, replacement and cementation. SEM elemental data explained elemental affinity groups and identified less common minerals such as cerium phosphate.

Key Words
Regolith, scanning electron microscopy, pit profiles, carbonate

Introduction
Much of the Wheatbelt of Western Australia is characterised by an ancient deeply weathered landscape of low relief formed under humid conditions and which is now experiencing a semiarid climate. The area is predominantly underlain by Archaean granitic and gneissic rocks that have been altered to lateritic profiles up to 30 metres or more deep (Johnston 1987). The complete laterite profile consists of saprolite overlying the fresh rock, overlain by the kaolinitic pallid zone, mottled zone, iron oxide rich duricrust and sandy topsoil (McArthur 1991). The main weathering products are kaolinite and iron oxides with primary quartz also being abundant. However carbonates, gypsum and many other evaporite minerals are now present, having accumulated in valley floor regolith under current semi-arid conditions. Figure 1 illustrates the stratigraphic organization of materials and some of the processes that have taken place in this complex landscape. Valley floor materials consist of diverse arrangements of alluvium, colluvium and residual lateritic regolith with all materials showing evidence of alteration by solute-rich groundwater under the semiarid conditions that have existed in the region within the past million years.
The focus of this paper is to develop an improved understanding of the materials present and the alteration processes that have occurred in this region.

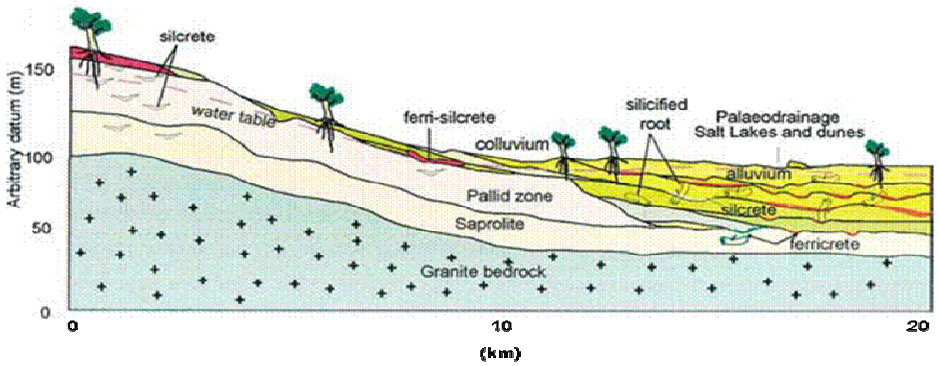

Figure 1. Illustration showing the materials present in valleys in SW Australia. From Gilkes *et al.* (2003).

Methods
Sample location and sampling method
Six sites in the WA wheatbelt were sampled. Pit profiles were taken every 200 metres along deep drains and at least 10 replicates of each morphologically distinct material type were taken.

Analytical methods
Samples were air-dried and discrete morphological components (matrix, mottles, and coarse fragments) separated. All samples were ground manually using an agate mortar and pestle. Soil minerals were

identified using powder x-ray diffraction (XRD). Traces 5.0.5 (Diffraction Technology 1999) and XPAS version 3.0 (Singh and Gilkes 1999) were used for mineral identification and data manipulation and Brindley and Brown (1980) for mineral identification.

Elemental composition was determined using a combination of x-ray fluorescence (XRF) of glass fusion beads (Norrish and Hutton 1969) and inductively coupled plasma mass spectrometry (ICP-MS) of diluted HNO_3-digested glass fusion beads

Polished thin sections were prepared by impregnating undisturbed soil with resin and kerosene was used as a lubricant in order to preserve soluble salts. Optical microscopy was used to describe fabric following criteria and nomenclature of Bullock *et al* (1985) and Stoops (2003). Scanning electron microscopy was used for imaging, microprobe analysis and element mapping.

Results

Field Morphology

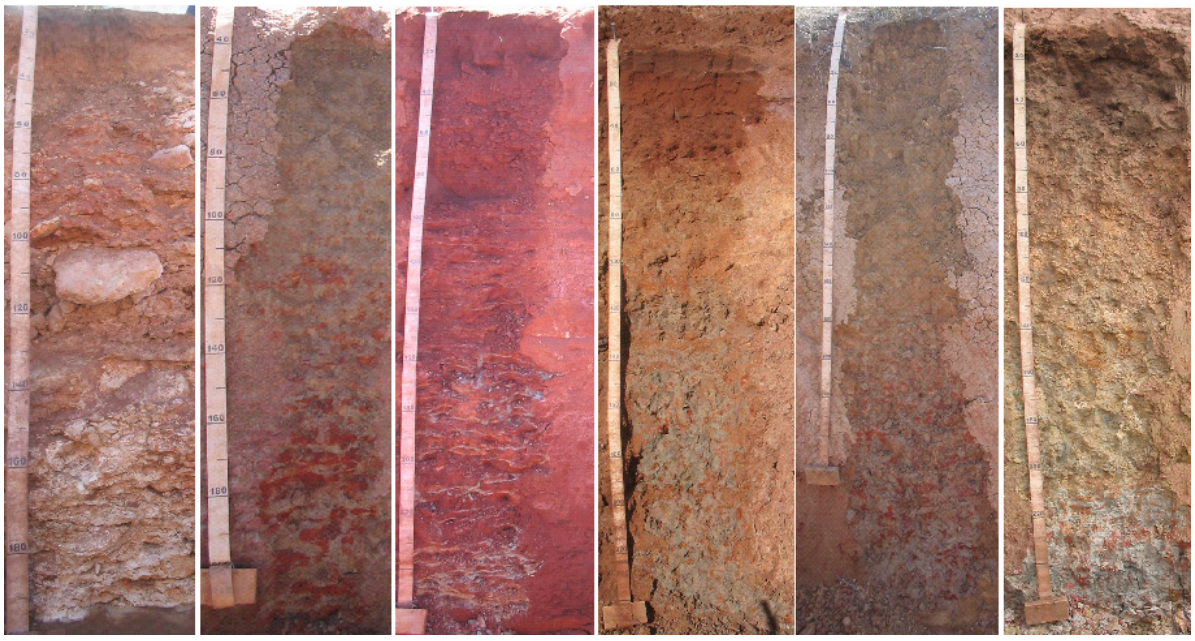

Figure 2. Representative soil profiles from the six sites sampled (from left to right); Three Springs, Pithara Morowa, Mongers 55, Dumbleyung and Wallatin Creek.

Pit photographs were taken at positions along drains. Information such as texture, structure, colour, strength, water status and the type and percentage of coarse fragments was recorded in the field with further morphological information collected in the laboratory. The six profiles included in Figure 2 are not only representative of each site; they collectively represent the materials encountered throughout the region. Three Springs was dominated by platey coarse material with as much as 80% present in some horizons. Sandy clay loam and clay loam were present above approximately 50cm.Fine material between the platey layers is light and silty light clay and consists predominantly of calcite and dolomite with very little actual clay present. Profile three (Morowa) was similar in structure to the first consisting mainly of platey red/brown hardpan through the centre of the profile and sandy loams near the surface. The photograph also shows horizontal veins of a non-cemented material. Profiles two, four, five and six (Pithara, Mongers 55, Dumbleyung and Wallatin Creek) show the mottling that is characteristic of the laterite profile. At all these sites loams in the top of the profiles tended to clay by 60cm. In general the percentage of mottles increased with depth and the distinction in colour between matrix and mottles became clearer. By the time the water table was reached up to 50% of mottles were cemented (by iron oxides) and were therefore classed as coarse fragments.

Mineralogy

The average mineralogical composition for each site is given in table 1. For all sites other than Three Springs materials were mostly comprised of quartz and kaolinite sometimes with feldspar and lesser amounts

of other minerals. Very little kaolinite was present in the Three Springs samples, these soils often containing smectite or illite instead together with substantial amounts of carbonates. The dominance of dolerite and calcite at Three Springs may reflect the different geology at this location where a variety of metamorphic rocks occur which is in contrast to the dominantly granitic setting for the other sites (McArthur 1991). However there are broad regional patterns in soil mineralogy in SW Australia with calcareous soils and sediments becoming more abundant north of the so called Menzies Line. The Menzies Line (ML) defines the boundary between two climatic regimes. The presence of calcareous soils is one of several features including differences in rainfall, geology, regolith mineralogy and ground and surface waters that separate the two zones. The boundary follows the 30°S parallel and runs roughly east-west before heading further north towards Shark Bay at the western boundary. This is however more a transitional zone dividing two overlapping areas than a sharp distinction (Butt *et al.* 1977).

Table 1. Summary table of the average mineralogy at each site.

site	quartz (%)	kaolinite (%)	feldspar (%)	calcite (%)	dolomite (%)
DU	56.7	26.9	2.4	2.4	4.8
MG	63.9	23.7	1.6	1.5	0.8
MW	46.9	36.7	3.8	4.8	0.0
PT	54.2	25.2	2.9	1.9	0.9
TS	20.0	5.3	0.3	10.5	50.9
WC	59.9	22.2	6.8	5.9	0.8
	halite (%)	**goethite (%)**	**hematite (%)**	**palygorskite (%)**	**smectite/illite (%)**
DU	0.1	1.4	4.5	0.0	0.9
MG	0.1	4.9	2.9	0.0	0.8
MW	0.6	0.0	0.4	0.0	7.2
PT	0.3	7.2	3.2	0.0	4.3
TS	1.5	0.0	0.0	2.8	8.7
WC	0.0	2.6	1.8	0.0	0.0

X-ray diffraction was used to determine the mineralogical composition of the samples represented by the two thin sections presented below (Figures 2 and 3). The sample shown in Figure 2 was dominated by dolomite and calcite with trace amounts of quartz and illite. The sample in Figure 3 contained a large amount of quartz, significant amount of feldspar and kaolinite.

Chemistry

Three hundred samples were analysed for 55 elements. Freeware R 2.7.2 (The R Foundation for Statistical Computing 2008) was used to summarise and draw out relationships in the data. Principle component analysis identified relationships between elements and established associations with minerals. Three components were considered, the first two components explained 47% of variability with component three explaining a further 7.7%; highlighting the diverse nature of the materials. Few clear element affinity groups occur; some elements (e.g. La, Ce, Pr, Nd, Sm, Eu, Gd, Tb, Dy, Ho, Er, Tm Yb and Lu) are tightly clustered as is commonly the case for the lanthanides and this cluster also contains Ni, Co, Mn and Cu. Mineralogical-chemical relationships include Ca, Mg and Sr being associated with calcite and dolomite and Fe, Cr Al and V being associated with goethite and hematite.

Microscopy

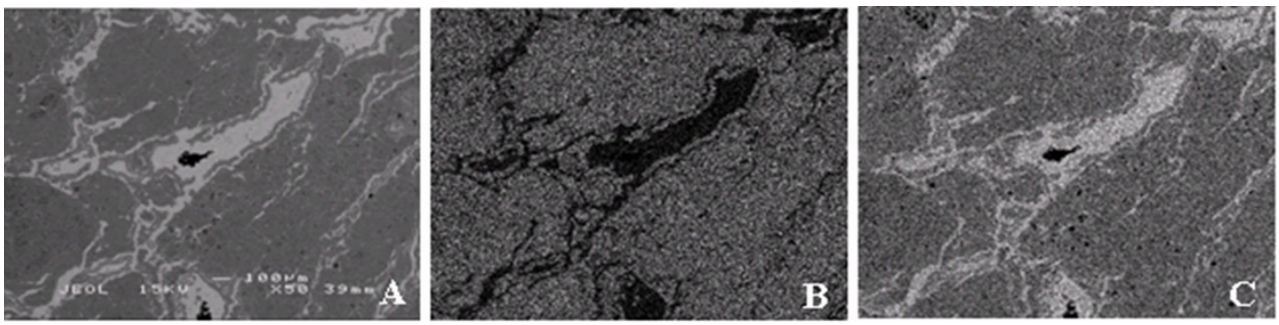

Figure 3. Scanning electron micrograph (A) of a carbonate dominated sample and the associated magnesium (B) and calcium (C) maps. The material contains little silicon and aluminium.

Scanning electron micrograph images in Figure 3 of a sample from Three Springs illustrate the dominance of Ca/Mg carbonates in this regolith. The sample contains little aluminium [clay minerals] or quartz as is also indicated by mineralogical and chemical analysis. It is therefore likely that any clay matrix was replaced, as opposed to being impregnated by authigenic calcite and dolomite that have crystallised from groundwater.

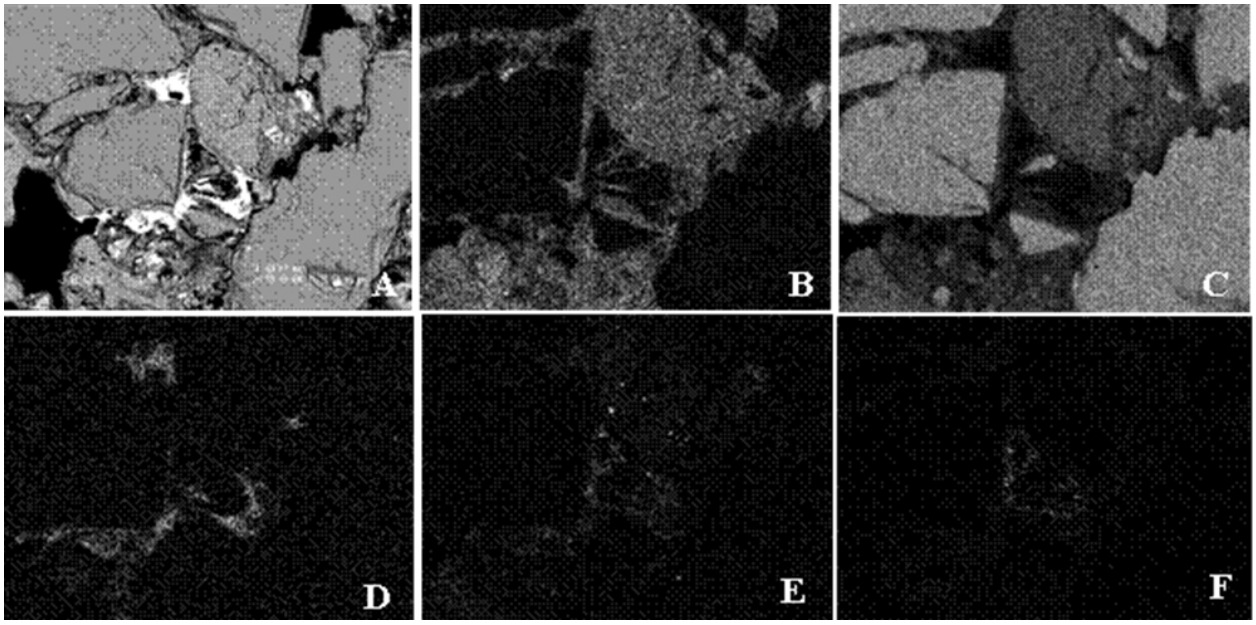

Figure 4. Back scattered electron image (A) of a matrix support sample and associated element maps for aluminium (B), silicon (C), cerium (D), calcium (E) and iron (F).

Figure 4 is of a relatively clay rich, matrix support sample, dominated by kaolinitic clay and angular quartz, both typical of the local saprolite derived from granite. The saprolite has formed *in situ* then subsequently invaded by groundwater from which diverse precipitates including iron oxides and cerium phosphate have formed.

Conclusions

Valley floor regolith in the wheatbelt of SW Australia exhibits complex variations in composition and morphology that reflect its long history of weathering and modification by ground water.

References

Brindley GW, Brown G (1980) 'Crystal Structures of Clay Minerals and Their X-Ray Identification' (Mineralogical Society, London, England).

Bullock P, Fedoroff N, Jongerius A, Stoops G, Tursina T, Babel U (1985) 'Handbook for soil thin section description.' (Waine Research Publications, Wolverhampton, England).

Butt CRM, Horwitz RC, Mann AW (1977) *Uranium occurrences in calcretes and associated sediments in Western Australia*. CSIRO Australia, Division of Mineralogy, Perth. Report: **FP16**.

George R, Clarke J, English P (2008) Modern and palaeogeographic trends in the salinisation of the Western Australian wheatbelt: a review *Australian Journal of Soil Research*. **46**, 751 – 767.

Gilkes R, Lee S, Singh Balbir (2003) The imprinting of aridity upon a lateritic landscape: an illustration from southwestern Australia *C.R. Geoscience* **335** (2003) 1207-1218.

Johnston CD (1987) Preferred water flow and localised recharge in a variable regolith. *In* A J Peck and D R Williamson (Editors), Hydrology and Salinity in the Collie River Basin, Western Australia. *Journal of Hydrology* **94**, 129-142.

McArthur WM (1991) Reference soils of south-western Australia (Department of Agriculture, Western Australia, Perth, Australia).

Norrish K, Hutton JT (1969) An accurate x-ray spectrographic method for the analysis of a wide range of geological samples *Geochimica et Cosmochimica Acta* **33**, 431-453.

Stoops G (2003) 'Guidelines for analysis and description of soil and regolith thin sections' (Soil Science Society of America, Wisconsin, USA).